

Combination of Optical and SAR Remote Sensing Data for Wetland Mapping and Monitoring

by

© **Meisam Amani**

A thesis submitted to the

School of Graduate Studies

In partial fulfillment of the requirements for the

Degree of Philosophy

Faculty of Engineering and Applied Science

Memorial University of Newfoundland

September 2018

St. John's, Newfoundland

✿ ✿ ✿ ✿ ✿ ✿ ✿ ✿ ✿ ✿ ✿
✿ DEDICATED TO ✿
✿ MY PARENTS ✿
✿ AND ✿
✿ MY WIFE, SAHEL ✿
✿ LOVE YOU FOR EVER ✿
✿ ✿ ✿ ✿ ✿ ✿ ✿ ✿ ✿ ✿ ✿

ABSTRACT

Wetlands provide many services to the environment and humans. They play a pivotal role in water quality, climate change, as well as carbon and hydrological cycles. Wetlands are environmental health indicators because of their contributions to plant and animal habitats. While a large portion of Newfoundland and Labrador (NL) is covered by wetlands, no significant efforts had been conducted to identify and monitor these valuable environments when I initiated this project. At that time, there were only two small areas in NL that had been classified using basic Remote Sensing (RS) methods with low accuracies. There was an immediate need to develop new methods for conserving and managing these vital resources using up-to-date maps of wetland distributions. In this thesis, object- and pixel-based classification methods were compared to show the high potential of the former method when medium or high spatial resolution imagery were used to classify wetlands. The maps produced using several classification algorithms were also compared to select the optimum classifier for future experiments. Moreover, a novel Multiple Classifier System (MCS), which combined several algorithms, was proposed to increase the classification accuracy of complex and similar land covers, such as wetlands. Landsat-8 images captured in different months were also investigated to select the time, for which wetlands had the highest separability using the Random Forest (RF) algorithm. Additionally, various spectral, polarimetric, texture, and ratio features extracted from multi-source optical and Synthetic Aperture Radar (SAR) data were assessed to select the most effective features for discriminating wetland classes. The methods developed during this dissertation were validated in five study areas to show their effectiveness. Finally, in collaboration with a team, a website

(<http://nlwetlands.ca/>) and a software package were developed (named the Advanced Remote Sensing Lab (ARSeL)) to automatically preprocess optical/SAR data and classify wetlands using advanced algorithms. In summary, the outputs of this work are promising and can be incorporated into future studies related to wetlands. The province can also benefit from the results in many ways.

Keywords: Wetland, Remote Sensing, Object-based Image Analysis, Separability analysis, SAR, Image Classification, Canada, Newfoundland and Labrador

ACKNOWLEDGEMENTS

I would like to take this opportunity to express my deepest thanks to those who helped me during different phases of my PhD. I would like to express my gratitude to my supervisor, Dr. Bahram Salehi, for his guidance, patience, and encouragement. Dr. Salehi introduced this interesting topic to me and trusted my abilities to contribute to this field. I also appreciate all the help, time, and valuable comments that I received from my co-supervisor, Dr. Brian Brisco. He was always available to help and provide a big-picture perspective on my view of the thesis. I am also thankful to Mr. Desmond Power, a member of my supervisory committee, for his valuable time and feedback. I am very grateful to my wife, Sahel, who worked with me on this project. Her presence, time, comments, and encouragements played a vital role in completing my thesis. I would also like to thank Ms. Jean Granger, the other member of our team. She was always kind to me and was ready to help me during various phases of my research. Additionally, I appreciate the time and guidance that I received from Dr. Cecilia Moloney and Dr. Weimin Huang.

Moreover, I would like to acknowledge the financial support of the Government of Canada through the Federal Department of Environment and Climate Change, and the Research & Development Corporation of Newfoundland and Labrador. I also would like to thank the Canada Center for Mapping and Earth Observation and Environment and Climate Change Canada for providing SAR imagery. Field data were collected by various organizations, including Ducks Unlimited Canada, Government of Newfoundland and Labrador Department of Environment and Conservation, and Nature Conservancy Canada. I thank these organizations for providing such valuable datasets.

I am truly grateful to my lovely mother and father, sisters, and brother for all their support during not only my PhD, but also every step of my life. I will never forget the love and support I received from you.

TABLE OF CONTENTS

ABSTRACT	iii
ACKNOWLEDGEMENTS	v
TABLE OF CONTENTS.....	vii
LIST OF TABLES	xiv
LIST OF FIGURES	xvii
ACRONYMS	xxii
CHAPTER 1. INTRODUCTION.....	1
1.1. Background	1
1.2. Motivations.....	6
1.3. Objectives.....	6
1.4. Contribution and novelty.....	7
1.5. Organizations of the dissertation	10
1.6. Co-authorship statement.....	12
1.7. Publications, presentations, software, website, teaching, and courses	13
1.7.1. Book chapter	13
1.7.2. Journal articles.....	13
1.7.3. Conference articles.....	16
1.7.4. Conference presentations	18
1.7.5. Software.....	19

1.7.6. Wetland website.....	20
1.7.7. Guest lecturer	21
1.7.8. Courses.....	21
References.....	22
CHAPTER 2. WETLAND CLASSIFICATION USING MULTI-SOURCE AND MULTI-TEMPORAL OPTICAL REMOTE SENSING DATA IN NEWFOUNDLAND AND LABRADOR, CANADA.....	26
Abstract.....	26
2.1. Introduction.....	27
2.2. Materials and methods	31
2.2.1. Study areas.....	31
2.2.2. In situ data	33
2.2.3. Aerial and satellite images	34
2.3. Methodology	36
2.4. Results and discussion.....	41
2.4.1. Comparison between different classifiers.....	41
2.4.2. The effect of the tuning parameters on classification accuracy	47
2.4.3. Comparison between pixel-based and object-based methods.....	49
2.4.4. Validation of the proposed methodology in other pilot sites	50
2.5. Conclusion.....	56
References.....	58

CHAPTER 3. EVALUATION OF MULTI-TEMPORAL LANDSAT 8 DATA FOR WETLAND CLASSIFICATION IN NEWFOUNDLAND, CANADA.....63

Abstract.....63

3.1. Introduction.....64

3.2. Study area.....65

3.3. Data.....65

3.4. Method.....66

3.5. Results.....67

3.6. Conclusion.....70

References.....70

CHAPTER 4. SPECTRAL ANALYSIS OF WETLANDS USING MULTI-SOURCE OPTICAL SATELLITE IMAGERY72

Abstract.....72

4.1. Introduction.....73

4.2. Study area and data80

 4.2.1. Study areas.....80

 4.2.2. Field data.....84

 4.2.3. Satellite data86

4.3. Methods88

 4.3.1. Preprocessing of satellite data.....89

 4.3.2. Variance analyses of field samples.....90

 4.3.3. Separability measures91

4.3.4. Separability analyses of other features	94
4.3.5. Wetland classification using selected features	95
4.4. Results and discussion.....	96
4.4.1. Variance analyses of field samples.....	96
4.4.2. Separability analyses of spectral bands	98
4.4.3. Separability analyses of other features	120
4.4.4. Wetlands classification using selected features.....	129
4.5. Conclusion.....	132
References.....	134
CHAPTER 5. SEPARABILITY ANALYSIS OF WETLANDS USING MULTI-SOURCE SAR DATA.....	141
Abstract.....	141
5.1. Introduction.....	142
5.2. Study areas and datasets	145
5.2.1. Study areas.....	146
5.2.2. Field data.....	149
5.2.3. Satellite data	151
5.3. Methodology	152
5.3.1. Preprocessing and feature extraction.....	152
5.3.2. Variance analysis of field samples	155
5.3.3. Separability measure	157

5.4. Results and discussion.....	157
5.5. Conclusion.....	175
References.....	177

**CHAPTER 6. A MULTIPLE CLASSIFIER SYSTEM TO IMPROVE MAPPING
COMPLEX LAND COVERS: A CASE STUDY OF WETLAND
CLASSIFICATION USING SAR DATA IN NEWFOUNDLAND, CANADA**184

Abstract.....	184
6.1. Introduction.....	185
6.2. Study area and data	186
6.2.1. Study area	186
6.2.2. Field data.....	188
6.2.3. Satellite data	189
6.3. Method.....	191
6.3.1. Pre-processing.....	193
6.3.2. SAR feature extraction	193
6.3.3. Segmentation.....	194
6.3.4. Proposed Multiple Classifier System.....	195
6.4. Results and discussion.....	199
6.5. Conclusion.....	206
References.....	207

CHAPTER 7. WETLAND CLASSIFICATION IN NEWFOUNDLAND AND LABRADOR USING MULTI-SOURCE SAR AND OPTICAL DATA INTEGRATION	210
Abstract.....	210
7.1. Introduction.....	211
7.2. Study areas and data.....	217
7.2.1. Study areas.....	217
7.2.2. Data.....	218
7.3. Methodology	221
7.3.1. Pre-processing.....	221
7.3.2. Segmentation.....	222
7.3.3. Feature extraction and selection	223
7.3.4. Classification	225
7.3.5. Accuracy assessment.....	227
7.4. Results and discussion.....	227
7.5. Conclusion.....	240
References.....	241
CHAPTER 8. SUMMARY, CONCLUSION, AND RECOMMENDATIONS ..	247
8.1. Summary.....	247
8.2. Conclusion.....	249
8.3. Recommendations.....	253
8.3.1. Separability analysis of wetlands using multi-temporal satellite data	253

8.3.2. Improving and validating the accuracy of the proposed MCS.....	254
8.3.3. Improving the accuracy of the Bog/Fen discrimination.....	254
8.3.4. Wetland classification using EWCS	255
8.3.5. Wetland classification using fuzzy methods	256
8.3.6. Wetland classification using deep learning methods.....	256
8.3.7. Improving wetland classification accuracy by incorporating DEM	257
8.3.8. Application of nanosatellites for wetland classification	257
References.....	258
APPENDIX.....	261

LIST OF TABLES

Table 1.1. Wetland Services (Mitsch and Gosselink, 2000; Hanson et al., 2008; Kimmel, 2010).	2
Table 2.1. The area and number of train and test data in Avalon pilot site.	34
Table 2.2. Evaluated features in this study.....	40
Table 2.3. Confusion matrix in terms of the number of pixels for the classification using the Random Forest algorithm with the User Accuracy, Producer Accuracy, errors of Commission ,and error of Omission (in %)......	47
Table 2.4. The information on the study areas, satellite and aerial data, and field data used for validation of the methodology.....	52
Table 2.5. The Overall Accuracy, Kappa Coefficient, mean Producer and User Accuracies for wetland classes in the validation pilot sites.	53
Table 3.1. The overall accuracies (OAs), as well as the average producer and user accuracies of wetland classes (APAs and AUAs) in the Avalon pilot site.	68
Table 4.1. Acronyms and corresponding description.	75
Table 4.2. The characteristics of the five wetland classes specified by the CWCS.	76
Table 4.3. The number of field samples (polygons) collected over five study areas.	86
Table 4.4. The satellite data used in this study.	87
Table 4.5. The spectral bands of RapidEye, Sentinel 2A, ASTER, and Landsat 8 used in this study (The wavelength range for each band is provided in the parentheses, and is in micrometers).	88
Table 4.6. The spectral indices, textural and ratio features evaluated in this study for separability analyses of wetland types.	95

Table 4.7. The most useful spectral bands for discriminating between each pair of wetland classes in late spring (June) using two distance measures. The spectral bands are ordered based on their separability measures (the spectral bands indicated in the upper right half of the table and the lower left half of the table were obtained using the T-statistics and U-statistics, respectively).113

Table 4.8. The best features for separating different wetland class pairs based on two separability measures: T-statistics and U-statistics.122

Table 4.9. The best features for wetland classification in the study areas.127

Table 4.10. The OA, Kappa coefficient, Mean PA and UA of wetland classes in the five study areas.....132

Table 5.1. Total number of field samples collected over all study areas.....151

Table 5.2. The SAR data used in this study.152

Table 5.3. SAR features investigated for separability analysis of wetland classes.153

Table 5.4. The most useful SAR features (provided in the upper right half of the table) and the decomposition methods (provided in the lower left half of the table) for discriminating between each pair of wetland classes. The features and decomposition methods are ordered based on their separability measures (refer to Table 5.3 for the acronyms of the selected SAR features).168

Table 6.1. Satellite data used in this study (Optical and SAR satellite data are used for segmentation and classification of the study area, respectively).....190

Table 6.2. Values of the tuning parameters of each non-parametric classifiers, which were used for wetland classification in this study.199

Table 6.3. The overall classification accuracy and mean producer’s and user’s accuracies of the wetland classes as well as the average accuracy, obtained by averaging these three accuracies, using each single classifier.....200

Table 6.4. The T value obtained for each wetland and non-wetland classes using each single classifier.....201

Table 7.1. The information on the aerial and satellite data.....220

Table 7.2. Evaluated features in this study.....225

Table. 7.3. Confusion matrix in terms of the number of pixels for the classification of the Deer Lake pilot site using the Random Forest algorithm.236

LIST OF FIGURES

Figure 1.1. Structure of the dissertation.....	10
Figure 1.2. The developed Advance Remote Sensing Lab (ARSel) software.....	20
Figure 1.3. The developed website for wetland classification in NL.....	21
Figure 2.1. Study areas: a) Avalon, b) Grand Falls-Windsor, c) Deer Lake, d) Gros Morne, and e) Goose Bay.....	33
Figure 2.2. (a) RapidEye imagery over a selected area in the Avalon pilot site. Segmentation results obtained by applying five bands of RapidEye imagery in three different levels of (b) level 1 (scale parameter=100), (c) level 2 (scale parameter=300), (d) level 3 (scale parameter=500).....	39
Figure 2.3. The Overall Accuracy and Kappa Coefficient for wetland classification in Avalon pilot site using the five machine learning algorithms: KNN, SVM, ML, CART, and RF.....	42
Figure 2.4. (a) Producer Accuracy and (b) User Accuracy for each of the wetland and non-wetland classes obtained by different classifiers for the Avalon pilot site.	44
Figure 2.5. (a) RapidEye image from the Avalon pilot site, (b) Classified image using the object-based Random Forest algorithm (Segmentation was performed using the multi-resolution algorithm, in which the scale=300, shape=0.1, and compactness=0.5).....	46
Figure 2.6. The effect of the variation in the tuning parameters: (a) Depth and (b) Minimum sample number, in the Random Forest classifier.	49
Figure 2.7. Classified image using the pixel-based Random Forest classifier.....	50

Figure 2.8. Producer Accuracy and User Accuracy for each of the wetland and non-wetland classes in (a) Grand Falls-Windsor, (b) Deer Lake, (c) Gros Morne, and (d) Goose Bay.....55

Figure 2.9. Classified image using the object-based Random Forest classifier in (a) Grand Falls-Windsor, (b) Deer Lake, (c) Gros Morne, and (d) Goose Bay.....56

Figure 3.1. (a) Study area (the Avalon pilot site), (b) Classified image obtained by the integration of multi-temporal Landsat 8 data.69

Figure 4.1. The upper left image illustrates the province of Newfoundland and Labrador, as well as the five study areas: (a) Avalon, (b) Grand Falls-Windsor, (c) Deer Lake, (d) Gros Morne, and (e) Goose Bay. The zoomed image also demonstrates the boundaries of different wetland classes obtained from the field work conducted in the Avalon study area.82

Figure 4.2. Spectral values of the field samples of two wetland classes.97

Figure 4.3. Separability measures of wetland class pairs in late spring (June) using the T-statistics and U-statistics. In each figure, the spectral band that provides the highest separability is highlighted (The numbers after the name of the spectral bands also indicate the number of the band. For example: ASTER_TIR14 is the TIR band (band 14) of ASTER).112

Figure 4.4. The spectral signature of wetlands, obtained from (a) RapidEye, (b) Sentinel 2A, (c) ASTER, and (d) Landsat 8.115

Figure 4.5. The red/orange appearance of bogs in the study areas.115

Figure 4.6. The box plots of the spectral bands, which provided the highest separability for wetland classes in late spring (June). The cross (×) mark indicates the mean value. The numbers after the name of the spectral bands indicate the

number of the band. For example: Sentinel2_RE6 is the Red Edge band (band 6) of Sentinel 2A.	120
Figure 4.7. The study areas and their corresponding classified maps.	131
Figure 5.1. Study areas.	147
Figure 5.2. SAR feature values for the field samples of wetland classes.	160
Figure 5.3. Three subclasses of the Bog class (a: treed bog, b: shrubby bog, c: open bog) and (d) the backscattering values of the field samples of the Bog class.....	161
Figure 5.4. Seaprability measure obtained from the SAR features for each pair of wetland classes using the U-test. The red bars indicate the best SAR features for discriminating various wetland class pairs (refer to Table 5.3 for acronym definitions).	165
Figure 5.5. Seaprability measure obtained from different decomposition methods for each pair of wetland classes using the U-test. The red bars indicate the most useful decomposition methods for differentiating various wetland class pairs.	167
Figure 5.6. Seaprability measure obtained from the (a) SAR features and (b) different decomposition methods for all wetland classes using the U-test (refer to Table 5.3 for acronym definitions).	169
Figure 5.7. Comparison between the amount of separability that each odd-bounce, double-bounce, and volume scattering provided for all wetland classes (refer to Table 5.3 for acronym definitions).	173
Figure 5.8. Comparison between the amount of separability that intensity layers of each satellite provided for all wetland classes.	175
Figure 6.1. (a) Study area and the location of the field samples, (b) A RADARSAT-2 imagery from the study area (The color composite image was obtained by the Freeman-Durden decomposition).	188

Figure 6.2. Flowchart of the method. Depth refers to the number of DTs. Minimum Sample Count indicates the minimum number of samples per node in each DT. C is the capacity constant and minimizes the error function. Gamma controls the shape of the hyperplane. K is the number of closest samples in the feature space. (MCS: Multiple Classifier System, ML: Maximum Likelihood, RF: Random Forest, DT: Decision Tree, KNN: K-Nearest Neighbor, SVM: Support Vector Machine).193

Figure 6.3. The classified map of the study area obtained from the proposed MCS.202

Figure 6.4. (a) Producer’s and (b) user’s accuracies of the wetland and non-wetland classes, and (c) the overall wetland classification accuracies and Kappa coefficients, obtained from the proposed MCS and the single classifiers (MCS: Multiple Classifier System, ML: Maximum Likelihood, RF: Random Forest, DT: Decision Tree, KNN: K-Nearest Neighbour, SVM: Support Vector Machine).205

Figure 7.1. Canadian Wetland Inventory progress map for wetland areas (<http://maps.ducks.ca/cwi/>).216

Figure 7.2. Study areas across Newfoundland and Labrador. a) Avalon, b) Grand Falls-Windsor, c) Deer Lake, d) Gros Morne, and e) Goose Bay.....218

Figure 7.3. Flow chart of the methodology.221

Figure 7.4. The maps of wetlands in a) Avalon, b) Grand Falls-Windsor, c) Deer Lake, d) Gros Morne, and e) Goose Bay.230

Figure 7.5. The overall classification accuracies, as well as the average producer and user accuracies of wetland classes in the five study areas.231

Figure 7.6. Producer Accuracy and User Accuracy for each of the wetland and non-wetland classes in a) Avalon, b) Grand Falls-Windsor, c) Deer Lake, d) Gros Morne, and e) Goose Bay.....233

Figure 7.7. Spectral and textural signatures of the Bog and Fen classes, obtained from Landsat 8 data acquired over the Avalon pilot site (B: band, NIR: Near Infrared, SWIR: Short Wave Infrared).235

Figure 8.1. Wetland classification using the CWCS and EWCS (Smith et al., 2007).256

ACRONYMS

A	Anisotropy
A12	Anisotropy ¹²
A2	ALOS-2
ALOS	Advanced Land Observing Satellite
Alpha _s	Symmetric scattering type magnitude
APA	Average Producer Accuracy
ARSeL	Advanced Remote Sensing Lab
ASTER	Advanced Spaceborne Thermal Emission and Reflection Radiometer
AUA	Average User Accuracy
CART	Classification and Regression Trees
CDEM	Canadian Digital Elevation Model
CDSM	Canadian Digital Surface Model
CNN	Convolutional Neural Network
CPU	Central Processing Unit
CWCS	Canadian Wetland Classification System
CWI	Canadian Wetland Inventory
dbl	Double-bounce scattering
DEM	Digital Elevation Model
derd	Double-bounce eigenvalues relative difference
DN	Digital Number
DSM	Digital Surface Model
DT	Decision Tree
DVI	Difference Vegetation Index
EWCS	Enhanced Wetland Classification System

FBD	Fine Beam Double Polarization
FDI	Forest Discrimination Index
FQ	Fine Quad
F-test	Fisher-test
GLCM	Gray-Level Co-occurrence Matrix
GPS	Global Positioning System
GPU	Graphics Processing Unit
H	Entropy
HH	Horizontal transmit and Horizontal receive polarization
hlx	Helix scattering
HV	Horizontal transmit and Vertical receive polarization
ISE	Intensity Shannon Entropy
IW	Interferometric Wide
Kd	Diplane scattering
Kh	Helix scattering
KNN	K-Nearest Neighbor
Ks	Sphere scattering
LA	Luenburg Anisotropy
LiDAR	Light Detection and Ranging
MCS	Multiple Classifier System
ML	Maximum Likelihood
N_derd	Normalized double-bounce eigenvalues relative difference
N_serd	Normalized single-bounce eigenvalues relative difference
NDMI	Normalized Difference Moisture Index
NDSI	Normalized Difference Soil Index

NDVI	Normalized Difference Vegetation Index
NDWI	Normalized Difference Water Index
NIR	Near Infrared
NISE	Normalized Intensity Shannon Entropy
NL	Newfoundland and Labrador
NOS	Non-Order Size
NPSE	Normalized Polarimetry Shannon Entropy
NRCan	Natural Resources Canada
NSE	Normalized Shannon Entropy
OA	Overall Accuracy
OBIA	Object-based Image Analysis
odd	Surface scattering
P	Pseudo probability
P_Alpha_s	Symmetric scattering type phase
PA	Producer Accuracy
PF	Polarization Fraction
PH	Pedestal Height
PSE	Polarimetry Shannon Entropy
R2	RADARSAT-2
RBF	Radial Basis Function
RE	Red Edge
RE-NDVI	Red Edge Normalized Difference Vegetation Index
RF	Random Forest
RS	Remote Sensing
RVI	Radar Vegetation Index

S1	Sentinel-1
SAM	Spectral Angle Mapper
SAR	Synthetic Aperture Radar
SAVI	Soil Adjusted Vegetation index
SE	Shannon Entropy
serd	Single-bounce eigenvalues relative difference
SRTM	Shuttle Radar Topography Mission
SVM	Support Vector Machine
SWIR	Short Wave Infrared
TIR	Thermal Infrared
TP	Total Power
UA	User Accuracy
UTM	Universal Transverse Mercator
VH	Vertical transmit and Horizontal receive polarization
vol	Volume scattering
VV	Vertical transmit and Vertical receive polarization
τ	Helicity
ψ	Orientation angle

CHAPTER 1. INTRODUCTION

1.1. Background

Wetlands provide various services of benefit to society, resulting in their receiving such monikers as “biological supermarkets” and “nature’s kidneys” (Mitsch and Gosselink, 2000). Services can range from providing habitat for unique or rare species to ameliorating potential flood situations (Mitsch and Gosselink, 2000; Hanson et al., 2008; Mahdavi et al., 2017b). Such services are derived from the natural functioning of wetlands, a result of the interacting ecological relationships amongst floral, faunal, geomorphological, biochemical, hydrological, and climatological features (Mitsch and Gosselink, 2000). Standard variations of these features define the different wetland classes and, therefore, wetland classes function differently and provide various services (National Wetlands Working Group, 1998). Peatlands, for example, are defined partially on the presence of extensive peat deposits, which build due to a wet climate and poorly drained soils (National Wetlands Working Group, 1998; Mitsch and Gosselink, 2000). This peat is frequently farmed as a source of fuel (Kimmel, 2010). Furthermore, marshes play a role in maintaining and stabilizing shorelines because they do often develop along the edge of water bodies (Mitsch and Gosselink, 2000). Wetlands in general are known for providing habitat to numerous species of plants and animals, many of which are unique to wetlands of certain types. Additionally, wetlands around the world are used for recreational activities, such as fowl hunting and berry-picking (Mahdavi et al., 2017b). Table 1.1 provides a summary of the services wetlands provide.

Table 1.1. Wetland Services (Mitsch and Gosselink, 2000; Hanson et al., 2008; Kimmel, 2010).

Wetland class	Services
Bog	Source of nutrients and organic carbon, water storage, groundwater recharge, carbon storage, fuel and fibre source, plant and animal habitat.
Fen	Flood regulation, climate regulation, water filtration, source of nutrients and organic carbon, carbon storage, plant and animal habitat.
Swamp	Flood regulation, erosion protection, climate regulation, water filtration, carbon storage, plant and animal habitat, recreation.
Marsh	Flood regulation, erosion protection, ground water recharge, climate regulation, water filtration, carbon storage, plant and animal habitat, recreation (fowl hunting).
Shallow Water	Flood regulation, erosion protection, water filtration, plant and animal habitat, recreation (fishing).

Newfoundland and Labrador (NL) contain many wetland areas, classification and monitoring of which are necessary for wetland conservation, provision of ecological goods and services, as well as managing water resources in the province. Furthermore, there is no accurate and reliable information about the numbers of wetlands in terms of area, type of them, their location, and their changes over time. In addition, urban expansion, agricultural activities, and hydroelectric projects

contributed to destroy wetland areas in NL (National Wetlands Working Group, 1988; Amani et al., 2017a, c). Therefore, the coordinated actions are needed to protect these valuable landscapes using new technologies. In this regard, Remote Sensing (RS) technology provides costly and up-to-date data to map wetlands with high accuracies and in a timely manner. However, it should be noted that wetlands share many ecological characteristics, which causes the identification of these areas to be challenging using satellite data.

Different types of RS data have so far been applied to classify wetlands, each with its own advantages and limitations. In this regard, it has been frequently reported that a combination of optical and Synthetic Aperture Radar (SAR) RS data provides the highest classification accuracy (Mahdavi et al., 2017a; Amani et al., 2017c; Mahdianpari et al., 2018). Optical satellites provide valuable information about the spectral characteristics of wetlands by using different spectral bands, such as Near Infrared (NIR), Red Edge (RE), and Short Wave Infrared (SWIR). Each of these spectral bands can be effectively applied to distinguish wetland classes. Additionally, the preprocessing of optical satellite data is relatively straightforward and there is even no need to preprocess some of optical data for classification applications. Furthermore, there are currently several optical satellites, including Sentinel-2A and Landsat-8, which provide free data to users and, thus, make them suitable for operational wetland mapping and monitoring. The main limitation of optical satellites is that they cannot capture appropriate images at nights, during cloudy times, or under bad weather conditions. On the other hand, SAR is more applicable in Canada because of the unfavorable weather conditions in most parts of the country, including NL. SAR signals are capable of penetrating through the clouds and into vegetation canopies, providing valuable

information about the water resources under wetland areas (Brisco et al., 2013). Furthermore, full-polarimetric SAR data enables us to derive and apply different decomposition methods to accurately discriminate wetlands. The parameters obtained by the decomposition techniques are more useful than main scattering contributions, because wetlands are complex environments and there is a significant similarity between their backscattering responses (Millard and Richardson, 2013; Gosselin et al., 2014; Hong et al., 2015). The mentioned characteristics make SAR images very effective for wetland mapping. A problem associated with SAR data, however, is the presence of speckle in the imagery. Speckle degrades the radiometric quality of SAR images. Thus, many speckle filtering approaches have been proposed to tackle this problem before processing SAR data (e.g., Lee et al., 1999; Mahdavi et al., 2017c).

Temporal resolution of satellites is also important for studies of changeable and dynamic environments, such as wetlands (Munyati, 2000; Dechka et al., 2002; Mahdavi et al., 2017a; Amani et al., 2017b). The vegetation, soil, and water in wetlands vary over time considerably. Water may or may not be present on wetlands, or the height and greenness of vegetation can vary in different dates. For instance, water content of wetlands is high in June because of high amount of rain and vegetation height is low, while in September, water content in wetland areas is generally lower than June and vegetation is more mature and elevated (Mahdavi et al., 2017b). In general, marsh is the most changeable wetlands, where it is affected by surface runoff, groundwater, and adjacent water bodies, and its water level can change even daily (Mahdavi et al., 2017b). Marsh can also experience period of inundation or dry-out. Shallow Water is also generally more separable in Spring than in Summer. Because in Summer, the vegetation is well grown and

are green and, consequently, it is difficult to separate from other wetland classes (especially emergent marsh), which are mostly green. However, there is not much vegetation on shallow water surface in Spring (mostly in early spring) and, thus, it is easy to be distinguished from other wetlands (Mahdavi et al., 2017b). Based on these explanations, classification of wetlands using single-date satellite imagery produces low accuracies because of the dynamic nature of wetlands. Combining multi-date satellite data has resulted in higher wetland classification accuracies compared to using single-date imagery (Dechka et al., 2002; Leahy et al., 2005; Henderson and Lewis, 2008; Mahdavi et al., 2017a; Amani et al., 2017a). In fact, if two types of wetlands are not separable in a particular date, their spectral responses will change in other dates in a way that we can distinguish them.

Various classification algorithms have so far been developed and applied to classify wetlands, the most common of which is the Random Forest (RF) algorithm (Amani et al., 2017a, c; Mahdavi et al., 2017b). RF is a non-parametric ensemble classifier and consists of many decision trees, which vote for the most popular class (Breiman, 2001). A classification algorithm can be applied to both pixels and objects. In general, object-based methods provide higher classification accuracy in terms of both visual interpretation and statistical analyses compared to pixel-based methods when medium to high spatial resolution imagery is used (Mahdavi et al., 2017b). In an object-based method, an image is partitioned into discrete segments based on the spatial and spectral attributes so that meaningful objects are generated. Thus, various features can be extracted and applied to increase the accuracy of a classification using the produced objects (Blaschke, 2010).

1.2. Motivations

While a large portion of NL is covered by wetlands, their location and extent, as well as how they change over time have not been properly investigated. In fact, NL was the only Atlantic Canadian province without a comprehensive wetland inventory at the initiation of this thesis. At that time, there were only two small areas in NL that were classified using basic RS methods. Additionally, it was argued that human activities, such as urbanization, industrialization, and farming in the province increasingly posed serious threats to these valuable environments over the last several decades. Thus, there was a considerable demand to map and monitor wetland areas in the province using advanced satellite-based methods.

1.3. Objectives

The main objective of this study was to develop advanced and innovative RS methods for wetland classification. To this end, various satellite data were utilized and the methods were validated in five different study areas to demonstrate their high potential and robustness for wetland mapping and monitoring. To achieve this main scope, the following specific objectives were considered:

- 1) Assess the object-based method for wetland classification and demonstrate how classification accuracy increases when this method is compared to common pixel-based methods.
- 2) Investigate the effects of segmentation scales on wetland classification accuracy.
- 3) Evaluate different classification algorithms for wetland identification and suggest the most accurate method for further studies.

- 4) Assess the effects of tuning parameters, defined in non-parametric classifiers, on wetland mapping accuracy.
- 5) Propose a Multiple Classifier System (MCS) to increase the classification accuracy of land covers with high levels of similarities, such as wetlands, in terms of both overall and class accuracies.
- 6) Assess various optical and SAR features using field data to identify and remove poor/noisy features before applying the classification procedure.
- 7) Investigate parametric and non-parametric separability measures for performing separability analysis of wetlands.
- 8) Conduct spectral and backscattering analyses of wetlands to select the most effective optical spectral bands, SAR features, decomposition methods, and textural features for wetland studies. To do this, multi-source optical (e.g., RapidEye, Sentinel-2A, Advanced Spaceborne Thermal Emission and Reflection Radiometer (ASTER), and Landsat-8) and SAR (e.g., RADARSAT-2, Sentinel-1, and Advanced Land Observing Satellite (ALOS)-2) data were investigated.
- 9) Evaluate multi-temporal satellite data to select the time, at which wetlands are more distinguishable and, consequently, the classification is the most accurate.
- 10) Validate the proposed methods for wetland classification in different study areas in NL to prove their high performance.

1.4. Contribution and novelty

As mentioned in subsection 1.2, wetland classification in NL was understudied, compared to other Canadian provinces, when this thesis began. Thus, it was first

necessary to evaluate several common RS methods for wetland classification in the province. In fact, the author of this dissertation is among the first researchers who used advanced RS techniques to accurately map wetlands in NL. Consequently, some parts of this thesis are related to comparing and evaluating common methods that have been conducted worldwide and in other Canadian provinces. For instance, the comparison between the object-based and pixel-based methods, as well as between different classification algorithms were investigated in this thesis. It should be noted that these initial analyses were necessary for the subsequent experiments and future wetland studies in the province. However, several new methods and approaches were proposed and discussed in most parts of the thesis, which are outlined as follows:

- The effects of tuning parameters for non-parametric algorithms on classification accuracy are extensively discussed in Chapter 2. There are many studies that have blindly applied non-parametric classifiers, such as RF, for wetland classification (e.g. Zhang et al., 2010; Corcoran et al., 2012; Millard and Richardson, 2013; Hong et al., 2015). However, this thesis demonstrates how important the tuning parameters are, as well as the need to select the most optimum values for the tuning parameters for each study.
- Although several studies have argued the separability of wetland species using spectral bands, the corresponding research is based on field spectrometry. Distinctively, this study comprehensively discusses the separability of wetlands using multi-source optical satellite data to select the most useful spectral band, spectral indices, spectral texture features, and optical satellite for wetland mapping (see Chapter 4). Based on the author's

literature review, this study is the first, which extensively discusses the separability analysis of wetlands using multi-source optical satellite data.

- There are currently many studies which evaluate the efficiency of various SAR features for wetland classification (e.g. Bourgeau-Chavez et al., 2009; Brisco et al., 2011; Millard and Richardson, 2013; White et al., 2015). However, there is no consistent conclusion of which SAR features provide the highest separability for wetland types. Thus, part of this thesis investigates the amount of separability that different SAR features and decomposition methods, extracted by various SAR systems, provide for wetland classification (see Chapter 5).
- The importance of pre-processing both field and satellite data and, thus, removing noisy and poor features for wetland classification are extensively discussed in Chapter 4 and Chapter 5.
- Increasing the classification accuracy of wetlands is a challenging task because wetlands are complex environments and the corresponding classes are significantly similar in satellite images. This task is more difficult when SAR data are solely applied for wetland classification using a limited number of features. In this study, a new MCS is proposed to increase the accuracy of wetland classification using minimal SAR features compared to individual classifiers (see Chapter 6).
- The amount and reasons for confusion between various wetland classes using RS methods are extensively discussed throughout the thesis (especially in Chapter 2 and Chapter 7).

1.5. Organizations of the dissertation

This dissertation is a paper-based thesis including eight chapters, six of which contain the peer-reviewed articles (Figure 1.1). Chapters 2-4 are based on optical satellite data, while Chapter 5 and 6 are based on SAR data. Finally, Chapter 7 is based on a combination of optical and SAR imagery. Figure 1.1 illustrates the organization of the thesis. A brief explanation of each chapter is also provided below.

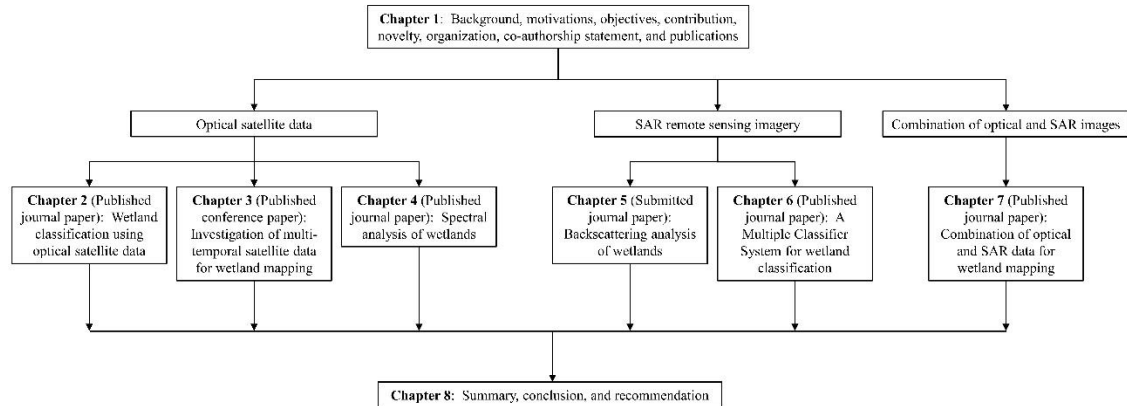


Figure 1.1. Structure of the dissertation.

Chapter 1, introduces the research background, motivation behind this research, the main objectives, novelty and contribution, as well as organization of the thesis. In addition, all the journal and conference papers, as well as conference presentations resulting from this research are provided at the end of this chapter. It is also worth noting that several journal and conference papers that are not directly related to the thesis, but, published during the course of this research are listed in subsection 1.7.

Chapter 2 evaluates multi-source and multi-temporal optical satellite data for wetland classification. Several analyses, such as comparison between various image classification algorithms, the effects of tuning parameters of the non-parametric classifiers on the classification accuracy, and comparison between object- and pixel-based image analyses are provided in this chapter.

In Chapter 3, multi-temporal optical satellite data are investigated to select the time that wetland classes are most separable and, therefore, the classification accuracy is highest.

Chapter 4 presents the separability analysis of wetland classes using multi-source optical RS data to select the most efficient optical bands and several other optical features for wetland studies.

Chapter 5 assesses the separability analysis of wetland species using multi-source SAR data. Various SAR features and decomposition techniques are investigated in this chapter to select the most optimum SAR features for wetland mapping.

In Chapter 6, a novel MCS is developed to increase the classification accuracy of complex landscapes. The MCS is applied to SAR data for classification of similar wetland classes using a limited number of features to show the potential of the proposed algorithm.

Chapter 7 combines various optical and SAR features to map wetlands using object-based classification methods.

The summary, conclusions, and recommendation for future studies are finally provided in Chapter 8.

1.6. Co-authorship statement

Mr. Meisam Amani (thesis author) is the main author for all articles pertaining to this thesis work, including those provided in Chapters 2-7. Other co-authors are: Dr. Bahram Salehi, Ms. Sahel Mahdavi, Ms. Jean Granger, Dr. Brian Brisco, Dr. Mohamed Shehata, and Dr. Alan Hanson. Mr. Meisam Amani was responsible for proposing and developing the main ideas contained in each research paper. Programming for the developed methods and data analysis were also performed by Mr. Meisam Amani. Moreover, all duties associated with the preparation, submission, and revision of each manuscript were also conducted by Mr. Meisam Amani. Dr. Bahram Salehi was the main supervisor of the thesis and provided funding and helped in developing the ideas through several meetings. He also provided minor revisions for some of the manuscripts. Ms. Sahel Mahdavi was a member of the team that worked on wetland classification in NL. The preprocessing of all SAR data used in this thesis was performed by her. Ms. Sahel Mahdavi also reviewed the research manuscripts and helped to improve the methods and papers considerably. Ms. Jean Granger was also another member of the team that worked on wetland classification in NL. A part of field collections was conducted by her. She also prepared all the field data used in this thesis. Ms. Jean Granger also helped in preparing the manuscripts and improved the research manuscripts in terms of grammar. Dr. Brian Brisco was the co-supervisor of the thesis work and considerably contributed to revising the research manuscripts with his prompt and valuable major/minor comments. Dr. Mohamed Shehata and Dr. Alan Hanson also reviewed one of the research manuscripts and suggested minor revisions.

1.7. Publications, presentations, software, website, teaching, and courses

1.7.1. Book chapter

I contributed to a book chapter related to my thesis subject:

- Salehi, B., Mahdianpari, M., **Amani, M.**, Mohammadimanesh, F., Granger, J., Mahdavi, S., & Brisco, B. (2018). A collection of novel algorithms for wetland classification with SAR and optical data. "Minor revision", *InTech Open*.

1.7.2. Journal articles

I was the first author of 5 published and submitted journal articles, which were all related to my thesis subject:

- * **Amani, M.**, Salehi, B., Mahdavi, S., Brisco, B., & Shehata, M. (2018). A Multiple Classifier System to improve mapping complex land covers: a case study of wetland classification using SAR data in Newfoundland, Canada. *International Journal of Remote Sensing*, 1-14.
- * **Amani, M.**, Salehi, B., Mahdavi, S., & Brisco, B. (2018). Spectral analysis of wetlands using multi-source optical satellite imagery. *ISPRS Journal of Photogrammetry and Remote Sensing*, 144, 119-136.
- * **Amani, M.**, Salehi, B., Mahdavi, S., & Brisco, B. (2018). Separability analysis of wetland using multi-source SAR data. "Major revision", *ISPRS Journal of Photogrammetry and Remote Sensing*.

* indicates the papers for which I was the corresponding author.

- * **Amani, M.**, Salehi, B., Mahdavi, S., Granger, J., & Brisco, B. (2017). Wetland classification in Newfoundland and Labrador using multi-source SAR and optical data integration. *GIScience & Remote Sensing*, 54(6), 779-796.
- * **Amani, M.**, Salehi, B., Mahdavi, S., Granger, J. E., Brisco, B., & Hanson, A. (2017). Wetland Classification Using Multi-Source and Multi-Temporal Optical Remote Sensing Data in Newfoundland and Labrador, Canada. *Canadian Journal of Remote Sensing*, 43(4), 360-373.

Additionally, I contributed to 5 journal articles, which were all related to my thesis:

- Mahdianpari, M., Salehi, B., Mohammadimanesh, F., Brisco, B., Mahdavi, S., **Amani, M.**, & Granger, J. (2018). Fisher Linear Discriminant Analysis of coherency matrix for wetland classification using PolSAR imagery. *Remote Sensing of Environment*, 206, 300-317.
- Mahdavi, S., Salehi, B., **Amani, M.**, Granger, J., Brisco, B., & Huang, W. (2018). A Dynamic Classification Scheme for Mapping Spectrally Similar Classes: Application to Wetland Classification. "Under review", *Remote Sensing of Environment*.
- Mahdavi, S., Salehi, B., **Amani, M.**, Brisco, B., & Huang, W. (2018). Change detection. "Under review", *IEEE Journal of Selected Topics in Applied Earth Observations and Remote Sensing*.
- Mahdavi, S., Salehi, B., **Amani, M.**, Granger, J. E., Brisco, B., Huang, W., & Hanson, A. (2017). Object-based classification of wetlands in Newfoundland and Labrador using multi-temporal PolSAR data. *Canadian Journal of Remote Sensing*, 43(5), 432-450.

* indicates the papers for which I was the corresponding author.

- Mahdavi, S., Salehi, B., Granger, J., **Amani, M.**, & Brisco, B. (2017). Remote sensing for wetland classification: a comprehensive review. *GIScience & Remote Sensing*, 1-36.

Moreover, I published, submitted, and contributed to 11 journal articles during three years of my PhD, which were not related to my thesis topic:

- * **Amani, M.**, Mobasheri, M. R., & Mahdavi, S. (2018). Contemporaneous estimation of Leaf Area Index and soil moisture using the red-NIR spectral space. *Remote Sensing Letters*, 9(3), 265-274.
- Ghahremanloo, M., Mobasheri, M. R., & **Amani, M.** (2018). Soil moisture estimation using land surface temperature and soil temperature at 5 cm depth. *International Journal of Remote Sensing*, 1-14.
- Mahdavi, S., **Amani, M.**, & Maghsoudi, Y. (2018). The effects of orbit type on Synthetic Aperture RADAR (SAR) backscatter. "Accepted", *Remote Sensing Letters*.
- Ghahremanloo, M., **Amani, M.**, & Mobasheri, M. R. (2018). Soil moisture estimation at different depths using field soil temperature at various depths and remotely sensed surface temperature. "Under review", *International Journal of Remote Sensing*.
- * Mobasheri, M. R., Ranjbaran, M., **Amani, M.**, Mahdavi, S. & Zabihi, H. R. (2018). Determination of soil total nitrogen content in an agricultural area using spectrometry data. "Under review", *Journal of Applied Remote Sensing*.

* indicates the papers for which I was the corresponding author.

- * Mobasheri, M. R., Beikpour, M., **Amani, M.**, & Mahdavi, S. (2018). Soil moisture estimation using water absorption bands. "Under review", *Journal of Applied Remote Sensing*.
- * **Amani, M.**, Salehi, B., Mahdavi, S., Masjedi, A., & Dehnavi, S. (2017). Temperature-Vegetation-soil Moisture Dryness Index (TVMDI). *Remote Sensing of Environment*, 197, 1-14.
- * Parsian, S., & **Amani, M.** (2017). Building extraction from fused LiDAR and hyperspectral data using the Random Forest algorithm. *GEOMATICA*, 71(4), 3-19.
- Mahdavi, S., Maghsoudi, Y., & **Amani, M.** (2017). Effects of changing environmental conditions on synthetic aperture radar backscattering coefficient, scattering mechanisms, and class separability in a forest area. *Journal of Applied Remote Sensing*, 11(3), 036015.
- Mobasheri, M. R., & **Amani, M.** (2016). Soil moisture content assessment based on Landsat 8 red, near-infrared, and thermal channels. *Journal of Applied Remote Sensing*, 10(2), 026011.
- * **Amani, M.**, Parsian, S., MirMazloumi, S. M., & Aieneh, O. (2016). Two new soil moisture indices based on the NIR-red triangle space of Landsat-8 data. *International Journal of Applied Earth Observation and Geoinformation*, 50, 176-186.

1.7.3. Conference articles

Furthermore, I was the first author of 3 published conference articles, which were all related to my thesis subject:

* indicates the papers for which I was the corresponding author.

- * **Amani, M.**, Salehi, B., Mahdavi, S., & Granger, J. (2017). An Operational Wetland Classification Model in Newfoundland and Labrador using Advanced Remote Sensing Methods. *IEEE Newfoundland Electrical and Computer Engineering Conference (NECEC)*.
- * **Amani, M.**, Salehi, B., Mahdavi, S., & Granger, J. (2017). Spectral analysis of wetlands in Newfoundland using Sentinel 2A and Landsat 8 imagery. *American Society for Photogrammetry and Remote Sensing (ASPRS) Annual Conference*.
- * **Amani, M.**, Salehi, B., Mahdavi, S., Granger, J., & Brisco, B. (2017). Evaluation of multi-temporal Landsat 8 data for wetland classification in Newfoundland, Canada. *IEEE International Geoscience and Remote Sensing Symposium (IGARSS)*.

Additionally, I contributed to 3 conference articles, which were all related to my thesis subject:

- Mahdavi, S., Salehi, B., **Amani, M.**, Granger, J., Brisco, B., & Huang, W. (2017). A Novel Method for Classification of Complicated Land Covers using Remote Sensing Techniques. *IEEE Newfoundland Electrical and Computer Engineering Conference (NECEC)*.
- Mahdavi, S., Salehi, B., **Amani, M.**, Granger, J., Brisco, B., & Huang, W. (2017). A comparison between different Synthetic Aperture Radar (SAR) sensors for wetland classification. *American Society for Photogrammetry and Remote Sensing (ASPRS) Annual Conference*.
- Mahdavi, S., Salehi, B., **Amani, M.**, Granger, J., Brisco, B., & Huang, W. (2017). Applying dynamic feature selection for object-based classification of wetlands

* indicates the papers for which I was the corresponding author.

in Newfoundland and Labrador. *IEEE International Geoscience and Remote Sensing Symposium (IGARSS)*.

Moreover, I published a conference article during my PhD, which were not related to my thesis topic:

- * **Amani, M.** (2017). Dryness estimation Using Three Variables of the Land Surface Temperature, Perpendicular Vegetation Index, and Soil Moisture Content. *IEEE Newfoundland Electrical and Computer Engineering Conference (NECEC)*.

1.7.4. Conference presentations

During 3 years of my PhD, I presented the outputs of my thesis at 10 conferences:

- Topic: Backscattering analysis of wetlands (Jun 2018). *39th Canadian Symposium on Remote Sensing, Saskatoon, SK, Canada*.
- Topic: Separability analysis of wetland classes using optical satellite data (Nov 2017). *Geomatics Atlantic Conference, St. John's, NL, Canada*.
- Topic: A new approach of fusing different classifiers to improve wetland classification using SAR data (Nov 2017). *Geomatics Atlantic Conference, St. John's, NL, Canada*.
- Topic: An Operational Wetland Classification Model in Newfoundland and Labrador using Advanced Remote Sensing Methods (Nov 2017). *26th Annual IEEE Newfoundland Electrical and Computer Engineering Conference, St. John's, NL, Canada*.

* indicates the papers for which I was the corresponding author.

- Topic: Evaluation of multi-temporal Landsat 8 data for wetland classification in Newfoundland, Canada (Jul 2017). *IEEE International Geoscience and Remote Sensing Symposium, Fort Worth, TX, USA.*
- Topic: Spectral analysis of wetlands in Newfoundland using Sentinel 2A and Landsat 8 imagery (Mar 2017). *ASPRS Annual Conference, Baltimore, MD, USA.*
- Topic: Object-based wetland classification in Newfoundland and Labrador using Random Forest algorithm (Feb 2017). *6th Spatial Knowledge and Information Canada Conference, Banff, AB, Canada.*
- Topic: New technologies for wetland classification (Oct 2016). *Newfoundland and Labrador's Green Economy Conference, St. John's, NL, Canada.*
- Topic: A wetland classification framework for Newfoundland and Labrador using multi-source SAR and optical data fusion (Jun 2016). *37th Canadian Symposium on Remote Sensing, Winnipeg, MB, Canada.*
- Topic: Newfoundland and Labrador's wetland classification using remote sensing satellite imagery (Mar 2016). *18th Annual Aldrich Multidisciplinary Graduate Research Conference, St. John's, NL, Canada.*

1.7.5. Software

I contributed to the development and maintenance of an RS software for land cover classification. The software, named Advance Remote Sensing Lab (ARSEL), comprises several advanced algorithms to preprocess optical and SAR imagery, as well as to classify land covers, such as wetlands. Figure 1.2 provides screenshots of the software.

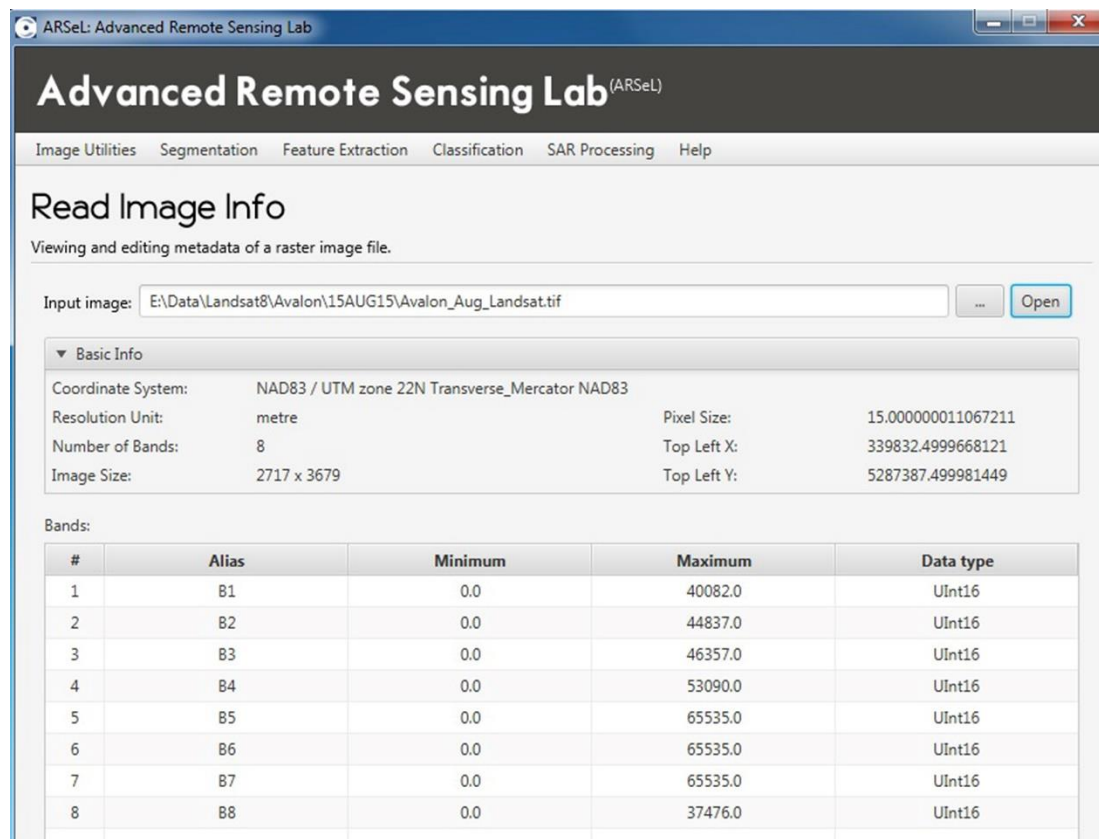


Figure 1.2. The developed Advance Remote Sensing Lab (ARSeL) software.

1.7.6. Wetland website

I contributed to the development and maintenance of a website (<http://nlwetlands.ca/>), the aim of which is to illustrate the location and extent of wetland areas in NL. Figure 1.3 illustrates several parts of the developed website.

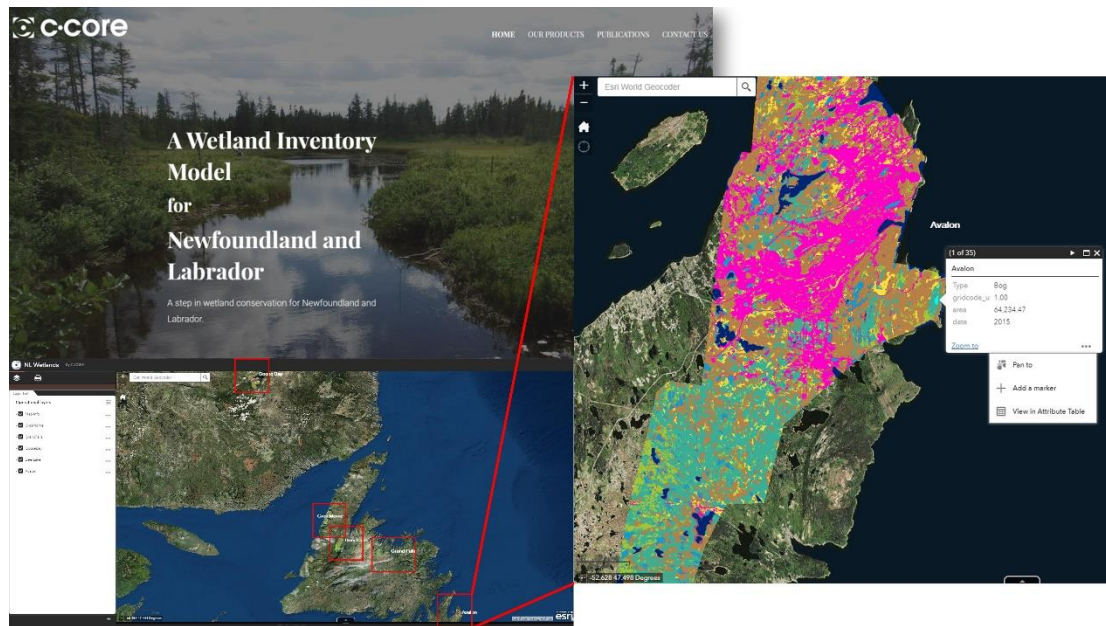


Figure 1.3. The developed website for wetland classification in NL.

1.7.7. Guest lecturer

I also taught two classes for two different courses in the Department of Geography, Memorial University of Newfoundland, which were related to my thesis topic:

- Guest lecturer for the course “Introduction to Remote Sensing” (Mar 2018).
Topic of presentation: Object-Based Image Analysis (OBIA).
- Guest lecturer for the course “Environmental Image Analysis” (Oct 2017).
Topic of presentation: Wetlands.

1.7.8. Courses

During my PhD, I passed four courses with average of 92/100.

- Applied Remote Sensing. GPA: 94/100.
- Advanced Technology of Remote Sensing. GPA: 94/100.
- Introduction to Systems and Signals. GPA: 91/100.

- Advanced Topics in Computer Vision. GPA: 89/100.

References

Amani, M., Salehi, B., Mahdavi, S., Brisco, B., & Shehata, M. (2018). A Multiple Classifier System to improve mapping complex land covers: a case study of wetland classification using SAR data in Newfoundland, Canada. *International Journal of Remote Sensing*, 1-14.

Amani, M., Salehi, B., Mahdavi, S., Granger, J. E., Brisco, B., & Hanson, A. (2017a). Wetland Classification Using Multi-Source and Multi-Temporal Optical Remote Sensing Data in Newfoundland and Labrador, Canada. *Canadian Journal of Remote Sensing*, 43(4), 360-373.

Amani, M., Salehi, B., Mahdavi, S., Granger, J., & Brisco, B. (2017b). Evaluation of multi-temporal Landsat 8 data for wetland classification in Newfoundland, Canada. *IEEE International Geoscience and Remote Sensing Symposium (IGARSS)*.

Amani, M., Salehi, B., Mahdavi, S., Granger, J., & Brisco, B. (2017c). Wetland classification in Newfoundland and Labrador using multi-source SAR and optical data integration. *GIScience & Remote Sensing*, 54(6), 779-796.

Blaschke, T. (2010). Object based image analysis for remote sensing. *ISPRS Journal of Photogrammetry and Remote Sensing*, 65(1), 2-16.

Bourgeau-Chavez, L. L., Riordan, K., Powell, R. B., Miller, N., & Nowels, M. (2009). Improving wetland characterization with multi-sensor, multi-temporal SAR and optical/infrared data fusion. *In Advances in geoscience and remote sensing. InTech*.

Breiman, L. (2001). Random forests. *Machine Learning*, 45(1), 5-32.

Brisco, B., Kapfer, M., Hirose, T., Tedford, B., & Liu, J. (2011). Evaluation of C-band polarization diversity and polarimetry for wetland mapping. *Canadian Journal of Remote Sensing*, 37(1), 82-92.

Brisco, B., Li, K., Tedford, B., Charbonneau, F., Yun, S., & Murnaghan, K. (2013). Compact polarimetry assessment for rice and wetland mapping. *International Journal of Remote Sensing*, 34(6), 1949-1964.

Corcoran, J., Knight, J., Brisco, B., Kaya, S., Cull, A., & Murnaghan, K. (2012). The integration of optical, topographic, and radar data for wetland mapping in northern Minnesota. *Canadian Journal of Remote Sensing*, 37(5), 564-582.

Dechka, J. A., Franklin, S. E., Watmough, M. D., Bennett, R. P., & Ingstrup, D. W. (2002). Classification of wetland habitat and vegetation communities using multi-temporal Ikonos imagery in southern Saskatchewan. *Canadian Journal of Remote Sensing*, 28(5), 679-685.

Gosselin, G., Touzi, R., & Cavayas, F. (2014). Polarimetric Radarsat-2 wetland classification using the Touzi decomposition: case of the Lac Saint-Pierre Ramsar wetland. *Canadian Journal of Remote Sensing*, 39(6), 491-506.

Hanson, A., Swanson, L., Ewing, D., Grabas, G., Meyer, S., Ross, L., ... & Kirkby, J. (2008). Wetland ecological functions assessment: an overview of approaches. *Canadian Wildlife Service Technical Report Series*, 497.

Henderson, F. M., & Lewis, A. J. (2008). Radar detection of wetland ecosystems: a review. *International Journal of Remote Sensing*, 29(20), 5809-5835.

- Hong, S. H., Kim, H. O., Wdowinski, S., & Feliciano, E. (2015). Evaluation of polarimetric SAR decomposition for classifying wetland vegetation types. *Remote Sensing*, 7(7), 8563-8585.
- Kimmel, K., & Mander, Ü. (2010). Ecosystem services of peatlands: Implications for restoration. *Progress in Physical Geography*, 34(4), 491-514.
- Leahy, M. G., Jollineau, M. Y., Howarth, P. J., & Gillespie, A. R. (2005). The use of Landsat data for investigating the long-term trends in wetland change at Long Point, Ontario. *Canadian Journal of Remote Sensing*, 31(3), 240-254.
- Lee, J. S., Grunes, M. R., & De Grandi, G. (1999). Polarimetric SAR speckle filtering and its implication for classification. *IEEE Transactions on Geoscience and remote sensing*, 37(5), 2363-2373.
- Mahdavi, S., Salehi, B., Amani, M., Granger, J. E., Brisco, B., Huang, W., & Hanson, A. (2017a). Object-based classification of wetlands in Newfoundland and Labrador using multi-temporal PolSAR data. *Canadian Journal of Remote Sensing*, 43(5), 432-450.
- Mahdavi, S., Salehi, B., Granger, J., Amani, M., & Brisco, B. (2017b). Remote sensing for wetland classification: a comprehensive review. *GIScience & Remote Sensing*, 1-36.
- Mahdavi, S., Salehi, B., Moloney, C., Huang, W., & Brisco, B. (2017c). Speckle filtering of Synthetic Aperture Radar images using filters with object-size-adapted windows. *International Journal of Digital Earth*, 1-27.
- Mahdianpari, M., Salehi, B., Mohammadimanesh, F., Brisco, B., Mahdavi, S., Amani, M., & Granger, J. (2018). Fisher Linear Discriminant Analysis of coherency

matrix for wetland classification using PolSAR imagery. *Remote Sensing of Environment*, 206, 300-317.

Millard, K., & Richardson, M. (2013). Wetland mapping with LiDAR derivatives, SAR polarimetric decompositions, and LiDAR–SAR fusion using a random forest classifier. *Canadian Journal of Remote Sensing*, 39(4), 290-307.

Mitsch, W. J., & Gosselink, J. G. (2000). The value of wetlands: importance of scale and landscape setting. *Ecological Economics*, 35(1), 25-33.

Munyati, C. (2000). Wetland change detection on the Kafue Flats, Zambia, by classification of a multitemporal remote sensing image dataset. *International Journal of Remote Sensing*, 21(9), 1787-1806.

National Wetlands Working Group. (1988). Wetlands of Canada. Ecological land classification series, no. 24. *Sustainable Development Branch, Environment Canada, Ottawa, Ontario, and Polyscience Publications Inc., Montreal, Quebec*, 452.

White, L., Brisco, B., Dabboor, M., Schmitt, A., & Pratt, A. (2015). A collection of SAR methodologies for monitoring wetlands. *Remote Sensing*, 7(6), 7615-7645.

Zhang, X., Feng, X., & Jiang, H. (2010). Object-oriented method for urban vegetation mapping using IKONOS imagery. *International Journal of Remote Sensing*, 31(1), 177-196.

CHAPTER 2. WETLAND CLASSIFICATION USING MULTI-SOURCE AND MULTI-TEMPORAL OPTICAL REMOTE SENSING DATA IN NEWFOUNDLAND AND LABRADOR, CANADA

Abstract

Newfoundland and Labrador (NL) is the only province in Atlantic Canada that does not have a wetland inventory system. As a consequence, both classifying and monitoring wetland areas are necessary for wetland conservation and human services in the province. In this study, wetlands in five pilot sites, distributed across NL, were classified using multi-source and multi-temporal optical remote sensing images. The procedures involved the application of an object-based method to segment and classify the images. To classify the areas, five different machine learning algorithms were examined. The results showed that the Random Forest (RF) algorithm in combination with an object-based approach was the most accurate method to classify wetlands. The average producer and user accuracies of wetland classes considering all pilot sites were 68% and 73%, respectively. The overall classification accuracies, which considered the accuracy of all wetland and non-wetland classes varied from 86% to 96% across all pilot sites confirming the robustness of the methodology despite the biological, ecological, and geographical differences among the study areas. Additionally, we assessed the effects of the tuning parameters on the accuracy of results, as well as the difference between pixel-based and object-based methods for wetland classification in this study.

Keywords: Remote Sensing, Wetlands, Object-based classification, Machine learning classifiers, Canada, Newfoundland and Labrador

2.1. Introduction

Wetlands play a pivotal role in physical and chemical limnology of surface water, reducing downstream flooding and erosion, collecting and storing runoff, as well as providing food, water, and shelter to a multitude of plants and animals. Furthermore, wetlands are globally important for the storage of carbon to help ameliorate the effects of human-induced greenhouse gases on atmospheric temperature (Tiner et al., 2015). While it is estimated that 36% of wetlands in Canada are located in Newfoundland and Labrador (NL, Warner and Rubec, 1997), no significant efforts have been made to properly assess wetland regions in the province using new technologies like remote sensing methods. The consequence is that there is no spatially explicit and consistent wetland distribution map in the province. On the other hand, human activities, including urbanization and agricultural activities have caused serious threats to these valuable landscapes in NL during the last decades. Therefore, monitoring of wetlands and producing up-to-date and reliable maps of these areas are important in terms of both biological habitats and human activities.

Traditionally, wetland classification requires field work, which is labor intensive, expensive, time consuming, and usually impractical due to poor accessibility. Consequently, it is only practical and valid for relatively small areas (Ozesmi and Bauer, 2002). Remote sensing, on the other hand, provides the required coverage to monitor different wetlands at various scales, and the corresponding data has

been efficiently applied to classify wetlands in time and space without prohibitive costs. Moreover, remote sensing offers repeated coverage that can be effectively used for change detection of wetlands over time (Schmitt and Brisco, 2013). Besides many advantages of remote sensing technology, there are several problems in detecting and classifying different types of wetlands using satellite imagery. There are considerable similarities between the ecological characteristics of wetlands, and therefore, different wetlands pose similar spectral signatures in optical satellite data. This situation is more serious for bog and fen, where they are sometimes categorized as one class (peatland). Furthermore, the life form and species composite of vegetation in wetlands can be various within and among years. Water may or may not be present on wetlands during different months (South, 1983). These specific characteristics of wetlands cause wetland classification to be a challenging task in remote sensing science.

Generally, wetland classification methodology using remotely sensed data is categorized into pixel-based or object-based classifications, the latter of which is also referred to as Object-Based Image Analysis (OBIA). While pixel-based analysis has long been the main approach in the classification of remote sensing imagery, OBIA has become increasingly commonplace over the past decades, with availability of very high resolution satellite imagery (Blaschke, 2010; Blaschke et al., 2014). A large number of researchers have reported that OBIA was superior to traditional pixel-based methods, when high or medium spatial resolution data were used (Blaschke, 2010; Zhang et al., 2010; Pu et al., 2011; Myint et al., 2011; Salehi et al., 2012a). Pixel-based classification methods cannot fully utilize the spatial information of high resolution imagery. However, the OBIA method enables the use of spatial information, extraction of various features, and reduction

of the data set. As a result, the classification of image objects not only uses the spectral information of objects, but also applies topological and hierarchical relationships between the image objects (Duro et al., 2012; Salehi et al., 2012a). Moreover, changing pixels to objects through OBIA reduces within-class spectral variation and therefore, reduces salt and pepper effects, which are common in pixel-based classification methods (Liu and Xia, 2010). Image segmentation is the first step in OBIA. The multi-resolution segmentation algorithm, proposed by Baatz and Schäpe (2000), is the most popular algorithm and has been extensively used by many researchers (Zhou and Troy, 2008; Myint et al., 2011; Duro et al., 2012; Salehi et al., 2013; Qian et al., 2014). The algorithm offers several segmentation parameters including scale, shape, and color. While segmenting the imagery enables us to analyze the spatial information of objects and produce different features, it should be noted that the accuracy of the final classification has a direct relationship to the segmentation. Therefore, the segmentation algorithm and its corresponding parameters should be wisely selected.

Whether pixels or objects are used for image classification, the extracted information (spectral and/or textural) can be subjected to different classifiers, such as K-Nearest Neighbor (KNN), Support Vector Machine (SVM), Maximum Likelihood (ML), Classification and Regression Trees (CART), and Random Forest (RF). It is worth noting that all of the above-mentioned algorithms are supervised algorithms. These types of classifiers use labeled training data as input to define models for predicting the class label of the test data (Cord and Cunningham, 2008).

Wetland classification is one of the most challenging issues in remote sensing science. This is because wetlands are complex areas, in which various classes are spectrally similar. This matter is more important for some classes, such as bog and

fen (both peat-producing wetlands), which have many vegetative similarities. In this paper, we assessed the performance of different machine learning classifiers for object-based wetland classification over different study areas in NL. In addition, several assessments on the effects of different levels of segmentation, various features, and the tuning parameters associated with the best performing classification algorithm were investigated. A comparison was also made between pixel-based and object-based classification methods. It is worth mentioning that although only optical satellite data were used for wetland classification in this study, many researchers have reported that using an integration of various remote sensing data, including optical, Synthetic Aperture RADAR (SAR), and Light Detection and Ranging (LiDAR) have resulted in higher classification accuracies. For example, Grenier et al. (2007) combined Landsat 7 and RADARSAT 1 data to classify wetlands in two pilot sites in Quebec. They evaluated multi-scale object-based classification and obtained 67% and 76% accuracies in the respective pilot sites. Moreover, Corcoran et al. (2012) investigated the fusion of optical, SAR, and DEM data for wetland mapping in northern Minnesota. Their results proved that integration of multi-source and multi-temporal remote sensing data during the growing season improved wetlands discrimination by reaching a classification accuracy of 75%. Gosselin et al. (2014) also assessed the Touzi incoherent target-scattering decomposition method for wetland mapping in Lac Saint-Pierre, Quebec. Then, they compared the results with those obtained from supervised ML classification using multi-temporal Landsat 5 data. They obtained an accuracy of approximately 78% by applying both methods. More recently, Chasmer et al. (2016) tested the cost effectiveness of LiDAR data for wetland classification in the boreal plains in Alberta. They obtained 57% accuracy, and concluded that terrain

morphology and vegetation structure information, obtained by LiDAR data, provided an accurate and cost-effective means for wetland identification.

2.2. Materials and methods

2.2.1. Study areas

In this study, wetlands in five pilot sites distributed across NL were classified into five classes: Bog, Fen, Marsh, Swamp, and Shallow Water, as specified by the Canadian Wetland Classification System (Warner and Rubec, 1997). Reasons for the selection of these pilot sites were both practical and ecological. Practically, these pilot sites were selected because they were near developed settlements with at least several road accessibilities over large areas. Much of NL is undeveloped, and as a result cannot be accessed easily and inexpensively. Accessibility via car was needed for field workers and areas located in and around settlements addressed this need. Additionally, these five pilot sites were familiar to the experts that were involved in collecting the field data. Because little work on mapping wetlands has been done in the province, the finding of potential wetland sites relied both on the analysis of satellite imagery and on any local knowledge held by the field workers. In this way, there was less time spent finding wetlands in unfamiliar areas. Ecologically, these wetlands represent different regional climates found across NL. For example, the Grand Falls and Deer Lake pilot sites experience more continental climates as a result of their inland locations, compared to that of the oceanic climates of the coastal sites. Differences in climate affect a regions wetland development (South, 1983).

First, the methodology was developed and evaluated in one of the pilot sites, the Avalon (Figure 2.1 (a)) and, then, it was validated in four other pilot sites (Grand Falls-Windsor, Deer Lake, Gros Morne, and Goose Bay). The Avalon pilot site is located in the northeastern portion of the Avalon Peninsula, Newfoundland, Canada, between the latitudes and longitudes of 47°39'57.91"N, 52°47'07.45"W and 47°15'01.11"N, 53°00'19.96"W. Encompassing an area of approximately 700 km², the Avalon pilot site is located within the Maritime Barren ecoregion, which is characterized by an oceanic climate as a result of the region's proximity to the Atlantic Ocean. The land cover is dominated by heathland barrens, balsam fir forests, urban regions, and agricultural areas (South, 1983). Urban and agricultural areas are the most prominent land covers in the northern portion of the pilot site, where the capital city of Newfoundland (St. John's) is located, while the southern regions are mostly covered by peatlands (bogs and fens).

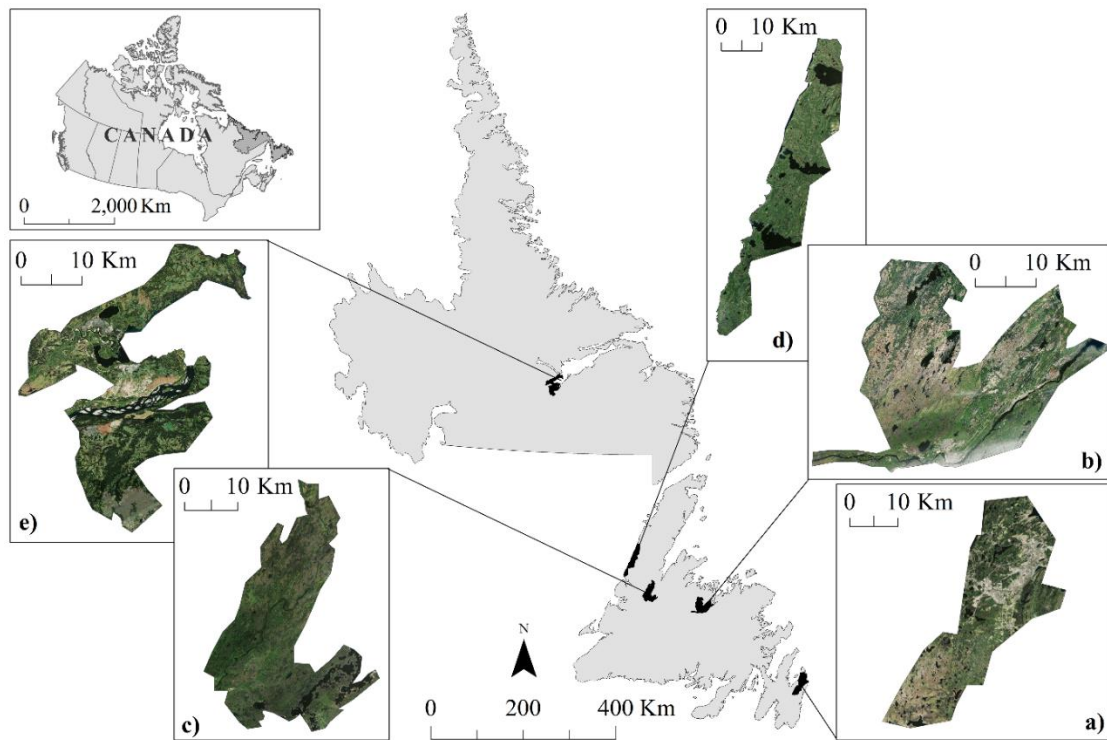


Figure 2.1. Study areas: a) Avalon, b) Grand Falls-Windsor, c) Deer Lake, d) Gros Morne, and e) Goose Bay.

2.2.2. In situ data

Field work was carried out between July and October 2015 to develop our methods for wetland classification. Potential wetland sites were selected based on the visual analysis of high resolution Google Earth imagery, their accessibility via public roads and trails, and the public or private ownership of lands. Visited wetlands in the field were labeled as one wetland class (i.e. Bog, Fen, Marsh, Swamp, and Shallow Water) using the classification key described in the Canadian Wetland Classification System (Warner and Rubec, 1997). In this system, wetland types are classified majorly based on broad soil, vegetation, and hydrology characteristics. According to the system proposed by these researchers and based on the presence of hydrophytic vegetation and/or water, each visited field site was first classified

as upland or wetland. The wetland sites were then classified as peatland (i.e. bog, fen, or swamp) or a mineral wetland (swamp, marsh, or shallow water) based on visual and textural analyses of the soil by ecological experts. Finally, each site was classified as one of the five wetland classes on the basis of examination of the dominant vegetation structure and hydrological characteristics. More explanation on the procedure for identifying wetland type in the field can be found in Warner and Rubec (1997). Ancillary information including GPS points, field notes on dominant vegetation, hydrology, surrounding landscape, and on-site photographs, was collected at each wetland site. Finally, the wetland boundary for each site was defined and carried out in the ArcMap 10.3.1 software using the GPS points, high resolution satellite and aerial imagery, as well as the ancillary information. Table 2.1 demonstrates the area and the number of polygons, obtained from the field data, which were used for training the algorithms, as well as for evaluating the accuracy of the classified maps.

Table 2.1. The area and number of train and test data in Avalon pilot site.

Pilot site	Total train area (ha)	Total test area (ha)	Number of train sites	Number of test sites
Avalon	414	385	113	109

2.2.3. Aerial and satellite images

Three different aerial and satellite data sets, Canadian Digital Surface Model (CDSM), RapidEye, and Landsat 8, were used to classify wetlands in the study areas. The CDSM forms part of the elevation system designed by Natural Resources Canada (NRCan, www.ccrs.nrcan.gc.ca). The CDSMs indicate the top

of features, such as the top of trees or building roofs, and were derived from radar interferometry data acquired during the Shuttle Radar Topography Mission (SRTM) performed by the space shuttle endeavor in 2000. The CDSM is a significantly improved product over flat, open ground compared to the Canadian Digital Elevation Model (CDEM), which is generated from sparse contour lines. Generally, the spatial resolution of the CDSM products is 75 arc sec (20 meters), with a horizontal accuracy between 3 to 100 meters. In this research, five tiles of the CDSMs were downloaded and used from www.geobase.ca. The vertical resolution of these tiles were approximately 10 meters, and the resolution in X, Y directions were 15×25 m² (Canadian Digital Surface Model 2013). After projecting these tiles into the correct projection system (Transvers Mercator, UTM 22N for Avalon area) and mosaicing them, they were resampled to 15×15 m² pixels using the nearest neighbor interpolation method. The nearest neighbor method was selected because it preserves original DN values and is simple to apply (Lillesand et al., 2014).

Two sets of RapidEye imagery, acquired on June 18, 2015 and October 22, 2015 over the Avalon area, were also used in this study. The RapidEye images were level 3A products, which were radiometrically and geometrically corrected, and aligned to a cartographic map projection (RapidEye, 2015). The ortho-rectified pixel size of RapidEye images is 5 meters, and they consist of five spectral bands: blue (440-510 nm), green (520-590 nm), red (630-685 nm), red edge (690-730 nm), and near infrared (760-850 nm).

Two sets of Landsat 8 images of level 1T products, which were acquired on June 19, 2015 and November 26, 2015 over the Avalon pilot site, were also downloaded from <http://espa.cr.usgs.gov/> and used in the analysis. The Landsat 8 level 1T

products are geometrically corrected with approximately 12 meters circular error and 90% confidence global accuracy (<http://landsat.usgs.gov/landsat8.php>). The images consist of 11 spectral bands with a spatial resolution of 30 meters in bands 1 to 7 and 9, 15 meters in band 8 (panchromatic), and 100 meters in bands 10 and 11 (thermal bands).

It is worth noting that all the images used in this study were finally resampled to 5 meters spatial resolution and were layer-stacked using the eCognition software.

2.3. Methodology

Previous studies have shown that the use of different classification techniques led to various classification results (e.g. Pal, 2005; McNerney and Nieuwenhuis, 2009; Song et al., 2012). Therefore, the initial focus of this research was on the comparison between the five different supervised machine learning classifiers: KNN, ML, SVM, CART, and RF. A brief explanation of each algorithm is provided in the following.

The KNN classifier, which is a non-parametric classification algorithm, is a simple machine learning algorithm that classifies an object based on the class attributes of its K-nearest neighbors in a feature space. In consequence, K is the key tuning parameter in the classifier, which can considerably affect the results of a classification. It is worth mentioning that usually more than one neighbor is assigned to improve classification accuracy (Cord and Cunningham, 2008).

SVM is another example of a non-parametric algorithm, which was first proposed by Vapnik and Chervonenkis (1971). The algorithm attempts to define the optimal hyperplane to effectively separate different classes. The kernel function is the

tuning parameter in the classifier used to map non-linear decision boundaries into linear boundaries in a higher dimension. The four most frequently used kernel functions in the SVM algorithm are linear, polynomial, Radial Basis Function (RBF), and sigmoid kernels (Kavzoglu and Colkesen, 2009).

The ML classifier is a probabilistic algorithm based on Bayesian statistics. It assumes that the feature vectors from each class are normally distributed, but not necessarily independently distributed. Using the training samples, the classifier first estimates the mean vectors and covariance matrices of the selected features for each class, and then applies them for image classification. The ML classifier can be a practical choice when the training samples are sufficient (Qian et al., 2014). In addition, there is no need to set any tuning parameter in the classifier.

CART, a well-known decision tree classification algorithm, which was first developed by Brieman et al. (1984), is also a non-parametric algorithm that has been widely used in image classification. This algorithm develops a decision tree in a binary recursive partitioning procedure by splitting the training data into several subsets based on an attribute value test, and then repeats this process on each derived subsets. The tree-growing process stops when no further splits are possible for subsets. The maximum depth of a decision tree is the key tuning parameter in the algorithm, which determines the complexity of the model. In general, a larger depth can build a relatively more complex decision tree with potentially a higher overall classification accuracy. However, too many nodes may also lead to over-fitting of the model (Qian et al., 2014).

The RF algorithm is an ensemble learning method that improves the accuracy of classification using a group of decision trees instead of one decision tree (Polikar,

2006; Rokach, 2010). After a large number of decision trees are generated, the most popular class is determined for each pixel based on the votes obtained from the decision trees. Furthermore, this classifier provides measures of variable importance that can be used for further interpretation (Pal, 2005).

The RapidEye imagery was selected to segment the study areas in a way that the objects were more similar to the real objects, because the imagery had the highest spatial resolution compared to the other data that we used in this research. In fact, an image with better spatial resolution generally provides more reasonable objects through segmentation procedure compared to a lower spatial resolution imagery. This will also consequently increase the accuracy of a wetland classification. Image segmentation was performed in the Trimble eCognition Developer 9 using the multi-resolution segmentation algorithm. The algorithm is a bottom-up approach that consecutively merges pixels or existing image objects into larger ones, based on the user-defined parameters (e.g. scale, shape, and compactness). The scale parameter, which is the most important parameter in the algorithm, defines the maximum standard deviation of the homogeneity criteria with regard to the weighted image layers for generating image objects. In general, smaller values of the scale parameter produce relatively smaller image objects, while larger values produce correspondingly larger objects. Since there are no generally accepted criteria for segmenting wetlands in the literature, we explored three different levels of segmentation by considering all of the classifiers to evaluate which level produces the most meaningful real-world objects (Figure 2.2). Finally, the value of 300 was selected as the best scale with a shape of 0.1 and compactness of 0.5 to ensure the segmentation of pure objects that contained only one land cover type.

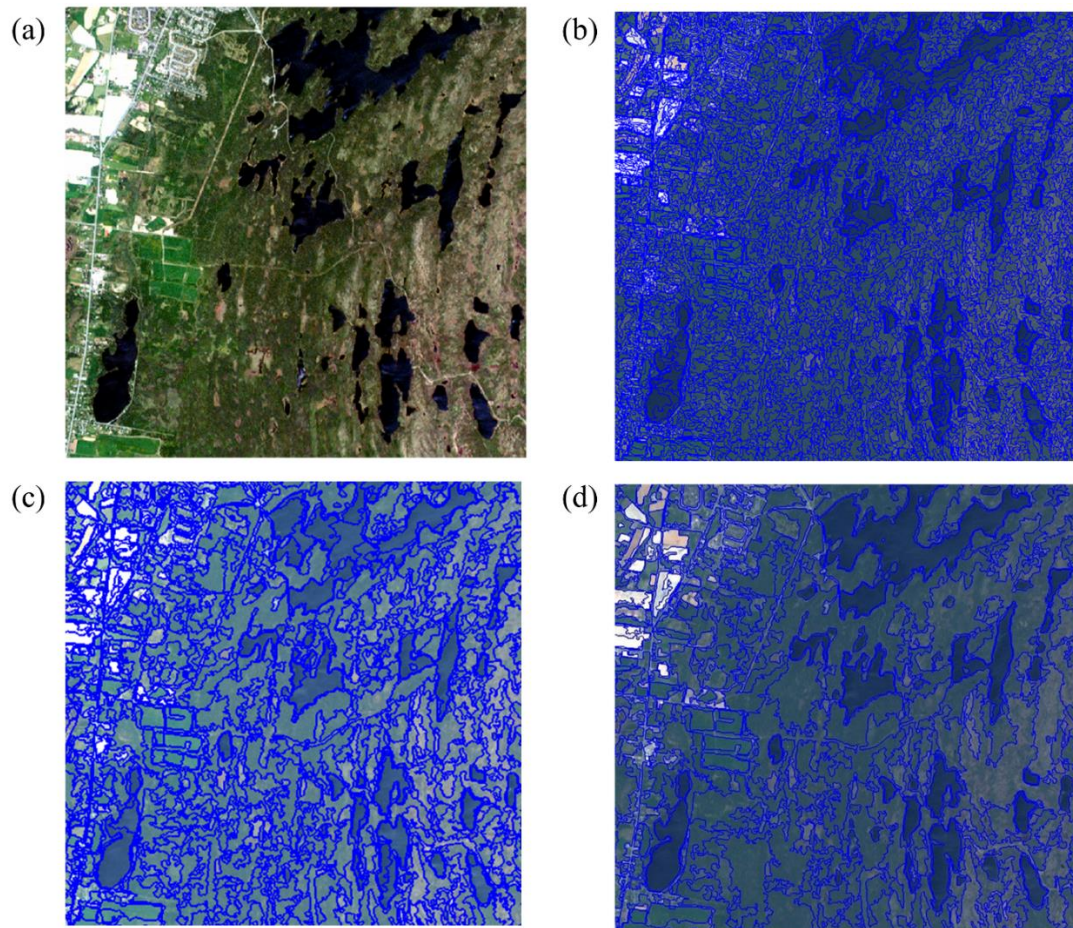


Figure 2.2. (a) RapidEye imagery over a selected area in the Avalon pilot site. Segmentation results obtained by applying five bands of RapidEye imagery in three different levels of (b) level 1 (scale parameter=100), (c) level 2 (scale parameter=300), (d) level 3 (scale parameter=500).

Various features, including topographic features, spectral features, texture features, as well as the features that are available in eCognition were evaluated to select those features that were most useful to discriminate different types of wetlands (Table 2.2).

Table 2.2. Evaluated features in this study.

Topographic features	Canadian Digital Surface Model, Slope, Aspect
Spectral features	Normalized Difference Water Index Normalized Difference Vegetation Index Normalized Difference Soil Index Soil Adjusted Vegetation index
Texture features	Standard deviation, GLCM (homogeneity, contrast, dissimilarity, entropy, moment, correlation)

To select the optimal features for separating various wetland classes, several toolboxes provided in eCognition software (e.g. “feature space optimization”, “sample editor”, and “sample selection information”) were used. The toolboxes provide useful information about attributes and histograms of image objects of different classes. Finally, we concluded that generally two features of mean and standard deviation values of the objects provided the most accurate results in the study areas. After inserting these two features into the five before-mentioned classifiers and evaluating the obtained results, we selected the best classifier to use in later experiments. It is worth noting that 50% of the field data was randomly used to train the algorithms and the other 50% was applied to evaluate the performance of the classifiers in delineating different wetland and non-wetland classes in the study areas (Table 2.1). The accuracy of the classifiers was also measured using the parameters of the Overall Accuracy (OA), Kappa Coefficient, Producer Accuracy (PA), and User Accuracy (UA), which were all derived from a confusion matrix. The OA is calculated by summing the number of correctly

classified pixels/objects and dividing by the total number of pixels/objects. The Kappa Coefficient also measures the agreement between classification and field data. A kappa value of 1 represents perfect agreement, while a value of 0 represents no agreement (Rossiter, 2004).

The settings of the tuning parameters in the classifiers are known to greatly affect classification accuracy (Pu et al., 2011; Duro et al., 2012; Qian et al., 2014). Therefore, different values were assigned to the tuning parameters in the selected classifier to see how these parameters could change the classification results and to select the optimum values for each of the tuning parameters.

Many studies have reported that OBIA typically outperforms the pixel-based methods when comparing overall classification accuracy using different remote sensing data (Blaschke, 2010; Zhang et al., 2010; Pu et al., 2011; Myint et al., 2011; Salehi et al., 2012b). Nevertheless, we compared these two approaches for wetland classification in the Avalon area.

2.4. Results and discussion

2.4.1. Comparison between different classifiers

Figure 2.3 demonstrates the OA and Kappa Coefficient calculated from each of the classifiers. It is worth noting that these results are the best results obtained by each classifier. In fact, different values for various tuning parameters in each classifier were tested and, finally, the best value was selected (see the following subsection for the results obtained for the best performing algorithm). According to the analyses, it was concluded that the RF algorithm had the best performance among

the five classifiers. The OA and Kappa Coefficient for this classifier were 90% and 0.87, respectively, which proved that the agreement between the actual classes and the classified classes was high. This may be due to the fact that RF employs a group of decision trees rather than a single decision tree to improve the classification accuracy. Moreover, RF is an effective classifier when using large datasets and estimate missing data. Finally, RF can operate better with complex relationships between estimators due to noise. After RF, the CART classifier provided the next best results with an OA and Kappa Coefficient of 88% and 0.85, respectively. The rest of classifiers, ML, SVM, and KNN showed the same results (OA= 87% and Kappa Coefficient= 0.82).

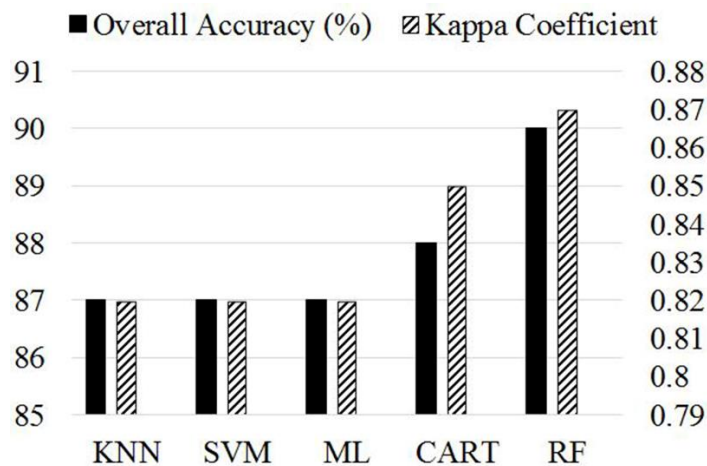


Figure 2.3. The Overall Accuracy and Kappa Coefficient for wetland classification in Avalon pilot site using the five machine learning algorithms: KNN, SVM, ML, CART, and RF.

The PA and UA for each of the wetland and non-wetland classes using different classifiers are illustrated in Figure 2.4. According to the figure, it is clear that the

accuracies for the non-wetland classes were higher than those of the wetland classes. The PAs for the Deep Water and Urban classes using different classifiers were almost at the same level and more than 95%, which demonstrated that separating these non-wetland classes from other classes was easier compared to the others. The most accurately identified wetland classes were Shallow Water and Bog. This was because the number of field samples for the Bog class were higher than other wetland classes and the Shallow Water class was spectrally more distinguishable than other wetlands. However, there were generally average accuracies and sometimes low accuracies for Fen, Marsh and Swamp (especially in the case of the Fen class using the classifiers other than RF). It is worth noting that there are situations where, even in the field, it is difficult to clearly distinguish between wetland classes, and as a result, wetlands were sometimes categorized as more than one class. For example, some wetlands were classified as Bog/Fen, Bog/Swamp, or Marsh/Shallow Water. The confusion between different wetlands during the field work will affect the final classification results. However, we tried to reduce this uncertainty by getting help from several ecological experts, who were familiar with the local study areas, for collecting field data. Moreover, it was tried to use those field data that we were completely sure about the type of wetland.

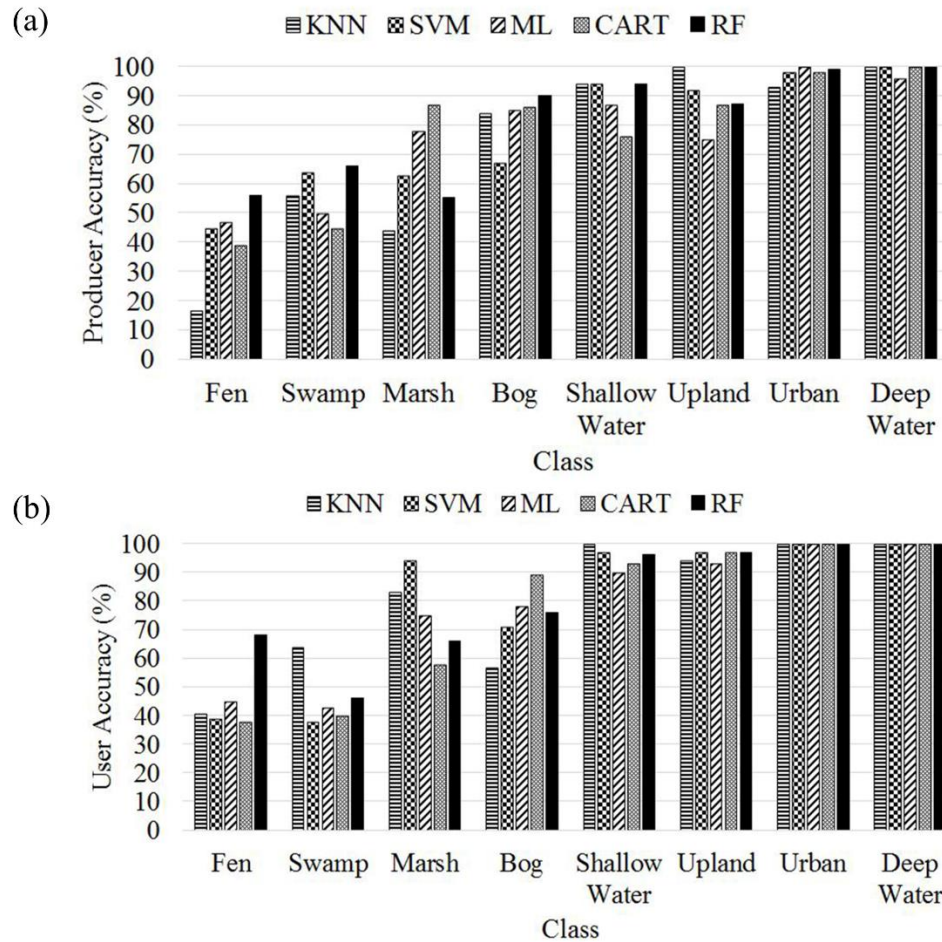


Figure 2.4. (a) Producer Accuracy and (b) User Accuracy for each of the wetland and non-wetland classes obtained by different classifiers for the Avalon pilot site.

Figure 2.5 (b) demonstrates the classified image obtained by the best classifier (RF), and Table 2.3 provides a detailed confusion matrix derived from this classifier based on the test data. It was concluded that identifying non-wetland classes was easier than wetland classes, in which the UAs and PAs for these three classes were on average more than 90%. There was confusion where Upland was misclassified as Swamp (2316 pixels) and Marsh (1295 pixels). This misclassification occurred

because swamps (treed wetlands) in our study area are not always easy to identify using aerial or satellite imagery and in many cases they are visually and spectrally similar to upland forests. The most accurately identified wetland classes were Shallow Water and Bog with PAs of 94% and 90%, and UAs of 96% and 76%, respectively. Only 92 pixels of the Shallow Water class were misclassified as Marsh. This can be explained by the fact that in the Avalon pilot site there are several emergent marsh areas that are spectrally similar to shallow water bodies containing lily pads on the water. Additionally, there was misclassification between the Marsh/Bog classes. More importantly, the highest confusion was between Bog/Fen, which had been expected before the analysis. This is rooted in the fact that bogs and fens (both peat-producing wetlands) have many ecological similarities. Even during field work, there were situations where it was unclear based solely on visual analysis if a wetland was certainly a bog or fen. It is interesting to note that merging these two classes into one wetland class (Bog/Fen) increased the OA of the classification to 92%.

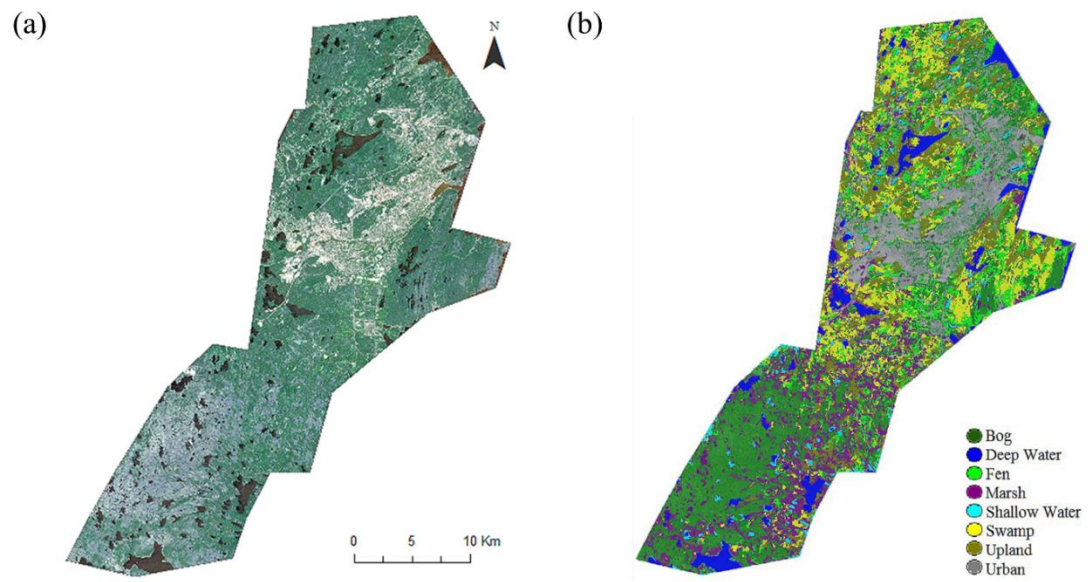


Figure 2.5. (a) RapidEye image from the Avalon pilot site, (b) Classified image using the object-based Random Forest algorithm (Segmentation was performed using the multi-resolution algorithm, in which the scale=300, shape=0.1, and compactness=0.5).

Table 2.3. Confusion matrix in terms of the number of pixels for the classification using the Random Forest algorithm with the User Accuracy, Producer Accuracy, errors of Commission ,and error of Omission (in %).

		Reference Data										
		B	F	M	SW	S	Up	DW	Ur	Total	C	UA
Classified Data	B	20279	4241	1476	0	590	0	0	83	26669	24	76
	F	1672	7368	841	0	987	0	0	0	10868	32	68
	M	541	70	3941	92	0	1295	0	0	5939	34	66
	SW	0	0	0	1445	0	0	60	0	1505	4	96
	S	78	740	859	0	3470	2316	0	32	7495	54	46
	Up	0	682	0	0	178	24304	0	0	25164	3	97
	DW	0	0	0	0	0	0	69312	0	69312	0	100
	Ur	0	0	0	0	0	0	0	19340	19340	0	100
	Total	22570	13101	7117	1537	5225	27915	69372	19455	166292		
	O	10	44	45	6	34	13	0	1			OA= 90
PA	90	56	66	94	66	87	100	99			K= 0.87	
OA: Overall Accuracy		B: Bog			S: Swamp			C: Commission				
K: Kappa Coefficient		F: Fen			Up: Upland			O: Omission				
PA: Producer Accuracy		M: Marsh			DW: Deep Water							
UA: User Accuracy		SW: Shallow Water			Ur: Urban							

2.4.2. The effect of the tuning parameters on classification accuracy

The tuning parameters of a classifier have significant impacts on classification accuracy. In this subsection, we discuss the effects of variation of the tuning parameters on the accuracy of the RF classifier. There are two important tuning

parameters in the classifier that can considerably affect the classification accuracy: depth and minimum sample number. The depth determines the complexity of the algorithm. In general, a larger depth will result in relatively more complex decision trees with more nodes in each decision tree. In addition, increasing the depth may result in a higher overall classification accuracy. However, it should be noted that too many nodes will lead to over-fitting of the RF classifier, which can result in accuracy reduction (Duro et al., 2012; Qian et al., 2014). The minimum sample number also indicates the minimum number of samples per node in each decision tree.

In our study, several values were assigned to each of these variables to assess their effects on the classification accuracy (depth = 5, 10, 15, 20, 25, 30, 40, 50, 100, minimum sample number = 2, 5, 10, 20, 30, 40), where the results are illustrated in Figure 2.6. It was concluded that the best overall classification accuracy (OA=90%) was generally achieved when the depth and minimum sample number were 20 and 5, respectively. According to Figure 2.6 (a), the overall classification accuracy increased to the highest level when the depth increased to 20. After 20, it decreased and then became stable when the maximum depth ≥ 30 , in which the OA was 87%. From Figure 2.6 (b), it is seen that the 5 minimum sample number resulted in the highest classification accuracy. With increasing sample number the OA decreased gradually to reach the lowest level of accuracy (74%) for sample number of 40.

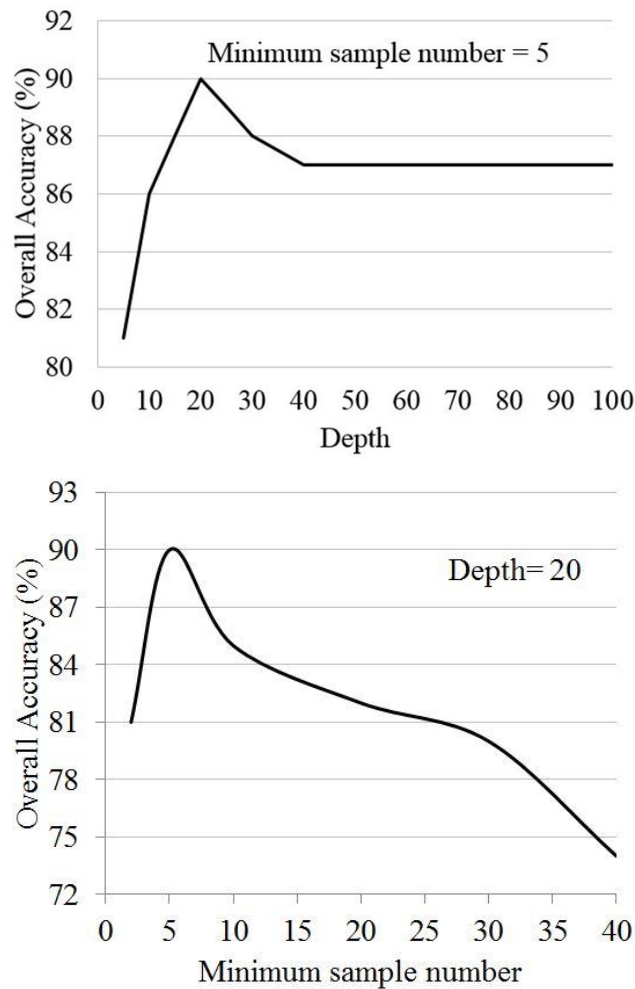


Figure 2.6. The effect of the variation in the tuning parameters: (a) Depth and (b) Minimum sample number, in the Random Forest classifier.

2.4.3. Comparison between pixel-based and object-based methods

Pixel-based and object-based image classification methods using the best examined machine learning algorithm (RF) can be compared in Figure 2.7 and Figure 2.5 (b). The pixel-based RF method (Figure 2.7) produced a speckled appearance, while the object-based RF method showed less speckle, in which the classified image was similar to actual objects in the Avalon pilot site. Furthermore, the OA and Kappa Coefficient for the pixel-based method were 77% and 0.7,

respectively, which were considerably lower than 90% and 0.87 observed for the object-based method (See Figure 2.3 and Table 2.3). These findings highlight the benefits of using object-based analysis instead of traditional pixel-based methods.

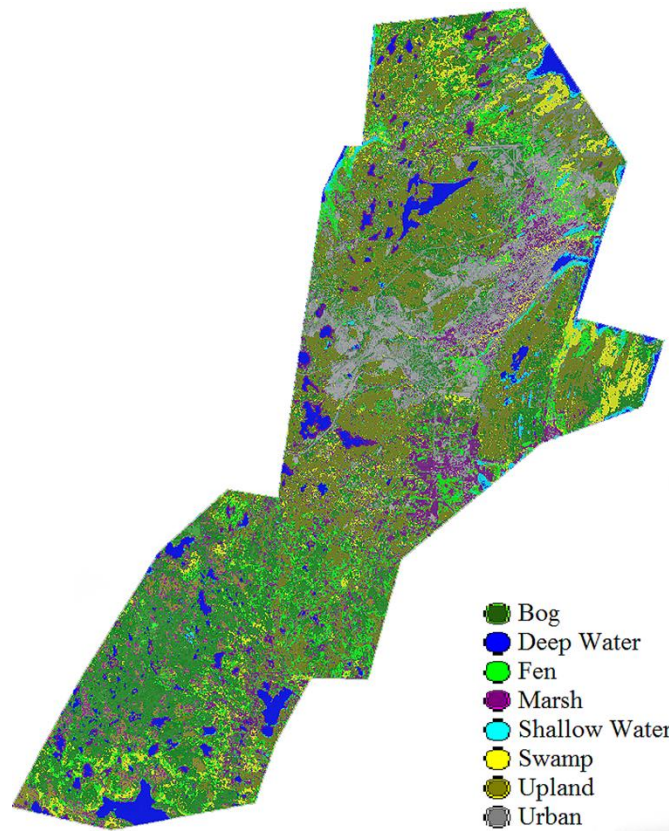


Figure 2.7. Classified image using the pixel-based Random Forest classifier.

2.4.4. Validation of the proposed methodology in other pilot sites

To show the effectiveness of the proposed approach for wetland classification, we selected four other pilot sites including Grand Falls-Windsor, Deer Lake, Gros Morne, and Goose Bay (Figure 2.1 (b, c, d, e)). These pilot sites (each approximately 700 km²) were selected to represent the different local ecologies distributed across NL. The information about these pilot sites, their respective land cover, the aerial

and satellite images that were used to classify each pilot site, as well as the number of classes for each pilot site are provided in Table 2.4. We have used multi-source and multi-temporal optical data (acquired between June and October 2015) for wetland classification. Moreover, the field data, collected between July and October 2015, does not exactly correspond to the acquisition date of the imagery. This temporal disparity across data sets must also be considered when evaluating image classification accuracy and associated uncertainties, particularly in the case of wetlands. This is because wetlands are highly dynamic in nature (Mitsch and Gosselink, 2000). This dynamic nature can result in wetlands looking visually different (amount of water, vegetation growth) during different years, months, and even days. For example, there may be excessive rain one day resulting in the flooding of what is typically marsh wetland. This flooding may be enough to completely cover any emergent vegetation, making the wetland appear more similar to shallow or deep water land cover. This same marsh, during a very dry summer, may completely dry out so that it looks more similar to upland. While certain species of vegetation on the ground may identify a dry area as a wetland, this can be difficult to identify via remote sensing methods. However, intriguingly, using multi-temporal and multi-source data increases the accuracy of classification as opposed to decreasing it. When we use features from more than one date or more than one source, we are actually increasing the amount of information that we have about an object. By using data from multiple dates and sources, we are augmenting the chance of separation of two classes. The reason is that maybe the two wetland classes are not distinguishable in the image acquired in one date/by one source, but they can be separated using the image taken at another date/using another source because wetlands change considerably within a year. Certainly,

using many dates to detect an object will not be helpful if the object does not change during a while.

Table 2.4. The information on the study areas, satellite and aerial data, and field data used for validation of the methodology.

Study area	Grand Falls- Windsor	Deer Lake	Gros Morne	Goose Bay
Land covers	Boreal forests, barrens, peatlands, water, agricultural and urban regions	Balsam and black spruce forests, peatlands, water, urban areas	balsam fir and black spruce forests, Peatlands, water, urban areas	Balsam fir, black spruce, and white birch forests, peatlands, water, urban regions
Images and date of acquisition	- One RapidEye (10/06/2015) - One Landsat 8 imagery (10/06/2015)	- One RapidEye imagery (18/06/2015) - One Landsat 8 imagery (04/08/2015) CDSM (Feb., 2010)	Two RapidEye imagery (18/06/2015, 06/09/2015)	- Two RapidEye imagery (01/07/2015, 04/10/2015) - One Landsat 8 imagery (09/08/2015)
Classes	- Wetland (Bog, Fen, Marsh, Shallow Water) - Non-wetland (Deep Water, Upland, Urban)	- Wetland (Bog, Fen, Marsh) - Non-wetland (Deep Water, Upland)	- Wetland (Bog, Marsh, Swamp) - Non-wetland (Deep Water, Upland, Urban)	- Wetland (Bog, Fen, Marsh, Shallow Water) - Non-wetland (Deep Water, Upland, Urban)
Total train area (ha)	358	84	537	327
Total test area (ha)	403	68	411	229
Number of train sites	70	31	54	30
Number of test sites	74	32	57	29

To classify the wetlands, each pilot site was segmented using its corresponding RapidEye Imagery, and then, two features of mean and standard deviation of pixels' values were inserted into the object-based RF algorithm to classify each area into pre-defined wetland and non-wetland classes (See Table 2.4). The OAs, Kappa Coefficients, as well as mean PAs and UAs for wetland classes in Grand Falls-Windsor, Deer Lake, Gros Morne, and Goose Bay are demonstrated in Table 2.5. The OAs and Kappa Coefficients obtained in different pilot sites were very close proving the robustness of the methodology.

Table 2.5. The Overall Accuracy, Kappa Coefficient, mean Producer and User Accuracies for wetland classes in the validation pilot sites.

	Grand Falls- Windsor	Deer Lake	Gros Morne	Goose Bay
Overall Accuracy (%)	90	86	96	87
Kappa Coefficient	0.87	0.8	0.93	0.84
Mean Producer				
Accuracy of wetland classes (%)	64	68	51	77
Mean User Accuracy of wetland classes (%)	73	50	94	80

The PA and UA for each of the evaluated classes in the corresponding study area are also demonstrated in Figure 2.8. Like the results achieved for the Avalon pilot site (Figure 2.4 and Table 2.3), the highest accuracies in the other four pilot sites

were obtained for non-wetland classes (between 95% and 100%). The lowest accuracies were also for Fen and Marsh classes in all study areas. According to Figure 2.8 (b and c), the PA and UA for Marsh class were different, which showed that the obtained results were not reliable. This fact was also observed for Fen class in Gros Morne and Goose Bay pilot sites (Figure 2.8 (c and d)). The reason could be rooted in the fact that the amount of field data and hence training data for these classes in the study areas was low. Figure 2.9 shows the classified images obtained by the RF classifier for each of the pilot sites. The obtained maps demonstrated clear separation between wetland and non-wetland classes. Based on the results, we concluded that there was high correlation between the reference and classified categories in all evaluated study areas. The authors believe that the proposed method is a promising approach to classify wetlands in different study areas; however, training data is important to improve the overall accuracy of the resultant classification.

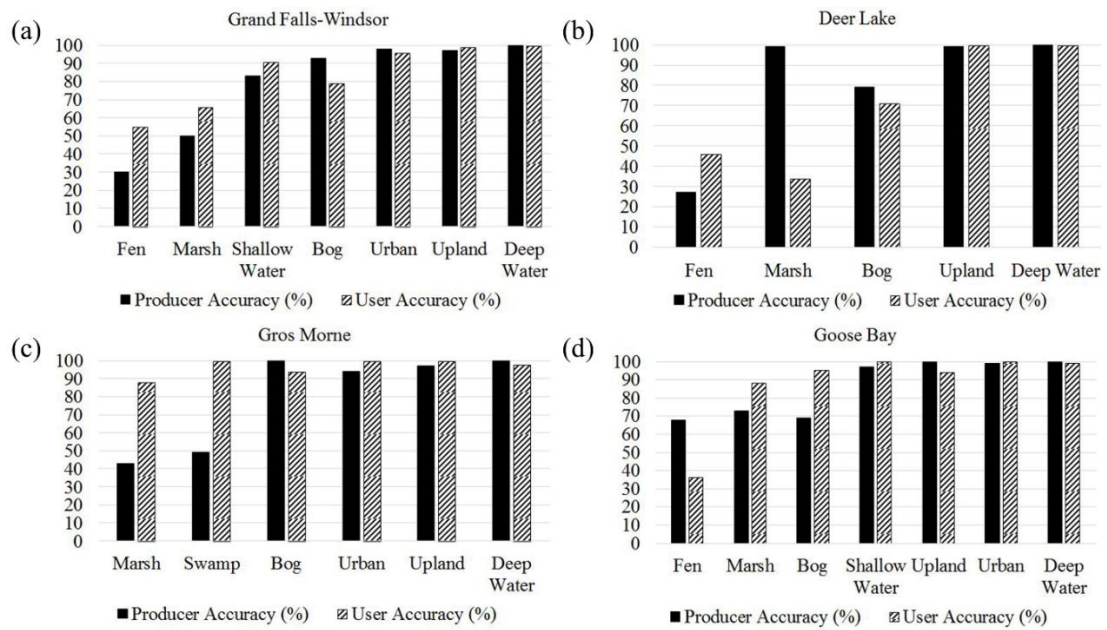


Figure 2.8. Producer Accuracy and User Accuracy for each of the wetland and non-wetland classes in (a) Grand Falls-Windsor, (b) Deer Lake, (c) Gros Morne, and (d) Goose Bay.

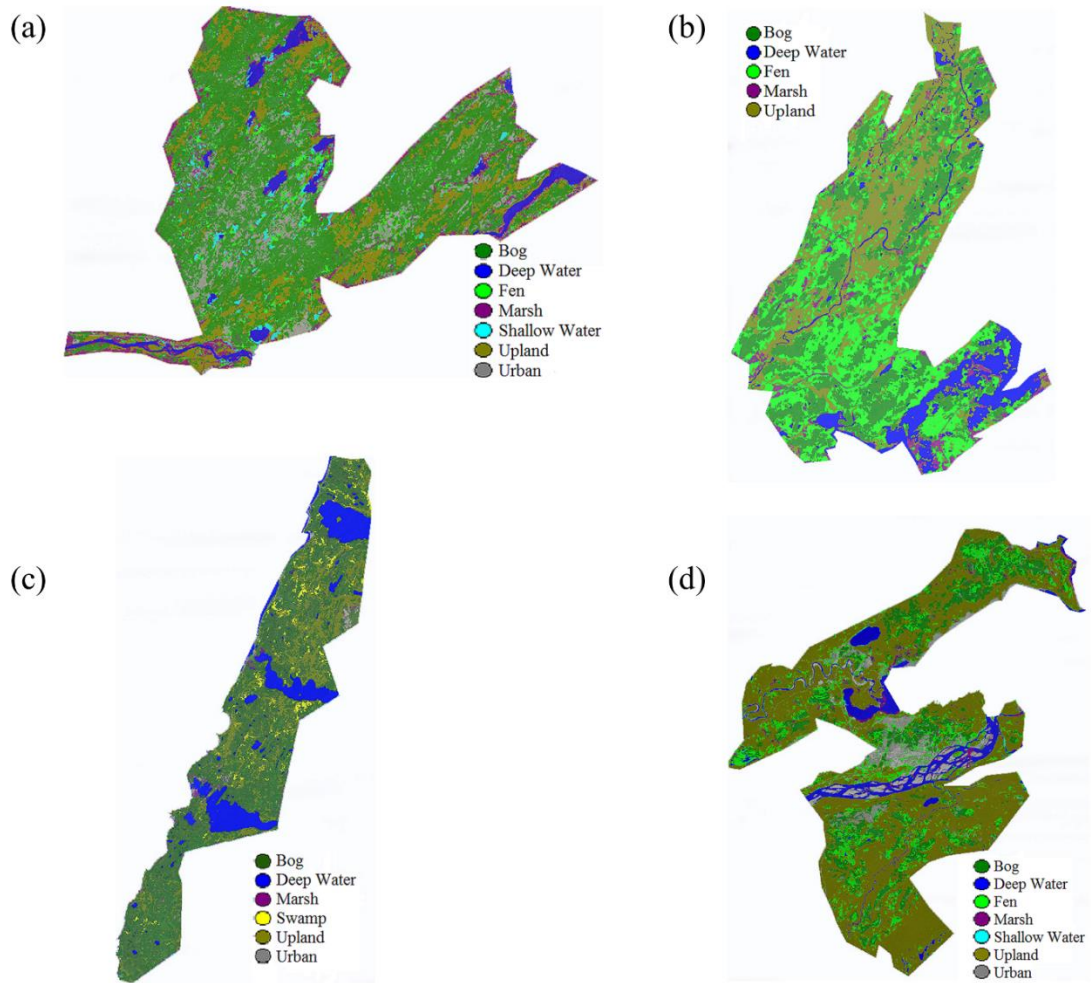


Figure 2.9. Classified image using the object-based Random Forest classifier in (a) Grand Falls-Windsor, (b) Deer Lake, (c) Gros Morne, and (d) Goose Bay.

2.5. Conclusion

Remote sensing satellites with different spatial and temporal coverages provide many useful tools for wetland classification and monitoring. The study showed that a fused multi-source and multi-temporal optical satellite data in combination with the OBIA approach is a promising approach for classifying wetlands in different study areas. A comparative assessment on the performance of five different machine learning classifiers: KNN, ML, SVM, CART, and RF showed that

the overall classification accuracies obtained by these classifiers were almost similar (between 87% and 90%), with the RF classifier outperforming the others. In addition, we concluded that the tuning parameters of the RF algorithm had noticeable impacts on the results and, therefore, the optimum values for these parameters should be calculated before analysis. The results also indicated that OBIA was superior to the traditional pixel-based method for wetland classification, as has already been proved by several researchers (e.g. Grenier et al., 2007; Dronova et al., 2011; Powers et al., 2012). All classes were depicted by the object-based method in a more realistic way in terms of generalized appearance and achieved accuracies compared to the pixel-based method that produced a speckled classified image. Finally, to show the high applicability and robustness of the proposed approach for wetland classification, four other pilot sites with various ecological characteristics were selected to classify wetlands. The results proved the high applicability of the methodology in different study areas. It was observed that non-wetland classes were classified with the highest accuracies (more than 90%). However, since there were many similarities between different wetland classes in terms of their spectral information, it was challenging to accurately differentiate among these classes. The most accurately identified wetland classes were Shallow Water and Bog, while average accuracies were achieved for Fen, Swamp, and Marsh. The overall classification accuracies considering all pilot sites were also between 86% and 96%. In conclusion, based on these levels of accuracies obtained from a confusion matrix, we concluded that the wetland classified maps using the RF algorithm were in strong agreement with real world land cover.

References

- Blaschke, T. (2010). Object based image analysis for remote sensing. *ISPRS Journal of Photogrammetry and Remote Sensing*, 65(1), 2-16.
- Blaschke, T., Hay, G. J., Kelly, M., Lang, S., Hofmann, P., Addink, E., ... & Tiede, D. (2014). Geographic object-based image analysis—towards a new paradigm. *ISPRS Journal of Photogrammetry and Remote Sensing*, 87, 180-191.
- Brieman, L., Friedman, J., Olshen, R., and Stone, C. (1984). Classification and regression trees. *Wadsworth & Brooks. Monterrey, CA*.
- Canadian Digital Surface Model, (2013). Canadian Digital Surface Model Product Specifications. *Government of Canada, Natural Resources Canada, Map Information Branch, Edition 1.1*.
- Chasmer, L., Hopkinson, C., Montgomery, J., & Petrone, R. (2016). A physically based terrain morphology and vegetation structural classification for wetlands of the Boreal Plains, Alberta, Canada. *Canadian Journal of Remote Sensing*, 42(5), 521-540.
- Corcoran, J., Knight, J., Brisco, B., Kaya, S., Cull, A., & Murnaghan, K. (2012). The integration of optical, topographic, and radar data for wetland mapping in northern Minnesota. *Canadian Journal of Remote Sensing*, 37(5), 564-582.
- Cord, M., and Cunningham, P. (Eds.). (2008). Machine learning techniques for multimedia: case studies on organization and retrieval. *Springer Science & Business Media*.
- Dronova, I., Gong, P., & Wang, L. (2011). Object-based analysis and change detection of major wetland cover types and their classification uncertainty during the low water period at Poyang Lake, China. *Remote Sensing of Environment*, 115(12), 3220-3236.

- Duro, D. C., Franklin, S. E., & Dubé, M. G. (2012). A comparison of pixel-based and object-based image analysis with selected machine learning algorithms for the classification of agricultural landscapes using SPOT-5 HRG imagery. *Remote Sensing of Environment*, 118, 259-272.
- Gosselin, G., Touzi, R., & Cavayas, F. (2014). Polarimetric Radarsat-2 wetland classification using the Touzi decomposition: case of the Lac Saint-Pierre Ramsar wetland. *Canadian Journal of Remote Sensing*, 39(6), 491-506.
- Grenier, M., Demers, A. M., Labrecque, S., Benoit, M., Fournier, R. A., & Drolet, B. (2007). An object-based method to map wetland using RADARSAT-1 and Landsat ETM images: test case on two sites in Quebec, Canada. *Canadian Journal of Remote Sensing*, 33(sup1), S28-S45.
- Kavzoglu, T., & Colkesen, I. (2009). A kernel functions analysis for support vector machines for land cover classification. *International Journal of Applied Earth Observation and Geoinformation*, 11(5), 352-359.
- Lillesand, T., Kiefer, R. W., & Chipman, J. (2014). Remote sensing and image interpretation. *John Wiley & Sons*.
- Liu, D., & Xia, F. (2010). Assessing object-based classification: advantages and limitations. *Remote Sensing Letters*, 1(4), 187-194.
- McInerney, D. O., & Nieuwenhuis, M. (2009). A comparative analysis of k NN and decision tree methods for the Irish National Forest Inventory. *International Journal of Remote Sensing*, 30(19), 4937-4955.
- Mitsch, W. J., & Gosselink, J. G. (2000). The value of wetlands: importance of scale and landscape setting. *Ecological Economics*, 35(1), 25-33.

- Myint, S. W., Gober, P., Brazel, A., Grossman-Clarke, S., & Weng, Q. (2011). Per-pixel vs. object-based classification of urban land cover extraction using high spatial resolution imagery. *Remote Sensing of Environment*, 115(5), 1145-1161.
- Ozesmi, S. L., & Bauer, M. E. (2002). Satellite remote sensing of wetlands. *Wetlands Ecology and Management*, 10(5), 381-402.
- Pal, M. (2005). Random forest classifier for remote sensing classification. *International Journal of Remote Sensing*, 26(1), 217-222.
- Polikar, R. (2006). Ensemble based systems in decision making. *IEEE Circuits and systems magazine*, 6(3), 21-45.
- Powers, R. P., Hay, G. J., & Chen, G. (2012). How wetland type and area differ through scale: A GEOBIA case study in Alberta's Boreal Plains. *Remote Sensing of Environment*, 117, 135-145.
- Pu, R., Landry, S., & Yu, Q. (2011). Object-based urban detailed land cover classification with high spatial resolution IKONOS imagery. *International Journal of Remote Sensing*, 32(12), 3285-3308.
- Qian, Y., Zhou, W., Yan, J., Li, W., & Han, L. (2014). Comparing machine learning classifiers for object-based land cover classification using very high resolution imagery. *Remote Sensing*, 7(1), 153-168.
- RapidEye, A. G. (2015). Satellite Imagery Product Specifications. *RapidEye Agency, product manual, Version 6.1*.
- Rokach, L. (2010). Ensemble-based classifiers. *Artificial Intelligence Review*, 33(1-2), 1-39.
- Rossiter, D. G. (2004). Statistical methods for accuracy assessment of classified thematic maps. *International Institute for Geo-information Science and Earth, Department of Earth Systems Analysis, Enschede, NL*, 46.

- Salehi, B., Zhang, Y., & Zhong, M. (2013). A combined object-and pixel-based image analysis framework for urban land cover classification of VHR imagery. *Photogrammetric Engineering & Remote Sensing*, 79(11), 999-1014.
- Salehi, B., Zhang, Y., Zhong, M., & Dey, V. (2012). A review of the effectiveness of spatial information used in urban land cover classification of VHR imagery. *International Journal of Geoinformatics*, 8(2).
- Salehi, B., Zhang, Y., Zhong, M., & Dey, V. (2012). Object-based classification of urban areas using VHR imagery and height points ancillary data. *Remote Sensing*, 4(8), 2256-2276.
- Schmitt, A., & Brisco, B. (2013). Wetland monitoring using the curvelet-based change detection method on polarimetric SAR imagery. *Water*, 5(3), 1036-1051.
- Song, X., Duan, Z., & Jiang, X. (2012). Comparison of artificial neural networks and support vector machine classifiers for land cover classification in Northern China using a SPOT-5 HRG image. *International Journal of Remote Sensing*, 33(10), 3301-3320.
- South, G. R. (1983). 10. Benthic marine algae. *Biogeography and Ecology of the Island of Newfoundland*, 48, 385.
- Tiner, R. W., Lang, M. W., and Klemas, V. V. (Eds.). (2015). *Remote Sensing of Wetlands: Applications and Advances*. CRC Press.
- Warner, B.G. and Rubec, C.D.A. (Eds.). (1997). The Canadian wetland classification system. *Wetlands Research Branch, University of Waterloo*.
- Zhang, X., Feng, X., & Jiang, H. (2010). Object-oriented method for urban vegetation mapping using IKONOS imagery. *International Journal of Remote Sensing*, 31(1), 177-196.

Zhou, W., & Troy, A. (2008). An object-oriented approach for analysing and characterizing urban landscape at the parcel level. *International Journal of Remote Sensing*, 29(11), 3119-3135.

CHAPTER 3. EVALUATION OF MULTI-TEMPORAL LANDSAT 8 DATA FOR WETLAND CLASSIFICATION IN NEWFOUNDLAND, CANADA

Abstract

Wetlands are important natural resources which provide many benefits to the environment. Consequently, mapping and monitoring wetlands has gained a considerable attention in recent years among remote sensing experts. Wetlands undergo a considerable change within a year. Thus, it is important to study how much various wetland types are distinguishable at different dates. This will help in choosing an appropriate image for wetland classification. On the other hands, combining various satellite images acquired on different dates is a promising approach to obtain a more accurate classified map compared to the map obtained by single-date satellite imagery. In this study, wetlands within a pilot sites, located in Newfoundland were first classified using each of the several available Landsat 8 data, captured in the three seasons of Spring, Summer, and Fall. By doing this, the separability of the wetland classes in each season was analyzed. Then, these multi-temporal data were integrated to obtain a more accurate map of wetlands. The overall classification accuracy of the final map was 88%, proving that using multi-temporal remote sensing data was necessary to obtain a more reliable and accurate map of the dynamic wetlands in the province.

Keywords: Remote Sensing, Wetland, Multi-temporal satellite data, Landsat 8, Newfoundland

3.1. Introduction

Wetlands are valuable natural resources because they provide many ecological functions and services (Woodward and Wui, 2001). Wetland areas are more important in Canada which contains 24% of the world's wetlands (National Wetlands Working Group, 1988). Therefore, it is highly required to monitor these valuable natural assets using new technologies. In this regard, remote sensing satellites providing timely and up-to-date images offer valuable and accurate information.

Wetlands are highly dynamic in nature and their environmental and physical characteristics vary across seasons and months (Mahdavi et al., 2017). This dynamicity can result in wetlands looking visually different (amount of water, vegetation growth) during different years, months, and even days. For example, there may be excessive rain one day resulting in the flooding of what is typically marsh wetland. This flooding may be enough to completely cover any emergent vegetation, making the wetland appear more similar to shallow or deep water land cover. This same marsh, during a very dry summer, may completely dry down so that it looks more similar to upland.

It is important in terms of operational purposes to determine in which date wetland classes are more separable. Additionally, we need to apply multi-temporal remote sensing data to monitor and detect changes in wetland regions during a period of time (Munyati, C., 2000). Using a single-date satellite data may

not result in a high accuracy for classification of wetlands. Therefore, multi-date imagery should be applied in studies of these dynamic lands (Siachalou et al., 2014; Mahdavi et al., 2017). Remote sensing satellites, in this regard, provide repeated coverage of the earth, and therefore, are suitable for monitoring changes in wetlands (Munyati, C., 2000; Schmitt et al., 2010; Siachalou et al., 2014; Mahdavi et al., 2017).

3.2. Study area

The study area was the Avalon pilot site, located in Newfoundland, Canada (Figure 3.1 (a)). The pilot site is approximately 700 km², and located within the Maritime Barren ecoregion. Wetlands of all five classes described by the Canadian Wetland Classification System (CWCS, National Wetlands Working Group, 1988) are found in the pilot site, though peatlands (bogs and fens) are dominant (South, 1983).

3.3. Data

The field work was conducted between July and October in 2015 and between June and August in 2016. Visited wetlands were assigned a wetland class (Bog, Fen, Marsh, Swamp, and Shallow Water) based on the CWCS. A GPS point was collected per wetland site visited. Then, the boundary for each wetland was delineated in ArcGIS using high spatial resolution satellite and aerial imagery (i.e., RapidEye and aerial orthophoto with 5 and 0.5 meters spatial resolutions, respectively). It is worth noting that three non-wetland classes of Deep Water, Upland, and Urban were also considered in this study.

In addition, three Landsat 8 images captured in different seasons (Table 3.1) were evaluated for wetland classification in this study. Landsat 8 has a temporal resolution of 16 days and contains 11 spectral bands in various parts of the electromagnetic spectrum, which can be effectively applied for wetland mapping. Landsat 8 was selected because the data are freely available and can be easily obtained at various times. As a result, the corresponding multi-date data are suitable for monitoring wetlands seasonally. It is worth noting that these multi-temporal data contained different imaging geometries, which can slightly affect the results and were not considered in this study.

3.4. Method

Since the Level 1T products of Landsat 8 data were used, geometric and radiometric corrections were not performed (<http://landsat.usgs.gov/landsat8.php>). However, the data were pan-sharpened to obtain the imagery with higher spatial resolution (15 meters). Moreover, instead of traditional pixel-based classification methods, an object-based Random Forest (RF) algorithm was selected to classify the Avalon pilot site. RF was selected because according to our analyses (Amani et al., 2017), it produced a higher classification accuracy compared to those produced by four other classifiers (i.e., Support Vector Machine, Maximum Likelihood, Decision Tree, and K-Nearest Neighbor). Field data was divided in half so that one half was used to train the algorithm and the other half was used to test the accuracy of the results. It is also worth mentioning that trial and error was used to select the most useful features to be inserted in the classification procedure. This was because the optimum tuning parameters depend on various factors, the most important of which was the

number of field samples. Finally, two features of mean and standard deviation of the objects values were used as the best features for distinguishing wetland classes.

Since the main focus of this study was evaluating multi-temporal satellite data for wetland classification, the satellite imagery acquired in each season (Table 3.1) was first classified by applying the selected features in an object-based RF classifier. By comparing the level of accuracy of each data, we concluded at which date wetlands were more separable by the algorithm. Then, a combination of the three images was applied to obtain a higher classification accuracy of wetlands in the study area.

3.5. Results

Table 3.1 displays the overall classification accuracy and the average producer and user accuracies of only wetland classes, obtained by applying the RF algorithm to each of the imagery. According to the results, the classification of the image, captured in August resulted in a higher accuracy compared to the other dates. This may be because August occurs during late in the summer, when vegetation has had a chance grow excessively, compared to other seasons. At this point, the various vegetative species have differentiated from one another. June may be too early in the growing season for vegetation to have developed since the winter. Similarly, by November, the vegetation is dying on the onset of winter, and as a result, many of the vegetative species have browned, and reduced in height and volume. Consequently, the growth and differentiation of unique vegetation associated with the various wetland classes during the summer may allow for better remotely sensed distinction between the classes.

Table 3.1. The overall accuracies (OAs), as well as the average producer and user accuracies of wetland classes (APAs and AUAs) in the Avalon pilot site.

Accuracy	June (2015/06/19)	August (2015/08/15)	November (2015/11/26)
OA (%)	86	88	81
APA (%)	60	64	56
AUA (%)	57	60	53

As explained, wetlands are dynamic environment and the type and the amount of changes are different across various wetlands. Consequently, different wetland classes may be more distinguishable on different dates. Therefore, combining satellite images obtained in various times of a year will result in higher classification accuracy. In this research, we integrated the three previous-mentioned Landsat 8 images to achieve a more accurate map of wetlands from the study area (Figure 3.1 (b)). As is clear, object-based classification produced a visually appealing generalized appearance of wetland and non-wetland classes. The overall classification accuracy, average producer accuracy of wetland classes, and average user accuracy of wetland classes were 88%, 68%, and 63%, respectively. These accuracies were statistically significant with p-value of less than 0.001. According to the results, it was concluded that combining multi-date images in a classification procedure provided more accurate results in terms of both visual interpretation and statistical analyses.

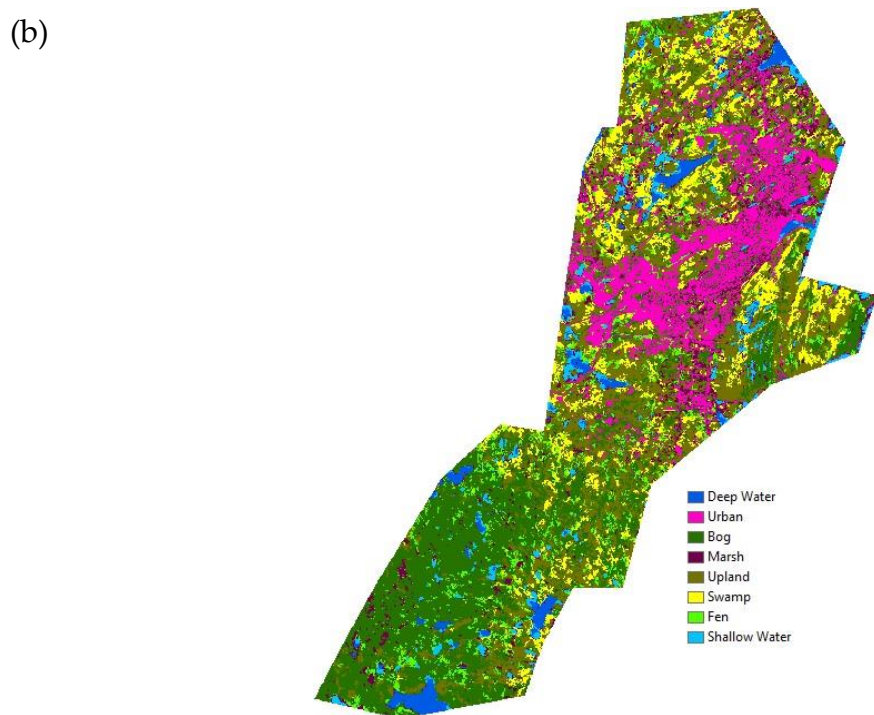
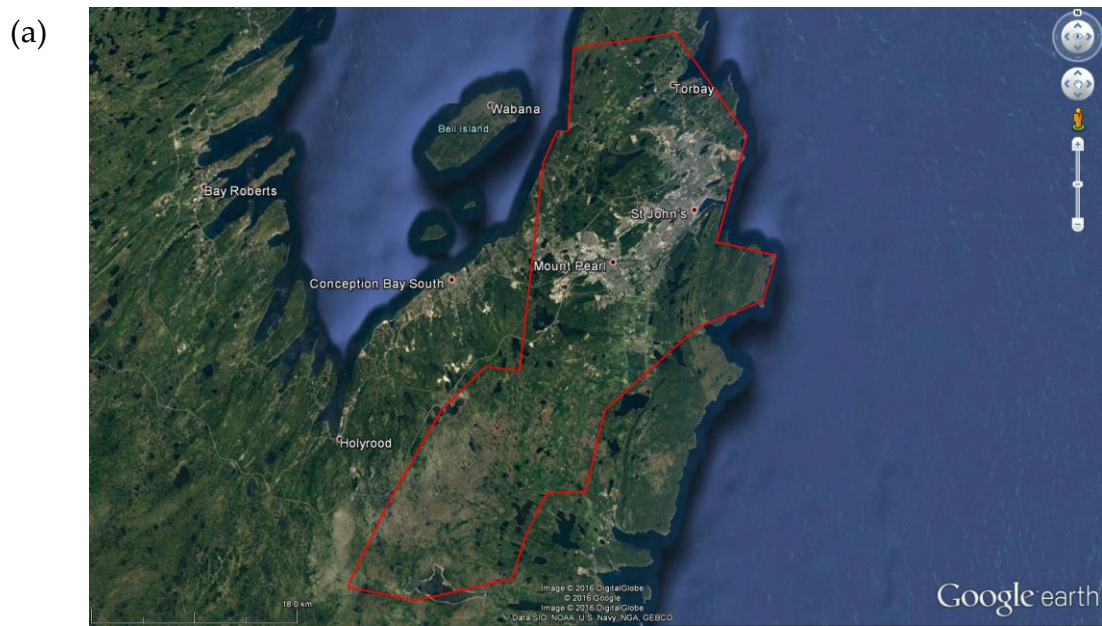


Figure 3.1. (a) Study area (the Avalon pilot site), (b) Classified image obtained by the integration of multi-temporal Landsat 8 data.

3.6. Conclusion

In this study, several analyses were carried out for concluding the best acquisition date for the images which are applied in wetland studies. Moreover, since wetlands can vary environmentally and visually during a year, using different satellite images, obtained at various times resulted in various classification accuracies. It was concluded that generally, the imagery captured in August produced a more reliable map with the highest accuracy compared to images acquired in June and November. In addition, we concluded that combining the data acquired at various dates provided a more accurate map compared to those of single-date imagery.

References

- Amani, M., Salehi, B., Mahdavi, S., Granger, J. E., Brisco, B., & Hanson, A. (2017). Wetland Classification Using Multi-Source and Multi-Temporal Optical Remote Sensing Data in Newfoundland and Labrador, Canada. *Canadian Journal of Remote Sensing*, 43(4), 360-373.
- Mahdavi, S., Salehi, B., Amani, M., Granger, J. E., Brisco, B., Huang, W., & Hanson, A. (2017). Object-based classification of wetlands in Newfoundland and Labrador using multi-temporal PolSAR data. *Canadian Journal of Remote Sensing*, 43(5), 432-450.
- Munyati, C. (2000). Wetland change detection on the Kafue Flats, Zambia, by classification of a multitemporal remote sensing image dataset. *International Journal of Remote Sensing*, 21(9), 1787-1806.

- National Wetlands Working Group. (1988). Wetlands of Canada. Ecological land classification series, no. 24. *Sustainable Development Branch, Environment Canada, Ottawa, Ontario, and Polyscience Publications Inc., Montreal, Quebec*, 452.
- Schmitt, A., Brisco, B., Kaya, S., & Murnaghan, K. (2010). Polarimetric change detection for wetlands. *IAHS Red Book*.
- Siachalou, S., Doxani, G., & Tsakiri-Strati, M. (2014). Time-series Analysis of High Temporal Remote Sensing Data to Model Wetland Dynamics: a Hidden Markov Model Approach. *In SENTINEL-2 for Science Workshop, Frascati, Italy*.
- South, G. R. (1983). 10. Benthic marine algae. *Biogeography and Ecology of the Island of Newfoundland*, 48, 385.
- Woodward, R. T., & Wui, Y. S. (2001). The economic value of wetland services: a meta-analysis. *Ecological Economics*, 37(2), 257-270.

CHAPTER 4. SPECTRAL ANALYSIS OF WETLANDS USING MULTI-SOURCE OPTICAL SATELLITE IMAGERY

Abstract

The separability of wetland types using different spectral bands is an important subject, which has not yet been well studied in most countries. This is particularly of interest in Canada because it contains approximately one-fourth of the total global wetlands. In this study, the spectral separability of five wetland classes, namely Bog, Fen, Marsh, Swamp, and Shallow Water, was investigated in Newfoundland and Labrador (NL), Canada, using field data and multi-source optical Remote Sensing (RS) images. The objective was to select the most useful spectral bands for wetland studies from four commonly used optical satellites: RapidEye, Sentinel 2A, ASTER, and Landsat 8. However, because the ultimate objective was the classification of wetlands in the province, the separability of wetland classes was also evaluated using several other features, including various spectral indices, as well as textural and ratio features to obtain a high level of classification accuracy. For this purpose, two separability measures were used: The T-statistics, calculated from the parametric t-test method, and the U-statistics, derived from the non-parametric Mann-Whitney U-test. The results indicated that the Near Infrared (NIR) band was the best followed by the Red Edge (RE) band for the discrimination of wetland class pairs. The red band was also the third most useful band for separation of wetland classes, especially for the delineation of the

Bog class from the other types. Although the Shortwave Infrared (SWIR) and green bands demonstrated poor separability, they were comparatively more informative than the Thermal Infrared (TIR) and blue bands. This study also demonstrated that ratio features and some spectral indices had high potential to differentiate the wetland species. Finally, wetlands in five study areas in NL were classified by inserting the best spectral bands and features into an object-based Random Forest (RF) classifier. By doing so, the mean Overall Accuracy (OA) and Kappa coefficient in the study areas were 86% and 0.82, respectively.

Keywords: Remote Sensing, Wetlands, Spectral analysis, Separability measures, Canada

4.1. Introduction

Wetlands are valuable natural resources that provide many ecological services to both flora and fauna. Their benefits are a result of the natural hydrological and biogeochemical processes carried out in these ecosystems. These processes, which are sometimes called wetland functions, include hydraulic storage and recharge, bio-geochemical transformation, biomass production, and habitat (Marton et al., 2015). In addition, these habitats are important forms of economic resources in many countries in the form of recreation, fishing, waterfowl hunting, and animal grazing (Marton et al., 2015; Guo et al., 2017). In recent times, wetlands have also become a popular topic in discussions of climate change because they contain 12% of the global carbon pool (Erwin, 2009; Guo et al., 2017).

Because of the valuable services that wetlands provide, the Ramsar Convention carried out a review of wetland inventories across the globe in an effort to analyze the extent, status, and effectiveness of inventories around the world, and to provide several specific recommendations as to how different countries can establish or improve on these important wetland tools (Finlayson et al., 1999). Consequently, attempts have been made to develop a wetland classification system based on the specific types of wetlands in each country (Ozesmi and Bauer, 2002; Tiner et al., 2015; Guo et al., 2017; Mahdavi et al., 2017b). For instance, there are two well-known wetland classification systems in Canada (National Wetlands Working Group, 1987; Smith et al., 2007): the Canadian Wetland Classification System (CWCS, refer to Table 4.1 for the list of acronyms) and the Enhanced Wetland Classification System (EWCS). The CWCS is the only Canada-wide classification system, which incorporates ecological characteristics of wetlands and their functions into the classification (National Wetlands Working Group, 1987). The CWCS categorizes wetlands into five classes based on their soil, water, and vegetation characteristics: Bog, Fen, Marsh, Swamp, and Shallow water. Table 4.2 summarizes the ecological characteristics of these five wetland classes (National Wetlands Working Group, 1987; Mitsch and Gosselink, 2000; Smith et al., 2007), which provides the framework for analyzing the spectral characteristics of wetlands.

Table 4.1. Acronyms and corresponding description.

Acronyms	Description
ASTER	Advanced Spaceborne Thermal Emission and Reflection Radiometer
B	Band
CWCS	Canadian Wetland Classification System
DEM	Digital Elevation Model
DVI	Difference Vegetation Index
EWCS	Enhanced Wetland Classification System
F-test	Fisher-test
ML	Maximum Likelihood
NIR	Near Infrared
NL	Newfoundland and Labrador
NDSI	Normalized Difference Soil Index
NDVI	Normalized Difference Vegetation Index
NDWI	Normalized Difference Water Index
OBIA	Object-Based Image Analysis
OA	Overall Accuracy
PA	Producer Accuracy
RF	Random Forest
RE	Red Edge
RE-NDVI	Red Edge Normalized Difference Vegetation Index
RS	Remote Sensing
SWIR	Shortwave Infrared
SAVI	Soil Adjusted Vegetation index
SAM	Spectral Angle Mapper
SAR	Synthetic Aperture RADAR
TIR	Thermal Infrared
UA	User Accuracy

Table 4.2. The characteristics of the five wetland classes specified by the CWCS.

Wetland class	Characteristics						
	Water Source	Water Table	Hydrology	Soil	pH	Nutrient Conditions	Vegetation Physiognomy
Bog	Ombrogenous	At or slightly below the surface	May have standing water	Organic	Acidic	Oligotrophic	Byrophytes (sphagnum moss), graminoids (sedges), ericaceous shrubs
Fen	Minerogenous	Fluctuating (at, slightly above, or slightly below the ground surface)	Standing or gently flowing water	Organic	Acidic to alkaline	Eutrophic, mesotrophic, oligotrophic	Bryophytes (brown and sphagnum mosses), graminoids (sedges), shrubs
Marsh	Minerogenous	At or below the ground surface	Standing or flowing water with fluctuating water levels	Mineral	Neutral to alkaline	Usually eutrophic	Aquatic emergent graminoids and shrubs
Swamp	Minerogenous	At or below the ground surface	Seasonal standing or flowing water	Organic or mineral	Alkaline to slightly acidic	Eutrophic, mesotrophic, oligotrophic	Trees and shrubs > 1m, forbs
Shallow Water	Minerogenous	At the surface	Seasonally stable standing or flowing water < 2m	Mineral	Neutral to alkaline	Usually eutrophic	Submerged and floating aquatic macrophytes

Note:

Water Source: The source of water that feeds a wetland. Ombrogenous wetlands receive water only from precipitation (rain, snow, and atmosphere), while Minerogenous wetlands receive water from multiple sources (e.g. precipitation and surface water flow).

Water Table: The upper portion of the zone of saturation, which is the area underground where the ground is totally saturated by water.

Soil: Wetland soils can be broadly defined as being Organic or Mineral. Organic soil is a result of a buildup of poorly decomposed organic (carbon) matter, while Mineral soil contains little or no organic matter, and can be described as mucky.

Nutrient Conditions: General nutrient quality of the wetland. Oligotrophic wetlands are poor in nutrients, mesotrophic wetlands have moderate levels of nutrients, and eutrophic wetlands have high levels of nutrients.

Vegetation Physiognomy: Describes the functional and morphological attributes of vegetation (e.g. shrubs have woody stems, and macrophytes are aquatic plants).

The characteristics and properties of wetlands can be effectively studied by measuring the spectral response of wetland types in different parts of the electromagnetic spectrum (Ozesmi and Bauer, 2002; Mahdavi et al., 2017b). In this regard, collecting the spectral information of wetlands can be performed using field spectrometry. However, besides the common limitations of field work (e.g. labor intensiveness, high expenses, and time limitation), inaccessibility has proven to be a major disadvantage when collecting wetland ground-truth data (Adam and Mutanga, 2009; Gallant, 2015; Mahdavi et al., 2017b). Because of these limitations, there is a need to develop a more effective and practical approach for analyzing the spectral characteristics of wetlands. In this regard, using the data collected by various optical RS satellites, characterized by different spatial, temporal, and spectral resolutions, is an optimum way to study the spectral characteristics of

wetlands (Ozesmi and Bauer, 2002; Gallant, 2015; Tiner et al., 2015; Guo et al., 2017; Mahdavi et al., 2017b).

Optical RS supplies images in various parts of the electromagnetic spectrum, including the visible and infrared (near, shortwave, and thermal). It should be noted that RS-based spectral analysis of wetlands requires knowledge of the spectral characteristics of vegetation and soils, as well as their correspondence with the vegetation cover and soil conditions in wetland areas (see National Wetlands Working Group (1987) for the characteristics of wetland species). Hyperspectral sensors may be the best choice for spectral analysis of wetlands. However, the corresponding data are generally expensive and difficult to obtain and process (Guo et al., 2017). Moreover, since there are not current hyperspectral orbital assets, it is necessary to figure out how to perform this using multispectral data. In addition, most current wetland inventories are based on the data acquired by multi-spectral satellites such as Landsat (Ozesmi and Bauer, 2002; Guo et al., 2017; Mahdavi et al., 2017b). Moreover, there are currently many satellites, which provide valuable multi-spectral imagery for users free of charge, including Landsat, Sentinel 2A, and Advanced Spaceborne Thermal Emission and Reflection Radiometer (ASTER). Thus, it is often more practical to use multi-spectral satellite data for wetland mapping, instead of hyperspectral data (Ozesmi and Bauer, 2002; Guo et al., 2017; Mahdavi et al., 2017b).

When using multi-spectral data, it is important to investigate the different spectral bands of satellites to see which provide the best separability for the wetland classes. Several studies have been conducted in this regard, most of which have argued that the Near Infrared (NIR) and Red Edge (RE) bands are the most useful for delineation of wetland types (Ozesmi and Bauer, 2002; Schmidt and Skidmore,

2003; Adam et al., 2010; Mutanga et al., 2012; Amani et al., 2017a; Mahdavi et al., 2017b). The Shortwave Infrared (SWIR) bands, which are sensitive to both soil and vegetation moisture, have also been reported to be useful for discriminating some wetland types (Crist and Cicone, 1984; Mahdavi et al., 2017b). Moreover, Thermal Infrared (TIR) bands have distinguished water bodies from vegetation and soil covers (Amani et al., 2017a; Mahdavi et al., 2017b). The TIR bands has also been reported to be helpful in identifying inundated wetlands (Leblanc et al., 2011; Mahdavi et al., 2017b).

There are currently many optical satellites that provide medium to high spatial resolution images. These data can be effectively used to obtain detailed information from wetlands. Furthermore, through the availability of medium and high spatial resolution imagery, the Object-Based Image Analysis (OBIA) can be applied in place of traditional pixel-based methods for wetlands classification. The OBIA works by grouping homogenous pixels to produce image objects and, then, uses the spatial, spectral, as well as topological features of objects to improve classification accuracy (Hay and Castilla, 2008). Many researchers have reported that the OBIA is superior to the pixel-based methods in wetland classification (e.g., Harken and Sugumaran, 2005; Laba et al., 2010 ; Mahdianpari et al., 2018; Mahdavi et al., 2017a; Amani et al., 2017b, c). For instance, Harken and Sugumaran (2005) compared the pixel-based Spectral Angle Mapper (SAM) method and a non-parametric object-based classification for wetlands classification in Iowa, USA. They applied hyperspectral imagery to overcome the limitation of multi-spectral data in providing the spectral information of wetlands, and obtained 92% and 64% Overall Accuracy (OA) using the OBIA and SAM, respectively. Laba et al. (2010) also used the IKONOS imagery for wetlands classification in Tivoli Bays, New

York, and demonstrated that wetland classification accuracy can be improved by including object-based textural features to a pixel-based Maximum Likelihood (ML) classifier. Moreover, Amani et al. (2017b) compared the results of OBIA with pixel-based classification in Newfoundland and Labrador (NL), Canada, and concluded that all wetland classes were identified more correctly using the OBIA method in terms of both visual appearance and statistical accuracies.

Considering important values of wetlands in Canada, currently, there are no comprehensive studies from Canada that analyze the spectral characteristics of wetlands using optical satellites. This study aims to investigate the separability of five wetland classes as defined by the CWCS using a combination of field data and multi-source optical satellite images. Other spectral features, including the textural and ratio features, as well as various spectral indices were also evaluated to select the most important features for discriminating different wetland class pairs. Finally, a combination of the best spectral bands and features was inserted to an object-based Random Forest (RF) algorithm to classify wetlands in five different study areas with various ecologies across NL, Canada.

4.2. Study area and data

4.2.1. Study areas

This research was carried out in five study areas (each approximately 700 km²) distributed across NL, Canada (Figure 4.1). The locations of these study areas were based on the following considerations:

- (1) For timely and efficient field work and to increase the visitation of as many wetlands as possible, the areas were located in proximity to populated areas where road access to a large amount of the study area is available.
- (2) Because NL has a largely variable geology and climate considering its size of 106,000 km² (South, 1983), the five study areas were selected to represent the islands regional variation in landscape and vegetation as adequate as possible.
- (3) Ancillary data, such as aerial photos, archived land cover maps, and Digital Elevation Model (DEM) were available from the study areas.

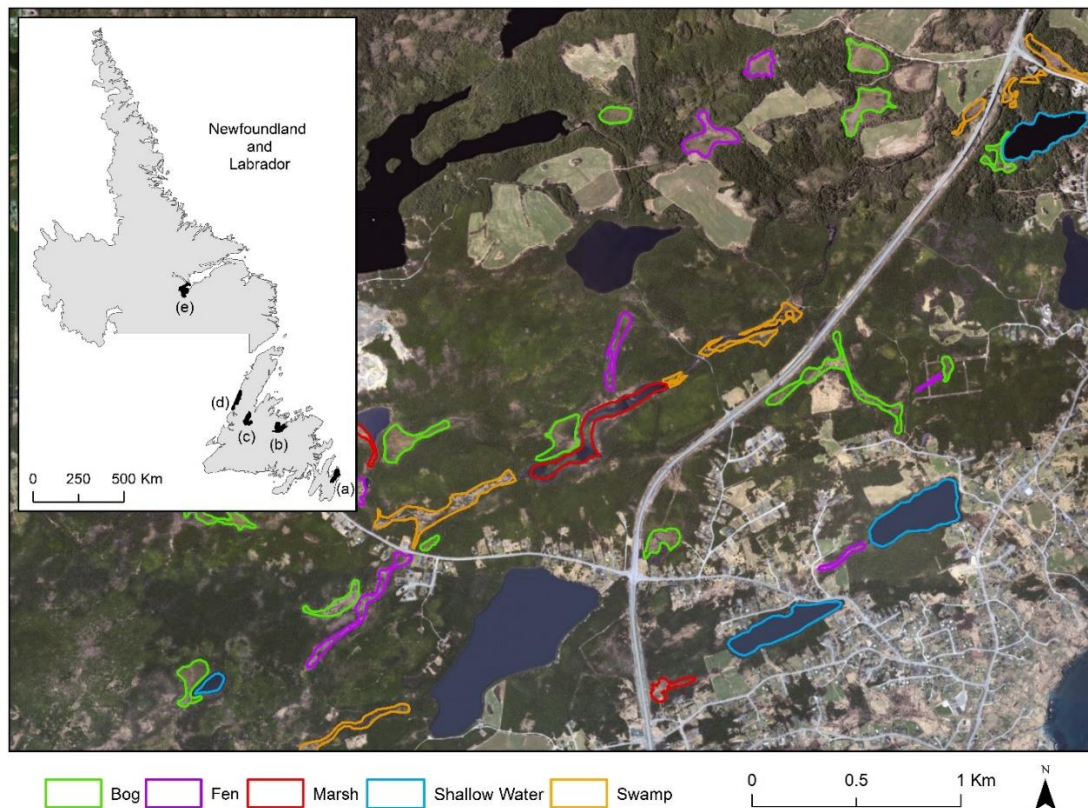


Figure 4.1. The upper left image illustrates the province of Newfoundland and Labrador, as well as the five study areas: (a) Avalon, (b) Grand Falls-Windsor, (c) Deer Lake, (d) Gros Morne, and (e) Goose Bay. The zoomed image also demonstrates the boundaries of different wetland classes obtained from the field work conducted in the Avalon study area.

The Avalon study area is located on the north-east portion of the Avalon Peninsula, on the south-east of Newfoundland, and is situated around the capital city of St. John's. Since the area is located in the Maritime Barrens ecoregion, it experiences an oceanic climate of foggy cool summers and short winters (Ecological Stratification Working Group, 1996). The landscape is also characterized by balsam fir forests, heathland dominated by ericaceous shrubs, moss, bogs, fens, and lichen

(South, 1983; Ecological Stratification Working Group, 1996), and the largest urban area presence in the province.

Closest to the Avalon is the Grand Falls-Windsor study area, in north-central Newfoundland. Being situated in the Central Newfoundland ecoregion, this study area experiences a continental climate specified by cool summers and cold winters (Ecological Stratification Working Group, 1996). In addition, the landscape is dominated by forests of balsam fir and black spruce, kalmia heathland, peatland (South, 1983; Ecological Stratification Working Group, 1996), and several urban areas.

The Deer Lake study area is approximately 130 km west of Grand-Falls Windsor, within the same Central Newfoundland ecoregion characterized by a continental climate (Ecological Stratification Working Group, 1996). Major land cover includes balsam and black spruce forest and peatlands (South, 1983). There is comparatively minor portions of urban areas within this study area, with only the small settlement of Howley within its borders.

The Gros Morne study area is located on the west coast of Newfoundland on the Great Northern Peninsula, adjacent to the Gulf of St. Lawrence. The study area falls in the Northern Peninsula ecoregion, which has an oceanic climate and experiences wind and fog (Ecological Stratification Working Group, 1996). In this study area, land cover is dominated by extensive low-lying peatlands (South, 1983). Moreover, moving east across the study area, the elevation dramatically increases, and the mountainous areas are covered in balsam fir and black spruce forests (South, 1983). Additionally, the Gros Morne National Park is located within the study area boundaries, as are several small communities, including Cow Head.

Goose Bay is the only study area located on the mainland near Happy Valley-Goose Bay, the largest town in Labrador. This study area falls within the Lake Melville ecoregion, characterized by humid but cool summers and cold winters (South, 1983). The landscape is covered by balsam fir, black spruce, white birch trees, and large portions of lichen dominated woodland. Furthermore, permafrost within wetlands is common in this study area due to the northern temperatures (Ecological Stratification Working Group, 1996).

4.2.2. Field data

The field work was conducted in all five study areas between July and October of 2015 and June and August of 2016 by 4 field teams made up of biologists and wetland ecologists. The goal of the field work was to ground-truth and classify five wetland types to act as testing and training data for the development of methods for the remote classification of wetlands across NL. Potential wetland sites within each study area were selected for investigation using the visual analysis of aerial and satellite imagery in the study areas. The requirements for site selection were as follows:

- (1) The site must be within 200 m of public road and pathways for ease-of accessibility.
- (2) The site should be located on public land.
- (3) The site must be a good example of one of the five wetland classes described by the CWCS.

If the visited site was in-fact a wetland, it was: (1) classified following the CWCS key, (2) one or several GPS points were collected within or as close to the wetland

as possible, (3) several pictures were taken, and (4) ancillary notes, including information on the dominant vegetation, hydrology, and surrounding upland, were recorded. It is also worth mentioning that there was no restriction on the size of wetlands during the first year (2015) of field work, resulting in several of the classified wetlands being quite small. However, more effort was paid to collecting wetlands of a size > 1 hectare where possible during the following year (i.e. 2016).

After completion of the field work, the GPS points were imported into ArcMap 10.3.1. Then, boundary delineation was conducted with the aid of several types of remotely sensed imagery, including high resolution ortho-photography, RapidEye imagery, and the satellite imagery base-map provided by Esri through the ArcMap. Boundaries were primarily delineated following the visible transition of dominant vegetation from wetland (the type of vegetation depends on the wetland class) to surrounding upland. Additionally, boundaries were determined conservatively to avoid including transitional areas where wetland vegetation may be mixed with upland vegetation. Table 4.3 provides the information of the total field samples (polygons) used in this study. It should be noted that the extracted polygons were the base of all analyses conducted in this study.

Table 4.3. The number of field samples (polygons) collected over five study areas.

Study area	Class	Number of polygons	Area (ha)
Avalon	Bog	83	269
	Fen	39	80
	Marsh	50	62
	Swamp	45	47
	Shallow Water	40	110
Grand Falls-Windsor	Bog	30	357
	Fen	61	194
	Marsh	45	102
	Swamp	30	47
	Shallow Water	21	52
Deer Lake	Bog	31	236
	Fen	54	121
	Marsh	24	19
	Swamp	40	56
	Shallow Water	23	68
Gros Morne	Bog	38	779
	Fen	31	98
	Marsh	31	50
	Swamp	42	48
	Shallow Water	27	64
Goose Bay	Bog	28	395
	Fen	29	139
	Marsh	21	78
	Swamp	23	35
	Shallow Water	11	19

4.2.3. Satellite data

In this study, data collected by four optical satellites, RapidEye, Sentinel 2A, ASTER, and Landsat 8, were investigated in late spring (Table 4). June was selected as this was the month that had the greatest amount of satellite data covering each of the study areas available for this research. In addition, each of the selected

satellites has valuable characteristics, which makes them suitable for operational wetland mapping and monitoring (Gallant 2015; Chatziantoniou et al., 2017; Amani et al., 2017b; Araya-López et al., 2018). For example, Gallant (2015) has mentioned that Landsat sensors have been traditionally popular for wetland mapping because of their rich temporal archive, wide coverage, and no cost for users. Moreover, except for RapidEye, the images captured by the other three satellites are freely available for users and, therefore, are appropriate for regional and national wetland studies. It is worth noting that since the images were acquired at different times (between June 5 and 25), various solar zenith angles can affect the results slightly, which was not considered in this study. Moreover, the satellites contained different spatial resolutions, which could affect the analyses slightly and was not considered in this research.

Table 4.4. The satellite data used in this study.

Study area	RapidEye	Sentinel 2A	ASTER	Landsat 8
Avalon	2015/06/18	-	2015/06/05	2015/06/19
Grand Falls- Windsor	2015/06/10	-	-	2015/06/10
Deer Lake	2015/06/18	2016/06/12	-	-
Gros Morne	2015/06/18	2016/06/25	2015/06/25	2015/06/15
Goose Bay	-	-	2015/06/23	2015/06/22

The characteristics of the applied spectral bands are also demonstrated in Table 4.5. According to this table, different spectral bands covering various parts of the electromagnetic spectrum, including visible, NIR, SWIR, as well as TIR, were

evaluated for separability analysis of wetlands in this study. It should be noted that because of the uncertainties involved with the SWIR bands of ASTER (bands 4-9) and the TIR band (band 11) of Landsat 8, they were excluded from this study. Moreover, the aerosol, water vapor, and cirrus bands of Sentinel 2A (bands 1, 9, and 10) and Landsat 8 (bands 1 and 9) are inappropriate for separability analysis of wetlands and, thus, were not investigated.

Table 4.5. The spectral bands of RapidEye, Sentinel 2A, ASTER, and Landsat 8 used in this study (The wavelength range for each band is provided in the parentheses, and is in micrometers).

RapidEye	Sentinel 2A	ASTER	Landsat 8
	B2_Blue (0.46-0.52)		B2_Blue (0.45-0.51)
	B3_Green (0.54-0.58)	B1_Green (0.52-0.6)	B3_Green (0.53-
B1_Blue (0.44-0.51)	B4_Red (0.65-0.68)	B2_Red (0.63-0.69)	0.59)
B2_Green (0.52-	B5_RE (0.698-0.712)	B3N_NIR (0.76-0.86)	B4_Red (0.64-0.67)
0.6)	B6_RE (0.733-0.747)	B10_TIR (8.13-8.48)	B5_NIR (0.85-0.88)
B3_Red (0.63-0.69)	B7_RE (0.773-0.793)	B11_TIR (8.48-8.83)	B6_SWIR (1.57-
B4_RE (0.69-0.73)	B8_NIR (0.784-0.9)	B12_TIR (8.93-9.28)	1.67)
B5_NIR (0.76-0.85)	B8A_RE (0.855-0.875)	B13_TIR (10.25-	B7_SWIR (2.11-
	B11_SWIR (1.565-	10.95)	2.29)
	1.655)	B14_TIR (10.95-	B10_TIR (10.6-
	B12_SWIR (2.1-2.28)	11.65)	11.19)

4.3. Methods

4.3.1. Preprocessing of satellite data

Since all the images were already geometrically corrected with accuracy of less than one pixel size, no further geometric corrections were carried out. Regarding the radiometric and atmospheric correction of the satellite data, the following steps were performed on each optical imagery to obtain the surface reflectance and temperature values.

- (1) The RapidEye surface reflectance data were derived using the Atmospheric and Topographic Correction Software (ATCORE) module of the PCI Geomatica software. The procedure is explained in details in Richter (2011).
- (2) The top of atmosphere reflectance Sentinel 2A data (Level 1C products) were first downloaded from <https://scihub.copernicus.eu/>. Then, these datasets were converted to surface reflectance data using the Sen2Cor version 2.3.1 radiative transfer atmospheric correction code (downloaded from the website of ESA Science Toolbox Exploitation Platform (STEP): <http://step.esa.int/main/third-party-plugins-2/sen2cor/>). More details regarding the Sen2Cor processing can be found in Gascon et al. (2017) and Li et al. (2018).
- (3) The ASTER level 2 surface reflectance products (AST_07XT) were used in this study (https://lpdaac.usgs.gov/dataset_discovery/aster/aster_products_table/ast_07xt_v003; Iwasaki and Tonooka, 2005). Regarding the thermal bands of ASTER, the level 2 Land Surface Temperature (LST) products (AST_08) were used (https://lpdaac.usgs.gov/dataset_discovery/aster/aster_products_table/ast_08_v003).

(4) The Landsat 8 surface reflectance data (level 2 products) were downloaded from <https://espa.cr.usgs.gov>, and were used. The Single-Channel method was also implemented to derive the LST values from the band 10 of Landsat 8.

4.3.2. Variance analyses of field samples

Field samples collected for RS applications should contain the highest possible accuracy. However, since wetlands are complex environments and each wetland class can contain several subclasses (National Wetlands Working Group, 1987), the spectral responses of different field samples within one wetland type can vary considerably. Consequently, when analyzing the spectral responses of different field samples from a particular wetland class, the values may not be in the same range and a large variance can be observed. Therefore, the variation of different field samples from each wetland class should be initially analyzed. To do this, the variance value of samples in each spectral band was calculated for each wetland class using Equation (1). Then, the spectral bands for which the field samples' values had significant variation were removed from the rest of the analyses.

$$Var = \frac{1}{N - 1} \sum_{i=1}^N (x_i - \mu)^2 \quad (4.1)$$

in which x_i indicates the value of a field sample, μ is the mean value of samples, and N is the number of field samples in a spectral band.

After analyzing the variance values of the field samples in individual classes, the variations of field samples within a spectral band were investigated for wetland class pairs. In fact, before performing any separability analysis of different classes in an image using spectral bands, we should be certain whether the classes of interest are separable using the applied spectral bands. This matter is more important for some RS applications, such as wetland classification, where the spectral characteristics of various field samples are different for a wetland class, as explained above. To be more precise, when analyzing the separability of two wetland classes using any spectral band, the variance value of field samples must be greater between rather than within classes in that particular band. To explore this, the Fisher-test (F-test) statistics (Equation (2)) was used and evaluated for each pair of wetland classes. Then, if the F-test value was less than one, we removed that spectral band for the class pairs from the subsequent analyses.

$$F = \frac{Var_B}{Var_W} \quad (4.2)$$

where Var_B and Var_W indicate the between and within variance values in each class pair, respectively. It is also worth mentioning that the F-test statistics can also be used for separability analysis, in which the class pair that has higher values in spectral band(s) will be more separable using the corresponding band(s).

4.3.3. Separability measures

So far, different separability measures have been developed and applied to perform feature selection with inconsistent results in RS science. It has been

frequently acknowledged that there is not a unique separability measure to select the most useful spectral band(s) for distinguishing various land cover classes (Yeung et al., 2005; Adam et al., 2010; Manevski et al., 2011; Proctor et al., 2013). Therefore, it was difficult to use the best method for selecting the most useful band or band combinations for discriminating different pairs of wetland classes in this study. After studying various separability measures, we ultimately implemented and used two distance measures of the T-statistics and U-statistics, calculated from the parametric t-test method and the non-parametric Mann-Whitney U-test method, respectively.

4.3.3.1. T-test

The t-test is a parametric test that determines whether the means of two classes are statistically different (Fay and Proschan, 2010; Mwangi et al., 2014). According to the pair-wised separability analysis in this study, an independent two-sample t-test was used. It has been reported that the two-sample t-test performs well, provided that the sample size of each class is greater than 15, and regardless of the distribution of data (Minitab, 1991; Ryan and Joiner, 2001). Additionally, the t-test is fast and straightforward to implement, and usually has more statistical power than most non-parametric tests (Minitab, 1991; Ryan and Joiner, 2001). The distance measure derived from the t-test method (called T-statistics) has different forms based on the assumptions of equal or unequal sample sizes and/or variances (Fay and Proschan, 2010; Mwangi et al., 2014). Since the sample size of various wetland classes in this study differed and the variance values varied significantly (see the previous subsection), the following form of the t-statistics, which assumes unequal sample sizes and unequal variances, was employed.

$$T - Statistics = \frac{|\mu_1 - \mu_2|}{\sqrt{\frac{Var_1}{n_1} + \frac{Var_2}{n_2}}} \quad (4.3)$$

in which μ_i , Var_i , and n_i indicate the mean, variance, and the number of field samples of class i , respectively.

4.3.3.2. Mann-Whitney U-test

The Mann-Whitney U-test is a non-parametric method that does not assume a normal distribution for the samples and evaluates the variance values of the data replaced by their ranks. In this method, instead of the difference in mean values, that of the median values of each spectral band is considered (Lehmann, 2004). It has been reported that if the data is assumed to have a normal distribution, the Mann-Whitney U-test has an efficiency of approximately 0.95 compared to the t-test (Lehmann, 2004). However, when the distribution is not normal and the sample size is large, the Mann-Whitney U-test is more efficient than the t-test (Conover, 1980). Furthermore, unlike parametric methods, the Mann-Whitney U-test is not seriously affected by outliers (Minitab, 1991; Ryan and Joiner, 2001). In this study, the U-statistics calculated from the Mann-Whitney U-test method (Equation (4)), was used to evaluate the amount of separability between the wetland class pairs.

$$U - Statistics = \min(U_1, U_2) \quad (4.4)$$

where U_i is the U value calculated for class i using the following equations:

$$U_1 = n_1 n_2 + \frac{n_1(n_1 + 1)}{2} - R_1 \quad (4.5)$$

$$U_2 = n_1 n_2 + \frac{n_2(n_2 + 1)}{2} - R_2 \quad (4.6)$$

in which n_i and R_i are the number of samples and the sum of the ranks for class i , respectively. It is also worth mentioning that since the number of field samples in this study was more than 20 for all wetland classes, analogous to the non-equal number of samples from each wetland classes did not affect the spectral analyses.

4.3.4. Separability analyses of other features

The final purpose of this research was the object-based classification of wetlands using multi-source satellite imagery. Although we could insert the most informative spectral bands, obtained from the separability analyses of spectral bands (calculated from the mean values of field samples), into the classification and produce the classified maps of wetlands, this will not result in the highest classification accuracy. The reason is that there may still be some classes that are not separable using only the mean values of samples. Since the object-based method was used in this study, many features could be considered for separability analysis of different wetlands and, consequently, for wetland classification. Therefore, besides the mean values of spectral bands, various spectral indices, texture and ratio features (Table 4.6) were also evaluated for distinguishing

wetland class pairs, as well as all wetland classes. To do this, the procedures, described in subsections 3.1 and 3.2 were performed on these features.

Table 4.6. The spectral indices, textural and ratio features evaluated in this study for separability analyses of wetland types.

	$Brightness, NDWI = \frac{Green - NIR}{Green + NIR}, DVI = NIR - Red, NDVI =$
Spectral indices	$\frac{NIR - Red}{NIR + Red}, RE-NDVI = \frac{NIR - RE}{NIR + RE}, NDSI = \frac{SWIR - NIR}{SWIR + NIR}, SAVI =$
	$\frac{(1+L)(NIR-Red)}{NIR+Red+L}; L = 0.5$
Ratio features	$\frac{Blue}{Brightness}, \frac{Green}{Brightness}, \frac{Red}{Brightness}, \frac{RE}{Brightness}, \frac{NIR}{Brightness}, \frac{SWIR}{Brightness}$
Texture features	Standard deviation of the polygons obtained from all spectral bands of the satellites.

4.3.5. Wetland classification using selected features

After performing the separability analyses of the spectral bands and the features listed in Table 4.6, the selected features were injected into an object-based RF classifier to obtain wetland maps of the study areas. The RF algorithm was selected because it performed better than other classifiers based on our previous studies (Amani et al., 2017b, c; Mahdavi et al., 2017a). RF has also been successful in many studies of classification of vegetation and complex environments, such as wetlands (Adam et al. 2010; Mutanga et al., 2012; Mahdianpari et al., 2017). Moreover, one of the benefits of using the RF classifier is that various data sources from different measurement scales can be easily incorporated into the classification (Adam et al., 2010). Since all the images used in this study had medium spatial resolution, the object-based method was used instead of the traditional pixel-based method. The

multi-resolution algorithm was first used to segment the image using the spectral and spatial information and, then, the classification is performed on the objects as the minimum unit of analysis (Duro et al., 2012). Both segmentation and classification were performed in the eCognition™ 9 software (Definiens, 2009). It is worth noting that both RF and multi-resolution algorithms contain different input parameters, which should be carefully selected to obtain a high classification accuracy. This matter is discussed in more details in our previous study (see Amani et al., 2017b).

4.4. Results and discussion

4.4.1. Variance analyses of field samples

As mentioned in subsection 3.1, Equation (1) was used for variance analysis of field samples and only the spectral bands for which the corresponding field samples had relatively similar reflectance values (lower variance) were used for the next experiments (see Figure 4.2 (a) as an examples). Figure 4.2 (b) illustrates a spectral band, for which the variation of reflectance values of field samples was high and, therefore, the band was removed from the next analyses. According to Table 4.5, there were 30 spectral bands extracted from four different optical sensors, from which the spectral responses of five wetland types were analyzed. Consequently, there were $30 \times 5 = 150$ features extracted from the images. Finally, 10 features were removed from the subsequent experiments based on variance values calculated from Equation (1).

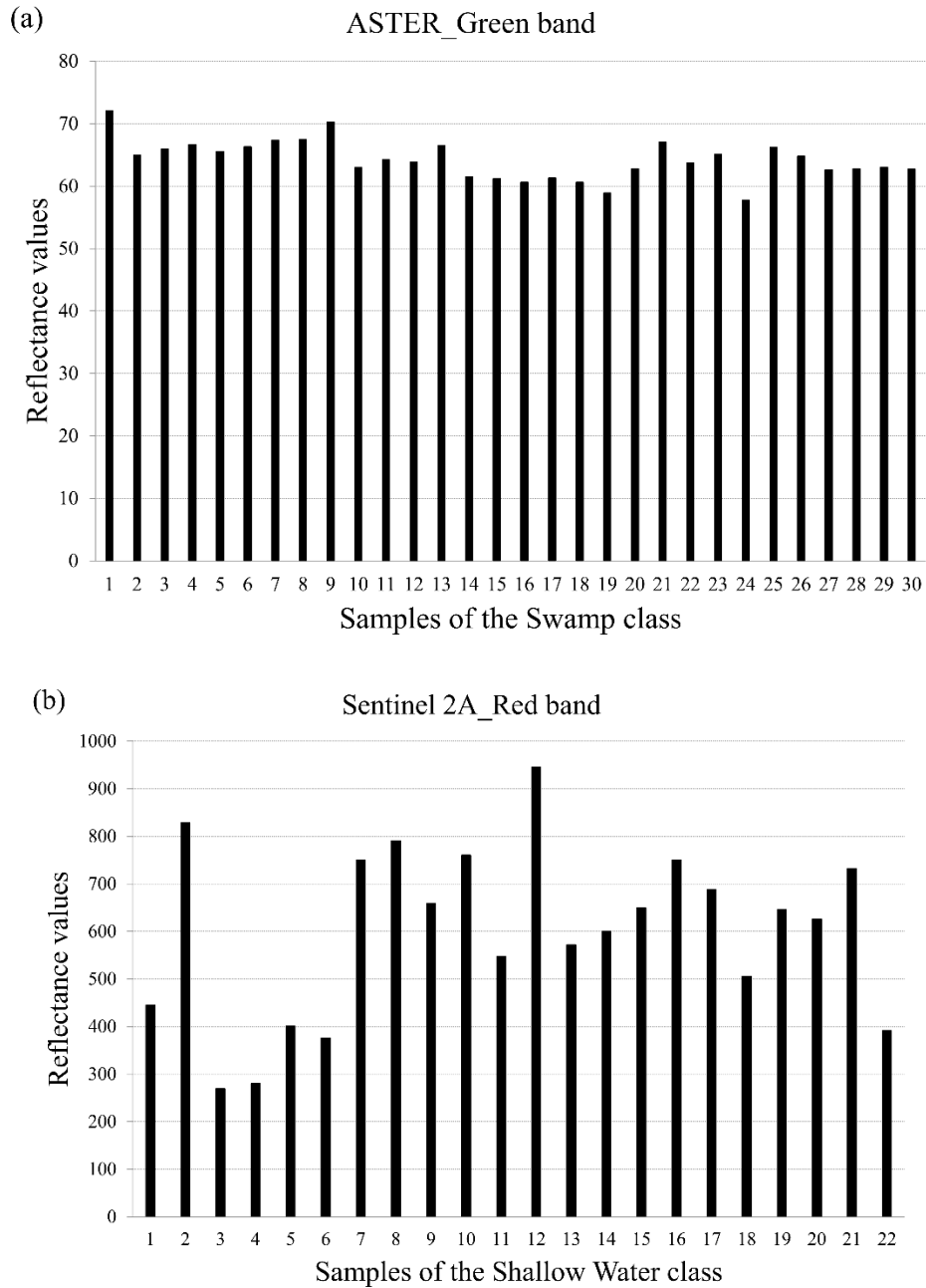


Figure 4.2. Spectral values of the field samples of two wetland classes.

After performing variance analyses on the individual wetland classes, variance analyses on wetland class pairs were then performed using the F-test statistics (Equation (2)). In this step, 13 features were removed from the next experiments.

Finally, an attempt was made to select the best features (out of 127 features) to classify wetlands using separability analyses, which are discussed in more detail in the next three subsections.

4.4.2. Separability analyses of spectral bands

Figure 4.3 illustrates the amount of separability between different wetland class pairs in various spectral bands, which was obtained using two measures: T-statistics and U-statistics. Based on the values of the T-statistics and U-statistics illustrated in Figure 4.3, the most useful spectral band(s) for distinguishing the different pairs of wetland types is also summarized in Table 4.7. As evident from this table, only one band is recommended for separating some pairs, however, multiple spectral bands are recommended for separating others. The separability of wetlands is also visualized by plotting the spectral signatures of the classes in Figure 4.4.

As clear from Figure 4.3 and Table 4.7, the results obtained by the T-test and U-test were not always consistent. This was expected as each of these methods considers different assumptions for samples distribution. However, both separability methods were considered in this study to obtain a comprehensive conclusion. It should be noted that the results obtained by the U-test were more trustful compared to the T-test in this study because the variance values of field wetland samples were considerably high (see subsection 3.1) and the data did not generally follow a normal distribution. Finally, the following results were obtained by considering the results of both distance measures.

The NIR band was the most useful spectral band for discriminating wetland classes. The NIR band is the most important band for vegetation studies, and is a useful band to study the biomass content of vegetation and its health. The NIR band is also helpful in distinguishing water bodies from land because water strongly absorbs the NIR light, while soil and vegetation reflects more energy in this region of spectrum (Schmidt and Skidmore, 2003; Manevski et al., 2011). Consequently, the NIR band is often the most helpful spectral bands in wetland studies, for which vegetation and water are two important components. For example, in all cases except for Bog/Swamp, Fen/Swamp, Marsh/Shallow Water, the NIR band was the best band to discriminate wetland class pairs (see Figure 4.3 and Table 4.7). According to Figure 4.3, the Landsat 8 NIR band produced the largest separability for wetland class pairs in 6 cases out of 10 cases. The results obtained from the spectral signatures (Figure 4.4) also supported these results, where the greatest variation was observed in the NIR bands. It is also worth noting that this difference was most significant for the Shallow Water class.

The RE bands produced the second best discrimination between wetland class pairs, as well as all wetland classes. The RE band provides valuable information about both biochemical and biophysical parameters of wetlands, such as chlorophyll content and the Leaf Area Index (LAI). This band is also useful in assessing the water deficit in wetland biomass (Filella and Penuelas, 1994; Mutanga and Skidmore, 2007). Moreover, the RE band has been widely used to monitor vegetation growth and, thus, was very useful for distinguishing wetlands, which are highly dynamic environments. For instance, in 5 out of 10 cases, the RE bands of the RapidEye and/or Sentinel 2A were selected as the best spectral bands using either the T-statistics or U-statistics in separating wetland type pairs (Figure

4.3). The RE bands were also among the best spectral bands to discriminate the Marsh class from other wetland classes using both the T-statistics and U-statistics (see Table 4.7). Moreover, more variation in the response of wetland classes was observed in the RE bands compared to that of the SWIR and visible bands (Figure 4.4).

Comparing the visible bands, the red band had the strongest power to delineate the wetland classes. This band was also better than the SWIR and TIR bands in the separation of wetland classes. The red band is useful in studies of vegetation, soil types, and geology. This spectral band is mostly used for detecting chlorophyll absorption in vegetation, as well as for evaluating the composite of the soil, where soils with rich iron-oxide have a high reflectance in this band (Schmidt and Skidmore, 2003; Manevski et al., 2011). Therefore, this band was very helpful for discriminating several wetlands, which contain different types of soils and vegetation with various amounts of chlorophyll content. For instance, according to the spectral signatures obtained from different satellites (Figure 4.4), bog wetlands reflected greater energy in the red band compared to the other wetland classes. The reason may be that bog wetlands in NL contain more sphagnum moss, which often has a red or orange appearance (see Figure 4.5. Note the red appearance of bog due to the presence of red sphagnum moss). As a consequence, this band was one of the best spectral bands to distinguish the Bog class from other wetland classes (see Figure 4.3 (e and f) as examples). In addition, the spectral signatures of wetlands obtained from the RapidEye and ASTER data also presented some differences between mean values of the Bog class from the other wetland classes in the red band (Figure 4.4). It is also worth mentioning that the red band has been used in distinguishing between vegetation and man-made

objects (Shettigara et al., 1995), and it was expected to be useful in delineating wetlands from urban areas.

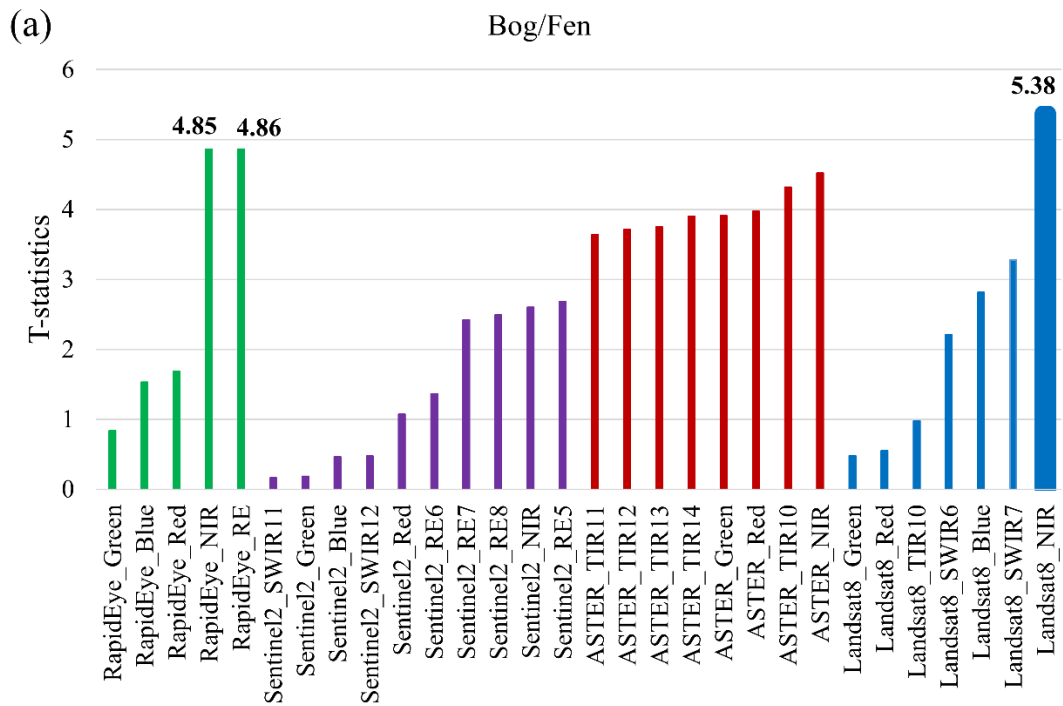
The SWIR bands exhibited poor separability, and were only helpful in some cases (e.g. for discriminating the Shallow Water class from the Bog and Fen classes). The SWIR band is sensitive to the moisture content in soil and vegetation. The reflectance in this band decreases as moisture content increases. This is helpful for discriminating wet from dry land covers (Crist and Cicone, 1984). However, since all types of wetlands are generally wet, this spectral band was not as informative as the NIR, RE, and red bands. As expected, this band is more useful for discriminating between wetlands and uplands.

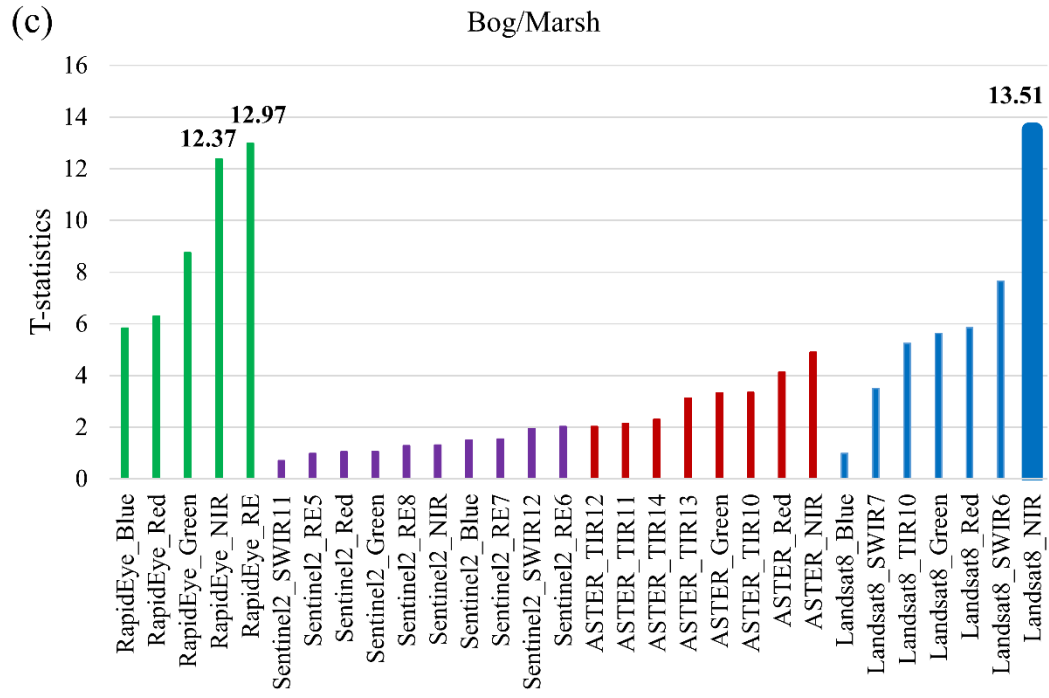
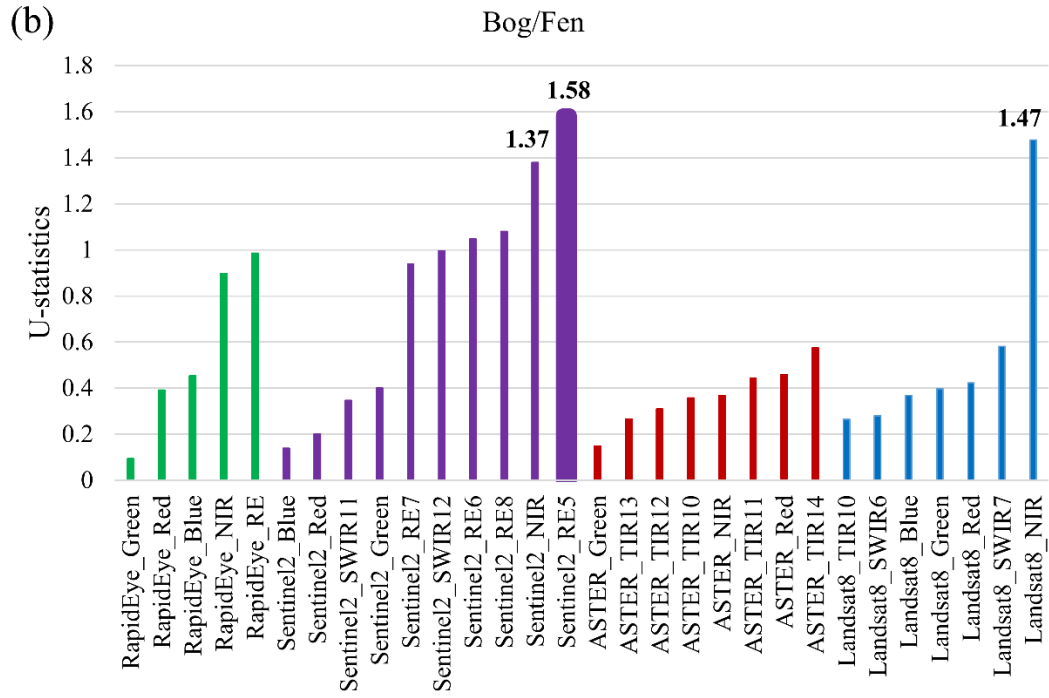
The green band is also useful in assessing plant vigor, as well as in isolating different types of vegetation, where healthy and green vegetation reflects more energy in this region (Adam et al., 2010). Although the green bands were not selected as the best spectral bands in Table 4.7, they were more appropriate for distinguishing wetland class pairs (Figure 4.3), as well as all wetland classes compared to the blue and TIR bands.

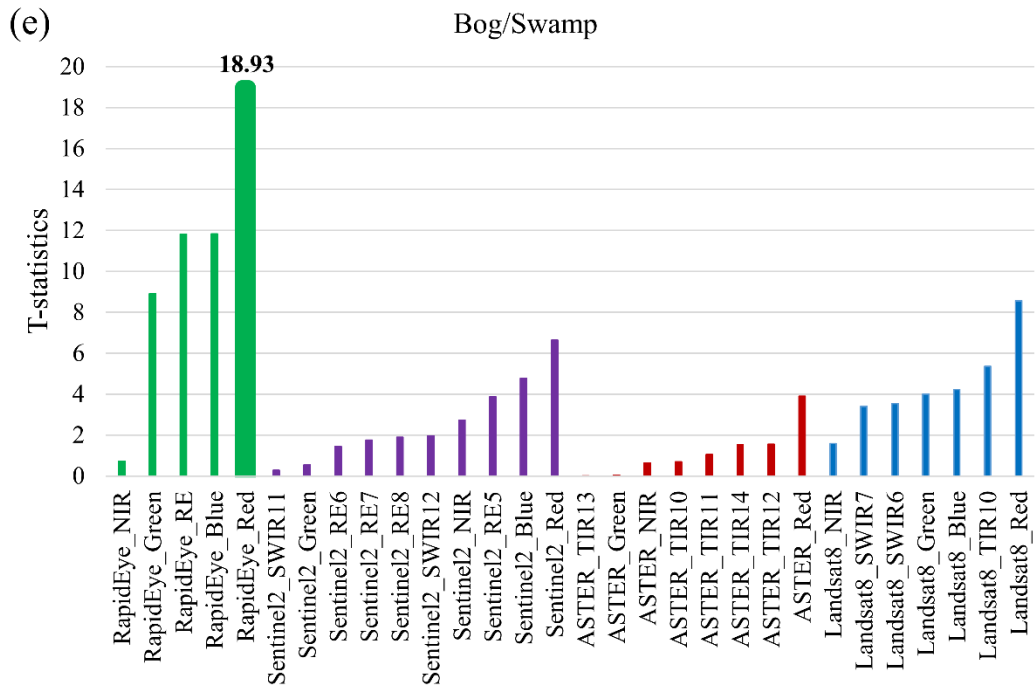
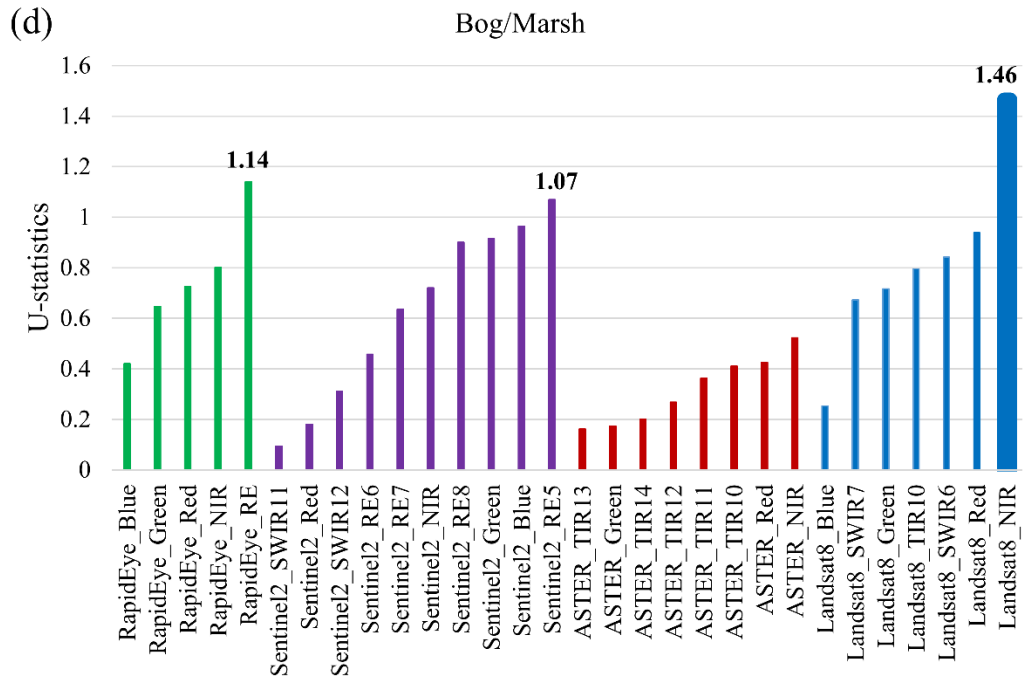
Although several studies have argued that the TIR bands had potential for the separability of water bodies from wetland vegetation (e.g. Leblanc et al., 2011; Amani et al., 2017a), this band was not as helpful as the other spectral bands for separating various wetland classes. One main reason for this result may be due to the coarse spatial resolution of TIR bands in satellite data compared to the other spectral bands resulting in mixed pixels.

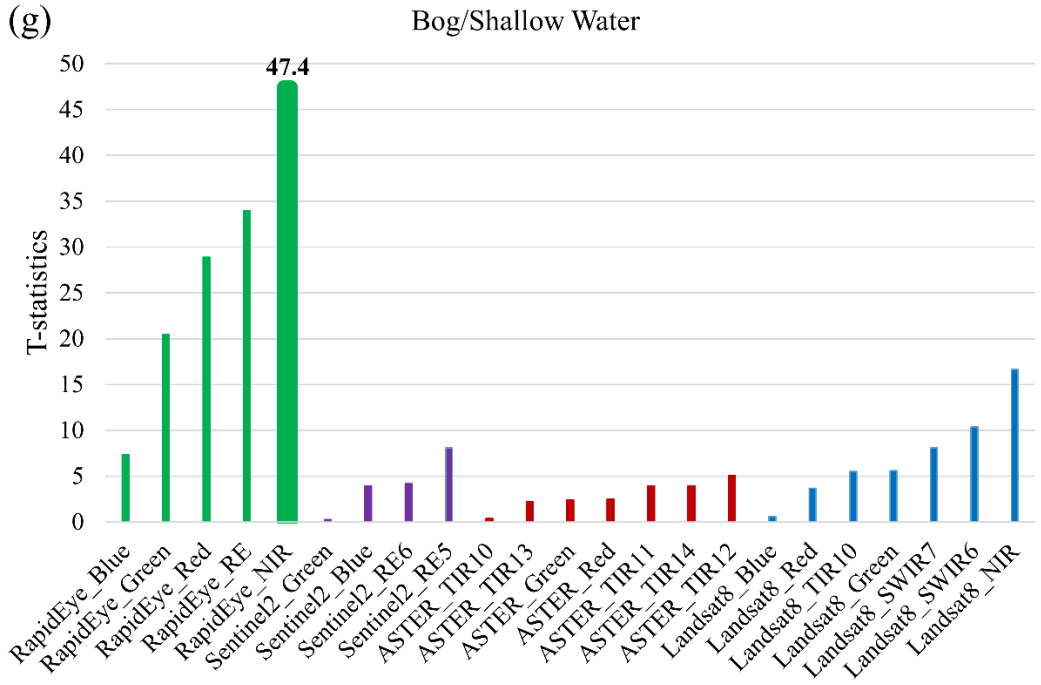
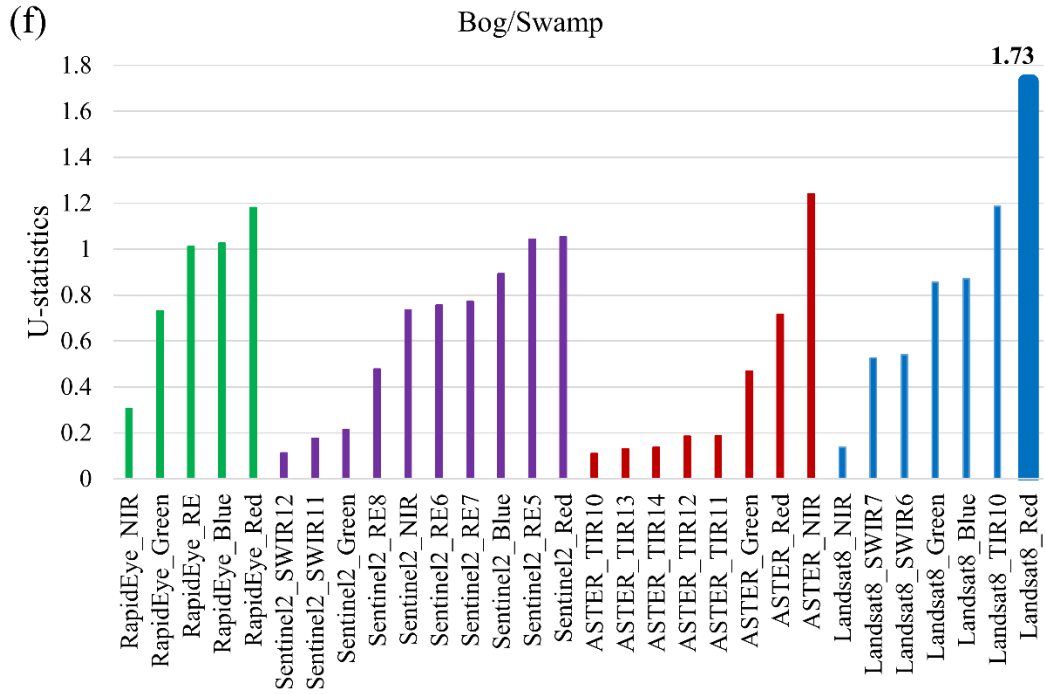
In addition, the result of the analyses in this study indicated that the pairs of wetland classes were more difficult to distinguish in the blue band, in which

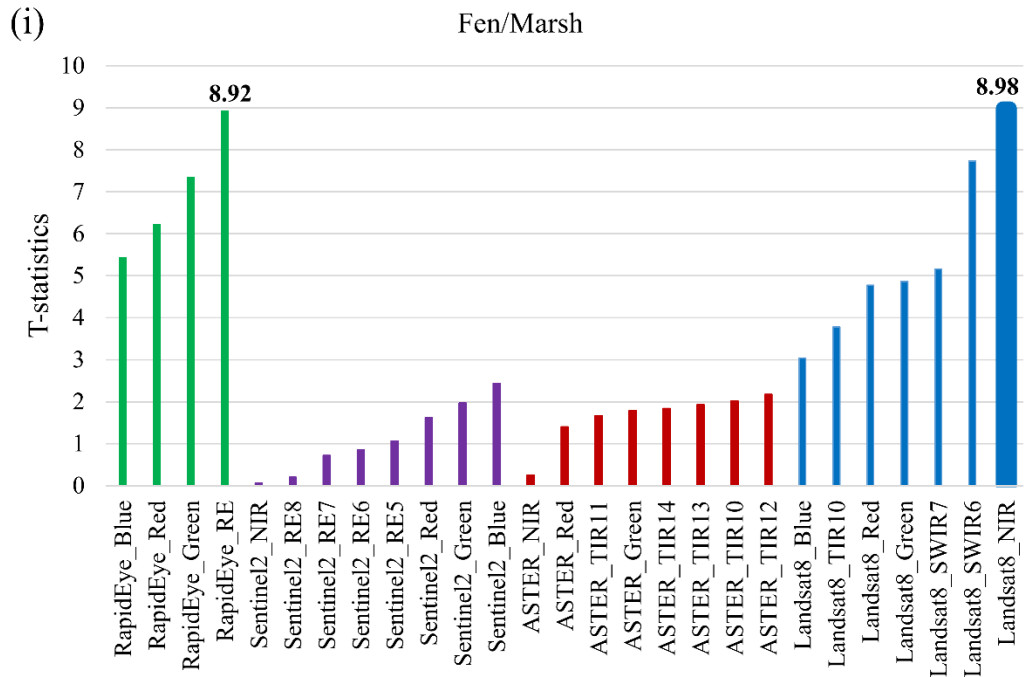
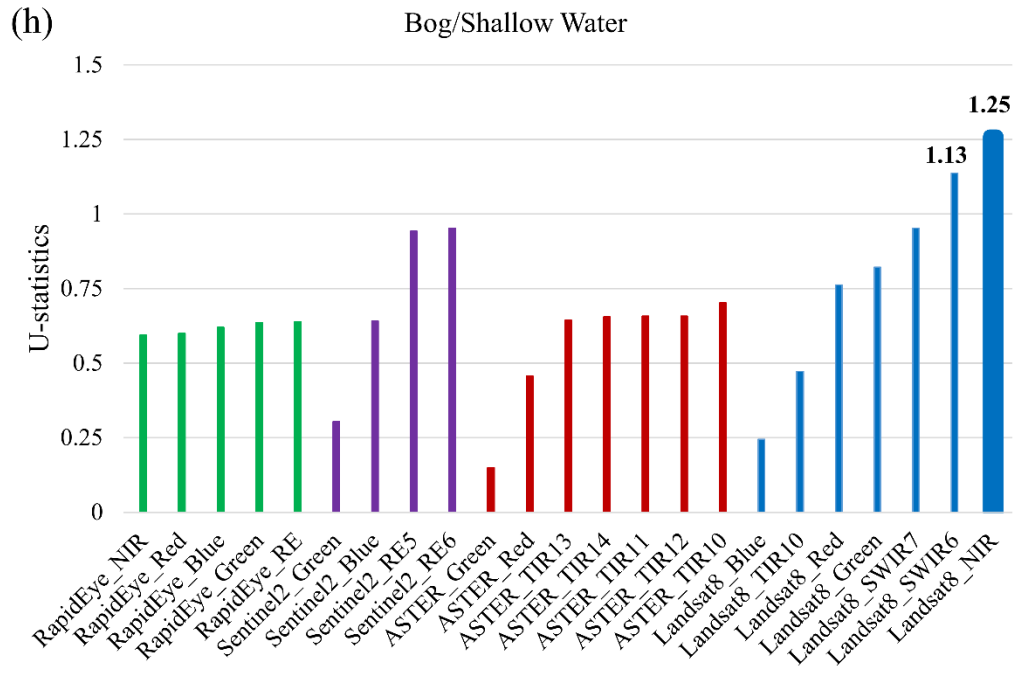
wetland classes were spectrally similar. For instance, as demonstrated in Figure 4.4, the highest overlap in the spectral signatures of wetlands was observed in the blue band of the satellites.

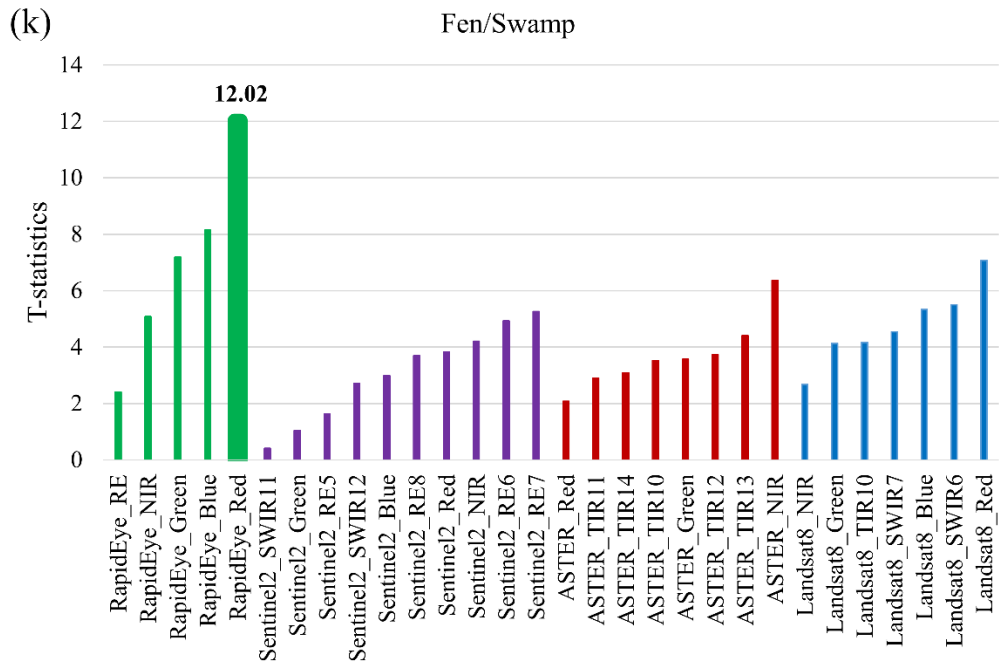
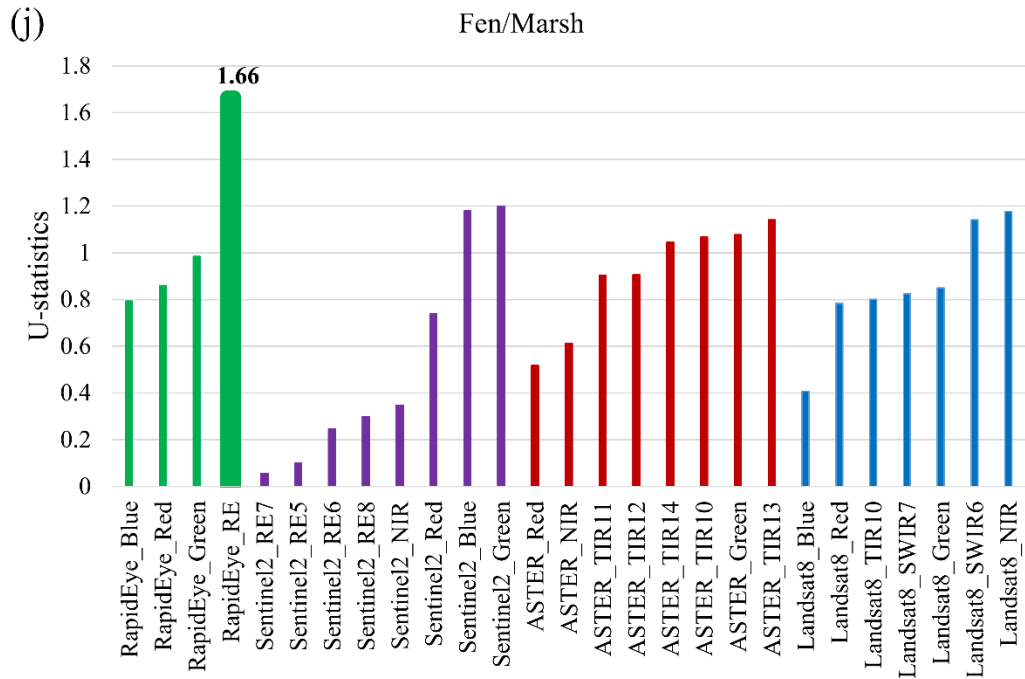


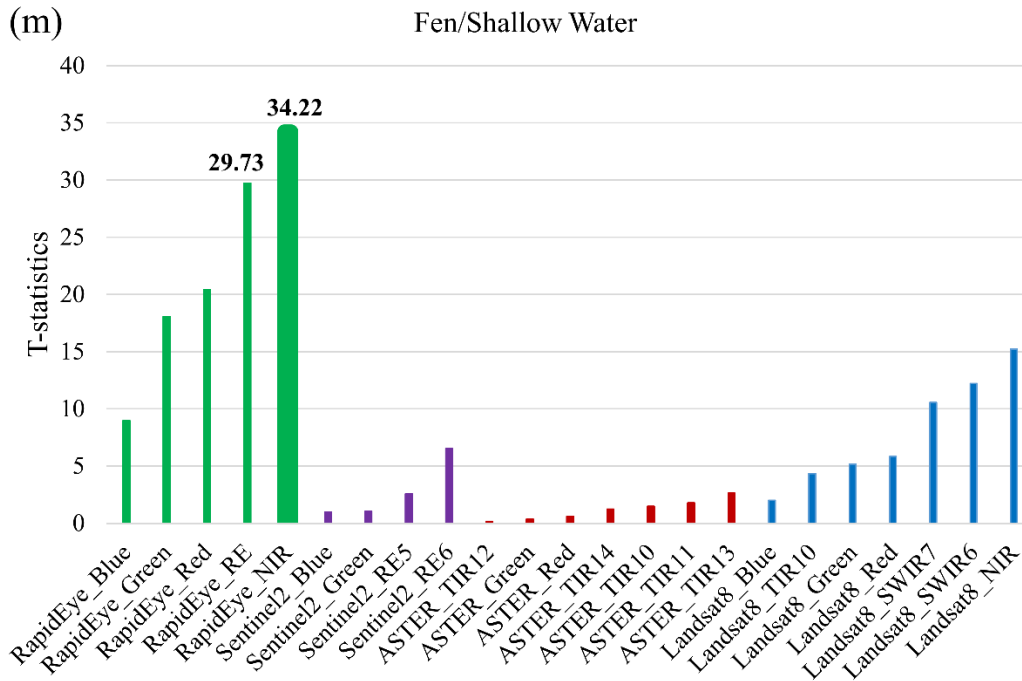
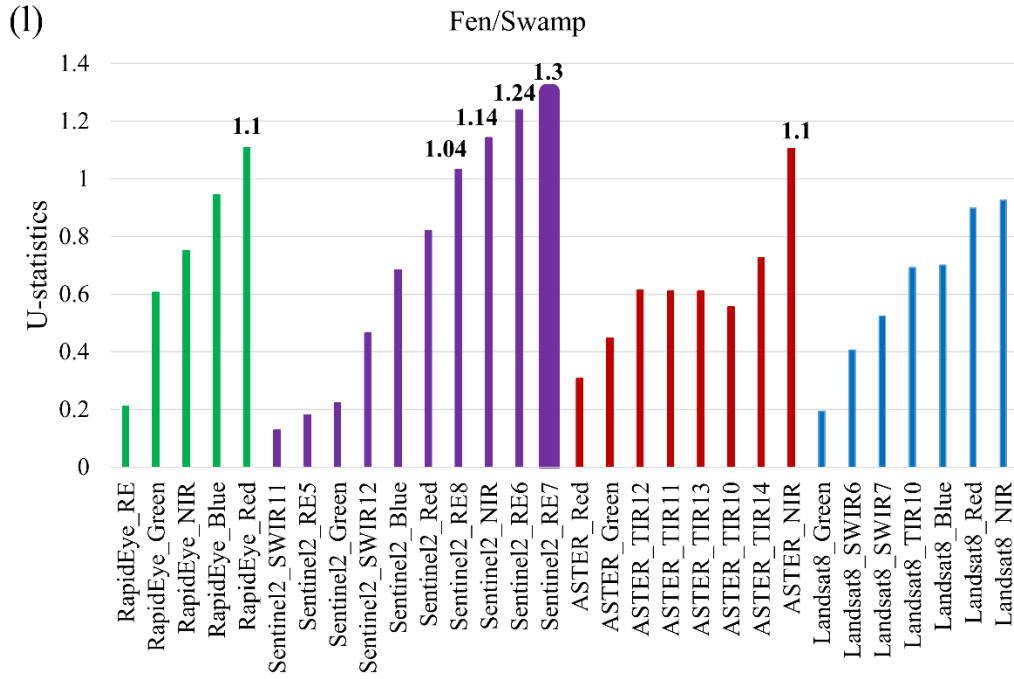


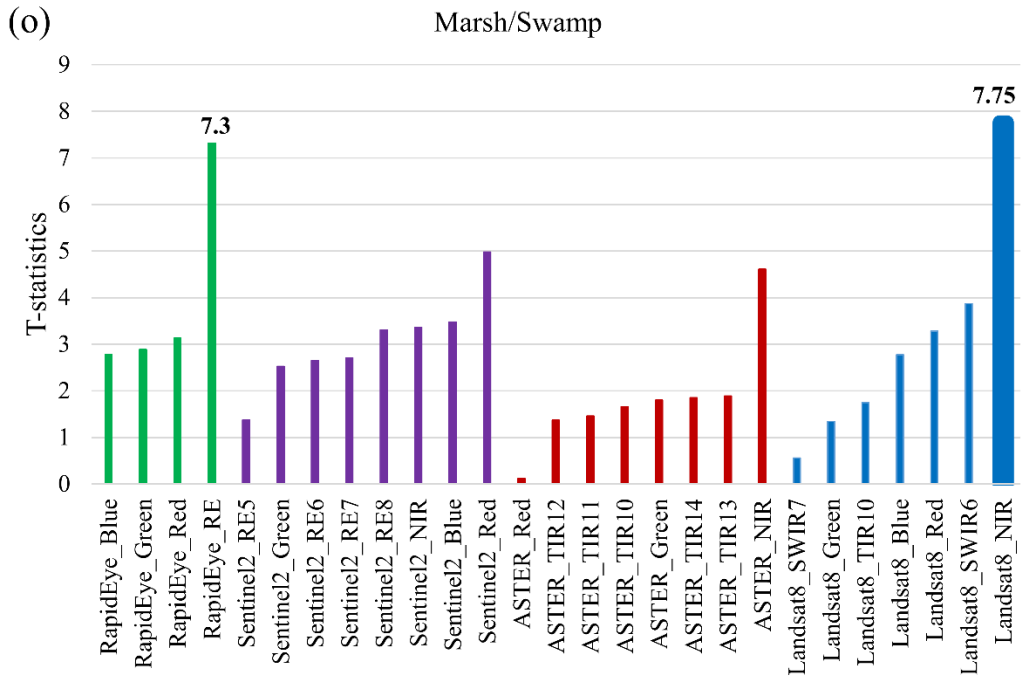
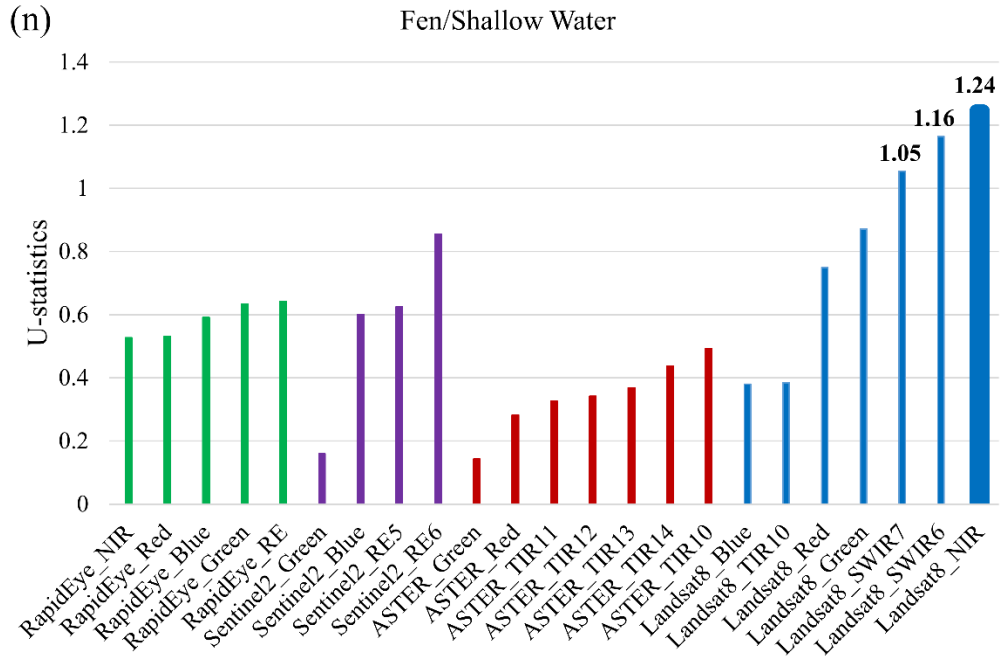


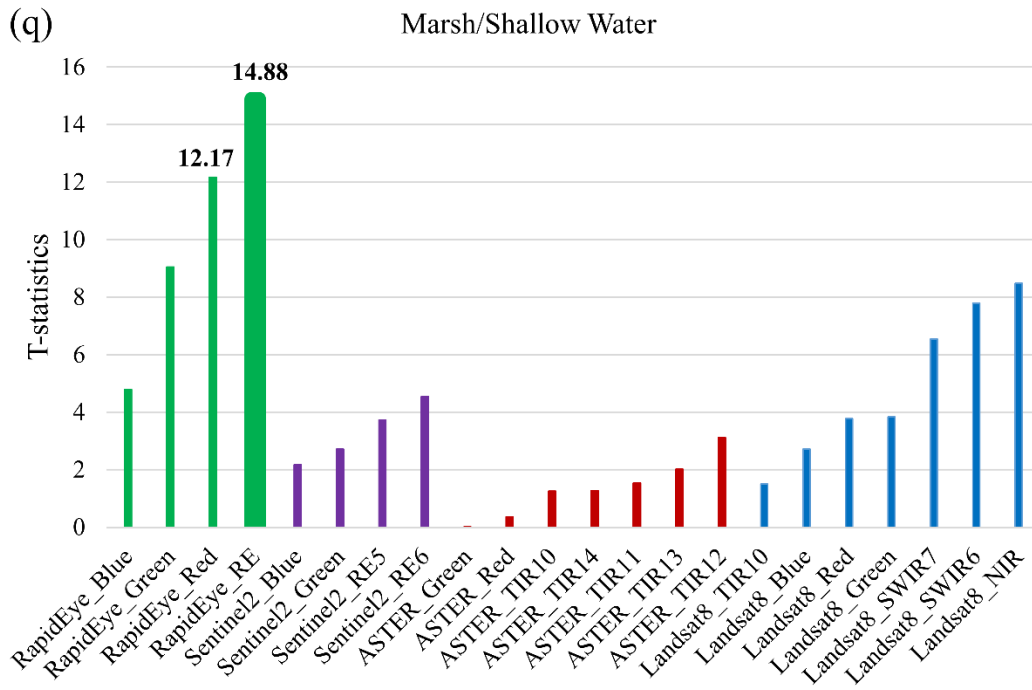
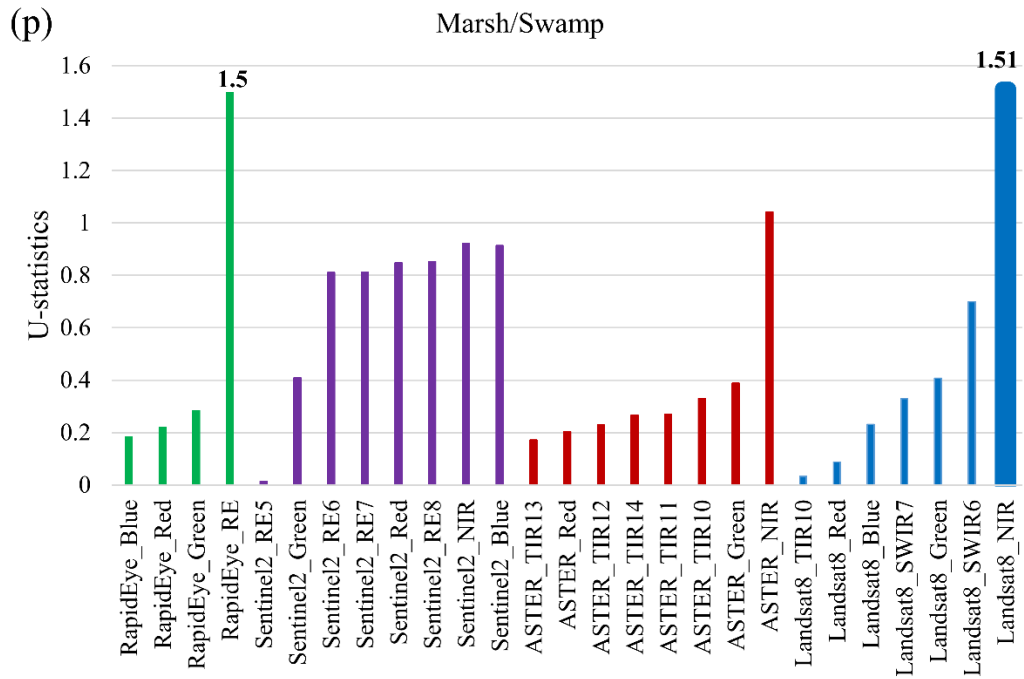


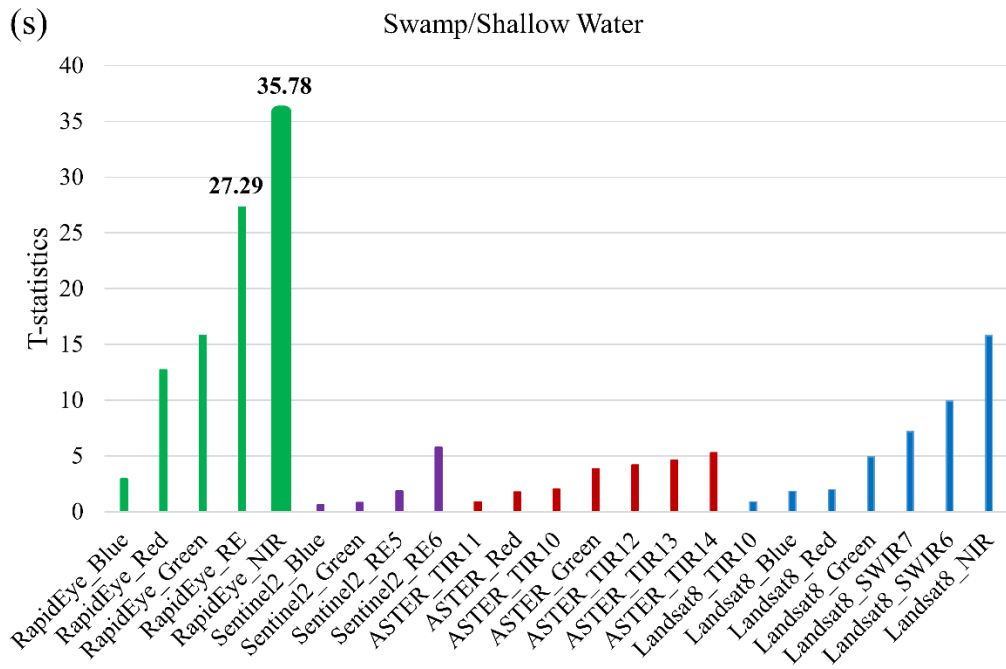
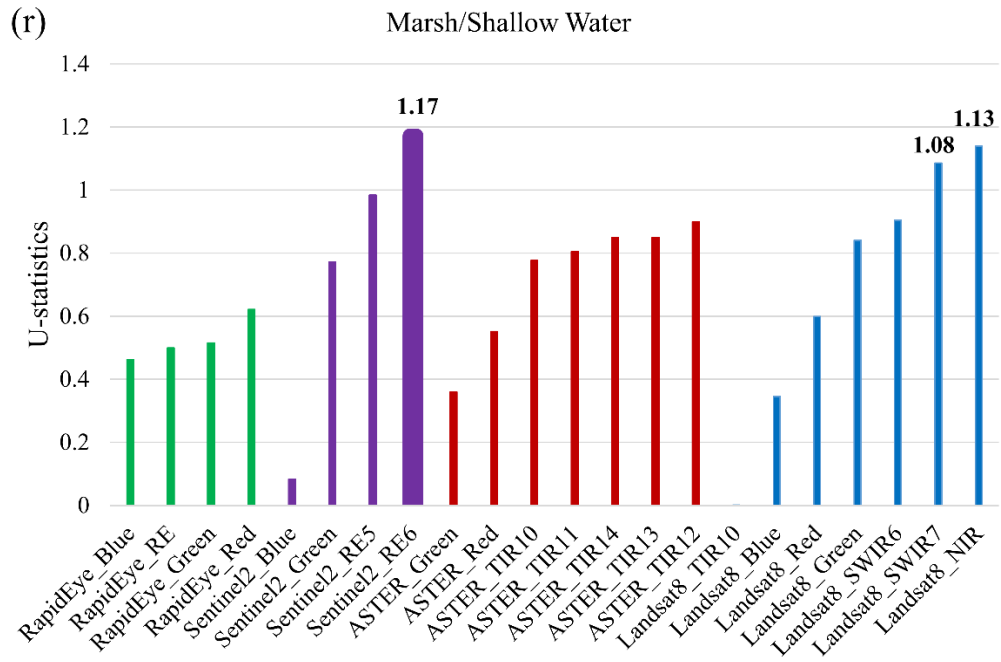












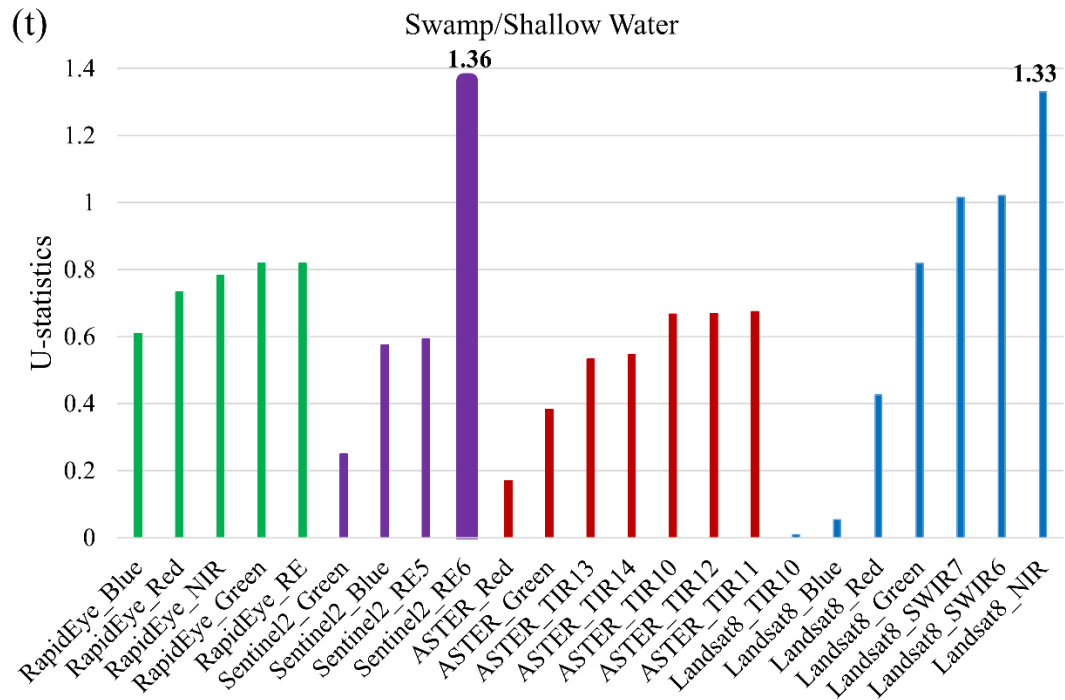
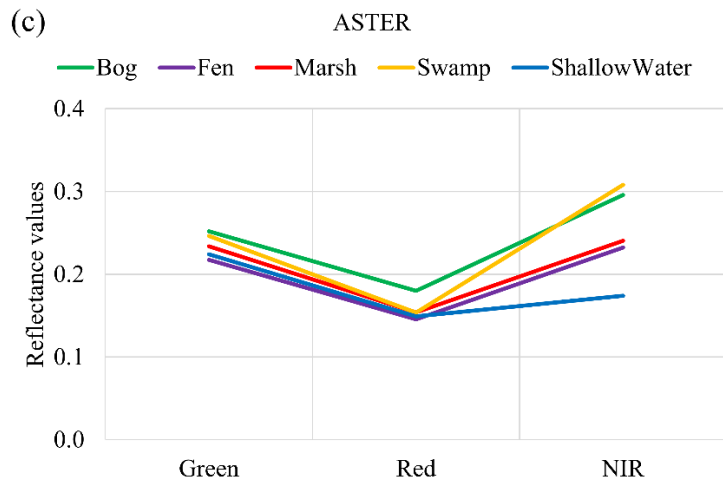
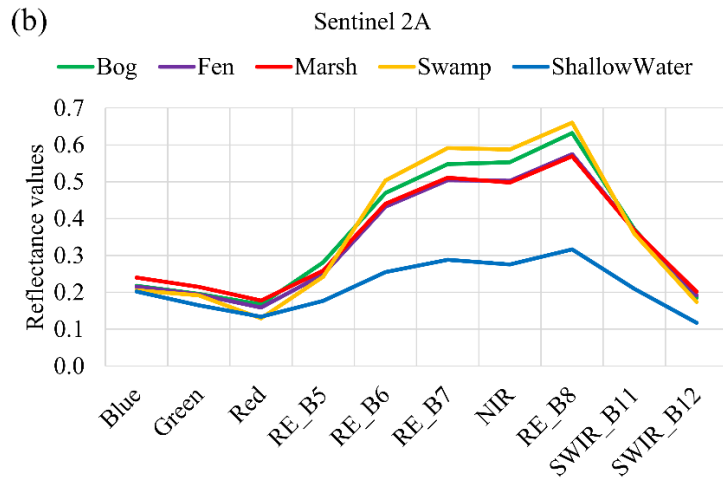
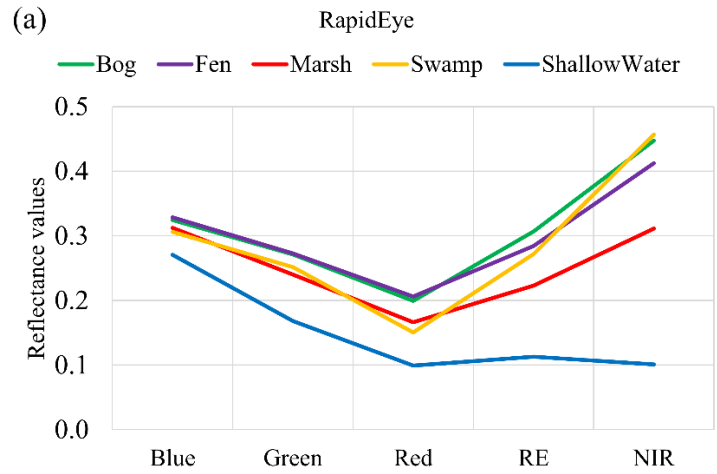


Figure 4.3. Separability measures of wetland class pairs in late spring (June) using the T-statistics and U-statistics. In each figure, the spectral band that provides the highest separability is highlighted (The numbers after the name of the spectral bands also indicate the number of the band. For example: ASTER_TIR14 is the TIR band (band 14) of ASTER).

Table 4.7. The most useful spectral bands for discriminating between each pair of wetland classes in late spring (June) using two distance measures. The spectral bands are ordered based on their separability measures (the spectral bands indicated in the upper right half of the table and the lower left half of the table were obtained using the T-statistics and U-statistics, respectively).

	Bog	Fen	Marsh	Swamp	Shallow Water
Bog	×	Landsat8 NIR RapidEye RE RapidEye NIR	Landsat8 NIR RapidEye RE RapidEye NIR	RapidEye Red	RapidEye NIR
Fen	Sentinel2 RE5 Landsat8 NIR Sentinel2 NIR	×	Landsat8 NIR RapidEye RE	RapidEye Red	RapidEye NIR
Marsh	Landsat8 NIR RapidEye RE Sentinel2 RE5	RapidEye RE	×	Landsat8 NIR RapidEye RE	RapidEye RE RapidEye Red
Swamp	Landsat8 Red	Sentinel2 RE7 Sentinel2 RE6 Sentinel2 NIR ASTER NIR RapidEye Red Sentinel2 RE8	Landsat8 NIR RapidEye RE	×	RapidEye NIR RapidEye RE
Shallow Water	Landsat8 NIR Landsat8 SWIR6	Landsat8 NIR Landsat8 SWIR6 Landsat8 SWIR7	Sentinel2 RE6 Landsat8 NIR Landsat8 SWIR7	Sentinel2 RE6	×



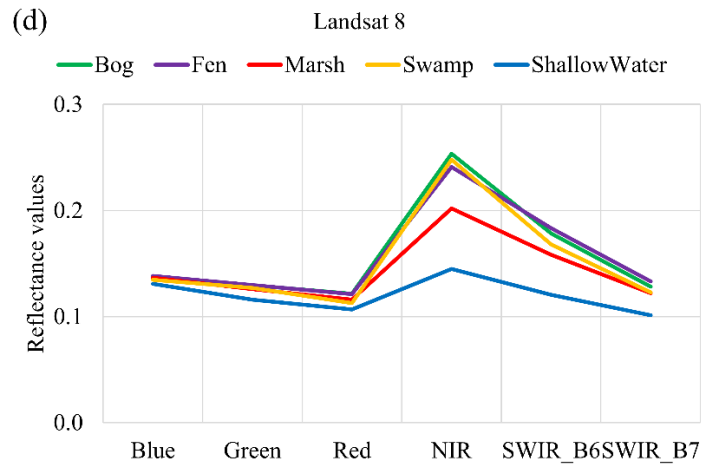


Figure 4.4. The spectral signature of wetlands, obtained from (a) RapidEye, (b) Sentinel 2A, (c) ASTER, and (d) Landsat 8.



Figure 4.5. The red/orange appearance of bogs in the study areas.

In addition, the following results were obtained based on the analyses of the spectral signatures of the wetland classes (Figure 4.4):

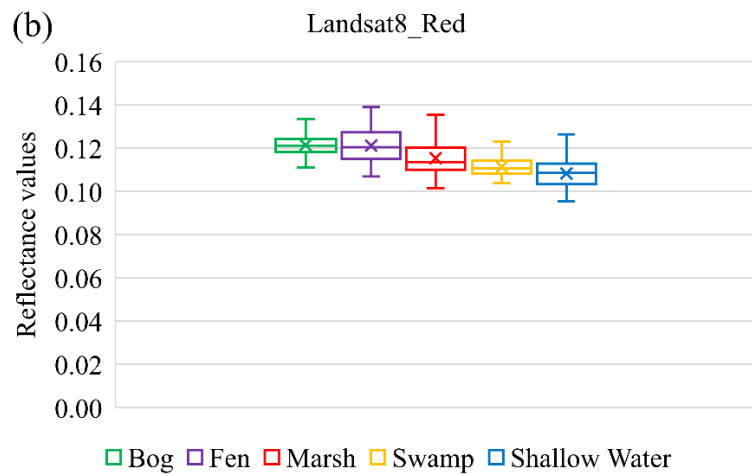
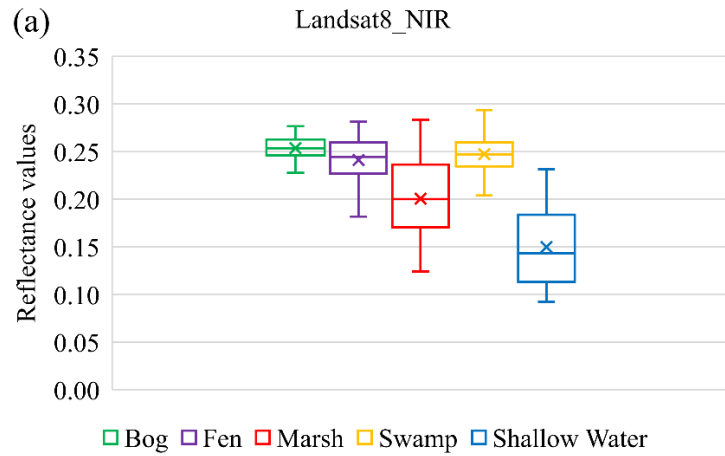
- (1) The spectral signatures of vegetated wetlands (i.e. Bog, Fen, Marsh, and Swamp) followed the same patterns, and were similar to the spectral signatures of green vegetation, for which the highest and lowest values were observed in the NIR and red bands, respectively.

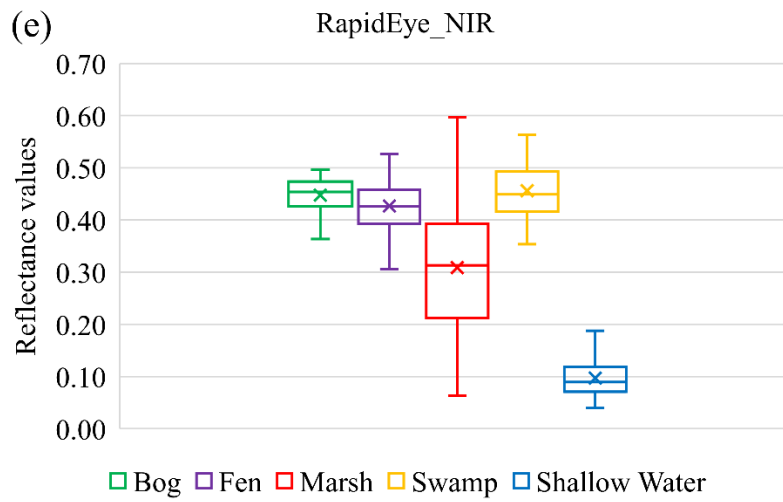
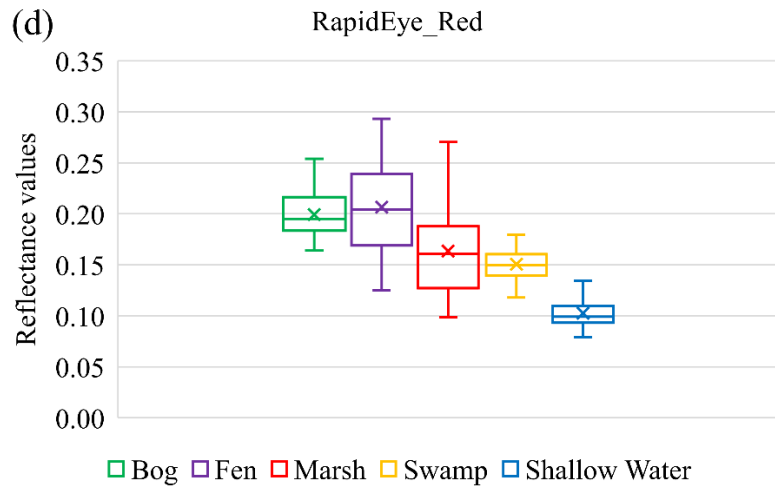
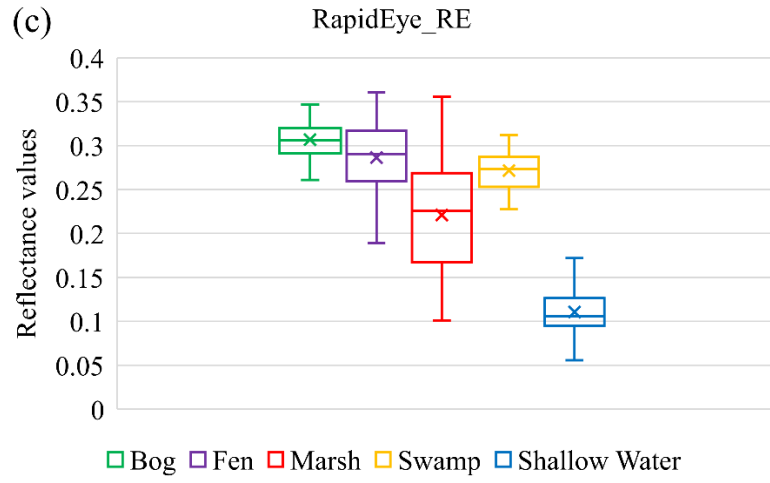
- (2) The spectral signatures of the Shallow Water class were not completely similar to the spectral signature of clean and open water. In fact, in some cases, the NIR values of the Shallow Water class were more than that of the visible bands. This can be explained by the fact that there were some aquatics beds with emergent vegetation in and on the shallow water bodies in the study areas.
- (3) The Shallow Water class was spectrally distinct from other wetland classes in all spectral bands.
- (4) The Shallow Water and Bog classes generally had the lowest and highest responses, respectively.
- (5) Compared to the other vegetated wetlands, the Marsh class presented the lowest spectral response in almost all spectral bands. This was because, generally, the Marsh class contains more open water than other vegetated wetland classes found in the study areas.

Figure 4.6 illustrates the distribution of the reflectance values for the wetland classes in the most effective spectral bands (see Table 4.7) using boxplots. Different wetland classes had similar reflectance values in the spectral bands, making the separation of complex wetlands a challenging task. This is also supported by the spectral signatures of the wetland classes (Figure 4.4), where there was considerable overlap between the values of wetland classes, especially between the vegetated wetland types.

Additionally, according to Figure 4.6, high variance was observed for some wetland classes, such as the Marsh and Shallow Water classes. This can be attributed to the fact that each of these wetland classes contained more than one land cover type, as described in the EWCS (Smith et al., 2007). The Marsh and

Shallow Water classes contain both vegetation and water (i.e. meadow/emergent marsh and aquatic bed/open water) and, therefore, their spectral responses were affected by both vegetation and water.





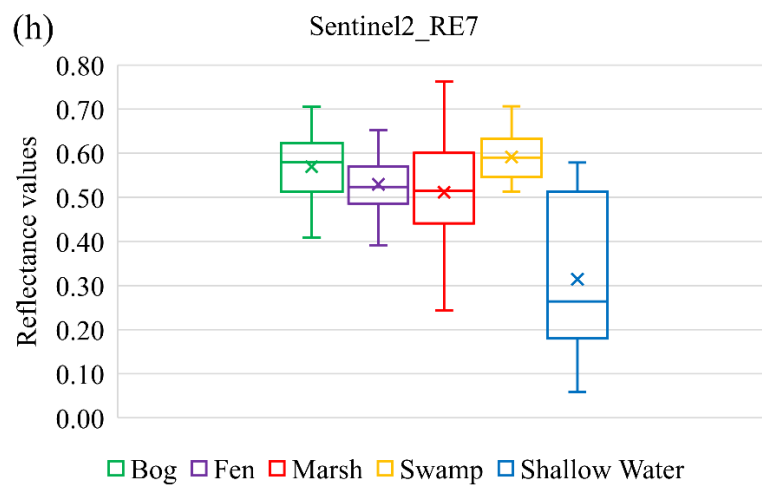
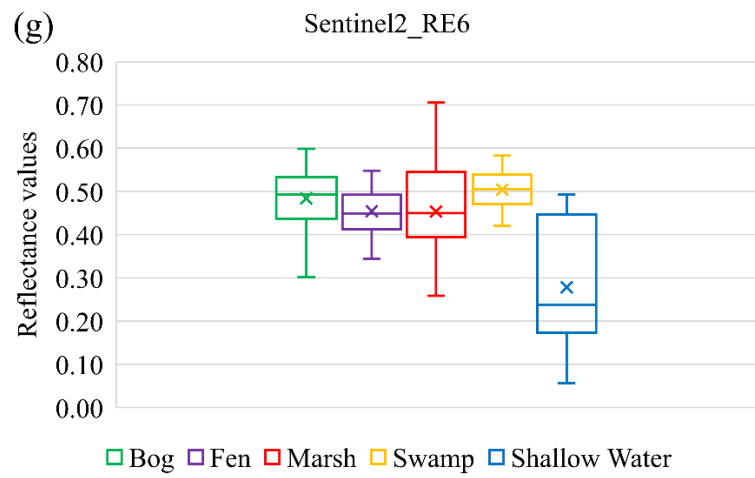
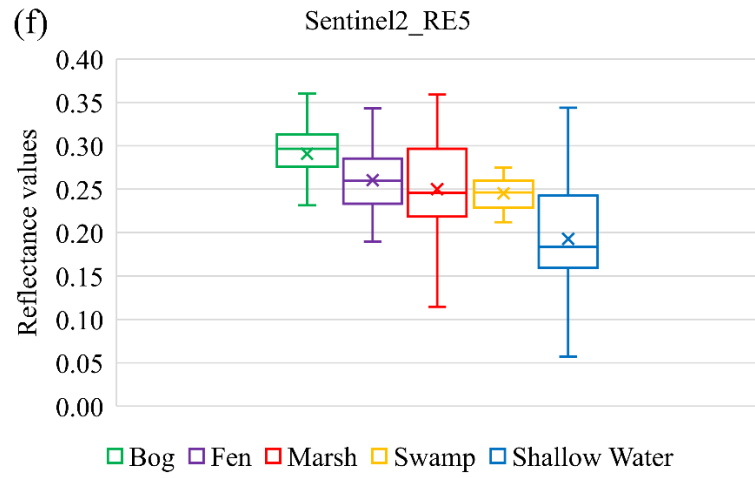


Figure 4.6. The box plots of the spectral bands, which provided the highest separability for wetland classes in late spring (June). The cross (×) mark indicates the mean value. The numbers after the name of the spectral bands indicate the number of the band. For example: Sentinel2_RE6 is the Red Edge band (band 6) of Sentinel 2A.

Based on the results, it is suggested to select those satellites for wetland classification that contain the NIR and RE bands. For instance, Sentinel 2A, which has four different RE bands can be one of the most useful optical satellites in this regard. However, the spatial resolution of the satellite data is also important, especially when OBIA is applied to classify wetlands. Thus, RapidEye with 5 meters spatial resolution and both the RE and NIR bands also provide valuable data for wetland studies. Additionally, the temporal resolution of optical satellites is important for dynamic wetland environments and, therefore, Sentinel 2A and RapidEye with approximately 5 days revisit time are more suitable than Landsat 8 and ASTER with 16 days temporal resolution.

4.4.3. Separability analyses of other features

It is clear that even with the best spectral bands, it was difficult to delineate the wetland classes. Therefore, in this subsection, other features are evaluated to ameliorate this task. All of the steps performed for selecting the best spectral bands (obtained from the mean reflectance values of the field samples) were performed for several other features, including spectral indices, texture and ratio features (see Table 4.6).

The variance analyses primarily showed that the brightness, mean and ratio values had the lowest variations and, therefore, the corresponding features were most reliable for wetland classification in the study areas. On the other hand, the highest variance in the values of field samples was observed for the standard deviation features and, thus, the corresponding features were removed from the rest of the analyses.

After performing variance analyses, the distance between the pairs of wetland classes was calculated using the T- and U-statistics and the best features, providing the highest separability were obtained (Table 4.8). Moreover, Table 4.9 demonstrates the spectral bands and features that provided the maximum spectral separation between all wetland classes, obtained from aggregating the results provided in Table 4.8. The frequency in Table 4.9 indicates how many times a spectral band or a feature was selected as the best feature for discriminating wetland pairs.

The ratio features were generally the most helpful features for discriminating wetland pairs. In this regard, the highest T- and U-statistics were obtained for the NIR, RE, Green, and Red ratios, respectively. It can also be seen from Table 4.9 that the wetland classes had greater potential of being separable using the RapidEye NIR and RE ratios and, thus, they were selected as the best features for 13, and 11 times, respectively.

The selected spectral indices were also helpful in discriminating different pairs of wetland classes. The Normalized Difference Water Index (NDWI), Normalized Difference Vegetation Index (NDVI), Difference Vegetation Index (DVI), and Soil Adjusted Vegetation index (SAVI) were the best spectral indices, respectively.

However, the Normalized Difference Soil Index (NDSI) was not as good as the other spectral indices. The reason was the NDSI considers the SWIR band, which was not as helpful as the other spectral bands (see previous subsection).

Additionally, the best spectral bands, selected in the previous subsection, were between the most useful features for discrimination wetland class pairs in this section. For example, either the NIR and RE bands were selected as one of the best features for distinguishing the wetland class pairs.

Table 4.8. The best features for separating different wetland class pairs based on two separability measures: T-statistics and U-statistics.

T-test		U-test	
Feature	T-statistics	Feature	U-statistics
Bog/Fen			
RapidEye RE Ratio	11.12	ASTER Green Ratio	2.79
Landsat8 SWIR7 Ratio	8.62	ASTER NDWI	2.44
Landsat8 NIR Ratio	8.18	RapidEye RE Ratio	2.10
RapidEye Green Ratio	7.78	Sentinel2 SWIR12 Ratio	1.88
Landsat8 NDSI6	7.25	Landsat8 NIR Ratio	1.87
RapidEye Blue Ratio	7.12	Sentinel2 Green Ratio	1.84
RapidEye NDVI	7.01	ASTER Red Ratio	1.82
RapidEye NIR Ratio	6.91	Sentinel2 NDWI	1.74
RapidEye_NIR	6.78	Sentinel2 Blue Ratio	1.69
Landsat8 NDSI7	6.64	Mean Landsat8 NIR	1.63
Bog/Marsh			

RapidEye RE Ratio	16.19	ASTER Green Ratio	3.14
RapidEye Green Ratio	15.57	ASTER NDWI	2.83
Landsat8 DVI	13.89	Sentinel2 Green Ratio	1.96
Landsat8 NIR	13.74	Sentinel2 NDWI	1.89
RapidEye RE	13.66	ASTER Red Ratio	1.85
Landsat8 NDSI7	13.47	RapidEye Green Ratio	1.73
Landsat8 NIR Ratio	12.74	Sentinel2 NDSI12	1.68
RapidEye NIR	12.37	Landsat8 NIR	1.54
RapidEye DVI	12.34	RapidEye RE Ratio	1.53
Landsat8 SAVI	12.14	Landsat8 NDWI	1.53

Bog/Swamp

RapidEye Red	19.9	Sentinel2 SAVI	2.04
RapidEye Red Ratio	17.5	Sentinel2 RE5 NDVI	2.02
RapidEye NDVI	14.47	Landsat8 Green Ratio	2.00
RapidEye RE NDVI	14.25	ASTER SAVI	1.95
RapidEye RE Ratio	14.22	Landsat8 Blue Ratio	1.93
RapidEye SAVI	13.43	ASTER DVI	1.89
RapidEye RE	13.24	Sentinel2 NDVI	1.89
RapidEye Blue	11.25	Sentinel2 RE6 Ratio	1.89
RapidEye NIR Ratio	11.09	Landsat8 NDVI	1.86
RapidEye Brightness	10.02	ASTER NDVI	1.80

Bog/Shallow Water

RapidEye NIR	48.42	ASTER Green Ratio	2.56
RapidEye DVI	43.28	RapidEye Green Ratio	2.31
RapidEye RE	33.30	ASTER NDWI	2.05

RapidEye Brightness	32.54	RapidEye NIR Ratio	1.99
RapidEye NIR Ratio	31.58	RapidEye RE Ratio	1.97
RapidEye RE Ratio	26.76	Sentinel2 NDWI	1.89
RapidEye NDWI	26.22	Sentinel2 Green Ratio	1.84
RapidEye Red	24.89	Sentinel2 Red Ratio	1.81
RapidEye Green Ratio	23.79	Sentinel2 NDSI12	1.81
RapidEye NDVI	21.38	Sentinel2 Blue Ratio	1.75
Fen/Marsh			
Landsat8 NIR	10.32	ASTER NIR Ratio	2.15
Landsat8 Blue Ratio	10.14	Sentinel2 Green Ratio	1.94
RapidEye Brightness	9.61	RapidEye Blue Ratio	1.80
Landsat8 NDWI	9.35	RapidEye Green Ratio	1.79
Landsat8 DVI	9.31	Sentinel2 NDWI	1.76
RapidEye Blue Ratio	8.77	ASTER NDVI	1.75
Landsat8 Brightness	8.59	ASTER DVI	1.697
RapidEye RE Ratio	8.58	ASTER SAVI	1.69
		Standard deviation	
RapidEye NIR Ratio	8.46	Sentinel2 RE5	1.69
Landsat8 NDVI	8.31	RapidEye NDWI	1.66
Fen/Swamp			
RapidEye NDVI	14.02	Landsat8 NIR Ratio	2.16
RapidEye Red Ratio	13.91	ASTER Red Ratio	2.01
RapidEye SAVI	13.07	ASTER NDWI	1.86
RapidEye NDWI	12.70	Landsat8 SAVI	1.85
RapidEye Red	11.75	Landsat8 NDVI	1.85

RapidEye NIR Ratio	11.60	ASTER Green Ratio	1.75
RapidEye RE6 NDVI	11.31	RapidEye NDVI	1.70
RapidEye Blue	10.95	Landsat8 DVI	1.67
RapidEye DVI	9.98	Sentinel2 NDVI	1.65
Standard deviation			
RapidEye Red	9.54	RapidEye DVI	1.64

Fen/Shallow Water

RapidEye NIR	31.39	RapidEye NDWI	2.47
RapidEye RE	26.78	RapidEye Blue Ratio	2.16
RapidEye Brightness	26.64	RapidEye Green Ratio	2.08
RapidEye DVI	26.52	Sentinel2 NDWI	2.08
RapidEye RE Ratio	26.25	Sentinel2 RE5 Ratio	1.93
RapidEye NIR Ratio	23.503	Sentinel2 Blue Ratio	1.90
RapidEye Green Ratio	22.37	Sentinel2 Red Ratio	1.86
RapidEye NDWI	21.50	ASTER NIR Ratio	1.82
RapidEye RE NDVI	20.61	Sentinel2 Green Ratio	1.77
RapidEye Green	19.64	ASTER DVI	1.74

Marsh/Swamp

RapidEye NDVI	16.65	Landsat8 SAVI	1.87
RapidEye DVI	15.36	Landsat8 NDVI	1.81
RapidEye SAVI	15.18	Sentinel2 SAVI	1.81
RapidEye RE NDVI	13.71	Landsat8 NIR Ratio	1.77
RapidEye Red Ratio	13.16	Landsat8 DVI	1.68
Landsat8 DVI	13.02	Landsat8 NIR	1.68
Landsat8 NDWI	12.96	ASTER DVI	1.62

RapidEye NDWI	12.66	Sentinel2 RE7 Ratio	1.60
RapidEye NIR Ratio	12.37	ASTER SAVI	1.59
Landsat8 Red Ratio	11.99	Sentinel2 RE6 Ratio	1.55

Marsh/Shallow Water

RapidEye Blue Ratio	16.94	RapidEye RE Ratio	2.45
RapidEye RE NDVI	16.38	RapidEye Green Ratio	2.15
RapidEye Brightness	15.57	RapidEye NDWI	2.07
RapidEye NIR	15.12	Sentinel2 Red Ratio	1.98
RapidEye NDWI	14.83	Sentinel2 RE5 Ratio	1.95
RapidEye NIR Ratio	14.57	Sentinel2 NDWI	1.94
RapidEye RE	14.12	Landsat8 Blue Ratio	1.87
RapidEye DVI	14.12	Sentinel2 Blue Ratio	1.75
RapidEye Red	12.827	Landsat8 NDWI	1.65
Standard deviation			
RapidEye NIR	12.64	Sentinel2 Green Ratio	1.64

Swamp/Shallow Water

RapidEye NIR	38.74	RapidEye Blue Ratio	1.84
RapidEye DVI	35.49	ASTER Green Ratio	1.68
RapidEye NIR Ratio	33.20	Sentinel2 NDWI	1.65
RapidEye RE Ratio	27.79	RapidEye Green Ratio	1.63
RapidEye Brightness	26.81	Sentinel2 Green Ratio	1.62
RapidEye RE NDVI	26.65	RapidEye NDWI	1.58
RapidEye NDWI	26.61	RapidEye Red Ratio	1.57
RapidEye RE	26.26	Landsat8 DVI	1.53
RapidEye NDVI	25.51	ASTER DVI	1.51

RapidEye SAVI	23.61	Sentinel2 Red Ratio	1.47
---------------	-------	---------------------	------

Table 4.9. The best features for wetland classification in the study areas.

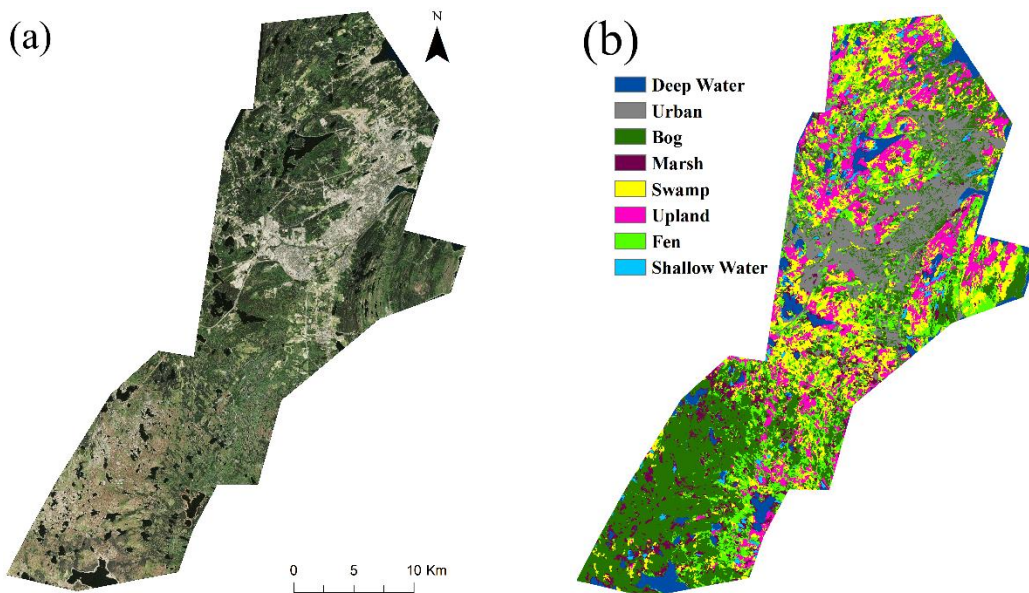
Feature	Frequency
RapidEye NIR Ratio	13
RapidEye RE Ratio	11
RapidEye NDWI	10
Landsat8 Green Ratio	9
RapidEye DVI	8
RapidEye NDVI	7
RapidEye NIR Ratio	7
Sentinel2 Green Ratio	7
Sentinel2 NDWI	7
Landsat8 DVI	6
RapidEye Brightness	6
RapidEye NIR	6
RapidEye RE	6
RapidEye RE NDVI	6
RapidEye Blue Ratio	6
ASTER DVI	5
ASTER Green Ratio	5
Landsat8 NIR	5
ASTER NDWI	4
Landsat8 NDVI	4
Landsat8 NDWI	4

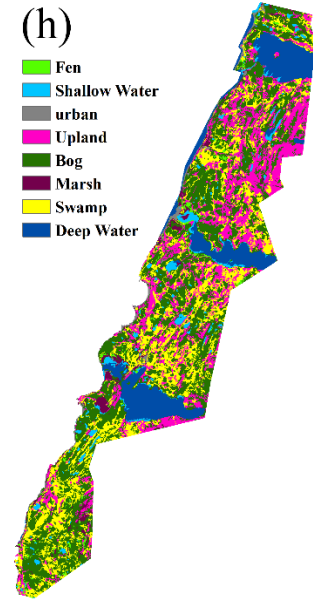
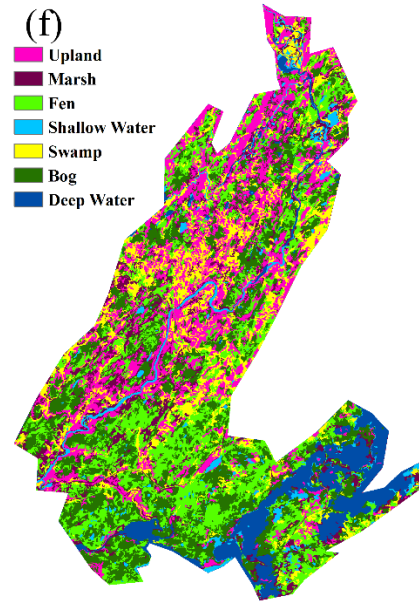
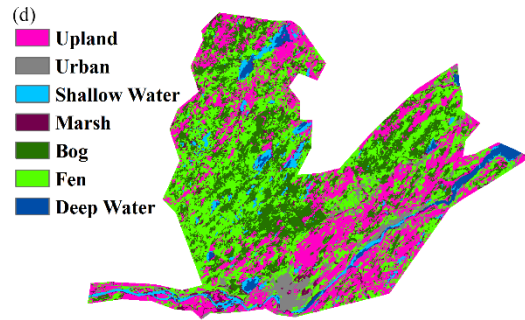
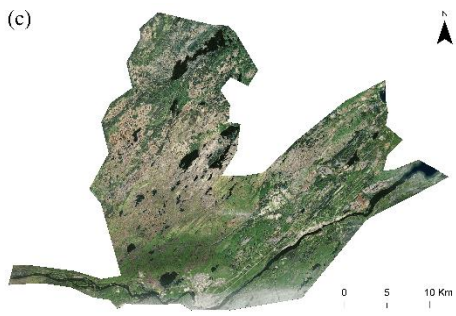
RapidEye Red	4
RapidEye Red Ratio	4
RapidEye SAVI	4
Sentinel2 Blue Ratio	4
Sentinel2 Red Ratio	4
ASTER Red Ratio	3
ASTER SAVI	3
Landsat8 Blue Ratio	3
Landsat8 SAVI	3
ASTER NDVI	2
ASTER NIR Ratio	2
Landsat8 NDSI7	2
RapidEye Blue	2
Sentinel2 NDSI12	2
Sentinel2 NDVI	2
Sentinel2 RE5 Ratio	2
Sentinel2 RE6 Ratio	2
Sentinel2 SAVI	2
Landsat8 Brightness	1
Landsat8 Green Ratio	1
Landsat8 NDSI6	1
Landsat8 Red Ratio	1
Landsat8 SWIR7 Ratio	1
RapidEye Green	1
RapidEye NIR (Standard deviation)	1

Sentinel2 RE5 NDVI	1
Sentinel2 RE7 Ratio	1
RapidEye Red (Standard deviation)	1
Sentinel2 RE5 (Standard deviation)	1

4.4.4. Wetlands classification using selected features

After selecting the best features for separating different wetland classes, they were injected into an object-based RF algorithm to obtain wetland maps from the study areas. To do this, half of the field samples was randomly used to train the algorithm and the other half was applied to evaluate the classification accuracy. Figure 4.7 illustrates the classified wetland maps.





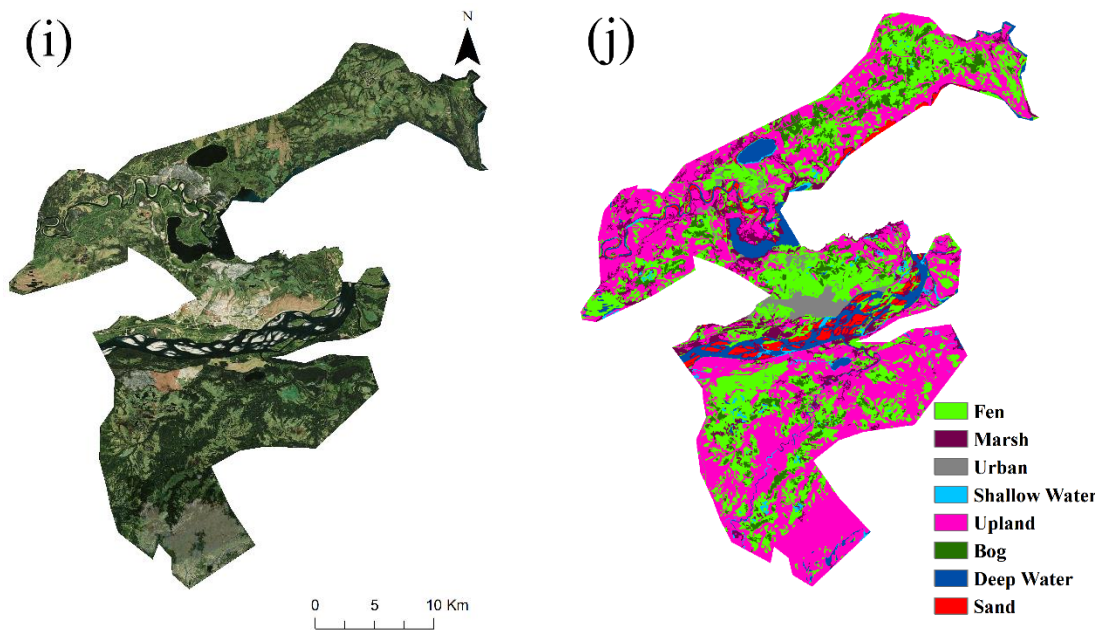


Figure 4.7. The study areas and their corresponding classified maps.

Based on the visual interpretation, which has been carried out by several ecological and RS experts using aerial imagery (pixel size=0.5 meters) and the ground truth data, it was concluded that all classes in most regions of the study areas were generally classified well. For example, according to the field measurements, the south of the Avalon study area, which is mostly covered by bogs, fens, and marshes, was correctly mapped in the classified image. Additionally, the areas surrounding deep waters, as well as the small water bodies, were classified as Shallow Water, which indicated that these regions were classified accurately. It was also concluded that the urban and deep water areas in most parts of the study areas have been identified correctly. The OAs, Kappa coefficients, and mean PAs and UAs for wetland classes in each study area are also provided in Table 4.10. According to the levels of classification accuracies, it was concluded that the

selected features in previous subsections had a high potential for the separation of different wetland classes in this study providing the accuracies more than 80%.

Table 4.10. The OA, Kappa coefficient, Mean PA and UA of wetland classes in the five study areas.

	Avalon	Grand Falls- Windsor	Deer Lake	Gros Morne	Goose Bay
OA (%)	88	84	82	89	86
Kappa coefficient	0.85	0.81	0.75	0.85	0.83
Mean PA of wetland classes (%)	75	68	73	71	76
Mean UA of wetland classes (%)	78	72	69	75	74

It is worth noting the main reason for low overall accuracies in this chapter compared to chapter 2 was the fact that multi-temporal satellite imagery was used in chapter 2, while single-date data (captured in June) were only applied to classify wetlands in this chapter. This also demonstrated high efficiency of multi-temporal data for increasing the accuracy of wetland classification.

4.5. Conclusion

The mapping and monitoring of wetlands using new technologies are important because they provide many beneficial services to both the environment and humans. In this regard, optical RS satellites provide valuable data. One main concern in utilizing the optical data is finding the most informative bands and

features for delineation of various wetland types. For this purpose, and to have a reliable and robust approach, the data acquired by four different optical satellites, including RapidEye, Sentinel 2A, ASTER, and Landsat 8 were investigated. Variance analyses should be carried out on the field data collected for wetland studies before performing any separability analysis. This is because wetlands are dynamic and complex environments and one wetland type can contain various land covers. Consequently, the spectral responses of the field samples of one particular wetland class can vary considerably. This fact is more important when using textural features (e.g. standard deviation values of field sample polygons), as there were high variances in their values and, thus, should be eliminated from the analyses. According to the spectral analyses, it was concluded that generally the NIR, RE, and red bands were the most useful spectral bands for the differentiation of wetland species, respectively. Thus, the corresponding ratio features and the spectral indices, derived from these bands (e.g. NDWI and NDVI) were among the best features for wetland classification. Additionally, these results demonstrated that the data acquired by some optical satellites, such as RapidEye and Sentinel 2A, which contain both NIR and RE bands may be the most appropriate for achieving high accuracy in wetland classifications. It was also concluded that the spectral responses of vegetated wetlands (i.e. Bog, Fen, Marsh, and Swamp) were very similar in some spectral bands and there were difficulties in discriminating them. Use of multi-temporal data or other types of RS data, such as SAR, might solve this problem. For instance, SAR data demonstrate a high potential for soil moisture estimation which is one of the main characteristics of wetlands. Thus, the separability analyses of wetlands should also be carried out using different types of SAR data to select the most useful SAR features to

differentiate wetlands. Furthermore, since wetlands are highly changeable over time (i.e. seasonally or even monthly), similar spectral analyses, performed in this study for the data captured in June, is suggested to be carried out using the satellite data acquired in other times to obtain a more versatile conclusion regarding the best spectral features for delineation of wetland classes. Finally, after selecting the most useful features for the delineation of wetland classes, they were used in an object-based RF algorithm to classify the wetlands in five different study areas. It was concluded that the selected spectral bands and features had a high potential for monitoring wetlands over various regions of NL.

References

- Adam, E., & Mutanga, O. (2009). Spectral discrimination of papyrus vegetation (*Cyperus papyrus* L.) in swamp wetlands using field spectrometry. *ISPRS Journal of Photogrammetry and Remote Sensing*, 64(6), 612-620.
- Adam, E., Mutanga, O., & Rugege, D. (2010). Multispectral and hyperspectral remote sensing for identification and mapping of wetland vegetation: a review. *Wetlands Ecology and Management*, 18(3), 281-296.
- Amani, M., Salehi, B., Mahdavi, S., Granger, J. (2017a). "Spectral analysis of wetlands in Newfoundland using Sentinel 2A and Landsat 8 imagery". In *IGFT 2017, ASPRS Annual Conference*.
- Amani, M., Salehi, B., Mahdavi, S., Granger, J. E., Brisco, B., & Hanson, A. (2017b). Wetland Classification Using Multi-Source and Multi-Temporal Optical Remote Sensing Data in Newfoundland and Labrador, Canada. *Canadian Journal of Remote Sensing*, 1-14.

Amani, M., Salehi, B., Mahdavi, S., Granger, J., & Brisco, B. (2017c). Wetland classification in Newfoundland and Labrador using multi-source SAR and optical data integration. *GIScience & Remote Sensing*, 1-18.

Araya-López, R. A., Lopatin, J., Fassnacht, F. E., & Hernández, H. J. (2018). Monitoring Andean high altitude wetlands in central Chile with seasonal optical data: A comparison between Worldview-2 and Sentinel-2 imagery. *ISPRS Journal of Photogrammetry and Remote Sensing*. In press.

Chatziantoniou, A., Psomiadis, E., & Petropoulos, G. P. (2017). Co-Orbital Sentinel 1 and 2 for LULC mapping with emphasis on wetlands in a mediterranean setting based on machine learning. *Remote Sensing*, 9(12), 1259.

Conover, W. J. (1980). Practical nonparametric statistics.

Crist, E. P., & Cicone, R. C. (1984). A physically-based transformation of Thematic Mapper data--The TM Tasseled Cap. *IEEE Transactions on Geoscience and Remote sensing*, (3), 256-263.

Definiens, A. G. (2009). Definiens eCognition developer 8 user guide. *Definens AG, Munchen, Germany*.

Duro, D. C., Franklin, S. E., & Dubé, M. G. (2012). A comparison of pixel-based and object-based image analysis with selected machine learning algorithms for the classification of agricultural landscapes using SPOT-5 HRG imagery. *Remote Sensing of Environment*, 118, 259-272.

Ecological Stratification Working Group (Canada), Center for Land, Biological Resources Research (Canada), & Canada. State of the Environment Directorate.

(1996). A national ecological framework for Canada. *Centre for Land and Biological Resources Research; Hull, Quebec: State of the Environment Directorate.*

Erwin, K. L. (2009). Wetlands and global climate change: the role of wetland restoration in a changing world. *Wetlands Ecology and Management*, 17(1), 71.

Fay, M. P., & Proschan, M. A. (2010). Wilcoxon-Mann-Whitney or t-test? On assumptions for hypothesis tests and multiple interpretations of decision rules. *Statistics Surveys*, 4, 1.

Filella, I., & Penuelas, J. (1994). The red edge position and shape as indicators of plant chlorophyll content, biomass and hydric status. *International Journal of Remote Sensing*, 15(7), 1459-1470.

Finlayson, C. M., Davidson, N. C., Spiers, A. G., & Stevenson, N. J. (1999). Global wetland inventory—current status and future priorities. *Marine and Freshwater Research*, 50(8), 717-727.

Gallant, A. L. (2015). The challenges of remote monitoring of wetlands. *Remote Sensing*, 7, 10938-10950.

Gascon, F., Bouzinac, C., Thépaut, O., Jung, M., Francesconi, B., Louis, J., ... & Languille, F. (2017). Copernicus Sentinel-2A calibration and products validation status. *Remote Sensing*, 9(6), 584.

Guo, M., Li, J., Sheng, C., Xu, J., & Wu, L. (2017). A Review of Wetland Remote Sensing. *Sensors*, 17(4), 777.

Harken, J., & Sugumaran, R. (2005). Classification of Iowa wetlands using an airborne hyperspectral image: a comparison of the spectral angle mapper classifier and an object-oriented approach. *Canadian Journal of remote sensing*, 31(2), 167-174.

Hay, G. J., & Castilla, G. (2008). Geographic Object-Based Image Analysis (GEOBIA): A new name for a new discipline. *Object-based image analysis*, 75-89.

Hey, D. L., Kostel, J. A., Crumpton, W. G., Mitsch, W. J., & Scott, B. (2012). The roles and benefits of wetlands in managing reactive nitrogen. *Journal of Soil and Water Conservation*, 67(2), 47A-53A.

Iwasaki, A., & Tonooka, H. (2005). Validation of a crosstalk correction algorithm for ASTER/SWIR. *IEEE transactions on Geoscience and Remote Sensing*, 43(12), 2747-2751.

Laba, M., Blair, B., Downs, R., Monger, B., Philpot, W., Smith, S., ... & Baveye, P. C. (2010). Use of textural measurements to map invasive wetland plants in the Hudson River National Estuarine Research Reserve with IKONOS satellite imagery. *Remote Sensing of Environment*, 114(4), 876-886.

Leblanc, M., Lemoalle, J., Bader, J. C., Tweed, S., & Mofor, L. (2011). Thermal remote sensing of water under flooded vegetation: New observations of inundation patterns for the 'Small' Lake Chad. *Journal of Hydrology*, 404(1), 87-98.

Lehmann, E. L. (2004). Elements of large-sample theory. *Springer Science & Business Media*.

Li, Y., Chen, J., Ma, Q., Zhang, H. K., & Liu, J. (2018). Evaluation of Sentinel-2A Surface Reflectance Derived Using Sen2Cor in North America. *IEEE Journal of Selected Topics in Applied Earth Observations and Remote Sensing*, (99), 1-25.

Mahdavi, S., Salehi, B., Amani, M., Granger, J. E., Brisco, B., Huang, W., & Hanson, A. (2017a). Object-based Classification of Wetlands in Newfoundland and Labrador Using Multi-Temporal PolSAR Data. *Canadian Journal of Remote Sensing*, 1-19.

Mahdavi, S., Salehi, B., Granger, J., Amani, M., & Brisco, B. (2017b). Remote sensing for wetland classification: a comprehensive review. *GIScience & Remote Sensing*, 1-36.

Mahdianpari, M., Salehi, B., Mohammadimanesh, F., & Motagh, M. (2017). Random forest wetland classification using ALOS-2 L-band, RADARSAT-2 C-band, and TerraSAR-X imagery. *ISPRS Journal of Photogrammetry and Remote Sensing*, 130, 13-31.

Mahdianpari, M., Salehi, B., Mohammadimanesh, F., Brisco, B., Mahdavi, S., Amani, M., & Granger, J. E. (2018). Fisher Linear Discriminant Analysis of coherency matrix for wetland classification using PolSAR imagery. *Remote Sensing of Environment*, 206, 300-317.

Manevski, K., Manakos, I., Petropoulos, G. P., & Kalaitzidis, C. (2011). Discrimination of common Mediterranean plant species using field spectroradiometry. *International Journal of Applied Earth Observation and Geoinformation*, 13(6), 922-933.

Marton, J. M., Creed, I. F., Lewis, D. B., Lane, C. R., Basu, N. B., Cohen, M. J., & Craft, C. B. (2015). Geographically isolated wetlands are important biogeochemical reactors on the landscape. *BioScience*, 65(4), 408-418.

- Minitab, C. (1991). Minitab reference manual (Release 7.1). *State Coll., PA16801, USA.*
- Mitsch, W. J., & Gosselink, J. G. (2000). *Wetlands (3rd Eds.)*. New York: Wiley.
- Mutanga, O., & Skidmore, A. K. (2007). Red edge shift and biochemical content in grass canopies. *ISPRS Journal of Photogrammetry and Remote Sensing*, 62(1), 34-42.
- Mutanga, O., Adam, E., & Cho, M. A. (2012). High density biomass estimation for wetland vegetation using WorldView-2 imagery and random forest regression algorithm. *International Journal of Applied Earth Observation and Geoinformation*, 18, 399-406.
- Mwangi, B., Tian, T. S., & Soares, J. C. (2014). A review of feature reduction techniques in neuroimaging. *Neuroinformatics*, 12(2), 229-244.
- National Wetlands Working Group. (1987). *Canada Committee on Ecological (Biophysical) Land Classification. The Canadian wetland classification system. Lands Conservation Branch, Canadian Wildlife Service, Environment Canada.*
- Ozesmi, S. L., & Bauer, M. E. (2002). Satellite remote sensing of wetlands. *Wetlands Ecology and Management*, 10(5), 381-402.
- Proctor, C., He, Y., & Robinson, V. (2013). Texture augmented detection of macrophyte species using decision trees. *ISPRS Journal of Photogrammetry and Remote Sensing*, 80, 10-20.
- Realmuto, V. J. (1990). Separating the effects of temperature and emissivity: Emissivity spectrum normalization. *In Proc. of the Second Thermal Infrared Multispectral Scanner (TIMS) Workshop, Jet Propulsion Lab., 1990 (pp. 31-35).*

Richter, R. (2011). Atmospheric/Topographic fro Satellite Imagery (ATCOR 2/3 User Guide, Version 8). *DLR-German Aerospace Center, Wessling, Germany.*

Ryan, B. F., & Joiner, B. L. (2001). *Minitab handbook*. Duxbury Press.

Schmidt, K. S., & Skidmore, A. K. (2003). Spectral discrimination of vegetation types in a coastal wetland. *Remote Sensing of Environment*, 85(1), 92-108.

Shettigara, V. K., Kempinger, S. G., & Aitchison, R. (1995). Semi-Automatic detection and extraction of man-made objects in multispectral aerial and satellite images. *Automatic Extraction of Man-Made Objects from Aerial and Space Images*, 63-72.

Smith, K. B., Smith, C. E., Forest, S. F., & Richard, A. J. (2007). A field guide to the wetlands of the boreal plains ecozone of Canada. *Ducks Unlimited Canada, Western Boreal Office: Edmonton, Alberta.*

South, R. (1983). Biogeography and Ecology of the Island of Newfoundland. 48. *Springer Science & Business Media.*

Tiner, R. W., Lang, M. W., & Klemas, V. V. (Eds.). (2015). Remote sensing of wetlands: applications and advances. *CRC Press.*

Yeung, K. Y., Bumgarner, R. E., & Raftery, A. E. (2005). Bayesian model averaging: development of an improved multi-class, gene selection and classification tool for microarray data. *Bioinformatics*, 21(10), 2394-2402.

CHAPTER 5. SEPARABILITY ANALYSIS OF WETLANDS USING MULTI-SOURCE SAR DATA

Abstract

Accurately classifying and monitoring wetlands using new technologies is important because of many services that wetlands provide to the environment. In this regard, Synthetic Aperture Radar (SAR) systems provide valuable data to separate different wetland classes. Using large amount of field samples collected during three years, 78 SAR features extracted from multi-source satellites were investigated to select the most important features and decomposition methods for discriminating five wetland classes: Bog, Fen, Marsh, Swamp, and Shallow Water. The results indicated that the ratio features obtained from the diagonal elements of the covariance matrix (extracted from full polarimetric data RADARSAT-2 imagery) and the intensity layers of the dual polarimetric data (i.e., the data acquired by Sentinel-1 and ALOS-2) were most useful for distinguishing wetland class pairs as well as all wetland classes. Additionally, the H/A/Alpha and Freeman-Durden decomposition techniques were selected as the best methods to discriminate wetlands. This study comprehensively discusses the efficiency of various SAR features/decomposition methods for wetland studies and the results are expected to help with creating sustainable policies and management for wetland protection and monitoring using remote sensing methods.

Keywords: Remote Sensing, Wetlands, SAR, Backscattering, Separability Analysis

5.1. Introduction

Wetlands are important natural resources for humans, animals, and plants, and provide many services at local, regional, and global scales. Wetlands provide food and shelter to animals and plants (Ozesmi and Bauer, 2002), store carbon produced by human activities (Roulet, 2000), protect coastlines and shorelines (Gedan et al., 2011), filter sediments and toxins (Vymazal, 2010), prevent natural hazards such as floods (Mitsch and Gosselink, 2000), and provide recreational and tourist activities (Tiner et al., 2015). Nevertheless, many wetlands are increasingly threatened by urbanization, industrialization, climate change, and agricultural activities (Tiner et al., 2015; Amani et al., 2017a, b; Mahdavi et al., 2017c). Thus, it is important to protect wetlands by mapping and monitoring these valuable landscapes using new technologies and sustainable methods. Since each country or region contains different wetland species, various classification systems are utilized. In Canada, the Canadian Wetland Classification System (CWCS) is predominantly used. This system classifies wetlands into five classes based on their functions and ecological characteristics: Bog, Fen, Marsh, Swamp, and Shallow Water (National Wetlands Working Group, 1997).

Using field work for wetlands classification has several limitations, which make this method inappropriate, especially for large scale applications (Mahdavi et al., 2017c). Moreover, because wetlands are usually located in remote places and have a high temporal variation, field measurements are not applicable in the long term (Henderson and Lewis, 2008; Gallant, 2015; Mahdavi et al., 2017b). However, satellites provide timely and cost-effective data, which are particularly useful, especially when applied to classify wetlands on regional and national scales. In

this regard, both optical and Synthetic Aperture Radar (SAR) data have been widely employed for wetland classification. Optical satellites are less capable of penetrating through the clouds, which restricts their applications when the weather conditions are not suitable. This is a major problem in Canada, where cloud cover is frequent. Furthermore, as optical sensors acquire spectral information regardless of the target's physical characteristics (e.g. vegetation height), they fail to discriminate between short vegetation and elevated vegetation wetlands, which have the same spectral but different physical characteristics (Mahdavi et al., 2017c). On the other hand, SAR systems provide many useful tools to overcome these limitations and, thus, are more applicable in Canada (Amani et al., 2018). SAR signals can penetrate through clouds and into vegetation canopies. Their penetration depth is directly proportional to the wavelength of the signal, and also depends on the structure and density of vegetation. SAR sensors also collect valuable information about the hydrology and ground conditions under vegetation canopies (Li et al., 2007). Moreover, several SAR satellites, such as RADARSAT-2, acquire full polarimetric data, which can be efficiently applied to delineate wetland classes (Brisco et al., 2011). In fact, polarimetric information along with SAR all-weather capabilities provide unique opportunities for wetland mapping (Touzi et al., 2007), and are currently deemed to be the most effective way for the characterization of target scattering (Touzi et al., 2009; Brisco et al., 2015).

When applying SAR data to classify wetlands, it is important to assess different channels, polarimetric features, and decomposition methods to see what features yield the best separability for wetland classes. Several studies have been conducted in this regard. In general, it has been argued that short wavelength SAR data are more appropriate to map herbaceous wetlands, such as Bog, Fen, and Marsh (Li

and Chen, 2005; Hong et al., 2015). However, long wavelength data (e.g. L band) are best to distinguish between forested or densely vegetated wetlands (e.g. Swamp) and uplands (Kasischke et al., 2003; Li and Chen, 2005; Hong et al., 2015, Mahdavi et al., 2017c). It has also been reported that the horizontal transmission and reception (HH) polarization is the most appropriate polarization for wetland mapping (Bourgeau-Chavez et al., 2009; Mahdavi et al., 2017c). Additionally, co-polarized data (i.e. HH and vertical transmission and reception (VV)) are useful in detecting flooded forest and inundation, as well as separating flooded and non-flooded wetlands (Mahdavi et al., 2017c). However, cross-polarized data (i.e. horizontal transmit and vertical receive (HV) or vice-versa) is helpful in discriminating between herbaceous and woody wetlands (e.g. delineating the Marsh and Swamp classes, Bourgeau-Chavez et al., 2009; Mahdavi et al., 2017c). The ratio of the polarizations have also proved helpful in wetland classification. For example, Brisco et al. (2011) reported that the ratios which include the HH polarization, obtained from airborne CV-580 C-band SAR data, had potential for delineation of flooded and non-flooded wetlands. Moreover, based on Bourgeau-Chavez et al. (2009), the ratio of L-HV and L-HH channels were considerably useful for classifying non-forested wetlands.

Polarimetric decompositions divide the total energy received from a sensor into different components each of which has a physical meaning. Applying SAR data through different polarimetric decomposition techniques enables effective discrimination of various wetlands. There are no consistent results in the literature regarding the best decomposition methods to classify wetlands. For instance, Brisco et al. (2011) investigated several decomposition methods, including Cloude-Pottier (Cloude, 1985), Freeman-Durden (Freeman and Durden, 1998), and Pauli

for the identification of wetland classes using Convai-580 C-band imagery. They reported that the wetland map produced by the Cloude-Pottier decomposition had the highest Overall Accuracy (OA = 65%) compared to the other two methods. Additionally, Millard and Richardson (2013) compared the classification results obtained by nine various approaches using three different decomposition methods: Freeman-Durden, Cloude-Pottier, and Touzi (Touzi, 2007). Based on their analyses, including the features extracted from the Touzi decomposition resulted in a higher classification accuracy compared to adding the other features extracted from the Freeman-Durden and Cloude-Pottier decompositions. Finally, White et al. (2015) investigated various decomposition methods for wetland classification in Canada. They argued that the $m\text{-}\chi$ decomposition had a higher accuracy compared to the Freeman-Durden decomposition when identifying changes from wet soil to open water within a season.

Although there are many studies which have applied various SAR data and different decomposition methods for wetland classification, there is no consistent conclusion on which SAR features are the most useful for discriminating different wetland classes. This might be because different studies have employed various sensor characteristics, and analyzed different study areas and wetland classes. However, the separability of five wetland classes using large amount of in situ data and for different channels of multi-source SAR data and various polarimetric features extracted from different decomposition methods are investigated in this study to obtain a reliable conclusion.

5.2. Study areas and datasets

5.2.1. Study areas

This research is part of a larger project for wetland inventory of Newfoundland and Labrador (NL), Canada. Multiple organizations, including federal, provincial, and local industries are involved in this project. After extensive discussion with project partners, five study areas were selected (Figure 5.1) to develop and evaluate the classification methods. Wetlands of all five classes described by the CWCS can be found in the study areas, though peatlands (bogs and fens) are dominant. It is widely acknowledged that wetland ecology and distribution is particularly controlled by climate and topography (Mitsch and Gosselink, 1993). Therefore, the study areas were selected such that they represent different local climates, ecoregions, and sub-regions of NL. Consequently, wetlands of these study areas can be considered representatives of the wetlands of all classes and ecologies in the province. A brief explanation of each study area is provided in the following subsections.



Figure 5.1. Study areas.

5.2.1.1. Avalon

Avalon is located in the northeastern portion of the Avalon Peninsula between the latitudes and longitudes of 47°39'57.91"N, 52°47'07.45"W and 47°15'01.11"N, 53°00'19.96"W. This study area is located within the Maritime Barren ecoregion and is characterized by an oceanic climate. Land cover within Avalon is dominated by extensive balsam fir forests, peatlands, heathland barrens, urban regions, and agricultural areas (South, 1983).

5.2.1.2. Grand Falls-Windsor

Grand Falls-Windsor is located in the north central portion of the Island of Newfoundland, between the latitudes and longitudes of 49°14'21.76"N, 55°45'06.68"W and 48°54'33.28"N, 55°41'51.05"W. This study area is located

within the Central Newfoundland ecoregion, an ecological sub-region of the island, which is characterized by a continental climate (Ecological Stratification Working Group, 1996). Boreal forest, barrens, and peatland dominate the majority of the study area (South, 1983), though there is several minor urban and agricultural areas in the south, where the town of Grand Falls-Windsor is located.

5.2.1.3. Deer Lake

Deer Lake is located in the north-east portion of the Island of Newfoundland, between the latitudes and longitudes of 49°34'28.54"N, 57°08'28.67"W and 49°08'19.74"N, 57°07'53.40"W. Falling within the North Central ecoregion of Newfoundland, Deer Lake and the surrounding area experience a continental climate, where summers are relatively hot and winters are cold and short compared to the rest of the island (Ecological Stratification Working Group, 1996). The land cover is dominated by extensive peatlands and balsam and black spruce forests (South, 1983). Within the South-East portion of the study area, there are several minor urban regions, such as the town of Howley and several other minor habitations along major roadways. It should be noted that much of the Northern portion of Deer Lake, which is dominated by forest and peatlands, is inaccessible via major roadways (South, 1983).

5.2.1.4. Gros Morne

Gros Morne is located on the Great Northern Peninsula on the west coast of Newfoundland, between the latitudes and longitudes of 50°15'26.55"N, 57°31'14.37"W and 49°34'53.01"N, 57°54'50.56"W. The climate in this area is oceanic due to the proximity to the Gulf of St. Lawrence to the west (Ecological

Stratification Working Group, 1996). Dominant land cover across Gros Morne includes low-lying peatlands, minor towns, and communities along the west coast. In addition, mountainous areas dominated by balsam fir and black spruce forests are located in the east (South, 1983).

5.2.1.5. Goose Bay

Goose Bay is located in central Labrador within the Lake Melville ecoregion between the latitudes and longitudes of 53°33'47.50"N, 60°10'17.59"W and 53°03'48.29"N, 60°22'06.09"W. The Lake Melville ecoregion is characterized by a climate of humid, cool summers, and cold winters. Generally, the landscape is dominated by extensive forests of balsam fir, black spruce, and white birch, interrupted by lowlands through which river valleys run. Permafrost also occurs in wetlands in this region as a result of Labrador's Northern latitude (Ecological Stratification Working Group, 1996). Small urban areas are also present in the centre of Goose Bay, where a portion of the town of Happy Valley-Goose Bay is located.

5.2.2. Field data

Field surveys were conducted in the summer and fall of 2015, 2016 and 2017. The potential wetland sites were first visited in the field and once it was confirmed that the site was in fact a wetland, it was labeled based on the wetland classes specified in the CWCS (i.e. Bog, Fen, Marsh, Swamp, and Shallow Water). The CWCS was selected in this study because:

- 1) Because the CWCS is country wide, the results of any classification in one province can be compared to that in another province. In other-words, the CWCS can act as a standard benchmark.
- 2) It has five general wetland classes and can be more easily identified by a various field work teams that may have different experiences classifying wetlands.

To classify wetlands based on the CWCS, the wetlands dominant vegetative structure, indicator species, and hydrological characteristics of each site were considered. The coordinates of each wetland site were collected using a hand-held Global Positioning System (GPS). Additionally, several other ancillary information, such as on-site pictures, dominant hydrology and vegetation were recorded. Because wetlands fall on a gradient (Zoltai and Vitt, 1995), there were often cases in the field where a wetland was not obviously classified as one class. In this case, the wetland was noted as being more than one potential class and was flagged for visitation in future field work. These sites were not used in this study. Other difficult examples included areas where hydrophytic vegetation were present, but with little or no evidence of water. This was often the case for the Marsh class, in which dry weather over summer removes much of the surface water. These sites were confirmed to be wetland using Google Earth's temporal slider to find evidence of water during different times of the year.

After collecting GPS points, the final step involved boundary delineation for each site, which was carried out in ArcMap 10.3.1 using the collected GPS points, high resolution satellite and aerial imagery, field ancillary information, and advice from biologists experienced in working with wetlands. Boundaries were drawn conservatively to avoid the potential inclusion of unclear, difficult to classify

transition areas between one land cover type (a particular wetland class) and another (a different wetland class or upland). The end result was numerous polygons representing individual wetland classes. Table 5.1 provides the information of the field samples used in this study for the backscattering analysis of five wetland classes.

Table 5.1. Total number of field samples collected over all study areas.

	Bog	Fen	Marsh	Swamp	Shallow Water
# Samples	210	214	171	180	122
Area (ha)	2036	632	311	233	313

5.2.3. Satellite data

Table 5.2 demonstrates the SAR data used in this study. Since the aim was to analyze the backscattering response of each wetland class in different SAR channels, the images acquired by RADARSAT-2 and Sentinel-1 C-band, and ALOS-2 L-band were considered in this study. As clear from Table 5.2, the images captured in August were selected because this was the month that had the greatest amount of satellite data covering each of the study areas available for this research.

Table 5.2. The SAR data used in this study.

	Avalon	Grand Falls- Windsor	Deer Lake	Gros Morne	Goose Bay
RADARSAT-2	2015/08/21	-	2015/08/10	2015/08/03	-
Sentinel-1	2015/08/20	2015/08/13	2015/08/15	2015/08/15	2015/08/20
	2015/08/		2015/08/18		2015/0823
ALOS-2	2015/08/02	-	-	-	-

5.3. Methodology

5.3.1. Preprocessing and feature extraction

The intensity channels were first extracted from the dual polarimetric data (i.e., the data acquired by Sentinel-1 and ALOS-2). The scattering matrix was also converted to the covariance matrix for full polarimetric data (i.e. RADARSAT-2 data). Then, a Lee enhanced filter (Lopes et al., 1990) and a PolSAR Lee filter (Lee et al., 1999) with window sizes of 7×7 pixels were applied to the intensity layers and the covariance matrix, respectively, to reduce speckle noise. All data were subsequently georeferenced and terrain-corrected using the 10 meters Canadian Digital Elevation Model (CDEM) and the Mapready™ software. Finally, various types of SAR features were extracted from RADARSAT-2 full polarimetric data using PolSARpro™ software (Table 5.3). These features along with the features extracted from the dual polarimetric data (Table 5.3) were investigated in this study for their capability in discriminating wetland classes. Based on Table 5.3, there were 78 features in total which were assessed in this study.

Table 5.3. SAR features investigated for separability analysis of wetland classes.

Sentinel-1	
5 features:	
horizontal transmit and horizontal receive polarization of Sentinel-1: S1_HH	
horizontal transmit and vertical receive polarization of Sentinel-1: S1_HV	
vertical transmit and vertical receive polarization of Sentinel-1: S1_VV	
Ratio features: $S1_HH/HV = \frac{ S_{HH} ^2}{ S_{HV} ^2}$, $S1_VV/HV = \frac{ S_{VV} ^2}{ S_{HV} ^2}$	
ALOS-2	
3 features:	
horizontal transmit and horizontal receive polarization of ALOS-2: A2_HH	
horizontal transmit and vertical receive polarization of ALOS-2: A2_HV	
Ratio feature: $A2_HH/HV = \frac{ S_{HH} ^2}{ S_{HV} ^2}$	
RADARSAT-2	
Covariance matrix (16 features)	Diagonal elements: $C11 = S_{HH} ^2$, $C22 = 2 S_{HV} ^2$, $C33 = S_{VV} ^2$ Total Power: $TP = S_{HH} ^2 + 2 S_{HV} ^2 + S_{VV} ^2$ Off-diagonal elements: $C12 = \sqrt{2} S_{HH} S_{HV}^*$, $C13 = S_{HH} S_{VV}^*$, $C21 = \sqrt{2} S_{HV} S_{HH}^*$, $C23 = \sqrt{2} S_{HV} S_{VV}^*$, $C31 = S_{VV} S_{HH}^*$, $C32 = \sqrt{2} S_{VV} S_{HV}^*$ (* indicate the complex conjugate operation) Ratio features: $R2_HH/HV = \frac{ S_{HH} ^2}{ S_{HV} ^2}$, $R2_VV/HV = \frac{ S_{VV} ^2}{ S_{HV} ^2}$, $R2_HH/VV = \frac{ S_{HH} ^2}{ S_{VV} ^2}$, $R2_HH/TP = \frac{ S_{HH} ^2}{TP}$, $R2_HV/TP = \frac{ S_{HV} ^2}{TP}$, $R2_VV/TP = \frac{ S_{VV} ^2}{TP}$
Coherency matrix (9 features)	Diagonal elements: $T11 = 0.5 S_{HH} + S_{VV} ^2$, $T22 = 0.5 S_{HH} - S_{VV} ^2$, $T33 = 2 S_{HV} ^2$ Off-diagonal elements: $T12 = 0.5(S_{HH} + S_{VV})(S_{HH} - S_{VV})^*$, $T13 = (S_{HH} + S_{VV})S_{HV}^*$, $T21 = 0.5(S_{HH} - S_{VV})(S_{HH} + S_{VV})^*$, $T23 = (S_{HH} - S_{VV})S_{HV}^*$, $T31 = S_{HV}(S_{HH} + S_{VV})^*$, $T32 = S_{HV}(S_{HH} - S_{VV})^*$ (* indicate the complex conjugate operation)
Freeman-Durden (3 features)	Surface scattering: odd_F Double-bounce scattering: dbl_F Volume scattering: vol_F
Van Zyl (Van Zyl, 1989), (3 features)	Surface scattering: odd_V Double-bounce scattering: dbl_V

Yamaguchi (Yamaguchi et al., 2005), (4 features)	Volume scattering: vol_V Surface scattering: odd_Y Double-bounce scattering: dbl_Y Volume scattering: vol_Y Helix scattering: hlx_Y
Krogager (Krogager, 1990), (3 features) H/A/Alpha (3 parameters)	Sphere scattering: Ks Diplane scattering: Kd Helix scattering: Kh Entropy: $H = -\sum_{i=1}^3 P_i \log_3(P_i)$ (where $P_i = \frac{\lambda_i}{\sum_{k=1}^3 \lambda_k}$, $\sum_{k=1}^3 P_k = 1$) Anisotropy: $A = \frac{\lambda_2 - \lambda_3}{\lambda_2 + \lambda_3}$ Alpha = $\sum_{i=1}^3 P_i \alpha_i$
Touzi (4 features)	Symmetric scattering type magnitude: Alpha_s Symmetric scattering type phase: P_Alpha_s Orientation angle: ψ Helicity: τ
Eigenvalue parameters (25 features)	Beta Delta Gamma First eigenvalue: Lambda1 Second eigenvalue: Lambda2 Third eigenvalue: Lambda3 First pseudo probability: $P1 = \frac{\lambda_1}{\lambda_1 + \lambda_2 + \lambda_3}$ Second pseudo probability: $P2 = \frac{\lambda_2}{\lambda_1 + \lambda_2 + \lambda_3}$ Third pseudo probability: $P3 = \frac{\lambda_3}{\lambda_1 + \lambda_2 + \lambda_3}$ Polarization Fraction: $PF = 1 - \frac{3\lambda_3}{\lambda_1 + \lambda_2 + \lambda_3}$ Polarization Asymmetry: $PA = \frac{P1 - P2}{PF}$ Luenburg Anisotropy: $LA = \sqrt{\frac{3}{2}} \sqrt{\frac{\lambda_2^2 + \lambda_3^2}{\lambda_1^2 + \lambda_2^2 + \lambda_3^2}}$ Anisotropy12: A12 Shannon Entropy: SE Normalized Shannon Entropy: NSE Polarimetry Shannon Entropy: PSE Normalized Polarimetry Shannon Entropy: NPSE Intensity Shannon Entropy: ISE

Normalized Intensity Shannon Entropy: NISE

Single-bounce eigenvalues relative difference: serd =

$\frac{\lambda_S - \lambda_{NOS3}}{\lambda_S + \lambda_{NOS3}}$ (λ_S is the eigenvalue for the single-bounce scattering and λ_{NOS3} indicates Non-Order Size (NOS) eigenvalue)

Normalized single-bounce eigenvalues relative difference:

N_serd

Double-bounce eigenvalues relative difference: derd =

$\frac{\lambda_D - \lambda_{NOS3}}{\lambda_D + \lambda_{NOS3}}$ (λ_D is the eigenvalue for the double-bounce scattering and λ_{NOS3} indicates Non-Order Size (NOS) eigenvalue)

Normalized double-bounce eigenvalues relative difference: N_derd

Radar Vegetation Index: $RVI = \frac{4\lambda_3}{\lambda_1 + \lambda_2 + \lambda_3}$

Pedestal Height: $PH = \frac{\lambda_3}{\lambda_1}$

Note: For a more complete description of the polarimetric features investigated in this study, interested readers can refer to Cloude and Pottier (1996), Maghsoudi (2011), and Hobart (2015).

5.3.2. Variance analysis of field samples

When analyzing the separability of land cover classes using field samples, it is necessary that the values of field samples extracted from a particular class are approximately within the same range. In addition, it should be guaranteed that the variance value of field samples must be greater between rather than within classes in a particular band. Variance analyses on the field samples are essential in wetland classification using SAR data because:

- (1) Wetlands are considerably complex environments, where each wetland class can contain several subclasses. For instance, the Bog class can be divided into Treed Bog, Shrubby Bog, and Open Bog, where each has various characteristics. On the other hand, some wetland classes, such as

Bog and Fen, can be considerably similar in terms of spectral and backscattering information

(2) SAR images are speckled as opposed to other satellite data, such as optical data (Mahdavi et al., 2018).

To perform variance analysis, the variance value of field samples, obtained from each SAR feature, was first calculated for each wetland class using Equation (1).

$$Var = \frac{1}{N - 1} \sum_{i=1}^N (x_i - \mu)^2 \quad (5.1)$$

where x_i is the value of a field sample, μ indicates the mean value of samples, and N refers to the number of field samples in a feature. Then, the features for which the field samples contained considerable variance were removed from the subsequent analyses. Additionally, the Fisher (F)-statistics (Equation (2)) was utilized to analyze the within and between class variances for wetland class pairs. Then, the features for which the F-statistics was less than one, were removed from the rest of analyses.

$$F = \frac{Var_B}{Var_W} \quad (5.2)$$

in which Var_W and Var_B refer to the within and between variance values in each class pair, respectively.

5.3.3. Separability measure

Many separability distances have so far been developed and used for discriminating land cover classes with inconsistent results and there is not a unique method to select the optimum features in a classification (Yeung et al., 2005; Adam et al., 2010; Proctor and Robinson, 2013). Thus, it was difficult to select the most appropriate separability measure in this study to select the best SAR features for delineating various wetland class pairs. Finally, since there were high variation between field samples (subsection 3.2) and the samples did not follow a normal distribution, the non-parametric Mann-Whitney U-test (Equation (3-5)) was used to assess the capabilities of various SAR features extracted from multi-source sensors for discriminating wetlands (Lehmann, 2004).

$$U - Statistics = \min(U_1, U_2) \quad (5.3)$$

$$U_1 = n_1 n_2 + \frac{n_1(n_1 + 1)}{2} - R_1 \quad (5.4)$$

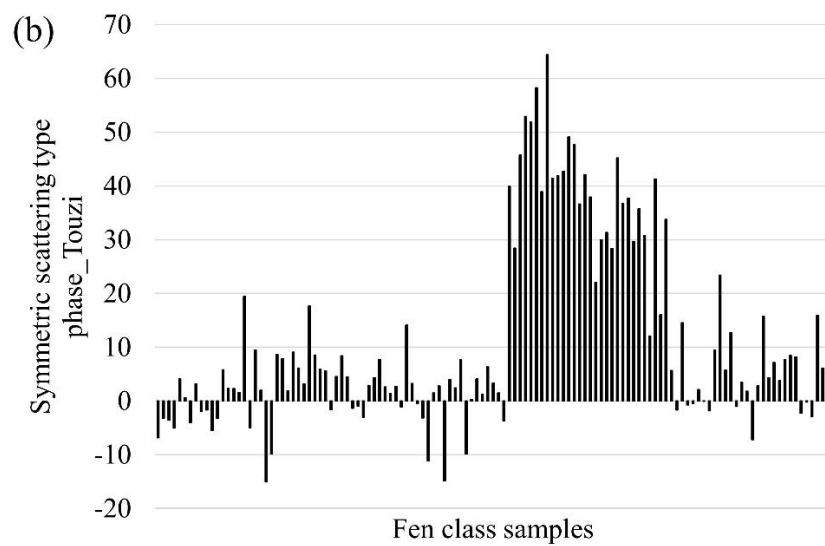
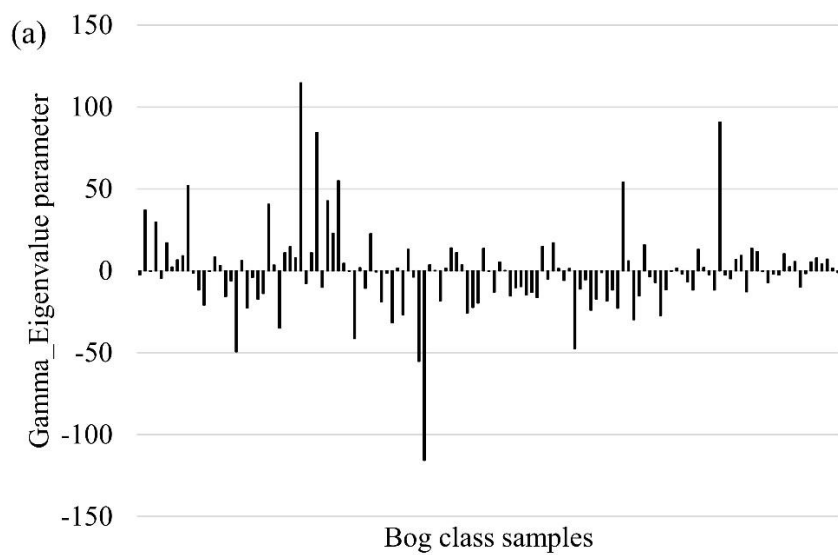
$$U_2 = n_1 n_2 + \frac{n_2(n_2 + 1)}{2} - R_2 \quad (5.5)$$

in which U_i is the U value calculated for class i . In addition, n_i and R_i are the number of samples and the sum of the ranks for class i , respectively.

5.4. Results and discussion

Equation (1) and Equation (2) were used to perform variance analyses on the individual classes and wetland class pairs, respectively. Figure 5.2 provides four

examples where the field samples for a specific class did not have the same values. The variance analyses were conducted for five wetland classes using 78 features (see Table 5.3). Finally, 23 features were removed from the subsequent experiments. These features were the off-diagonal elements of both covariance and coherency matrices, P_Alpha_s , ψ , τ , Delta, Gamma, $derd$, SE, NSE, PSE, ISE, and NISE. To be more precise, the results of the variance analyses showed that all the off-diagonal elements of the covariance and coherency matrices, which contain phase information, provided noisy results and, thus, were not identified as suitable features for the separability analysis of wetland classes. Moreover, although several studies have argued that the Touzi decomposition was very helpful in wetland classification (e.g. Touzi, 2007 and Touzi et al., 2009), the results of the variance analyses in this study demonstrated that three out of four components of this technique provided noisy results and were not recommended to be inserted in the wetlands classification procedure. The results of this study demonstrated that the Touzi decomposition method should be evaluated more in future studies to have a more reliable conclusion of the effectiveness of this technique for wetland classification. Several eigenvalue parameters were also detected as noisy features and were removed in the variance analyses step. For instance, 5 out of 6 components related to the Shannon Entropy were not selected as proper features for separability analysis of wetlands. Moreover, the Delta and Gamma features, which are considered as the components of the Cloude-Pottier decomposition, demonstrated high variance values for the field samples and were removed from the next experiments.



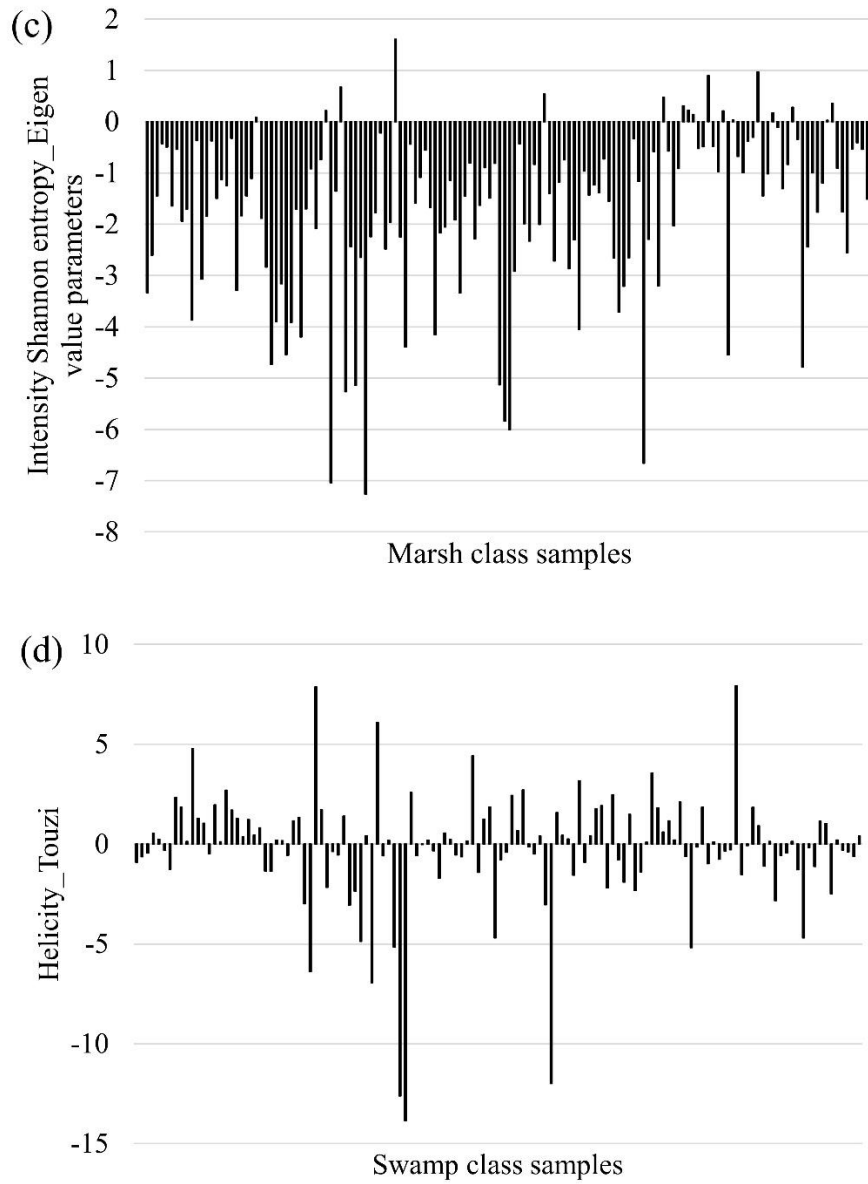


Figure 5.2. SAR feature values for the field samples of wetland classes.

Based on the variance analyses, it was also observed that the field samples of the wetland classes obtained from some of the SAR features should be divided into more than one class (see Figure 5.3 (d)). This is because each of the five main wetland classes, specified by the CWCS, can contain several subclasses, the

backscattering responses of which may differ. This fact demonstrates why some wetland classification systems, such as the Enhanced Wetland Classification System (EWCS), categorize wetland classes into several subclasses (19 wetland subclasses in the case of the EWCS). For instance, the Bog class is divided into three subclasses in the EWCS (Figure 5.3 (a-c)): treed bog, shrubby bog, and open bog. Consequently, when analyzing the backscattering characteristics of the field samples of the Bog class using some of the SAR features, a three-modal signature was observed (Figure 5.3 (d)).

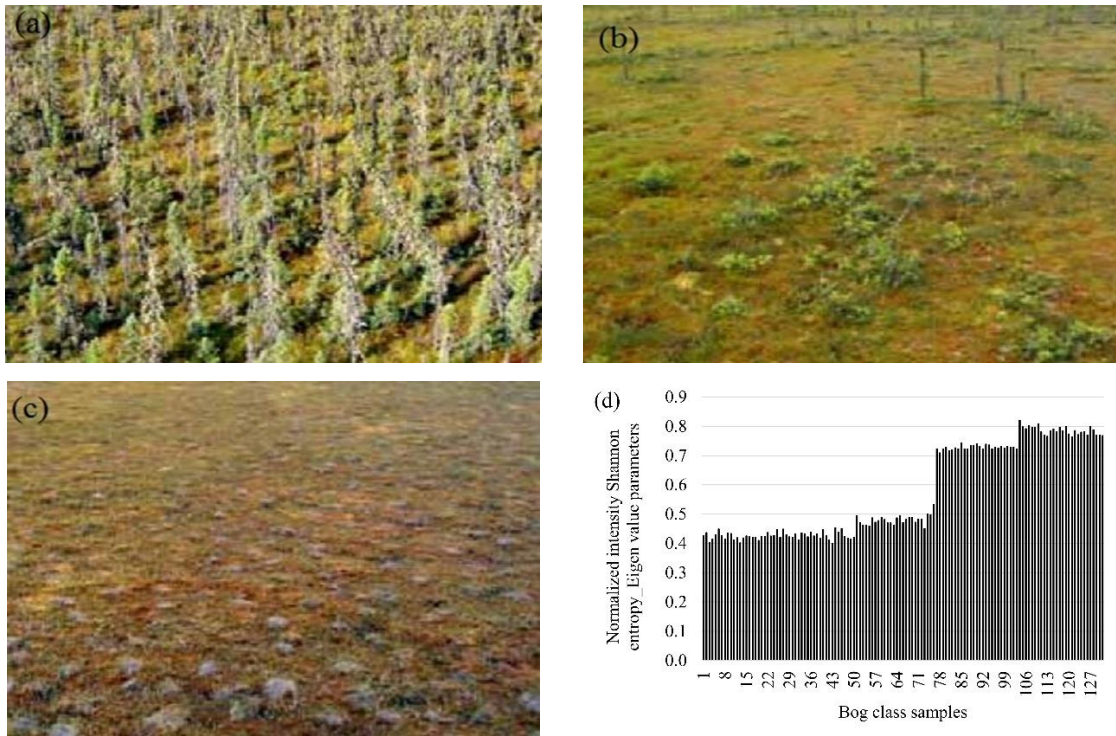
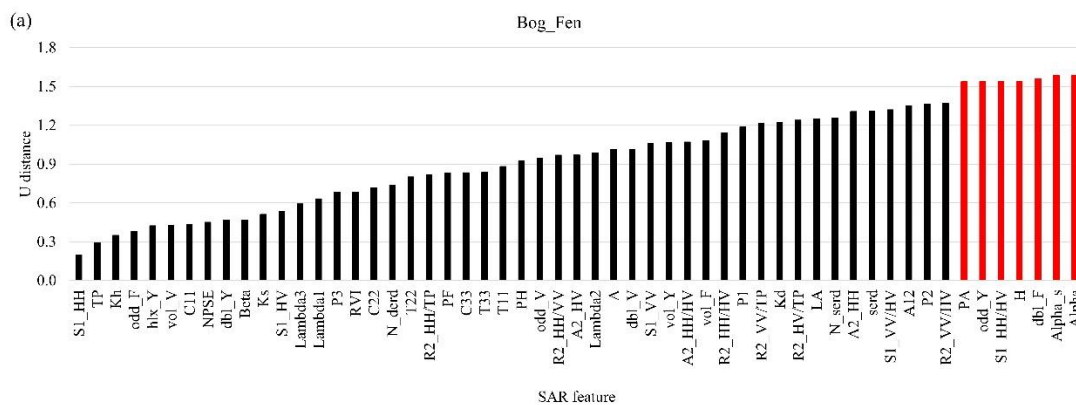
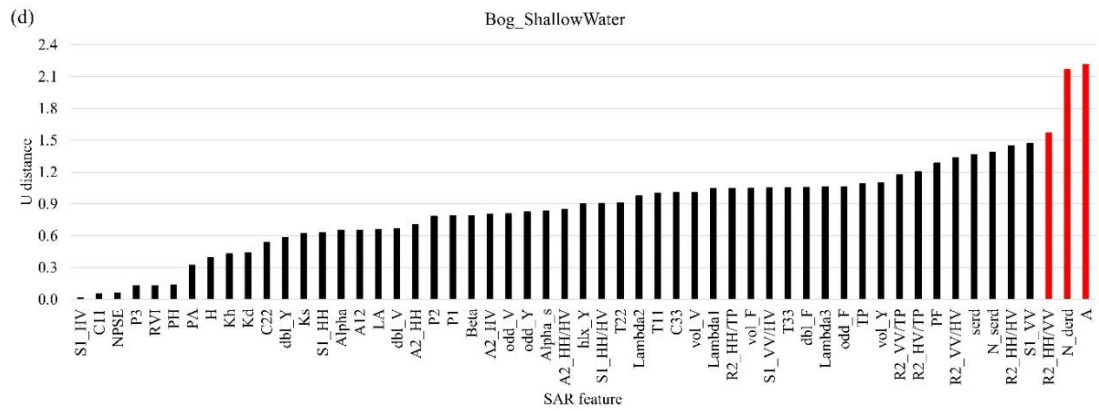
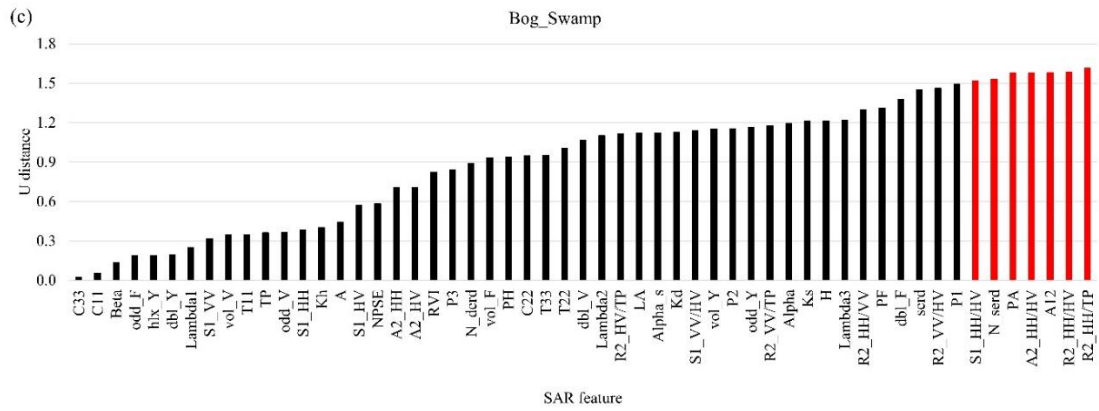
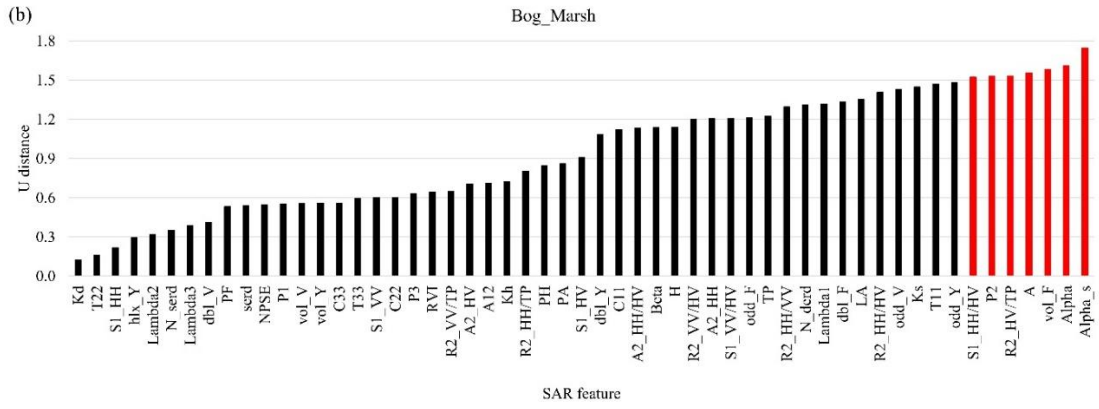
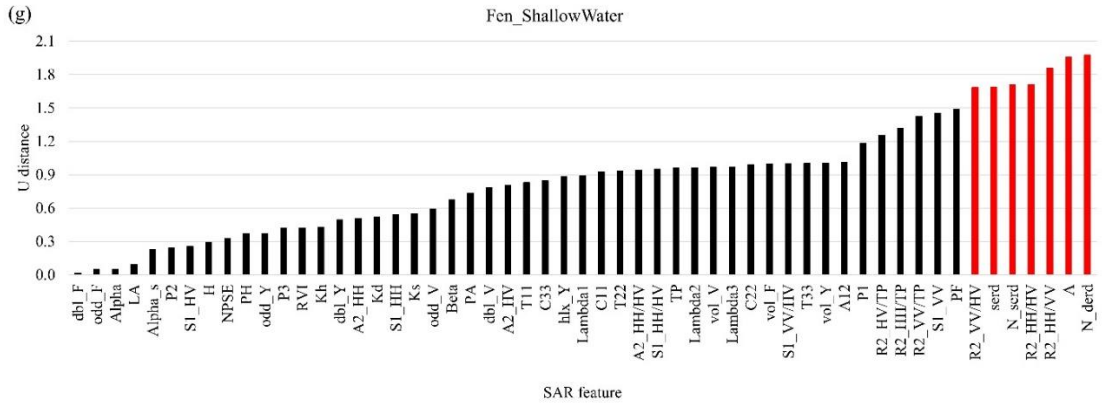
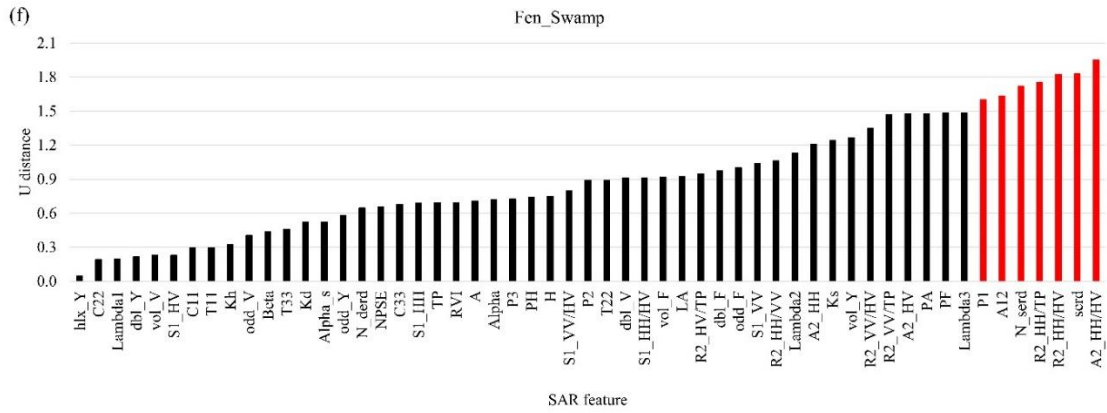
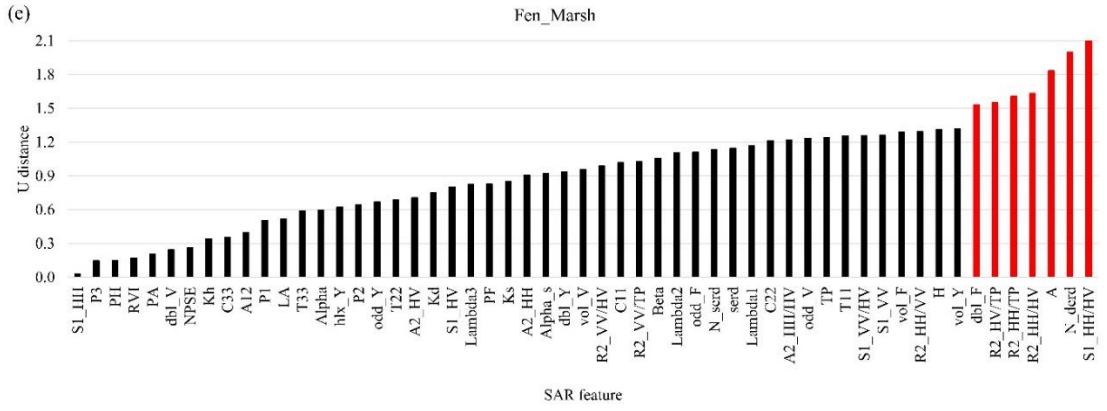


Figure 5.3. Three subclasses of the Bog class (a: treed bog, b: shrubby bog, c: open bog) and (d) the backscattering values of the field samples of the Bog class.

Separability analysis was performed using the Mann-Whitney U-test on the 55 remaining SAR features after variance analyses. Figure 5.4 demonstrates the amount of separability that each feature provides for each wetland class pair using U distance. In this study, the features that provided the separability measures exceeding 1.5 (red bars in Figure 5.4) were selected as the most useful features for distinguishing the class pairs. Figure 5.5 also shows the separability of each pair of wetlands using the five decomposition techniques investigated in this study. The red bars correspond to the decomposition methods which were the most useful in separating wetland class pairs (The U distance > 1 was considered a proper separability in this step). The results of Figure 5.4 and Figure 5.5 are summarized in Table 5.4 and can be used as a reference table for selecting the best SAR features and decomposition methods to distinguish wetland class pairs. In addition, the values of the U distance for each pair of wetland classes in Figure 5.4 and Figure 5.5 were aggregated to evaluate the amount of separability that each SAR feature/decomposition method provided for all wetland classes, the results of which are illustrated in Figure 5.6.







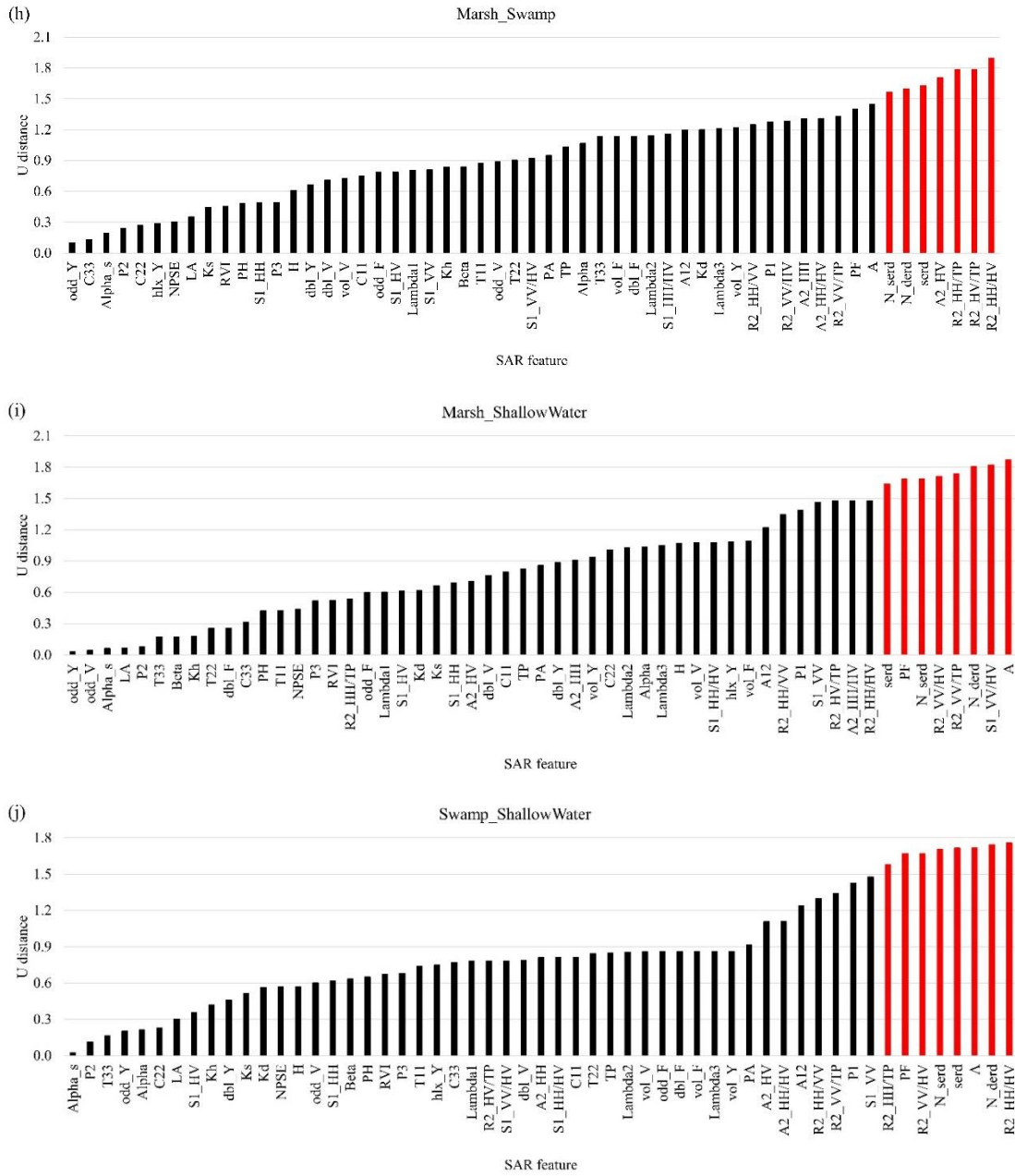
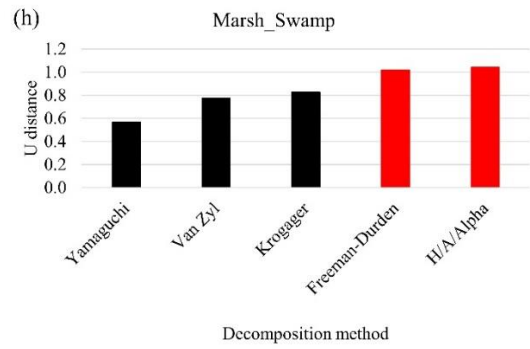
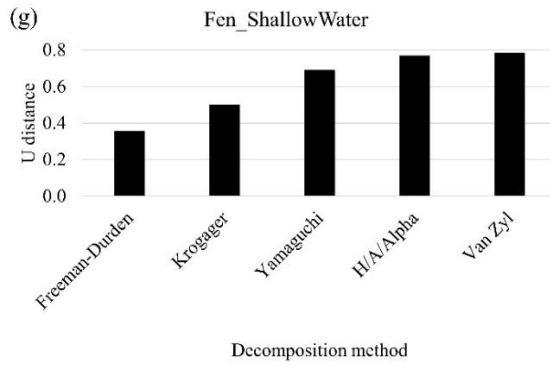
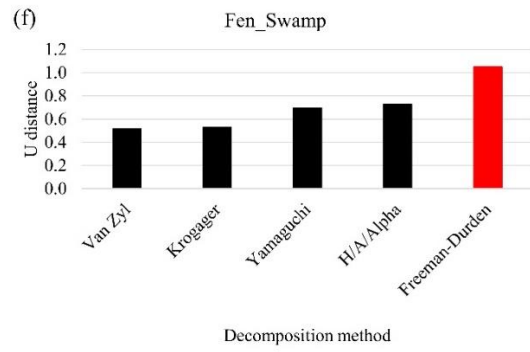
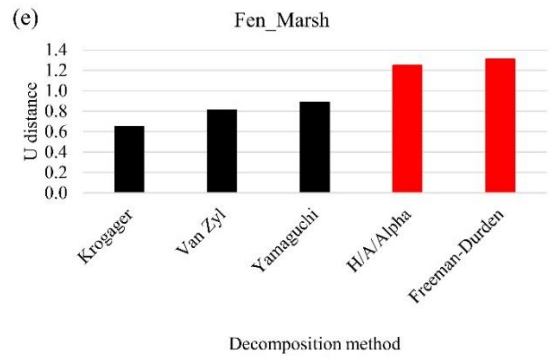
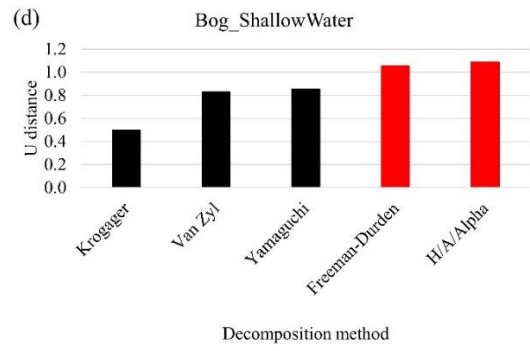
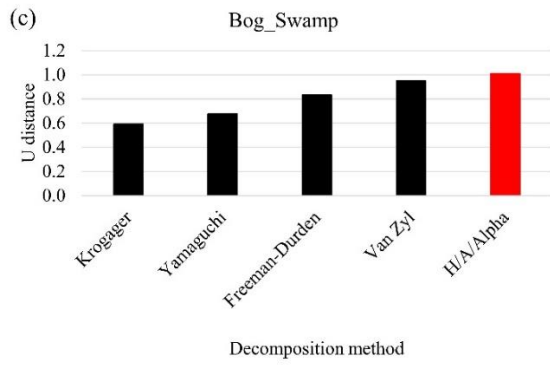
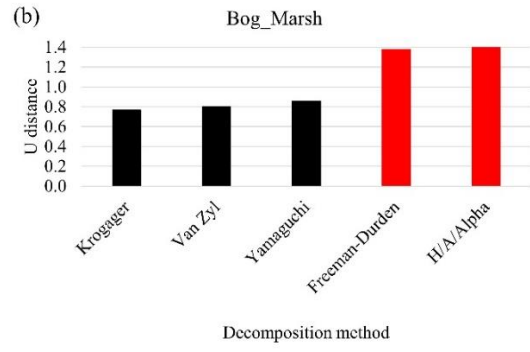
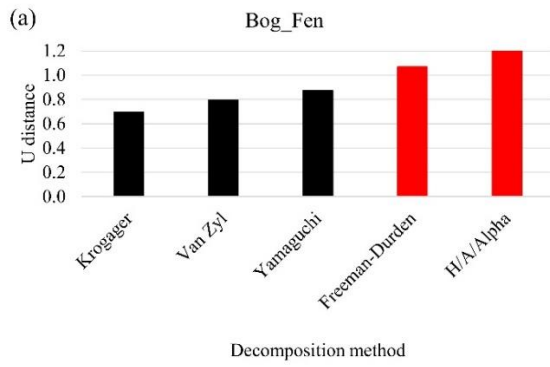


Figure 5.4. Seaprability measure obtained from the SAR features for each pair of wetland classes using the U-test. The red bars indicate the best SAR features for discriminating various wetland class pairs (refer to Table 5.3 for acronym definitions).



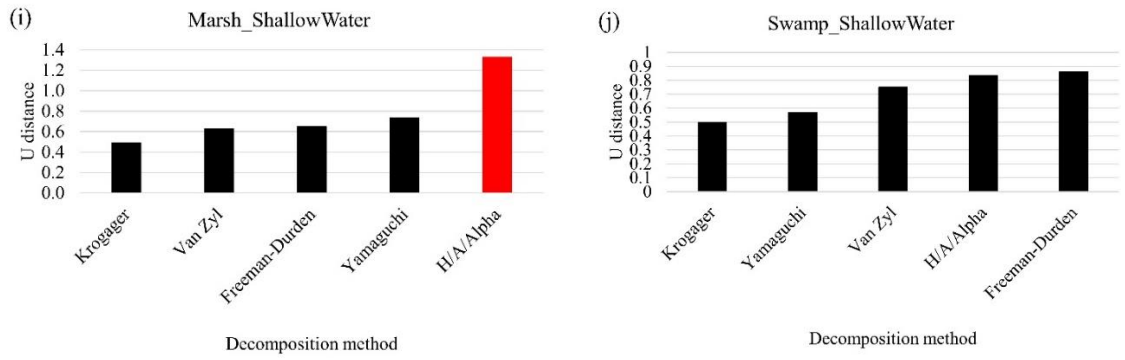


Figure 5.5. Seapability measure obtained from different decomposition methods for each pair of wetland classes using the U-test. The red bars indicate the most useful decomposition methods for differentiating various wetland class pairs.

Table 5.4. The most useful SAR features (provided in the upper right half of the table) and the decomposition methods (provided in the lower left half of the table) for discriminating between each pair of wetland classes. The features and decomposition methods are ordered based on their separability measures (refer to Table 5.3 for the acronyms of the selected SAR features).

	Bog	Fen	Marsh	Swamp	Shallow Water
Bog	×	Alpha	Alpha_s	R2_HH/TP	A
		Alpha_s	Alpha	R2_HH/HV	N_derd
		dbl_F	vol_F	A12	R2_HH/VV
		H	A	A2_HH/HV	
		S1_HH/HV	R2_HV/TP	PA	
		odd_Y	P2	N_serd	
		PA	S1_HH/HV	S1_HH/HV	
Fen	H/A/Alpha	×	S1_HH/HV	A2_HH/HV	N_derd
	Freeman-Durden		N_derd	serd	A
			A	R2_HH/HV	R2_HH/VV
			R2_HH/HV	R2_HH/TP	R2_HH/HV
			R2_HH/TP	N_serd	N_serd
			R2_HV/TP	A12	serd
			dbl_F	P1	R2_VV/HV
Marsh	H/A/Alpha	Freeman-Durden	×	R2_HH/HV	A
	Freeman-Durden	H/A/Alpha		R2_HV/TP	S1_VV/HV
				R2_HH/TP	N_derd
				A2_HV	R2_VV/TP
				serd	R2_VV/HV
				N_derd	N_serd
				N_serd	PF
					serd
Swamp	H/A/Alpha	Freeman-Durden	H/A/Alpha	×	R2_HH/HV
			Freeman-Durden		N_derd
					A
					serd
					N_serd
					R2_VV/HV
					PF
					R2_HH/TP

Shallow Water	H/A/Alpha Freeman-Durden	-	H/A/Alpha	-	×
---------------	-----------------------------	---	-----------	---	---

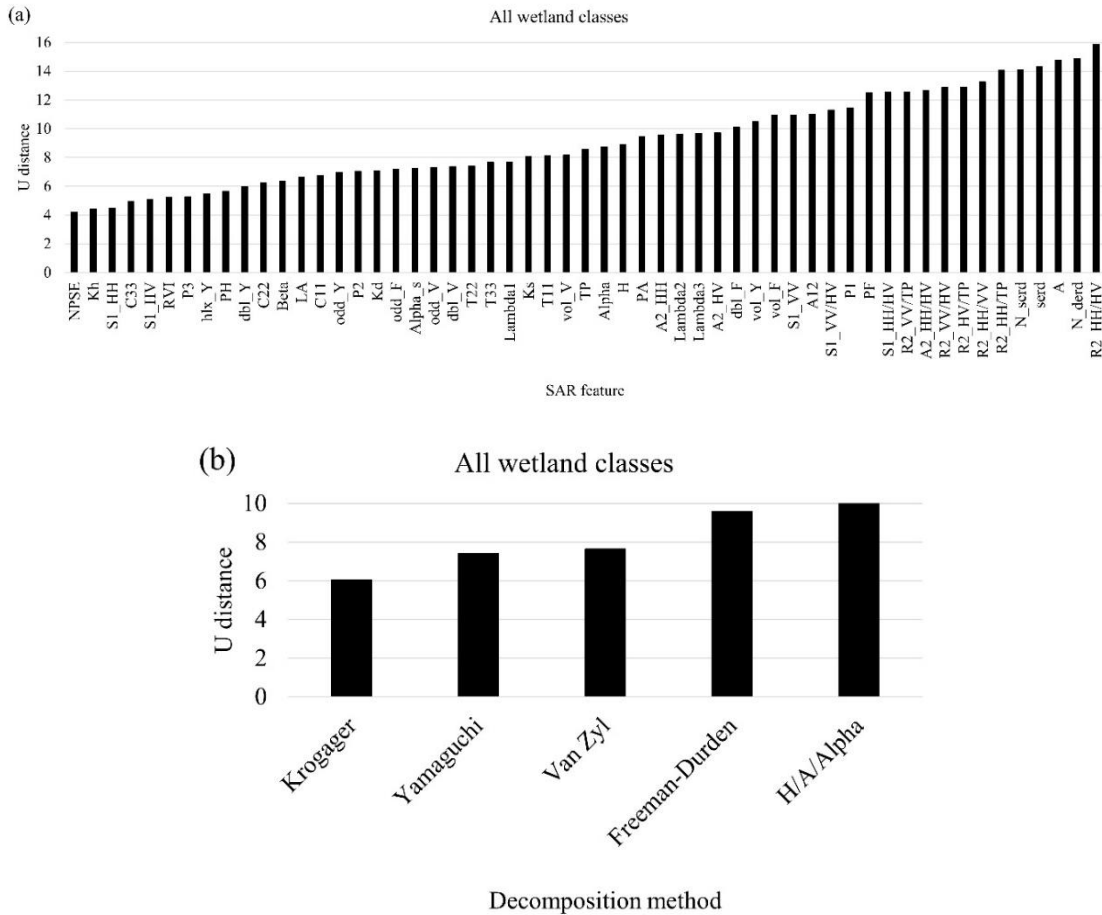


Figure 5.6. Seapability measure obtained from the (a) SAR features and (b) different decomposition methods for all wetland classes using the U-test (refer to Table 5.3 for acronym definitions).

Based on Figure 5.5 and Figure 5.6 (b), the H/A/Alpha decomposition was the most efficient method for differentiating wetland class pairs and, thus, for all wetland classes in this study. The H/A/Alpha is an eigenvector-based decomposition

method and is obtained based on the eigen decomposition of the coherency matrix (Maghsoudi, 2011). This method can effectively represent the characteristics of natural targets, such as wetland classes (Mahdianpari et al., 2018), by incorporating the information of the heterogeneity of targets (using H component), importance of secondary scattering mechanism (using A component), and dominant scattering mechanism (using the Alpha angle). Based on Figure 5.5, this method was selected as the best decomposition technique in 6 out of 10 class pairs. Additionally, three features extracted from this method were most often among the best for discriminating wetland class pairs (see Figure 5.4 and Table 5.4). For instance, except the case of separating the Swamp class from the Bog, Fen, and Marsh classes (3 cases), one (or more than one) of these three components, usually Anisotropy, was among the most efficient SAR features for distinguishing the pairs of wetland classes (see Table 5.4).

In addition, the results of this study showed that besides the H, A, and Alpha, some other SAR features, which were derived from eigenvalues of the coherency matrix (i.e., 25 features illustrated in Table 5.3) provided a high potential for wetlands discrimination. In this regard, three features of *serd*, *N_serd*, and *N_derd* (introduced by Allain et al., 2005) demonstrated a strong power for delineating wetland species. As clear from Figure 5.4, Table 5.4, and Figure 5.6 (a), *serd*, *N_serd*, and *N_derd* were frequently selected as the most efficient SAR features for separation of different wetland classes. For example, one (or more than one) of these three features proved to be effective in 8 out of 10 cases (Table 5.4). The authors (Allain et al., 2005) derived these parameters from the averaged coherency matrix considering the reflection symmetry hypothesis, and demonstrated their effectiveness in classifying natural media.

The Freeman-Durden was the second most effective decomposition method in discriminating various wetlands. Unlike other decomposition methods investigated in this study, Freeman-Durden is based on the physics of SAR scattering and provides valuable information about naturally incoherent scatterers such as wetlands (Freeman and Durden, 1998; Mahdavi et al., 2017a). This method decomposes the scattering energy into three physical mechanisms: single-bounce, double-bounce, and volume scattering. In fact, the Freeman-Durden model provides independent descriptors which are properly associated with wetland classes. For instance, the *odd_F*, *dbl_F*, and *vol_F* features were considerably helpful in identifying the open water (e.g. the Shallow Water class), flooded wetlands (e.g. the Swamp class), and herbaceous wetlands (e.g. the Bog and Fen classes), respectively.

The Van Zyl decomposition method was selected as the third most effective method. Although the Van Zyl decomposition is a modified version of the Freeman-Durden technique and the methods utilize similar components, the Van Zyl was not as helpful as the Freeman-Durden method. The reason might be the fact that the Van Zyl does not completely consider the physical characteristics of targets and is more bound to pure mathematical models (Maghsoudi, 2011).

Although the Yamaguchi uses three elements of the odd-bounce, double-bounce, and volume scattering, it was less helpful than the Freeman-Durden and Van Zyl decompositions for wetland class separation. The reason is rooted in the fact that the Yamaguchi employs the helix component (*hlx_Y*) along with the three main mechanisms (i.e. *odd_Y*, *dbl_Y*, *vol_Y*), while the *hlx_Y* is mostly useful for characterizing complex urban structures and less helpful in identifying natural targets such as wetlands (Yamaguchi et al., 2005; Hong et al., 2015). Consequently,

the averaged separability measure obtained by its components was low. This is reflected in Figure 5.4 and Figure 5.6 (a) where the hlx_Y is among the poorest features for delineating wetland species. Thus, the Yamaguchi was not generally considered helpful in this study. However, the other three components of this decomposition method demonstrated their usefulness in some cases. For instance, odd_Y was among the best features for differentiating the Bog and Fen classes (Table 5.4).

Additionally, the results provided in Figure 5.7 demonstrated that the volume component obtained by three decompositions of the Freeman-Durden, Van Zyl, and Yamaguchi was the best element to discriminate wetland classes compared to two other components (i.e., single- and double-bounce). This was because volume scattering is the most important mechanism for most wetlands, such as herbaceous and forested wetland types (Mahdavi et al., 2017c; Mahdianpari et al., 2018). The double-bounce scattering was also the second most efficient component by providing the U distance = 23.46 (see Figure 5.7). The double-bounce is a powerful element to identify flooded areas, which is the case of wetland environments, and especially useful for distinguishing flooded swamps from other wetland classes (Brisco et al., 2015). The single-bounce mechanism was relatively the least useful feature (U distance = 21.44, Figure 5.7). This was because single bounce is mostly effective in classifying open water bodies (Mahdavi et al., 2017c), while most of the wetland classes in the study areas were vegetated (e.g. Bog, Fen, Marsh, and Swamp).

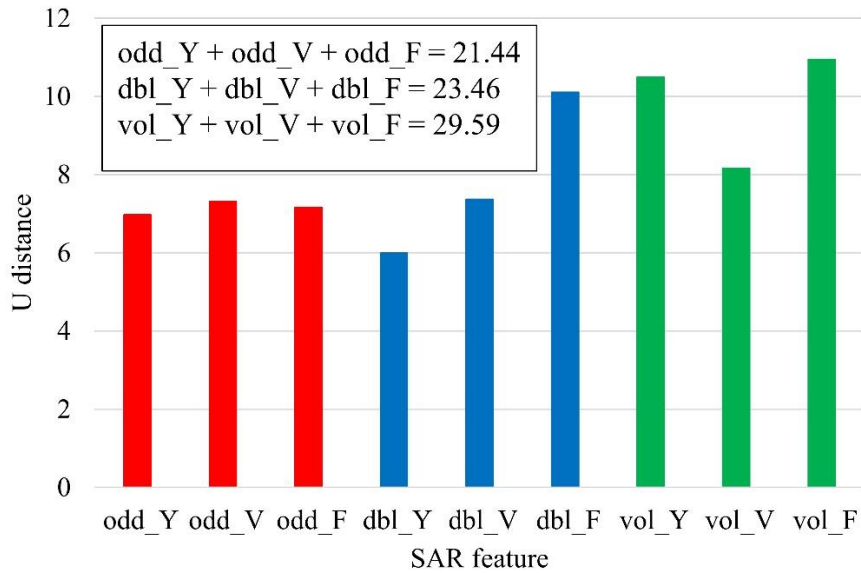


Figure 5.7. Comparison between the amount of separability that each odd-bounce, double-bounce, and volume scattering provided for all wetland classes (refer to Table 5.3 for acronym definitions).

Furthermore, the results indicated that the wetland classes were more difficult to separate using the Krogager decomposition method. For example, this decomposition was selected as the least useful technique in 7 out of 10 cases (see Figure 5.5). This was also observed when the features extracted from this method were assessed for separability analysis. For instance, the results demonstrated in Figure 5.4 showed that the K_s , K_d , and K_h were among the poorest features in terms of wetland class pairs discrimination. The most important reason was that the Krogager is a coherent decomposition technique and is more useful in identifying man-made features, such as those presented in urban areas, and is less applicable for classifying natural random targets like wetlands (Maghsoudi, 2011; Hobart, 2015).

Comparing all the features investigated in this study, the ratio features, especially those calculated from the RADARSAT-2 full polarimetric data, were the best SAR features for separation of the wetland classes. Deriving ratio of SAR images reduces speckle within them (Rignot and Van Zyl, 1993; Mahdavi et al., 2017c) and, thus, the corresponding features are less noisy and more appropriate for separating wetland classes. Based on Table 5.4, these features were among the optimum features in all 10 cases. Moreover, ratio features provided the highest separability in 5 out of 10 cases (see Figure 5.4). This proved that the relative values of SAR channels were considerably more promising than the absolute values of channels and can provide higher accuracy for wetland classification. As is clear from the results, although the intensity layers were not typically selected as the best features, the ratio features calculated from the intensity layers of all satellites were among the most efficient SAR features in the majority of cases considering individual class pairs and all wetland classes together. In fact, the ratio features reveal meaningful differences between two intensity channels, which might not be detectable when using a single-channel imagery (Rignot and Van Zyl, 1993).

As expected, the features extracted from the full polarimetric RADARSAT-2 data were generally much more informative than the features obtained by the dual polarimetric data (i.e., the data acquired by Sentinel-1 and ALOS-2). This was because wetlands are complex environments and contain complex scattering characteristics. Thus, full polarimetric data can detect this complexity using various decomposition methods. However, the dual polarimetric ratio features were considerably helpful in the separability analyses and proved to be useful in the absence of full polarimetric imagery.

The amount of separability obtained by the intensity layers ($|S_{HH}|^2$, $|S_{HV}|^2$, and $|S_{VV}|^2$) of ALOS-2 (L-band), Sentinel-1 and RADARSAT-2 (C-band) considering all wetland classes are illustrated in Figure 5.8. Comparing the results, ALOS-2 intensity layers were the most useful with U distance of 9.64. This was because L-band penetrates further into the vegetation canopy and can detect flooded vegetation through double-bounce scattering (Brisco et al., 2011; Mahdavi et al., 2017c). This was primarily observed when separating the Swamp class from other wetland types because Swamp trees were mostly flooded in the study areas and C-band cannot penetrate through these trees.

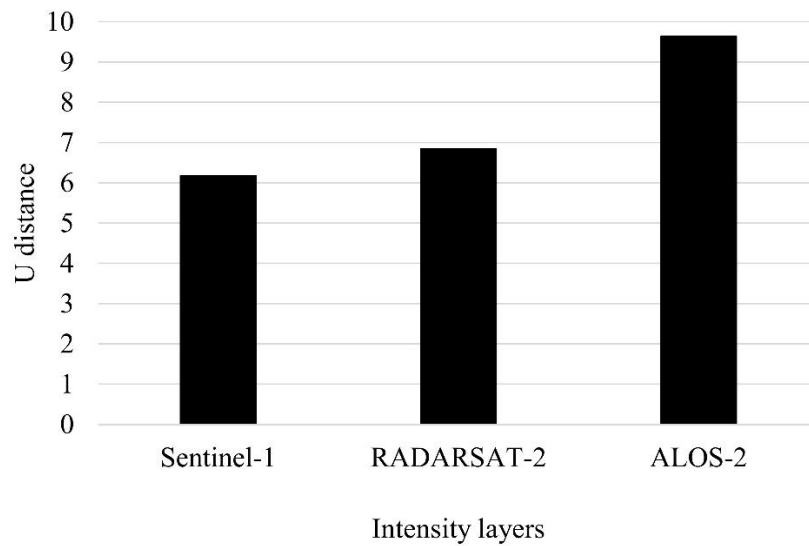


Figure 5.8. Comparison between the amount of separability that intensity layers of each satellite provided for all wetland classes.

5.5. Conclusion

Although several studies have investigated the separability of wetlands using various SAR features, the most important SAR features for differentiating wetland

species have been inconsistent. In this study, various SAR features (78 features) extracted from the dual C-band and L-band SAR systems (Sentinel-1 and ALOS-2, respectively), as well as full polarimetric RADARSAT-2 data (C-band) were assessed to obtain reliable and robust information about the most effective features/decomposition methods for separating classes in wetland studies. To this end, several variance analyses were initially performed on the field samples to remove inappropriate features. This step is critical in the separability analysis of wetlands because they are dynamic landscapes and can contain different subclasses. The complexity of wetland classes increases the variance values of their field samples and, thus, causes the separation of wetlands to be challenging using remote sensing data. Additionally, this illustrates why a non-parametric separability approach, such as the Mann-Whitney U-test, should be used for separability analysis of wetlands. By performing variance analyses on field samples, it was concluded that although several SAR features have proved to be promising for wetland classification, they should be removed before a classification procedure because of the noisy results obtained from them. In addition, the results of the separability analyses indicated that the ratio features, especially those obtained from the diagonal elements of the covariance matrix (e.g. $R2_{HH}/HV$, $R2_{HH}/TP$), were the best. It was also concluded that several SAR features extracted from the eigenvalue decomposition of the coherency matrix, such as $serd$, N_{serd} , and N_{derd} , provided a high potential for delineating wetland classes. Moreover, it was observed that dual polarimetric data, especially those obtained by the intensity layers of Sentinel-1, were not as useful as RADARSAT-2 full polarimetric data. This was because full polarimetric data enables us to use various decomposition methods that are considerably helpful in

separating complex wetlands. In this regard, the H/A/Alpha and Freeman-Durden techniques were the most useful decomposition methods, the corresponding components of which were among the most effective features. Furthermore, the results showed that the coherent decomposition methods, such as Krogager, were not suitable for identifying the naturally distributed targets such as wetland species. Finally, it was concluded that L-band was more important than C-band for wetland studies, and provided a high potential for detecting woody wetlands, such as swamps.

References

Adam, E., Mutanga, O., & Rugege, D. (2010). Multispectral and hyperspectral remote sensing for identification and mapping of wetland vegetation: a review. *Wetlands Ecology and Management*, 18(3), 281-296.

Amani, M., Salehi, B., Mahdavi, S., Brisco, B., & Shehata, M. (2018). A Multiple Classifier System to improve mapping complex land covers: a case study of wetland classification using SAR data in Newfoundland, Canada. *International Journal of Remote Sensing*, 1-14.

Amani, M., Salehi, B., Mahdavi, S., Granger, J. E., Brisco, B., & Hanson, A. (2017a). Wetland Classification Using Multi-Source and Multi-Temporal Optical Remote Sensing Data in Newfoundland and Labrador, Canada. *Canadian Journal of Remote Sensing*, 43(4), 360-373.

Amani, M., Salehi, B., Mahdavi, S., Granger, J., & Brisco, B. (2017b). Wetland classification in Newfoundland and Labrador using multi-source SAR and optical data integration. *GIScience & Remote Sensing*, 54(6), 779-796.

- Bourgeau-Chavez, L. L., Riordan, K., Powell, R. B., Miller, N., & Nowels, M. (2009). Improving wetland characterization with multi-sensor, multi-temporal SAR and optical/infrared data fusion. *In Advances in geoscience and remote sensing. InTech.*
- Brisco, B., Ahern, F., Hong, S. H., Wdowinski, S., Murnaghan, K., White, L., & Atwood, D. K. (2015). Polarimetric decompositions of temperate wetlands at C-band. *IEEE Journal of Selected Topics in Applied Earth Observations and Remote Sensing*, 8(7), 3585-3594.
- Brisco, B., Kapfer, M., Hirose, T., Tedford, B., & Liu, J. (2011). Evaluation of C-band polarization diversity and polarimetry for wetland mapping. *Canadian Journal of Remote Sensing*, 37(1), 82-92.
- Cloude, S. R. (1985). Target decomposition theorems in radar scattering. *Electronics Letters*, 21(1), 22-24.
- Cloude, S. R., & Pottier, E. (1996). A review of target decomposition theorems in radar polarimetry. *IEEE Transactions on Geoscience and remote sensing*, 34(2), 498-518.
- Ecological Stratification Working Group (Canada), Center for Land, Biological Resources Research (Canada), & Canada. State of the Environment Directorate. (1996). A national ecological framework for Canada. *Centre for Land and Biological Resources Research; Hull, Quebec: State of the Environment Directorate.*
- Freeman, A., & Durden, S. L. (1998). A three-component scattering model for polarimetric SAR data. *IEEE Transactions on Geoscience and Remote Sensing*, 36(3), 963-973.

- Gallant, A. 2015. The Challenges of Remote Monitoring of Wetlands. *Remote Sensing*, 7: 10938–10950.
- Gedan, K. B., Kirwan, M. L., Wolanski, E., Barbier, E. B., & Silliman, B. R. (2011). The present and future role of coastal wetland vegetation in protecting shorelines: answering recent challenges to the paradigm. *Climatic Change*, 106(1), 7-29.
- Henderson, F. M., & Lewis, A. J. (2008). Radar detection of wetland ecosystems: a review. *International Journal of Remote Sensing*, 29(20), 5809-5835.
- Hobart, G. (2015). A System of Mapping Historical Wildfire Events in the Boreal Forest using Polarimetric Radar. *Doctoral dissertation*.
- Hong, S. H., Kim, H. O., Wdowinski, S., & Feliciano, E. (2015). Evaluation of polarimetric SAR decomposition for classifying wetland vegetation types. *Remote Sensing*, 7(7), 8563-8585.
- Kasischke, E. S., Smith, K. B., Bourgeau-Chavez, L. L., Romanowicz, E. A., Brunzell, S., & Richardson, C. J. (2003). Effects of seasonal hydrologic patterns in south Florida wetlands on radar backscatter measured from ERS-2 SAR imagery. *Remote Sensing of Environment*, 88(4), 423-441.
- Krogager, E. (1990). New decomposition of the radar target scattering matrix. *Electronics Letters*, 26(18), 1525-1527.
- Lee, J. S., Grunes, M. R., & De Grandi, G. (1999). Polarimetric SAR speckle filtering and its implication for classification. *IEEE Transactions on Geoscience and remote sensing*, 37(5), 2363-2373.
- Lehmann, E. L. (2004). Elements of large-sample theory. *Springer Science & Business Media*.

Li, J., & Chen, W. (2005). A rule-based method for mapping Canada's wetlands using optical, radar and DEM data. *International Journal of Remote Sensing*, 26(22), 5051-5069.

Li, J., Chen, W., & Touzi, R. (2007). Optimum RADARSAT-1 configurations for wetlands discrimination: a case study of the Mer Bleue peat bog. *Canadian Journal of Remote Sensing*, 33(sup1), S46-S55.

Lopes, A., Touzi, R., & Nezry, E. (1990). Adaptive speckle filters and scene heterogeneity. *IEEE Transactions on Geoscience and remote sensing*, 28(6), 992-1000.

Maghsoudi, Y. (2011). Analysis of Radarsat-2 full polarimetric data for forest mapping. *Degree of PhD, Department of Geomatics Engineering, University of Calgary.*

Mahdavi, S., Maghsoudi, Y., & Amani, M. (2017a). Effects of changing environmental conditions on synthetic aperture radar backscattering coefficient, scattering mechanisms, and class separability in a forest area. *Journal of Applied Remote Sensing*, 11(3), 036015.

Mahdavi, S., Salehi, B., Amani, M., Granger, J. E., Brisco, B., Huang, W., & Hanson, A. (2017b). "Object-based classification of wetlands in Newfoundland and Labrador using multi-temporal PolSAR data". *Canadian Journal of Remote Sensing*, 43(5), 432-450.

Mahdavi, S., Salehi, B., Granger, J., Amani, M., & Brisco, B. (2017c). Remote sensing for wetland classification: a comprehensive review. *GIScience & Remote Sensing*, 1-36.

- Mahdavi, S., Salehi, B., Moloney, C., Huang, W., & Brisco, B. (2018). Speckle filtering of Synthetic Aperture Radar images using filters with object-size-adapted windows. *International Journal of Digital Earth*, 11(7), 703-729.
- Mahdianpari, M., Salehi, B., Mohammadimanesh, F., Brisco, B., Mahdavi, S., Amani, M., & Granger, J. E. (2018). Fisher Linear Discriminant Analysis of coherency matrix for wetland classification using PolSAR imagery. *Remote Sensing of Environment*, 206, 300-317.
- Millard, K., & Richardson, M. (2013). Wetland mapping with LiDAR derivatives, SAR polarimetric decompositions, and LiDAR-SAR fusion using a random forest classifier. *Canadian Journal of Remote Sensing*, 39(4), 290-307.
- Mitsch, W. J., & Gosselink, J. G. (2000). The value of wetlands: importance of scale and landscape setting. *Ecological Economics*, 35(1), 25-33.
- Mitsch, W., and J. G. Gosselink. (1993). Wetlands. (2nd Eds.). *New York, NY: Van Nostrand Reinhold*.
- National Wetlands Working Group. (1997). The Canadian Wetland Classification System. *Wetlands Research Branch, University of Waterloo*.
- Ozesmi, S. L., & Bauer, M. E. (2002). Satellite remote sensing of wetlands. *Wetlands Ecology and Management*, 10(5), 381-402.
- Proctor, C., He, Y., & Robinson, V. (2013). Texture augmented detection of macrophyte species using decision trees. *ISPRS Journal of Photogrammetry and Remote Sensing*, 80, 10-20.
- Rignot, E. J., & Van Zyl, J. J. (1993). Change detection techniques for ERS-1 SAR data. *IEEE Transactions on Geoscience and Remote sensing*, 31(4), 896-906.

- Roulet, N. T. (2000). Peatlands, carbon storage, greenhouse gases, and the Kyoto protocol: prospects and significance for Canada. *Wetlands*, 20(4), 605-615.
- South, G. R. (1983). 10. Benthic marine algae. *Biogeography and Ecology of the Island of Newfoundland*, 48, 385.
- Tiner, R. W., M. W. Lang, and V. V. Klemas, (Eds.). (2015). Remote Sensing of Wetlands: Applications and Advances. *Boca Raton: CRC Press, Taylor and Francis Group*.
- Touzi, R. (2007). Target scattering decomposition in terms of roll-invariant target parameters. *IEEE Transactions on Geoscience and Remote Sensing*, 45(1), 73-84.
- Touzi, R., Deschamps, A., & Rother, G. (2009). Phase of target scattering for wetland characterization using polarimetric C-band SAR. *IEEE Transactions on Geoscience and Remote Sensing*, 47(9), 3241-3261.
- Van Zyl, J. J. (1989). Unsupervised classification of scattering behavior using radar polarimetry data. *IEEE Transactions on Geoscience and Remote Sensing*, 27(1), 36-45.
- Vymazal, J. (2010). Constructed wetlands for wastewater treatment. *Water*, 2(3), 530-549.
- White, L., Brisco, B., Dabboor, M., Schmitt, A., & Pratt, A. (2015). A collection of SAR methodologies for monitoring wetlands. *Remote Sensing*, 7(6), 7615-7645.
- Yamaguchi, Y., Moriyama, T., Ishido, M., & Yamada, H. (2005). Four-component scattering model for polarimetric SAR image decomposition. *IEEE Transactions on Geoscience and Remote Sensing*, 43(8), 1699-1706.

Yeung, K. Y., Bumgarner, R. E., & Raftery, A. E. (2005). Bayesian model averaging: development of an improved multi-class, gene selection and classification tool for microarray data. *Bioinformatics*, 21(10), 2394-2402.

Zoltai, S. C., & Vitt, D. H. (1995). Canadian wetlands: environmental gradients and classification. *Vegetatio*, 118(1-2), 131-137.

Allain, S., FerroFAMIL, L., & Potier, E. (2005, October). New eigenvalue-based parameters for natural media characterization. *In Radar Conference, EURAD 2005. European (pp. 177-180). IEEE.*

CHAPTER 6. A MULTIPLE CLASSIFIER SYSTEM TO IMPROVE MAPPING COMPLEX LAND COVERS: A CASE STUDY OF WETLAND CLASSIFICATION USING SAR DATA IN NEWFOUNDLAND, CANADA

Abstract

There are currently various classification algorithms, each with its own advantages and limitations. It is expected that fusing different classifiers in a way that the advantages of each are selected can boost the accuracy in the classification of complex land covers, such as wetlands, compared to using a single classifier. Classification of wetlands using remote sensing methods is a challenging task because of considerable similarities between wetland classes. This fact is more important when utilizing Synthetic Aperture Radar (SAR) data, which contain speckle noise. Consequently, discriminating wetland classes using only SAR data is generally not as accurate as using some other satellite data, such as optical imagery. In this study, a new Multiple Classifier System (MCS), which combines five different algorithms, was proposed to improve the classification accuracy of similar land covers. This system was then applied to classify wetlands in a study area in Newfoundland, Canada, using multi-source and multi-temporal SAR data. The results demonstrated that the proposed MCS was more accurate for the classification of wetlands in terms of both overall and class accuracies compared to applying one specific algorithm. Therefore, it is expected that the proposed system improves the classification accuracy of other complex landscapes.

Keywords: remote sensing, wetlands, SAR, Multiple Classifier System, Canada

6.1. Introduction

Various classification algorithms have been proposed and applied in different fields of remote sensing, each of which has its own advantages and disadvantages. Therefore, combining different types of classifiers and using the advantages of each algorithm should result in a higher classification accuracy compared to using a particular classification algorithm. This process is named the Multiple Classifier System (MCS) or classifier ensemble in the literature (Briem et al., 2002; Du et al., 2012). Many MCSs have so far been proposed and utilized in different applications of remote sensing and have proved their potential. For instance, Steele (2000) used two new MCSs for land cover classification. The first method (called the product rule) was a simple and general method of fusing several classification rules into a single rule. In the second method, they proposed a non-parametric classifier that incorporated spatial information from different classifiers. Their results indicated that the product rule may increase classification accuracy with little additional expenses. Briem et al. (2002) also compared different single classifiers with various MCSs, including consensus-theoretic classifiers, bagging and boosting algorithms for classification of land cover using multi-source satellite data. They reported that all MCSs outperformed the single classification algorithms in terms of overall classification accuracies. In addition, Ceamanos et al. (2010) used a MCS of Support Vector Machines (SVMs) to improve classification of hyperspectral data. Their proposed system demonstrated higher overall and class accuracies compared to a standard SVM method. Finally, Maghsoudi et al. (2012) used an ensemble of SVMs

to classify the Petawawa experimental forest, in Ontario, Canada, using RADARSAT-2 data. They reported that their fusion system improved the classification accuracy considerably over a single classifier system.

Wetlands are complex landscapes, the classes of which are considerably similar in terms of spectral and backscattering information obtained by remote sensing satellites. In this regard, Synthetic Aperture Radar (SAR) data has been widely applied to classify wetlands. However, using the SAR data alone did not result in high accuracies compared to using some other satellite data, such as those captured by optical sensors (Amani et al., 2017b). This is first of all due to the nature of wetlands, which share many ecological characteristics. Moreover, SAR data contain speckle noise, which makes image segmentation and classification more challenging (Mahdavi et al., 2017a, b). In this study, a MCS is developed to improve wetland classification in a study area in Newfoundland, Canada using multi-source and multi-temporal SAR data. The main objective for proposing this system was increasing the classification accuracy of land covers with high levels of similarities, such as wetlands, in terms of both overall and class accuracies. The performance of the proposed system was also compared with single classifiers in the identification of several wetland classes.

6.2. Study area and data

6.2.1. Study area

The potential of the proposed MCS for classifying wetlands was assessed in the Avalon study area (Figure 6.1), located in the north-eastern portion of the Avalon

Peninsula on the Island of Newfoundland, Canada (Latitude= 47.2503° N to 47.6661° N, Longitude= 52.7862° W to 53.0056° W). This study area is 637 km², and belongs to the Maritime Barren ecoregion. It is generally dominated by balsam fir forests, heathland barrens, agricultural, and urban areas (South, 1983). Wetlands of all five classes, identified by the Canadian Wetland Classification System (CWCS, Ecological Stratification Working Group, 1996): i.e., Bog, Fen, Marsh, Swamp, and Shallow Water are found in the study area. However, like major part of the province, peatlands (i.e., Bog and Fen) are more widespread than other wetland classes (Ecological Stratification Working Group, 1996).

Although wetlands provide similar services, such as supporting recreational activities and providing habitat to numerous species of plants and animals, the way in which these services are derived via function and the quality/quantity of such services may differ amongst class (Hanson et al., 2008). For example, peatlands play an important role in climate change because peat is a substantial source and sink of carbon. Marshes, which typically form along the edge of water bodies, are also capable of filtering water pollutants and other particles via the presence of tall grasses and microbial species (Hanson et al., 2008; Kimmel and Mander, 2010).

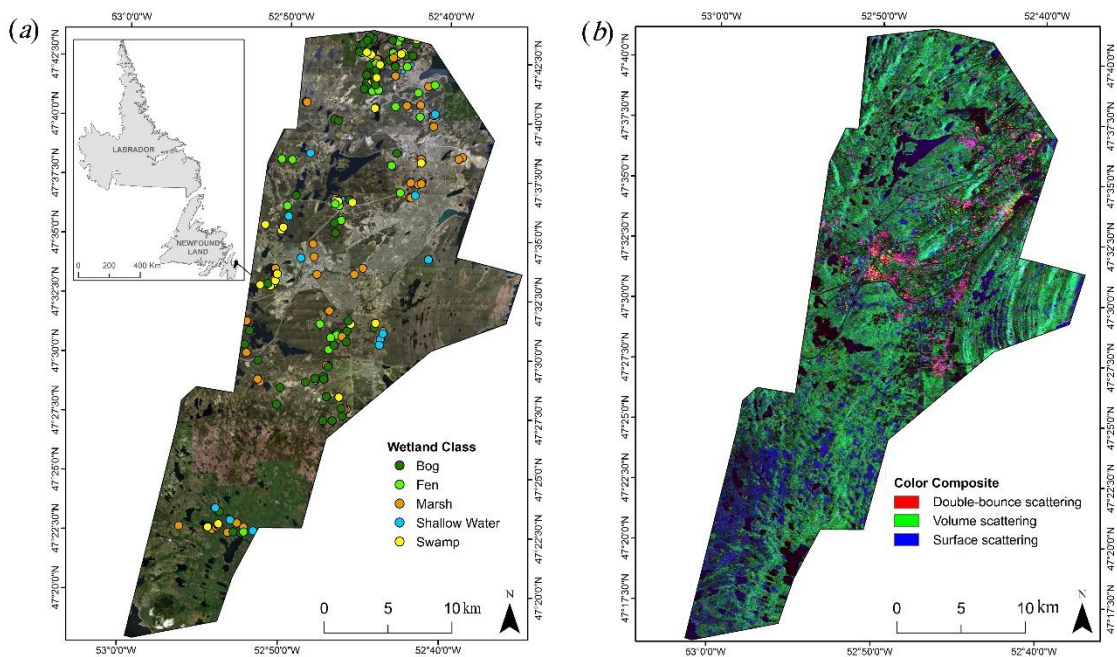


Figure 6.1. (a) Study area and the location of the field samples, (b) A RADARSAT-2 imagery from the study area (The color composite image was obtained by the Freeman-Durden decomposition).

6.2.2. Field data

The field work was conducted in summer and fall 2015, 2016, and 2017. In the field, each site was first differentiated from upland and, then, identified as a wetland class based on the CWCS. Several Global Positioning System (GPS) points and ancillary information, including the on-site photographs as well as notes on surrounding land covers and topography, were also taken at each site to help with future delineation steps. In the laboratory, wetland boundary delineation and polygon creation were carried out using ArcMap 10.3.1. The GPS points collected in the field identifying the location of wetlands were uploaded into ArcMap and superimposed over high spatial resolution satellite and aerial imagery (i.e., RapidEye and aerial orthophoto with 5 and 0.5 meters spatial resolutions,

respectively). Then, boundary delineation for each GPS point was performed using these high resolution data as well as the ancillary information collected in the field. Finally, there were 83, 39, 50, 45, 40 polygons, which were all more than 1 hectare, for the Bog, Fen, Marsh, Swamp, and Shallow Water classes, respectively. 50% of these field data, which were selected randomly, were used to train the classifiers, and the other 50% remained for accuracy assessment of the classified wetland maps.

6.2.3. Satellite data

A combination of different SAR data from the Advance Land Observing Satellite (ALOS-1 and -2) L band, RADARSAT-2 C band, and Sentinel-1 C band, were employed to classify wetlands in the study area (Table 6.1). Moreover, a high resolution RapidEye image was used to segment the study area. This is discussed in more detail in subsection 3.3.

Table 6.1. Satellite data used in this study (Optical and SAR satellite data are used for segmentation and classification of the study area, respectively).

Optical satellite	Date	Level	Spectral band	Spectral range (nm)	Spatial resolution (m)	
RapidEye	18/062015	3A	Blue	440-510	5	
			Green	520-590		
			Red	630-685		
			Red edge	690-730		
			NIR	760-850		
SAR satellite	Date	Mode	Polarization type	Intensity channels	Incident angle range (°)	Nominal resolution range × azimuth (m)
RADARSAT-2	10/062015	FQ4	Quad	HH, VV,	22.1-24.1	13.1×12.2
	21/08/2015			HV, VH		
Sentinel-1	20/08/2015	IW	Dual	VV, VH	30-45	8×16
ALOS-1	29/082010	FBD	Dual	HH, HV	7.9-60	20×20
ALOS-2	2/082015	FBD	Dual	HH, HV	8-70	9.1×9.1

FQ: Fine Quad, IW: Interferometric Wide, FBD: Fine Beam Double Polarization, HH: horizontal transmit and horizontal receive polarizations, VV: vertical transmit and vertical receive polarizations, HV: horizontal transmit and vertical receive polarizations, VH: vertical transmit and horizontal receive polarizations, NIR: Near Infrared, Level 3A: In this product, radiometric, geometric, and sensor corrections are applied to the data.

6.3. Method

The flowchart of the proposed MCS to improve the accuracy of complex landscapes is illustrated in Figure 6.2 and discussed in more details in the following subsections.

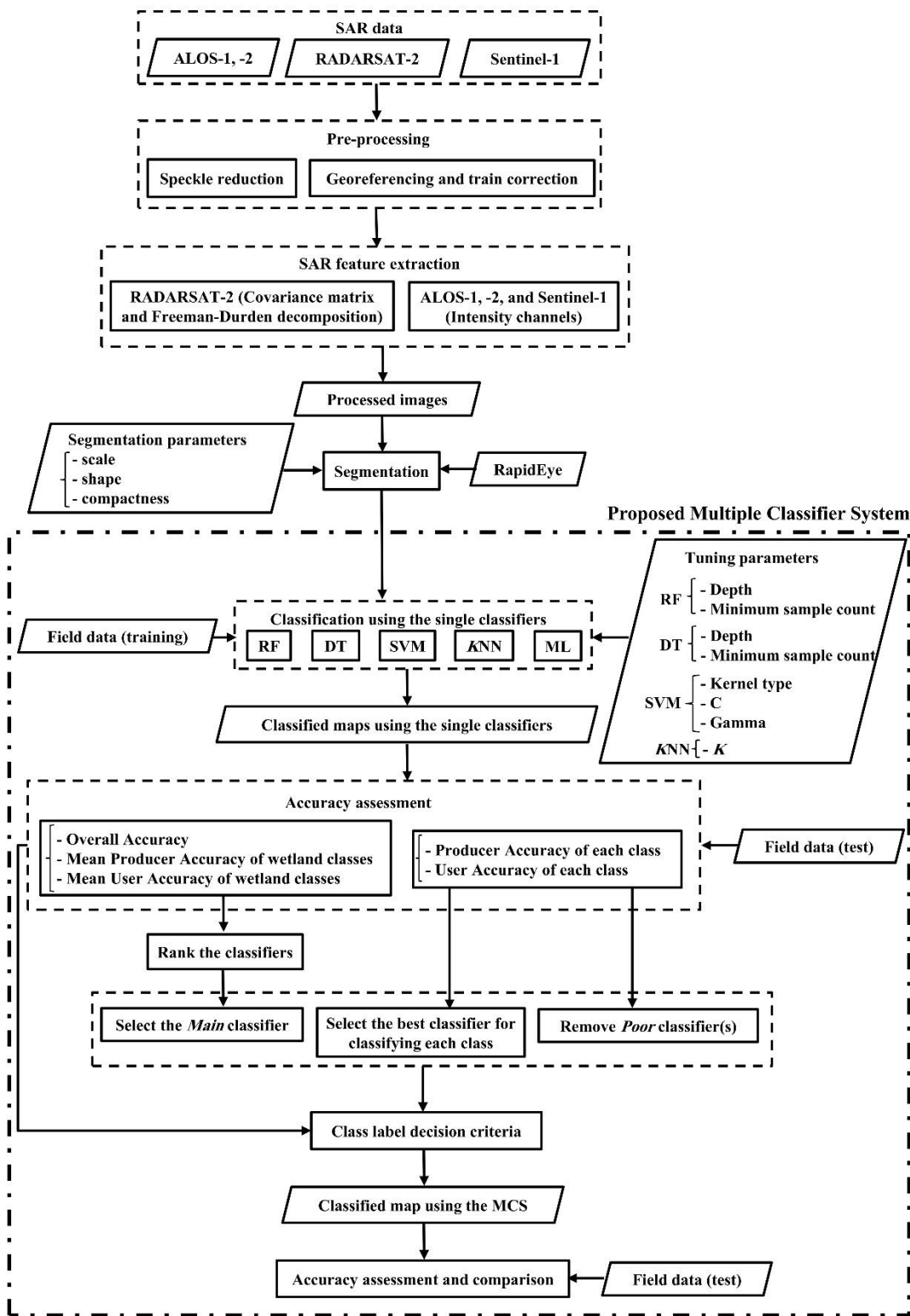


Figure 6.2. Flowchart of the method. Depth refers to the number of DTs. Minimum Sample Count indicates the minimum number of samples per node in each DT. C is the capacity constant and minimizes the error function. Gamma controls the shape of the hyperplane. K is the number of closest samples in the feature space. (MCS: Multiple Classifier System, ML: Maximum Likelihood, RF: Random Forest, DT: Decision Tree, KNN: K-Nearest Neighbor, SVM: Support Vector Machine).

6.3.1. Pre-processing

Geometric and radiometric corrections were not performed on the RapidEye image because it was already corrected by the RapidEye products providers (see Table 6.1). Regarding the SAR data, the intensity layers were first extracted from the Sentinel-1 and ALOS-1, -2 data (see Table 6.1), and the scattering matrix was first converted to the covariance matrix for full polarimetric RADARSAT-2 data. Then, a 7×7 pixels Lee enhanced filter (Lopes et al.,1990) was applied to the intensity layers and a 7×7 pixels PolSAR Lee filter (Lee et al., 1999) was applied to the covariance matrix to reduce the effects of speckle noise on the SAR data. Subsequently, the data were georeferenced and terrain-corrected using the Mapready™ software. Finally, all the SAR data were resampled to 12.5 m spatial resolution using the nearest-neighbour resampling method.

6.3.2. SAR feature extraction

The intensity layers of the Sentinel-1 and ALOS-1, -2 data (see Table 6.1), as well as the components of the covariance matrix (9 components) and the Freeman-Durden decomposition (Freeman and Durden, 1998, 3 components), extracted

from the RADARSAT-2 data, were used in this study. The covariance matrix is shown in Equation (6.1), in which S_{PQ} is an element of the scattering matrix. P and Q also indicate the scattering and incident polarizations, respectively. In addition, S_{PQ}^* refers to the complex conjugate of S_{PQ} .

$$C = \begin{bmatrix} \langle |S_{HH}|^2 \rangle & \langle \sqrt{2} S_{HH} S_{HV}^* \rangle & \langle S_{HH} S_{VV}^* \rangle \\ \langle \sqrt{2} S_{HV} S_{HH}^* \rangle & \langle 2|S_{HV}|^2 \rangle & \langle \sqrt{2} S_{HV} S_{VV}^* \rangle \\ \langle S_{VV} S_{HH}^* \rangle & \langle \sqrt{2} S_{VV} S_{HV}^* \rangle & \langle |S_{VV}|^2 \rangle \end{bmatrix} \quad (6.1)$$

The Freeman-Durden Decomposition assigns three scattering mechanisms to polarimetric SAR data. The first mechanism is odd or surface scattering and is related to the Bragg scattering from a rough surface. The second mechanism is even or double-bounce scattering and refers to scattering from dihedrals, such as trunk-ground or water-trunk interactions for swamp trees. The third mechanism is volume scattering and is modelled by randomly oriented dipoles for tree or vegetation canopies (Mahdavi et al., 2017).

6.3.3. Segmentation

A pixel-based classification method produces generally a noisy appearance and inaccurate classification results compared to the Object Based Image Analysis (OBIA) when applying medium and/or high spatial resolution satellite data (Amani et al., 2017a). This is more serious when using SAR data, which contain considerable amount of speckle noise (Mahdavi et al., 2017a, b). In addition, OBIA has proved to be more accurate in various wetland studies (e.g. Laba et al., 2010; Amani et al., 2017a, b; Mahdavi et al., 2017a; Mahdianpari et al., 2018). Therefore,

an OBIA was used for wetland classification in this study. The first step of OBIA is segmenting the study area, which was performed using a RapidEye 5 m spatial resolution image. An optical imagery was used for this purpose because segmenting SAR data alone, which contain salt and pepper appearance due to the speckle noise, does not provide meaningful objects (Mahdavi et al., 2017a; Mahdianpari et al., 2018). The multi-resolution segmentation algorithm (Baatz and Schäpe, 2000) was used in this study. The algorithm divides an image into many segments from which homogeneous and meaningful objects are generated using several initial parameters. The three most important parameters in this algorithm are scale, shape, and compactness, which mainly control the size and shape of the produced objects, as well as the within-object variance. Selecting the optimum values for these parameters is an important step in the classification procedure because they can significantly affect the final classification accuracy. In this study, the following values for each of these parameters were utilized based on our previous analyses (see Amani et al., 2017a, b): scale=300, shape=0.1, and compactness=0.5. Amani et al., (2017a, b) explored three various levels of segmentation by assigning different values for each of these parameters. Finally, they concluded that using the above-mentioned values in the segmentation procedure provided the objects that sufficiently corresponded to the real-world objects in the study area.

6.3.4. Proposed Multiple Classifier System

6.3.4.1. Classification using single classifiers

The first step in the proposed MCS was obtaining wetland maps using each of the

single classifiers. In this study, five classification algorithms were used, one of which was a parametric classifier: Maximum Likelihood (ML), and four of which were non-parametric classifiers: Random Forest (RF), Decision Tree (DT), K-Nearest Neighbor (KNN), and SVM. It should be noted that the number and type of the classifiers in this step is optional. We used these five classifiers because they are available in the eCognition software.

Each of the non-parametric classifiers requires several tuning parameters that should be determined before analysis (See Figure 6.2 for the tuning parameters of each classifier). In this study, the trial and error method was used to select the optimum values of these tuning parameters since there is no consistent method for this in the literature.

Finally, the study area was classified using each of the single classifiers and the produced maps were used in the next steps of the MCS, as explained in the following subsections. The statistical parameters obtained from the confusion matrix were used for accuracy assessment of each classifier. These parameters were the overall accuracy, kappa coefficient, producer's accuracy and user's accuracy of each class, as well as mean PA and UA of wetland classes.

6.3.4.2. Selection of the Main classifier

The five single classifiers were first ranked based on the values of the OA, and mean PA and UA of wetland classes. Then, the classifier that produced the highest values for these three parameters was selected as the *Main* classifier for the next experiments. To do so, these three types of accuracies were averaged and the classifier with the highest average accuracy was selected as the *Main* classifier. In

the case where two or more classifiers have the equally highest accuracy, one of them should be selected randomly as the *Main* classifier.

6.3.4.3. Selection of the best classifier for classifying each class and removing Poor classifier(s)

In this step, the best classifier for each individual wetland and non-wetland class was selected based on the PA and UA of each individual class. For this, a threshold (Equation (6.2)), named as T , was defined and calculated for each class in each classifier. The base of defining this threshold was that the purpose in each classification was to increase the values of both PA and UA and decrease their differences. For instance, to define which classifier is the best for classifying the Bog class, first T was calculated for the Bog class in each classifier, and then, the classifier that produced the highest T value was used to classify the Bog class in the next steps. In addition, the classifier(s) that were not selected for any of the classes (*Poor* classifier(s)) were removed.

$$T = ((PA) + (UA)) - (|(PA) - (UA)|) = 2 \times \min ((PA), (UA)) \quad (6.2)$$

6.3.4.4. Class label decision criteria

After determining: (1) the *Main* classifier, (2) the best classifier for each wetland and non-wetland class, and (3) removing the *Poor* classifier(s), the classified maps obtained from only the useful classifiers were overlaid. By doing so, each pixel had as many labels as the number of useful classifiers. For instance, assume that RF was selected as the *Main* classifier, RF was selected as the best classifier (highest T

value) for identification of two classes of Bog and Swamp, SVM was selected as the best classifier to map the Fen and Shallow Water classes, and ML was selected as the best classifier for classifying the Marsh class (In this case, the DT and KNN were removed and were considered as the *Poor* classifiers). Moreover, assume that the order of the layers in the overlaid map were the classified maps obtained from RF, SVM, and ML. Therefore, a random pixel containing class labels of [Swamp, Fen, Bog] had two *matched* labels (i.e., Swamp and Fen obtained by RF and SVM). Based on the number of *matched* labels, the following criteria were considered to decide the final class label for each pixel:

- (1) If there is no *matched* label, use the label obtained by the *Main* classifier.
- (2) If there is only one *matched* label, use that *matched* label.
- (3) If there are two or more than two *matched* labels, there are no equal *matched* labels (like the example mentioned above, i.e., [Swamp, Fen, Bog]), and the *Main* classifier is among the selected classifiers, then use the *matched* label obtained by the *Main* classifier.
- (4) If there are two or more than two *matched* labels, there are no equal *matched* labels, and the *Main* classifier is not among the selected classifiers, select one of the *matched* labels randomly.
- (5) If there are two or more than two *matched* labels, and there are equal *matched* labels, use the *matched* label that had the highest vote. For instance, a random pixel with the class labels of [Swamp, Fen, Fen] in the above example will finally had Fen label.

After defining the label of each pixel using the proposed MCS, described above, the accuracy of the obtained map was assessed and compared with the result of each single classifier.

6.4. Results and discussion

As mentioned in subsection 3.4.1, each non-parametric classifier has several tuning parameters, which considerably affect the classification accuracy and, thus, affect the accuracy of the proposed MCS. To select the best value for each of the tuning parameters, various values were assigned to each of the parameters and, then, the optimum values were selected based on both visual interpretation and statistical accuracies of the obtained maps. Finally, the values demonstrated in Table 6.2 were used.

Table 6.2. Values of the tuning parameters of each non-parametric classifiers, which were used for wetland classification in this study.

	RF and DT		SVM		KNN
Depth	Minimum sample count		Kernel type	C	Gamma K
20	5		RBF	1000000	0.01 5

RF: Random Forest, DT: Decision Tree, KNN: K-Nearest Neighbor, SVM:

Support Vector Machine, RBF: Radial Basis Function.

Depth refers to the number of DTs.

Minimum sample count indicates the minimum number of samples per node in each DT.

C is the capacity constant and minimizes the error function.

Gamma controls the shape of the hyperplane.

K is the number of closest samples in the feature space.

Table 6.3 illustrates the accuracy of the classified maps produced by each single classifier. Clearly, the RF classifier produced the highest average accuracy and, therefore, was selected as the *Main* classifier in the proposed MCS.

Table 6.3. The overall classification accuracy and mean producer’s and user’s accuracies of the wetland classes as well as the average accuracy, obtained by averaging these three accuracies, using each single classifier.

Accuracy measure	SVM	KNN	ML	DT	RF
Overall accuracy (%)	80	81	82	83	83
Mean producer’s accuracy of wetland classes (%)	38	42	46	43	49
Mean user’s accuracy of wetland classes (%)	44	46	38	34	48
Average accuracy (%)	54	56	55	53	60

ML: Maximum Likelihood, RF: Random Forest, DT: Decision Tree, KNN: K-Nearest Neighbor, SVM: Support Vector Machine.

Table 6.4 also demonstrates the *T* values obtained from the single classifiers for each wetland and non-wetland class. Based on the results, RF was selected as the best classifier to map the two classes of Bog and Marsh, DT was selected as the best algorithm to classify the Deep Water class, SVM was selected as the best classifier for identification of the Swamp and Shallow Water classes, and ML was selected as the best classifier for mapping three classes of the Fen, Upland and Urban. Furthermore, KNN was removed from the next steps as it produced the highest *T* value for none of the classes (i.e., *Poor* classifier).

Table 6.4. The T value obtained for each wetland and non-wetland classes using each single classifier.

<i>T</i> values by class								
Classifier	Bog	Fen	Marsh	Swamp	Shallow Water	Deep Water	Upland	Urban
RF	146.9	101.2	73.5	18.38	33.8	190.4	186	137.5
DT	122.2	83.1	46.6	15.4	34	199.4	190.3	129.9
SVM	39.6	102.8	36.5	46.3	91.3	187.1	188.3	130.4
ML	143.2	104.1	67.7	22.5	35.5	190.4	191.4	144
KNN	135.2	97.6	66.2	28.1	60.5	169.9	188.4	129.2

The bold values indicate which classifier produced the highest *T* value for each class.

ML: Maximum Likelihood, RF: Random Forest, DT: Decision Tree, KNN: *K*-Nearest Neighbor, SVM: Support Vector Machine.

After selecting the *Main* classifier and the best classifier for each class, the decision criteria for selecting the class label of each pixel (see subsection 3.4.4) were considered and implemented in MATLAB software. Finally, the classified map using the proposed MCS was obtained (Figure 6.3). Based on the visual interpretation using high spatial ortho-photos and experts' knowledge, it was concluded that the classified map is in high accordance with the actual land cover of the study area. Based on the produced map, Bog, Fen, Marsh, Swamp, and Shallow Water covered approximately 15%, 13.5%, 7.5%, 7.5%, and 2% of the study area (637 km²), respectively.

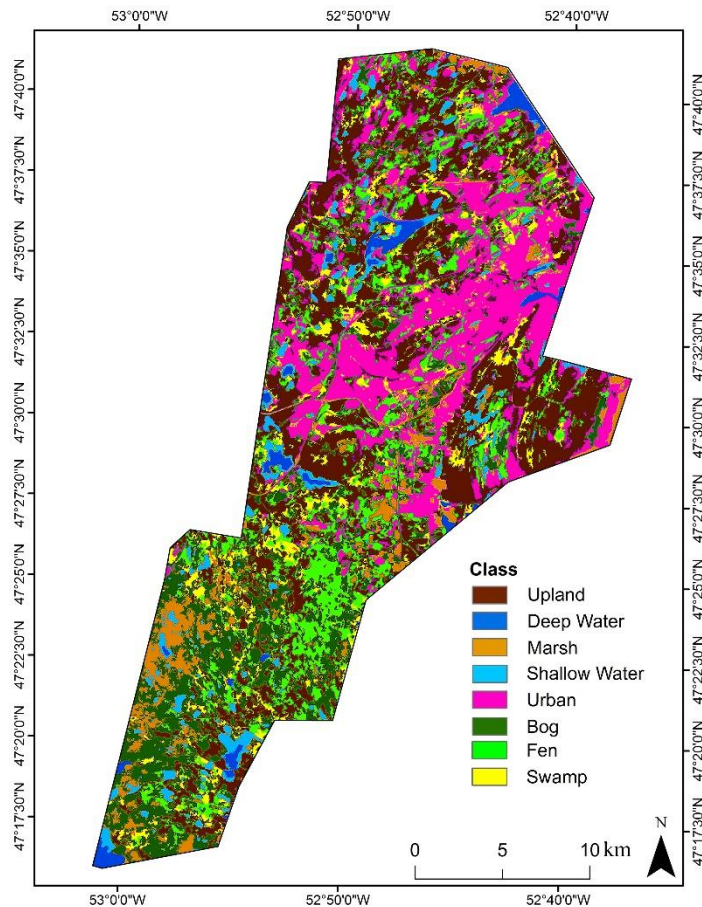


Figure 6.3. The classified map of the study area obtained from the proposed MCS.

The comparison between the statistical classification accuracies of each single classifier and the proposed MCS is illustrated in Figure 6.4. As can be seen from Figure 6.4 (a) and (b), except for the PA of the Fen class and UA of the Swamp class, the MCS produced the highest PA and UA values for all wetland and non-wetland classes compared to each single classifier. In addition, the OA and Kappa coefficient of the classified map obtained from the MCS were considerably higher than those obtained from the single classifiers (Figure 6.4 (c)). The proposed MCS

outperformed the single classifiers by increasing the OA and Kappa coefficient by 5%-8% and by 9%-16%, respectively. It is worth noting that the obtained increments were statistically significant (p -value <0.001).

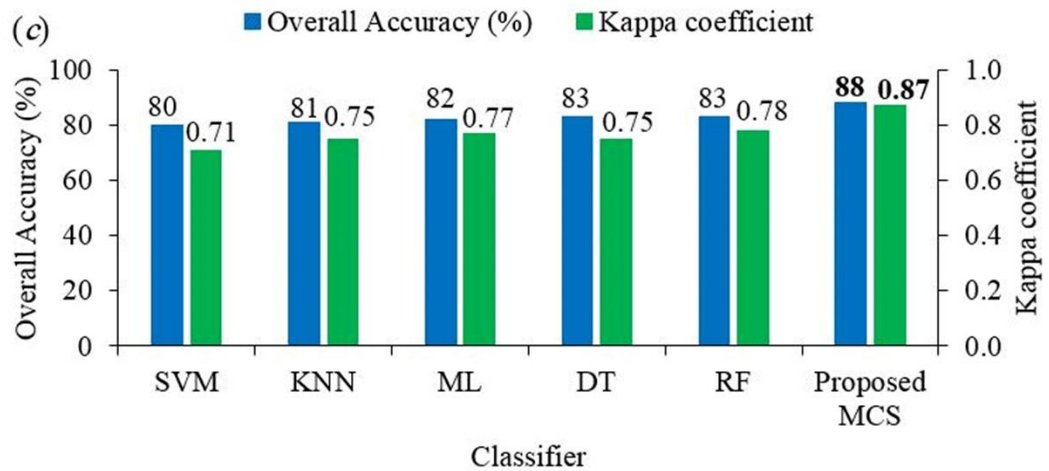
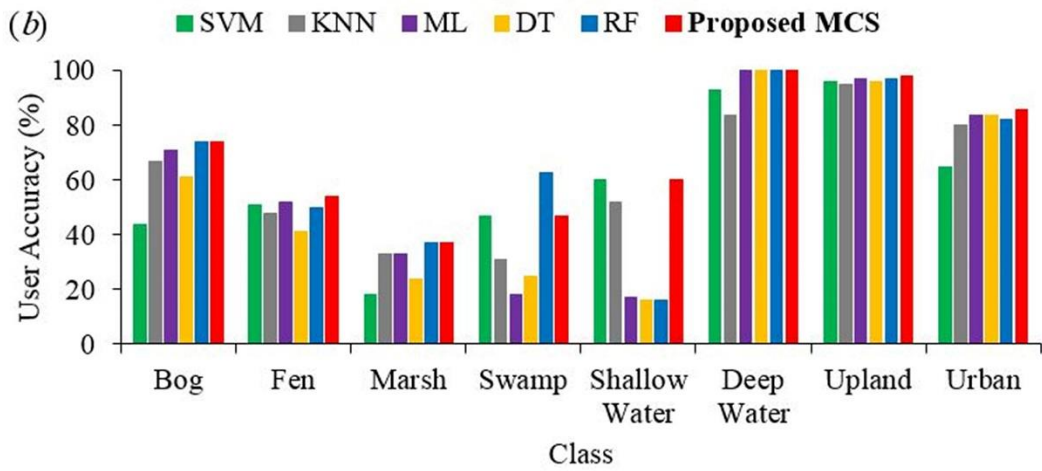
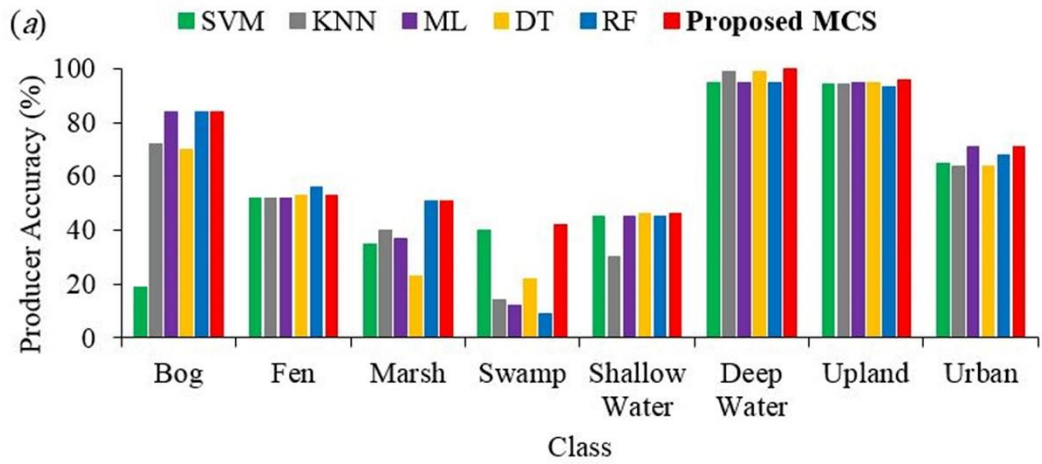


Figure 6.4. (a) Producer's and (b) user's accuracies of the wetland and non-wetland classes, and (c) the overall wetland classification accuracies and Kappa coefficients, obtained from the proposed MCS and the single classifiers (MCS: Multiple Classifier System, ML: Maximum Likelihood, RF: Random Forest, DT: Decision Tree, KNN: K-Nearest Neighbour, SVM: Support Vector Machine).

Although an OBIA approach was used in this study, there is no limitation in applying the proposed MCS in pixel-based methods. Additionally, although only five classifiers with limited SAR features were considered and used in the MCS, there are no limitations in using the type and the number of classifiers and features in the proposed system. In fact, using more classifiers with better performances and various types of features will consequently result in a higher classification accuracy in the final map obtained by the MCS. However, a feature selection method should be applied to remove the redundant features if more features are available for the classification. This is because increasing the number of features may only increase the accuracy of the classification until a certain level and, then, the accuracy will decrease due to including the redundant information (Landgrebe, 2005). The proposed MCS can also be applied to various types of satellite data. For example, if a combination of SAR and optical data is used, most of the single classifiers will produce higher classification accuracy compared to using only SAR data. Therefore, the MCS will also provide higher accuracy compared to using one type of satellite data. However, it should be noted that increasing the number of classifiers and input features as well as using more types of satellite data will result in the computational complexity and increase the

processing time. Thus, we should aim for an optimum balance between the accuracy of the MCS and the time of processing. For example, in this study, the execution time for the segmentation of the study area was approximately 7 minutes using eCognition software in a PC i7 with 3.6 GHz CPU and 32GB RAM. Regarding the classification time, the study area was classified in approximately 1 minute using the individual classifiers (varied between 55-63 seconds) and 14 minutes using the proposed MCS. Although the processing time of the proposed system was higher than that of the individual classifiers, based on the obtained accuracies (Figure 6.4) and considering the fact that obtaining even a few percentages in the classification accuracy of the complex land covers is significantly challenging, we recommend the proposed MCS for classifying complex environments such as wetlands.

6.5. Conclusion

Different classification algorithms have so far been applied to classify complex land covers such as wetlands using remote sensing data. In this study, it was first concluded that there are several limitations to achieve a high wetlands classification accuracy when applying a single classifier to SAR data. Thus, a MCS was proposed and developed to improve wetlands identification using SAR data in the province. Based on the results, it was concluded that the proposed MCS provided higher overall and class accuracies compared to using a single classifier. The results of this study can be shared with other provinces of Canada to help with developing policies for continues and effective mapping and protecting wetlands. Finally, we believe that since the proposed MCS demonstrated a high potential to delineate similar wetland classes, it can be effectively applied to classify any type

of other complex land covers.

References

- Amani, M., Salehi, B., Mahdavi, S., Granger, J. E., Brisco, B., & Hanson, A. (2017a). Wetland Classification Using Multi-Source and Multi-Temporal Optical Remote Sensing Data in Newfoundland and Labrador, Canada. *Canadian Journal of Remote Sensing*, 43(4), 360-373.
- Amani, M., Salehi, B., Mahdavi, S., Granger, J., & Brisco, B. (2017b). Wetland classification in Newfoundland and Labrador using multi-source SAR and optical data integration. *GIScience & Remote Sensing*, 1-18.
- Baatz, M., and A. Schäpe. (2000). Multiresolution Segmentation: An Optimization Approach for High Quality Multi-Scale Image Segmentation. *Angewandte Geographische Informations Verarbeitung XII*, 58(12), 12–23.
- Briem, G. J., Benediktsson, J. A., & Sveinsson, J. R. (2002). Multiple classifiers applied to multisource remote sensing data. *IEEE Transactions on Geoscience and remote sensing*, 40(10), 2291-2299.
- Ceamanos, X., Waske, B., Benediktsson, J. A., Chanussot, J., Fauvel, M., & Sveinsson, J. R. (2010). A classifier ensemble based on fusion of support vector machines for classifying hyperspectral data. *International Journal of Image and Data Fusion*, 1(4), 293-307.
- Du, P., Xia, J., Zhang, W., Tan, K., Liu, Y., & Liu, S. (2012). Multiple classifier system for remote sensing image classification: A review. *Sensors*, 12(4), 4764-4792.
- Ecological Stratification Working Group (Canada), Center for Land, Biological Resources Research (Canada), & Canada. State of the Environment Directorate.

- (1996). A national ecological framework for Canada. *Centre for Land and Biological Resources Research; Hull, Quebec: State of the Environment Directorate.*
- Freeman, A., & Durden, S. L. (1998). A three-component scattering model for polarimetric SAR data. *IEEE Transactions on Geoscience and Remote Sensing*, 36(3), 963-973.
- Hanson et al. (2008). Wetland Ecological Functions Assessment: An Overview of Approaches. *Canadian Wildlife Service Technical Report Series. Atlantic Region.* 487. 59pp.
- Kimmel, K., & Mander, Ü. (2010). Ecosystem services of peatlands: Implications for restoration. *Progress in Physical Geography*, 34(4), 491-514.
- Laba, M., Blair, B., Downs, R., Monger, B., Philpot, W., Smith, S., ... & Baveye, P. C. (2010). Use of textural measurements to map invasive wetland plants in the Hudson River National Estuarine Research Reserve with IKONOS satellite imagery. *Remote Sensing of Environment*, 114(4), 876-886.
- Landgrebe, D. A. (2005). Signal theory methods in multispectral remote sensing. *John Wiley & Son. Inc., Hoboken, New Jersey.* 29.
- Lee, J. S., Grunes, M. R., & De Grandi, G. (1999). Polarimetric SAR speckle filtering and its implication for classification. *IEEE Transactions on Geoscience and remote sensing*, 37(5), 2363-2373.
- Lopes, A., Touzi, R., & Nezry, E. (1990). Adaptive speckle filters and scene heterogeneity. *IEEE Transactions on Geoscience and remote sensing*, 28(6), 992-1000.
- Maghsoudi, Y., Collins, M., & Leckie, D. G. (2012). Polarimetric classification of Boreal forest using nonparametric feature selection and multiple classifiers. *International Journal of Applied Earth Observation and Geoinformation*, 19, 139-150.

- Mahdavi, S., Maghsoudi, Y., & Amani, M. (2017). Effects of changing environmental conditions on synthetic aperture radar backscattering coefficient, scattering mechanisms, and class separability in a forest area. *Journal of Applied Remote Sensing*, 11(3), 036015.
- Mahdavi, S., Salehi, B., Amani, M., Granger, J. E., Brisco, B., Huang, W., & Hanson, A. (2017a). Object-based classification of wetlands in Newfoundland and Labrador using multi-temporal PolSAR data. *Canadian Journal of Remote Sensing*, 1-19.
- Mahdavi, S., Salehi, B., Moloney, C., Huang, W., & Brisco, B. (2017b). Speckle filtering of Synthetic Aperture Radar images using filters with object-size-adapted windows. *International Journal of Digital Earth*, 1-27.
- Mahdianpari, M., Salehi, B., Mohammadimanesh, F., Brisco, B., Mahdavi, S., Amani, M., & Granger, J. E. (2018). Fisher Linear Discriminant Analysis of coherency matrix for wetland classification using PolSAR imagery. *Remote Sensing of Environment*, 206, 300-317.
- South, G.R. (1983). *Biography and Ecology of the Island of Newfoundland. Massachusetts: Kluwer Boston, Inc. Print*, 48.
- Steele, B. M. (2000). Combining multiple classifiers: An application using spatial and remotely sensed information for land cover type mapping. *Remote Sensing of Environment*, 74(3), 545-556.

CHAPTER 7. WETLAND CLASSIFICATION IN NEWFOUNDLAND AND LABRADOR USING MULTI- SOURCE SAR AND OPTICAL DATA INTEGRATION

Abstract

A vast portion of Newfoundland and Labrador is covered by wetland areas. Notably, it is the only province in Atlantic Canada that does not have a wetland inventory system. Wetlands are important areas of research because they play a pivotal role in ecological conservation and impact human activities in the province. Therefore, classifying wetland types and monitoring their changes are crucial tasks recommended for the province. In this study, wetlands in five pilot sites, distributed across Newfoundland and Labrador, were classified using the integration of aerial imagery, Synthetic Aperture Radar (SAR), and optical satellite data. First, each study area was segmented using the object-based method, and then various spectral and polarimetric features were evaluated to select the best features for identifying wetland classes using the Random Forest (RF) algorithm. The accuracies of the classifications were assessed by the parameters obtained from confusion matrices, and the overall accuracies varied between 81% and 91%. Moreover, the average producer and user accuracies for wetland classes, considering all pilot sites, were 71% and 72%, respectively. Since the proposed methodology demonstrated high accuracies for wetland classification in different study areas with various ecological characteristics, the application of future classifications in other areas of interest is promising.

Keywords: Wetland, Remote Sensing, Object-based classification, Random Forest, Newfoundland and Labrador

7.1. Introduction

A wetland is an area of land that shares characteristics with both dry upland and waterbodies in such a way as to establish a unique ecosystem that is identified by the presence of water, be it temporary or permanent, hydric soils, and/or hydrophytic vegetation. Wetlands are described as the “kidneys” of the environment because of the vital role they play in the water and chemical cycles. Wetlands provide essential ecological services, including filtering and purifying water, preventing flooding, protecting shorelines, controlling erosion, and storing carbon produced by human activities (Barbier et al., 1988; Rundquist et al., 2001; Tiner et al., 2015; Nyarko et al., 2015). Wetlands are also highly productive environments in terms of both land and water habitats for various plants and animals (Mitsch and Gosselink, 1993).

There are generally two methods for wetland classification: *in situ* and remote sensing. *In situ* methods require intensive field work, which is laborious, expensive, and time-consuming. In contrast to these traditional methods, remote sensing satellites provide multi-spectral data, multi-temporal coverage, and enable the cost effective mapping of wetlands (Kumar and Sinha, 2014). Consequently, remote sensing is the most practical way for classifying and monitoring wetlands in a timely manner over a large area. Two technologies routinely used for land cover applications are optical remote sensing and Synthetic Aperture Radar (SAR), both of which have advantages and disadvantages. Due to the spatial and temporal

complexities associated with wetlands, a suite of satellite data and more accurate methodologies should be applied to accurately classify wetlands. Therefore, many researchers have reported that a combination of SAR and optical remote sensing data provide a more promising approach for wetland studies than either alone (Wang et al., 1998; Li and Chen, 2005; Grenier et al., 2007; Gosselin et al., 2014).

Currently, because there are different medium and high spatial resolution imagery available, the Object-Based Image Analysis (OBIA) approach has been extensively applied instead of the traditional pixel-based techniques for wetland classification (Grenier et al., 2007; Reif et al., 2009; Salehi et al., 2013; Shiraishi et al., 2014). The OBIA method segments pixels into groups called objects. Various spectral and textural features extracted from the generated objects can be included in the classification procedure so that more accurate results can be achieved. In addition, it is possible to define different mathematical relationships, including various remote sensing indices, and use them as additional layers in the image classification procedure. Furthermore, topological and hierarchical relationships between image objects can be incorporated into OBIA to improve efficiently the accuracy of classification (Duro et al., 2012; Salehi et al., 2012).

To date, different classification algorithms, including the Support Vector Machine (SVM), Maximum Likelihood (ML), Classification And Regression Tree (CART), K-Nearest Neighbor (KNN), and Random Forest (RF), have been applied in various studies. It has been frequently reported that RF is superior to the other classifiers in land cover classification using satellite data (Pal, 2005; Mutanga et al., 2012; Whiteside and Bartolo, 2015). The algorithm is an ensemble learning method that improves the accuracy of classification by using a group of decision trees rather than a single decision tree. The RF algorithm is also capable of dealing with

an enormous amount of data, as well as complex relationships between estimators due to noise. Moreover, RF provides the means of selecting the important variables of research interest that can be used for further interpretation (Breiman, 2001).

Due to the values of wetlands, Canada established the Canadian Wetland Inventory (CWI) system to develop advanced methods for mapping and monitoring these valuable ecosystems. The system is an initiative to classify wetlands across Canada following the guidelines outlined by the Canadian Wetland Classification System (CWCS), as well as using remote sensing methods (Warner and Rubec, 1997). The CWCS is an ecologically-based system that describes the characteristics of wetlands based on vegetation, soil, water chemistry, and hydrological parameters. Warner and Rubec (1997) have identified five wetland classes in Canada through the CWCS: Bog, Fen, Marsh, Swamp, and Shallow water of less than 2 m in depth. After selecting the CWCS as the official classification system of the CWI, many researchers attempted to classify wetlands in Canada using this system. For example, Brisco et al. (2011) evaluated the applicability of polarization diversity and polarimetry data captured by an airborne CV-580 C-band SAR for wetland mapping in southwestern Manitoba. The overall classification accuracies in their study varied from 50% to 60% using the conventional separability analysis and maximum likelihood classification. Moreover, Powers et al. (2012) developed new object-based texture measures (geotex) and a decision-tree classifier to distinguish 15 wetland types in McMurray, Alberta using SPOT-5 imagery. The highest overall classification accuracy was 68% in their research. Schmitt and Brisco (2013) also estimated wetland changes in Gagetown, New Brunswick using multi-temporal RADARSAT 2 images. They compared three decomposition methods to detect the flooding

extent, as well as its temporal change. The image comparison along the time series was also performed using the curvelet-based change detection method. In addition, Gosselin et al. (2014) compared the wetlands classified maps in Lac Saint-Pierre, Quebec using the SAR (RADARSAT 2) and Optical (Landsat 5) data, and obtained the accuracies of 77% and 79%, respectively. Finally, Dabboor et al. (2015) explored the potential of the compact polarimetric SAR mode for wetland monitoring in Manitoba. They investigated the ability of compact polarimetric data to monitor wetlands using the Wishart-Chernoff distance and compared to the results obtained from fully polarimetric data.

Although the value of wetlands has already been recognized in Canada to some degree, no significant efforts have been made to properly assess wetland regions in Newfoundland and Labrador (NL) using remote sensing methods. It is estimated that Canada has about 24% of the global wetland areas, and of the approximately 14% of Canada's land mass that is covered by wetlands, 5% are found in NL (Warner and Rubec, 1997). Over the last few decades, extensive loss of wetlands has also occurred in the province as a result of agricultural activities, urbanization, and industrialization. Therefore, the need for a wetland inventory system to guide conservation programs and resource management has become more important for the province.

According to the CWI progress wetland map (Figure 7.1), prepared by Ducks Unlimited Canada, only two small regions in NL have been mapped using satellite data. The small area in Newfoundland (Avalon area, Figure 7.1) has been mapped based on the CWI scheme and using a combination of the Landsat ETM+ and RADARSAT 1 data (Mahoney and Hanson, 2006). An overall classification accuracy of 60% was obtained in this study, and the researchers have reported that

they faced many difficulties in discriminating between fens and bogs. Wetlands in a small area in Labrador (East of Minipi Lake within Eagle Plateau, Figure 7.1) has also been classified into the four categories of fens, bogs, swamps, and shallow water using a fused Landsat ETM+ and RADARSAT 1 data (Mahoney et al., 2007). The researchers used a small amount of field data for training the algorithm and a pan-sharpened IKONOS images for accuracy assessment. Mahoney et al. (2007) applied a fuzzy method to improve the accuracy of distinguishing between fens and bogs, and the overall classification accuracy was increased from 57% to 79% compared to a deterministic classification approach. It is also worth mentioning that several sporadic field surveys across NL have been conducted at different times, for different purposes, and often with various standards and methods. The aim of most of these field studies was identifying peatlands (bogs and fens), as this is the dominant type of wetland in NL (Price, 1992; Hoag and Price, 1995).

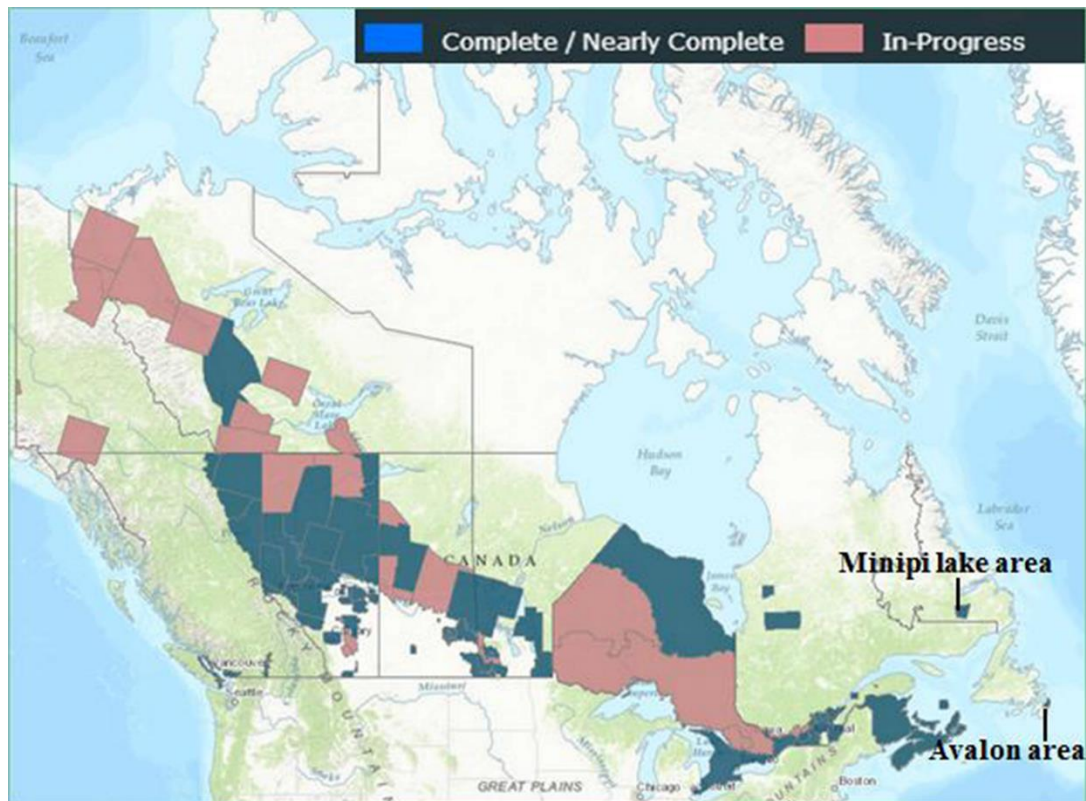


Figure 7.1. Canadian Wetland Inventory progress map for wetland areas (<http://maps.ducks.ca/cwi/>).

The objective of this study is to develop an approach for operational wetland mapping, which can efficiently deal with wetland complexity in NL, and to considerably improve the accuracy of wetland classification. For this, a combination of aerial imagery, SAR and optical satellite data were applied. The procedure involves the application of the OBIA method to segment the imagery, and the RF algorithm to classify wetlands in different study areas with various ecologies. Various spectral, SAR, texture, and ratio features were also evaluated for discrimination wetland types in this study. The accuracies of the classifications were then assessed by the parameters obtained from confusion matrices including the overall accuracies and the average producer and user accuracies for wetland

classes. The results are finally discussed with respect to wetland classification in NL.

7.2. Study areas and data

7.2.1. Study areas

In this study, wetlands in five pilot sites distributed across NL (Figure 7.2) are classified into five classes of Bog, Fen, Marsh, Swamp, and Shallow Water. The pilot sites were selected so as to represent the different local ecologies. It is widely acknowledged that wetland ecology and distribution is in part controlled by climate and topography (Mitsch and Gosselink, 1993). Consequently, wetlands of all classes and ecologies in NL are represented within these pilot sites, with different ratios of distribution, though like much of Newfoundland, peatlands are dominant. This will ensure that any methodologies subsequently developed will not only accurately classify wetlands in one local area of NL, but will also be robust enough to allow for the accurate classification of all wetlands across the entire province.

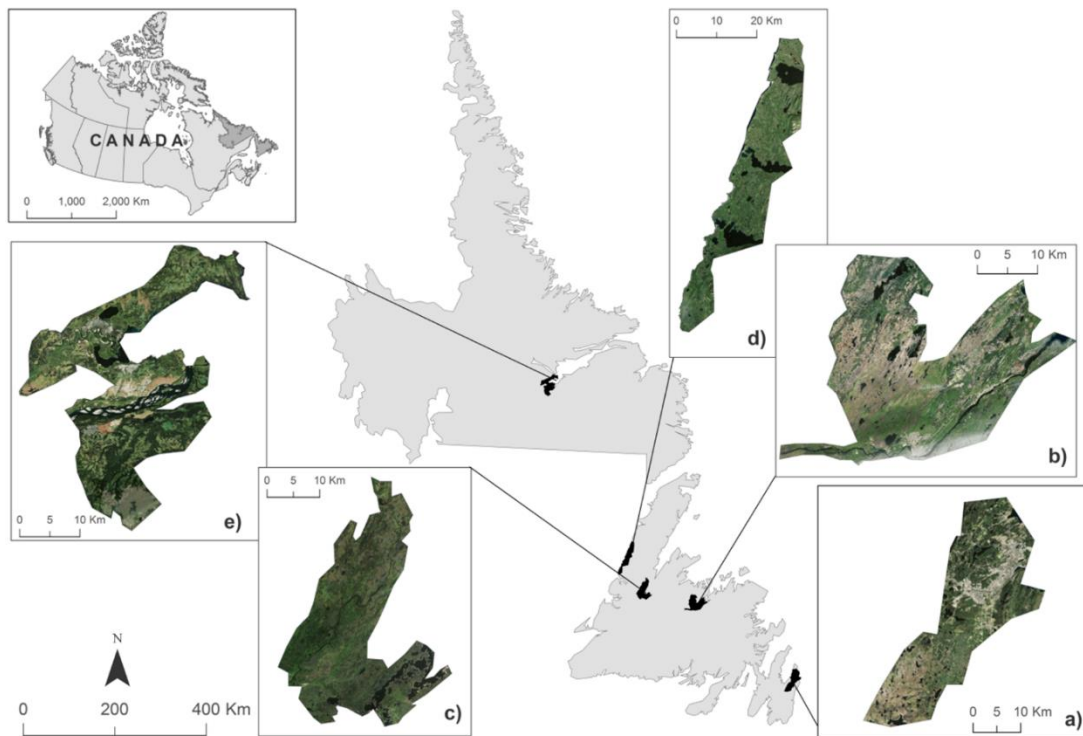


Figure 7.2. Study areas across Newfoundland and Labrador. a) Avalon, b) Grand Falls-Windsor, c) Deer Lake, d) Gros Morne, and e) Goose Bay.

7.2.2. Data

The field program was conducted between July and October in 2015 and between June to August in 2016, to support the development and testing of our methods for wetland classification in NL. Potential wetland sites were selected based on the visual analysis of high resolution aerial photography, their accessibility via public roads and trails, and the public or private ownership of the lands. Visited sites were identified down to class level (Bog, Fen, Marsh, Swamp, and Shallow Water) based on the classification key described by the CWCS (Warner and Rubec, 1997). Moreover, ancillary data, including GPS points, on-site photographs, and field notes on dominant vegetation, hydrology, and surrounding landscape were collected at each wetland site. Finally, the data was inserted into ArcMap 10.3.1,

where the wetland boundary for each site was delineated and digitized. To do so, high resolution satellite and aerial photography, as well as other ancillary data were used.

Four different types of aerial and satellite imagery, including the Canadian Digital Surface Model (CDSM), RapidEye, Landsat 8 Operational Land Imager (OLI), and Radarsat 2 SAR data were used to classify wetlands in the study areas. Table 7.1 provides the information about the data sets that were applied in each study area. All types of imagery, including the aerial photography, optical, and SAR satellite imagery were evaluated for wetland classification in the Avalon, Gros Morne, and Goose Bay pilot sites. However, the SAR data and RapidEye imagery were unavailable for the Grand Falls-Windsor and Deer Lake pilot sites, respectively, and hence were not included in the classification of these two study areas.

Table 7.1. The information on the aerial and satellite data.

Study area	Data	Date of acquisition
Avalon	- One RapidEye imagery	2015/06/18
	- Two Landsat 8 imagery	2015/06/19 , 2015/11/26
	- Two Radarsat 2 imagery	2015/06/10 , 2015/08/21
	- CDSM	February 2000
Grand Falls- Windsor	- One RapidEye imagery	2015/06/10
	- Two Landsat 8 imagery	2015/06/10, 2015/08/04
	- CDSM	February 2000
Deer Lake	- One Landsat 8 imagery	2015/08/04
	- Three Radarsat 2 imagery	2015/06/23 , 2015/08/10 and 2015/10/18
	- CDSM	February 2000
Gros Morne	- Two RapidEye imagery	2015/06/18 , 2015/09/06
	- Two Landsat 8 imagery	2015/06/15 , 2015/07/17
	- Three Radarsat 2 imagery	2015/06/16, 2015/08/03 and 2015/10/14
	- CDSM	February 2000
Goose Bay	- Two RapidEye imagery	2015/07/01 , 2015/10/04
	- Two Landsat 8 imagery	2015/06/22 , 2015/08/09
	- Two Radarsat 2 imagery	2015/06/30 , 2015/10/04
	- CDSM	February 2000
CDSM: Canadian Digital Surface Model		

7.3. Methodology

The image analysis methodology for wetland classification in the current study is depicted in Figure 7.3. The satellite images were selected separately for each pilot site (see Table 7.1). However, for all five pilot sites the same procedure was used for image segmentation, feature extraction and selection, selection of training samples, as well as setting tuning parameters in the RF classifier.

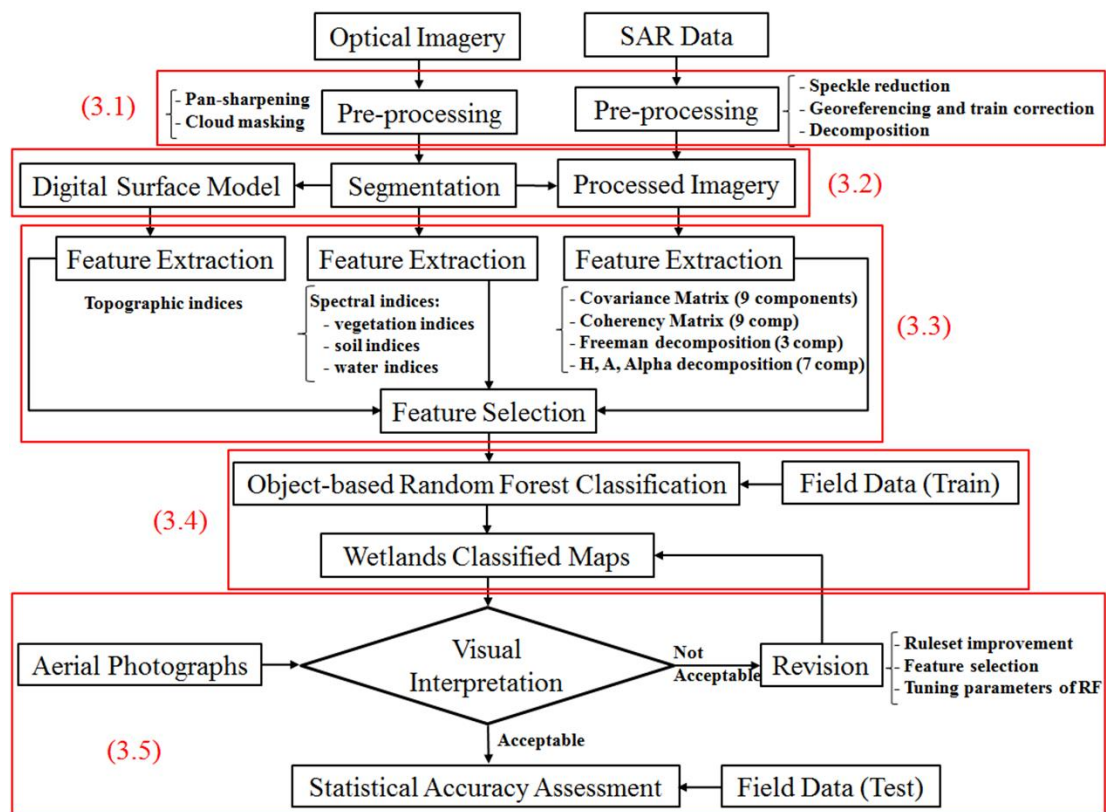


Figure 7.3. Flow chart of the methodology.

7.3.1. Pre-processing

Pre-processing was performed on both optical and SAR data. The geometric and radiometric corrections were not carried out on the optical imagery (CDSM,

RapidEye, and Landsat 8), because these products were already radiometrically and geometrically corrected with an accuracy of less than half pixel size (www.ccrs.nrcan.gc.ca; RapidEye, 2011; <http://landsat.usgs.gov/landsat8.php>). However, since some of the optical imagery contained cloud cover, cloud masking was performed on those images. Moreover, the Landsat 8 data were pan-sharpened to obtain images with higher spatial resolution (15 m). RADARSAT 2 images were acquired in Fine-resolution Quad-polarimetric (FQ) beam modes and presented in the form of a scattering matrix with a spatial resolution of 12.5 m. Since a scattering matrix provides absolute phase information that can be distorted during processing steps, it was converted to covariance matrix containing relative phase information. After extraction of the covariance matrix, a 7*7 Lee PolSAR filter was applied to the images to reduce the effect of speckle noise. The Lee filter was selected because it is a commonly-used polarimetric filter, which preserves polarimetric information (Lee et al., 1999). Then, the covariance matrix was terrain corrected to remove the effect of geometric distortions, such as foreshortening, layover and shadow, and then was geocoded. Finally, the coherency matrix, Freeman-Durden decomposition (Freeman and Durden, 1998) and H/A/ α decomposition (Cloude and Pottier, 1997) were extracted to be used along with the covariance matrix for classification.

7.3.2. Segmentation

The RapidEye imagery was used to segment all study areas except the Deer Lake pilot site, where the pan-sharpened Landsat 8 was used for segmentation. The RapidEye imagery was selected because it has the highest spatial resolution (5 m) compared to the other optical and SAR data used in this study. Furthermore, since

the SAR data contain speckle noise, using this type of imagery for segmentation will result in obtaining objects that do not correspond to real-world objects. The multi-resolution image segmentation algorithm (Baatz and Schäpe, 2000), implemented in the eCognition Developer™ 9 software (Definiens, 2009), was used to segment the study areas. The algorithm merges neighboring pixels based on several user-defined parameters, namely the scale, shape, and compactness, the most important of which is the scale parameter. In the present work, the scale parameter was adjusted until the resultant image objects visually represented the features of interest (i.e., wetland classes). Finally, the value of 300 was assigned to create pure objects that were sufficiently large for visual clarity and to separate and classify different types of wetlands.

7.3.3. Feature extraction and selection

Different object-based features can be extracted in the eCognition Developer™ software (Definiens, 2009) and applied during the classification procedure. Furthermore, numerous features are available within the software. In this study, various features, including topographic, spectral, SAR, and ratio features obtained from both optical and SAR data, as well as texture features calculated from the Grey Level Co-occurrence Matrix (GLCM) matrix, were initially extracted (See Table 7.2). Then, all of these features were evaluated to select only those features that were most useful to distinguish different types of wetlands. The eCognition Developer™ software provides measures of variable importance for separating different classes in a classification procedure through the “feature space optimization”, “sample editor”, and “sample selection information” tool boxes. In this study, we used these tool boxes and several other analyses, including

comparing the histograms of each feature among wetland and non-wetland classes to determine the selection of optimal object features. According to our analyses, the following features were generally more helpful to separate various categories in the study areas:

- 1) The Normalized Difference Vegetation Index (NDVI).
- 2) The Normalized Difference Water Index (NDWI).
- 3) The Mean and standard deviation values of objects derived from the visible and Near Infrared (NIR) bands.
- 4) The Mean and standard deviation values of objects derived from the Freeman decomposition components and three diagonal components of the covariance matrix ($|S_{HH}|^2$, $2|S_{HV}|^2$, $|S_{VV}|^2$. S_{HH} , S_{HV} , S_{VV} refer to the scattering elements at HH, HV, and VV channels, respectively).
- 5) Both optical and SAR ratio features, given in Table 7.2.

Table 7.2. Evaluated features in this study.

Topographic features	CDSM, Slope, Aspect																				
Spectral features	Normalized Difference Water Index = $\frac{G-NIR}{G+NIR}$ Modified Normalized Difference Water Index = $\frac{G-MIR}{G+MIR}$ Difference Vegetation Index = NIR-R Normalized Difference Vegetation Index = $\frac{NIR-R}{NIR+R}$ Red Edge Normalized Difference Vegetation Index = $\frac{NIR-RE}{NIR+RE}$ Forest Discrimination Index = NIR-(RE+B) Normalized Difference Soil Index = $\frac{SWIR-NIR}{SWIR+NIR}$ Soil Adjusted Vegetation index = $\frac{(1+L)(NIR-R)}{NIR+R+L}$; L=0.5 Normalized Difference Moisture Index = $\frac{NIR-SWIR}{NIR+SWIR}$																				
SAR features	Covariance matrix (9 components) Coherency matrix (9 components) Freeman decomposition (double, odd, and volume scattering) H, A, α , decomposition (alpha, anisotropy, beta, delta, entropy, gamma, lambda)																				
Ratio features	<table border="0" style="width: 100%; text-align: center;"> <thead> <tr> <th style="border-bottom: 1px solid black;">B</th> <th style="border-bottom: 1px solid black;">G</th> <th style="border-bottom: 1px solid black;">R</th> <th style="border-bottom: 1px solid black;">NIR</th> <th style="border-bottom: 1px solid black;">SWIR</th> </tr> </thead> <tbody> <tr> <td>Brightness</td> <td>Brightness</td> <td>Brightness</td> <td>Brightness</td> <td>Brightness</td> </tr> <tr> <td>$\frac{ S_{HV} ^2}{ S_{HH} ^2}$</td> <td>$\frac{ S_{HV} ^2}{ S_{VV} ^2}$</td> <td>$\frac{ S_{HH} ^2}{ S_{VV} ^2}$</td> <td>$\frac{ S_{HV} ^2}{TP}$</td> <td>$\frac{ S_{HH} ^2}{TP}$</td> </tr> <tr> <td>$\frac{ S_{HV} ^2}{ S_{VV} ^2}$</td> <td>$\frac{ S_{HH} ^2}{ S_{VV} ^2}$</td> <td>$\frac{ S_{VV} ^2}{TP}$</td> <td></td> <td></td> </tr> </tbody> </table>	B	G	R	NIR	SWIR	Brightness	Brightness	Brightness	Brightness	Brightness	$\frac{ S_{HV} ^2}{ S_{HH} ^2}$	$\frac{ S_{HV} ^2}{ S_{VV} ^2}$	$\frac{ S_{HH} ^2}{ S_{VV} ^2}$	$\frac{ S_{HV} ^2}{TP}$	$\frac{ S_{HH} ^2}{TP}$	$\frac{ S_{HV} ^2}{ S_{VV} ^2}$	$\frac{ S_{HH} ^2}{ S_{VV} ^2}$	$\frac{ S_{VV} ^2}{TP}$		
B	G	R	NIR	SWIR																	
Brightness	Brightness	Brightness	Brightness	Brightness																	
$\frac{ S_{HV} ^2}{ S_{HH} ^2}$	$\frac{ S_{HV} ^2}{ S_{VV} ^2}$	$\frac{ S_{HH} ^2}{ S_{VV} ^2}$	$\frac{ S_{HV} ^2}{TP}$	$\frac{ S_{HH} ^2}{TP}$																	
$\frac{ S_{HV} ^2}{ S_{VV} ^2}$	$\frac{ S_{HH} ^2}{ S_{VV} ^2}$	$\frac{ S_{VV} ^2}{TP}$																			
Texture features	GLCM (homogeneity, contrast, dissimilarity, entropy, moment, correlation)																				
<p>Note: B: blue, G: green, R: red, RE: red edge, NIR: near infrared, MIR: mid infrared, SWIR: short wave infrared, CDSM: Canadian Digital Surface Model, HH: Horizontal transmit and Horizontal receive polarizations, VV: Vertical transmit and Vertical receive polarizations, HV: Horizontal transmit and Vertical receive polarizations, TP: Total power = $S_{HH} ^2 + 2 S_{HV} ^2 + S_{VV} ^2$</p>																					

7.3.4. Classification

According to our analysis carried out using the eCognition Developer™ software, the RF classifier had the best performance compared to the SVM, ML, CART, and

KNN in all five study areas. Therefore, we used the object-based RF classification method for this research. The RF algorithm applies a user-defined feature vector to several trees in the forest. All trees are trained with the same features but on various training sets, which are generated randomly from the original training data. After training, each tree assigns a class label to the test data. Then, the results of all decision trees are fused, and finally, the majority of votes determine the class label for each object. There are two important tuning parameters in the RF algorithm implemented in the eCognition Developer™ software that can considerably affect the classification accuracy: depth and minimum sample number. The depth determines the number of nodes in each tree, and the minimum sample number indicates the minimum number of samples per node in each tree. In this study, after assigning different values to these parameters, it was concluded that the optimum values for the depth and the minimum sample number were 20 and 5, respectively. Moreover, we have used a maximum of 50 trees in the RF algorithm in each pilot site. It is also worth noting that half of the field data were randomly used to train the algorithms while the other half was applied to evaluate the performance of the algorithm in discriminating different wetland and non-wetland classes. It is also worth noting that the objects with the size of less than 1 hectare were merged with the biggest surrounding objects to reduce the speckle noise of classified maps. Finally, classified images in the five wetland classes of Bog, Fen, Marsh, Swamp, and Shallow Water, plus four non-wetland classes of Deep Water, Upland, Urban, and Sand for each pilot site were produced.

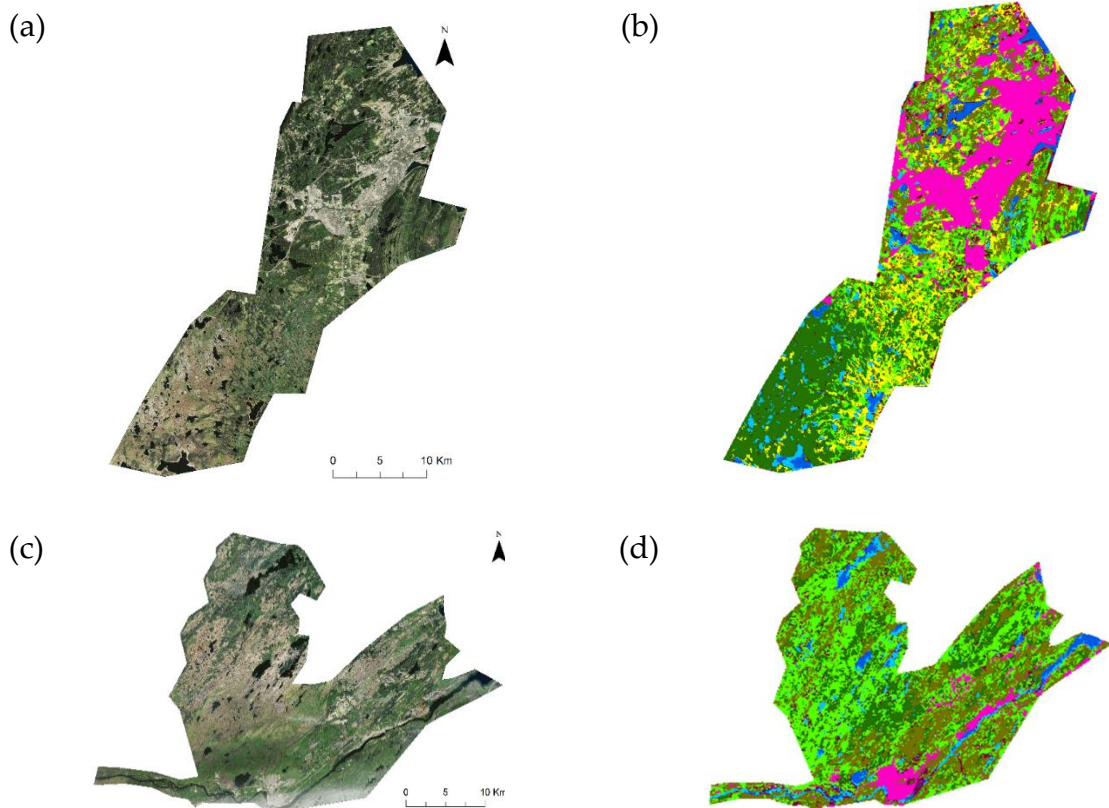
7.3.5. Accuracy assessment

Two types of accuracy assessment were carried out for the classified images. First, the maps were analyzed and interpreted visually using high spatial resolution ortho-photo images (0.5 m) to see if the classes visually correspond to real objects. If the results were not satisfactory, the classifications were improved by either changing the ruleset in the algorithm, selecting more useful features, or changing the tuning parameters in the RF classifier. Finally, when the maps were visually acceptable, the statistical accuracy assessment was conducted using a confusion matrix. To do this, after defining a boundary (polygon) for each field data in ArcGIS, as explained in section 2.2, all polygons were randomly and independently divided into two groups, in which 50% were used to train the RF algorithm and the other 50% remained to test the classification results. It is worth mentioning that the parameters of the Overall Accuracy (OA), Kappa Coefficient, Producer Accuracy (PA), and User Accuracy (UA), all of which were derived from a confusion matrix were calculated and used for accuracy assessment. The OA considers both wetland and non-wetland classes; however, since we were primarily interested in the efficiency of the proposed methodology for classifying wetlands, the average PA and UA of each five wetland classes were also presented to obtain a more reasonable conclusion.

7.4. Results and discussion

Figure 7.4 demonstrates the results of wetland classification obtained by the object-based RF algorithm in the five study areas. According to the maps, wetlands occupy approximately 68%, 63%, 64%, 65%, and 41% of the Avalon, Grand Falls-Windsor, Deer Lake, Gros Morne, and Goose Bay pilot sites, respectively. It is

evident that the classified images provide a visually adequate depiction of wetland and non-wetland classes. The obtained maps are noiseless and clean, and the delineated classes are visually realistic and correspond to the real-world objects based on the visual interpretation of the ecological experts who participated in collecting field data and were familiar with the study areas. For instance, most of small water bodies were classified as the Shallow Water class, indicating that these regions were classified accurately. Moreover, the deep water regions were classified correctly and the areas surrounding deep waters were also correctly identified as Shallow Water and Marsh classes (i.e., emergent marsh). Urban areas were also determined correctly.



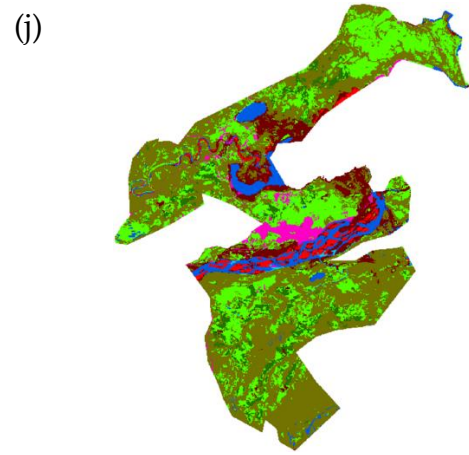
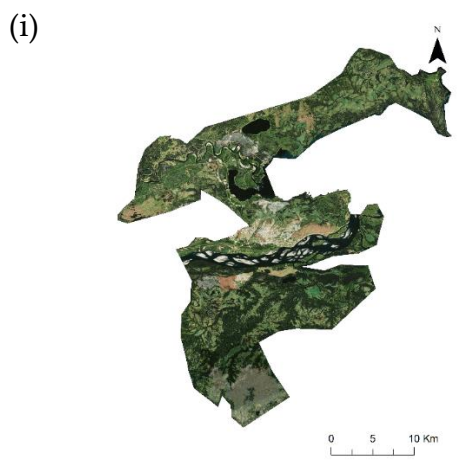
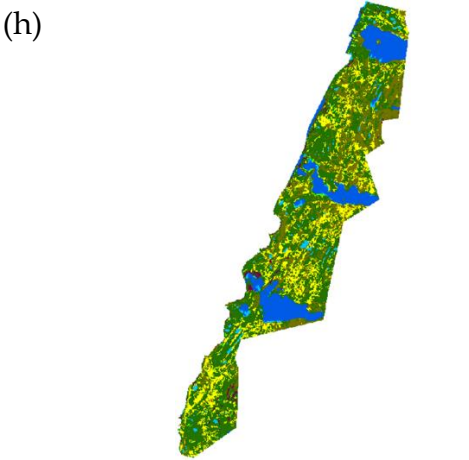
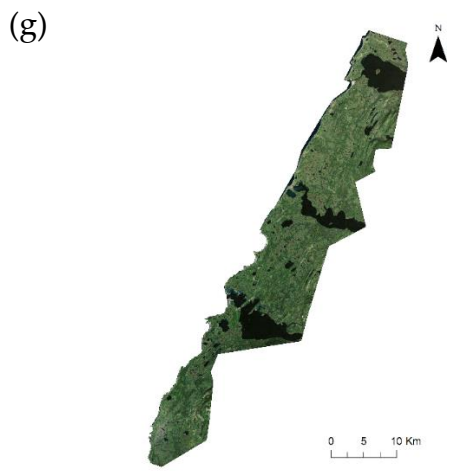
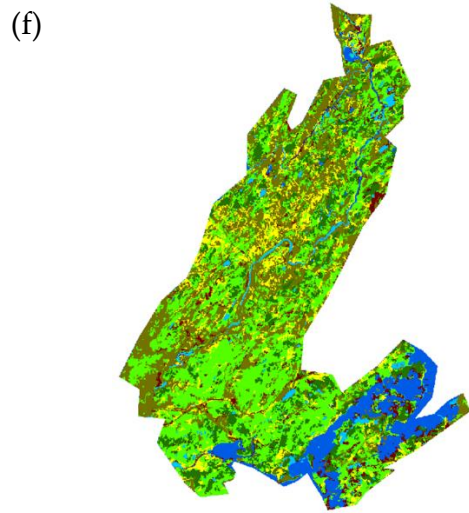
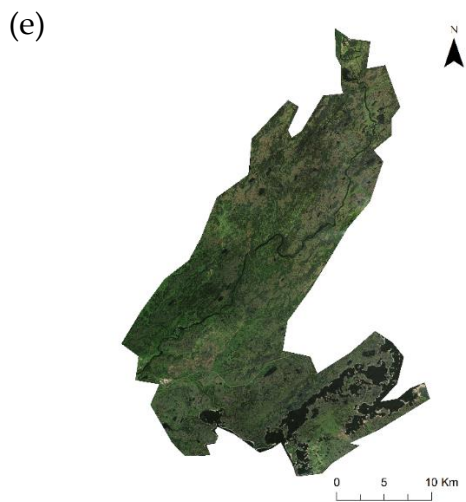




Figure 7.4. The maps of wetlands in a) Avalon, b) Grand Falls-Windsor, c) Deer Lake, d) Gros Morne, and e) Goose Bay.

As demonstrated in Figure 7.5, the OAs for the classification of the Avalon, Grand Falls-Windsor, Deer Lake, Gros Morne, and Goose Bay pilot sites were 92%, 87%, 81%, 92%, and 85%, respectively. The Kappa Coefficients were 0.89, 0.84, 0.76, 0.88, and 0.83 for the study areas, respectively. The average PAs of only wetland classes were 73%, 71%, 77%, 57%, and 77% in the Avalon, Grand Falls-Windsor, Deer Lake, Gros Morne, and Goose Bay pilot sites, respectively. Moreover, the average UAs of the wetland classes in the Avalon, Grand Falls-Windsor, Deer Lake, Gros Morne, and Goose Bay pilot sites were 72%, 80%, 65%, 71%, and 72%, respectively. Considering the complexity of wetlands in the study areas, these levels of accuracy proves the robustness and high performance of the proposed methodology in different study areas with various ecological characteristics.

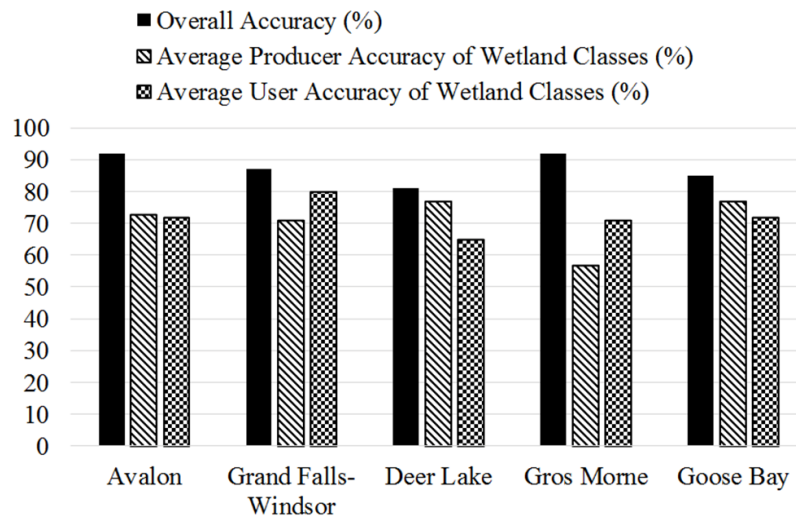
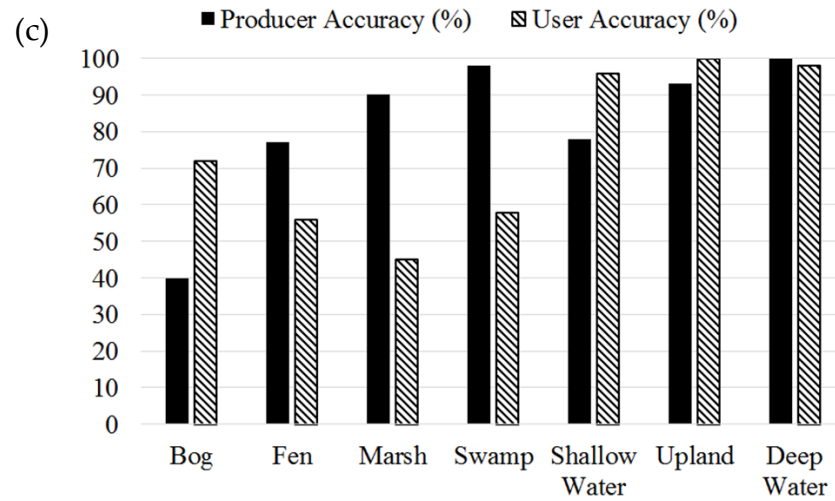
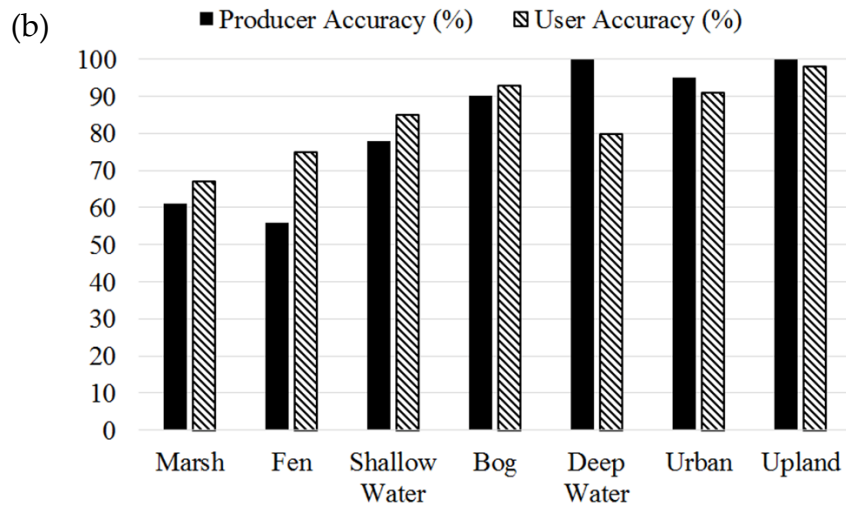
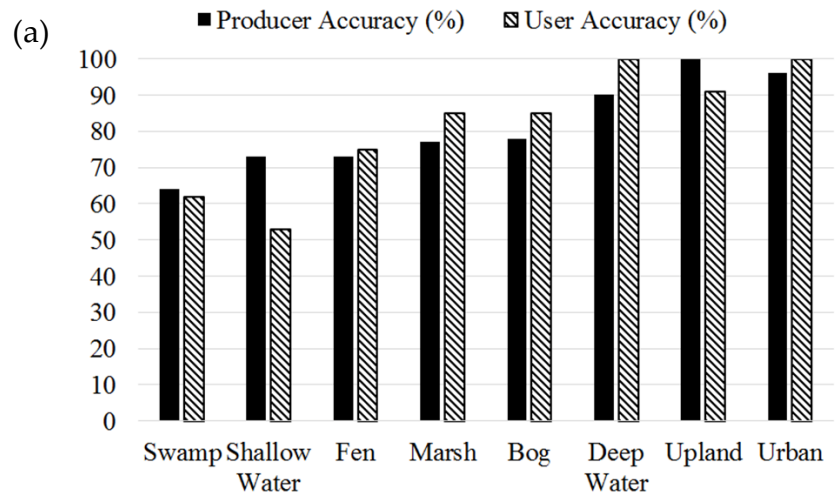


Figure 7.5. The overall classification accuracies, as well as the average producer and user accuracies of wetland classes in the five study areas.

Individual class accuracies, including both PA and UA, for the wetland and non-wetland classes in the corresponding study area were generated using confusion matrices, and are demonstrated in Figure 7.6.



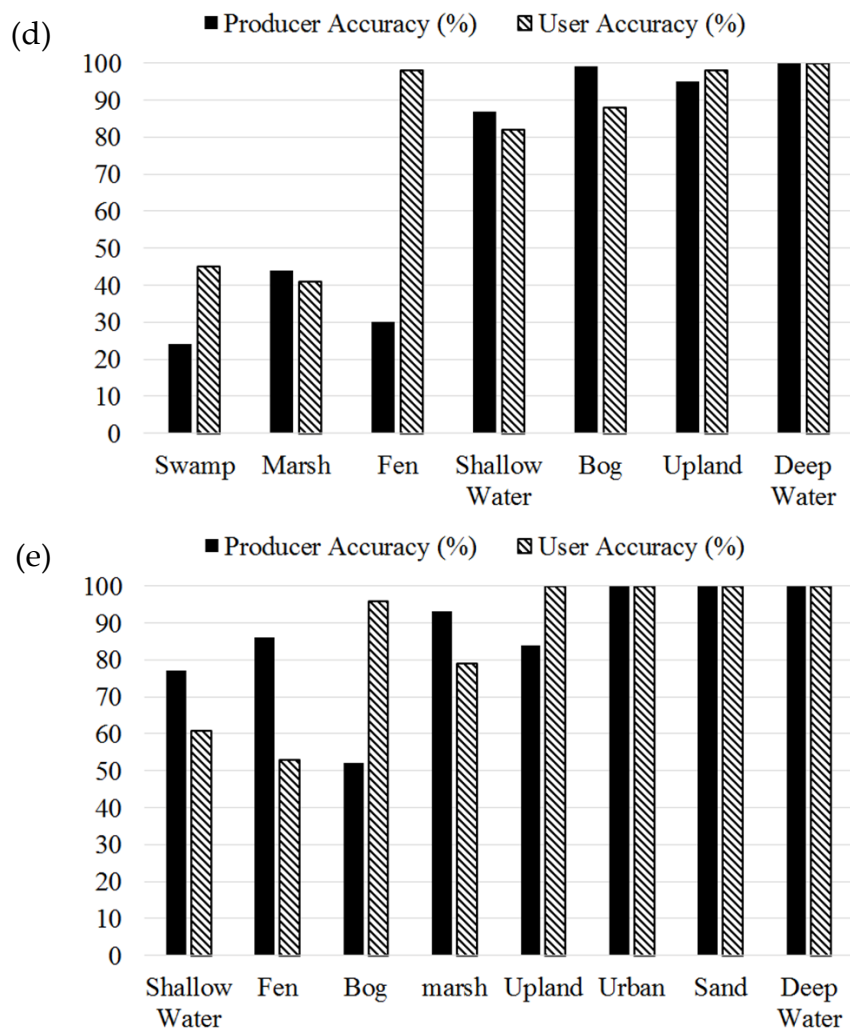


Figure 7.6. Producer Accuracy and User Accuracy for each of the wetland and non-wetland classes in a) Avalon, b) Grand Falls-Windsor, c) Deer Lake, d) Gros Morne, and e) Goose Bay.

As expected, the accuracies for the non-wetland classes were generally higher than those for wetland classes in all pilot sites. This is rooted in the fact that the non-wetland classes were easily distinguishable because they pose different spectral signature or backscattering energy compared to the other classes. Furthermore, since there were more train and test data for these classes relative to the wetland

classes, the RF algorithm performed more appropriate in identifying these classes. However, there were many difficulties in discriminating wetland classes, especially for the Fen/Bog, and Swamp/Upland classes, in which they were misclassified interchangeably. This can be explained by the fact that these wetland types are spectrally or texturally similar in remotely sensed data (Henderson and Lewis, 2008). These are discussed in more detail below.

The confusion between wetland classes was more severe for the Bog/Fen classes, for which our analyses showed that the spectral and textural signatures of these classes were generally overlapped in most cases, and there were no observable differences between their spectral and textural profiles (Figure 7.7). Since bog and fen are ecologically similar, even in the field there were situations where there was difficulty clearly distinguishing between them. As a result, these two types of wetlands were sometimes categorized as the same class (i.e. Peatland). This confusion can be easily seen in the accuracies obtained for the Deer Lake, Gros Morne, and Goose Bay pilot sites. According to Figure 7.6 (c and e), the PA for the Bog class was low (high error of omission) in the Deer Lake and Goose Bay pilot sites. It is possible that many of the bogs were misclassified as Fen in these pilot sites. Conversely, the PA for the Fen class was low in the Gros Morne pilot site (Figure 7.6 (d)), which means that many of the fens may have been incorrectly classified as Bog. To explain the high confusion between the Bog and Fen classes, the detailed confusion matrix obtained from the classification of the Deer Lake pilot site is provided as an example in Table 7.3. According to this Table, it was concluded that most of the bogs were mistakenly classified as Fen. The error of omission for the Bog class in this pilot site was 60%, proving that this class was highly underestimated during the classification. There were also many fens (1937

pixels out of 13316 pixels) that were misclassified as the Bog class. The resulting confusions between the Bog and Fen classes in the study areas are in accordance with many related studies. There are only a few studies that could separate these classes with an acceptable accuracy using remote sensing data. For example, Touzi et al. (2007) reported that some polarimetric parameters, extracted from the Touzi decomposition, were useful for separating bogs and fens.

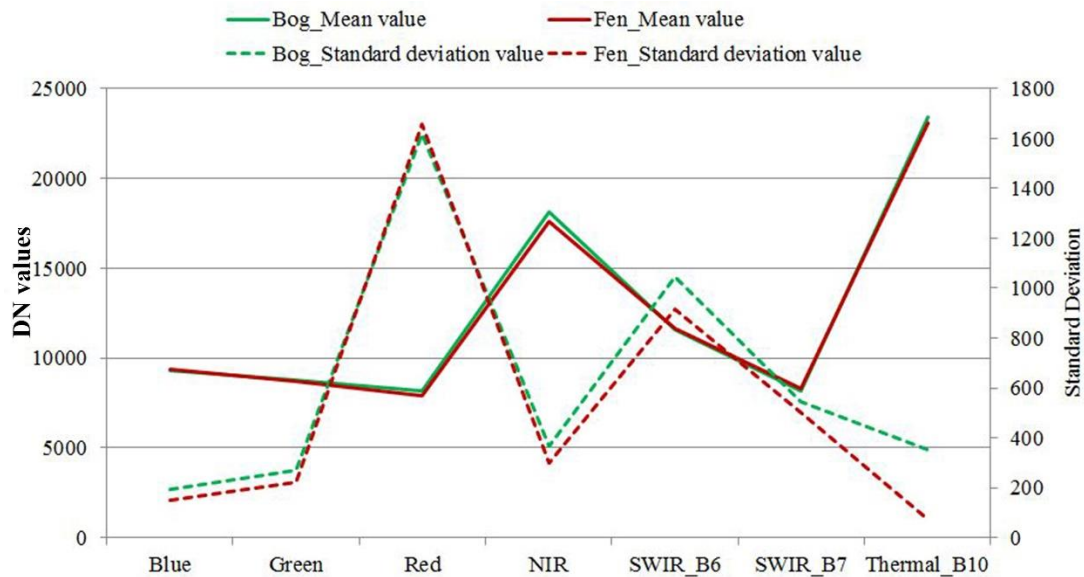


Figure 7.7. Spectral and textural signatures of the Bog and Fen classes, obtained from Landsat 8 data acquired over the Avalon pilot site (B: band, NIR: Near Infrared, SWIR: Short Wave Infrared).

Table. 7.3. Confusion matrix in terms of the number of pixels for the classification of the Deer Lake pilot site using the Random Forest algorithm.

		Reference Data									
		Up	M	F	SW	S	B	DW	Total	C (%)	UA(%)
Classified Data	Up	13951	16	35	0	0	16	0	14018	1	99
	M	336	1255	1074	70	0	27	0	2762	55	45
	F	105	21	10191	185	0	7718	0	18220	44	56
	SW	0	104	0	2230	0	0	0	2334	5	95
	S	654	0	79	0	1051	0	0	1784	42	58
	B	22	0	1937	0	0	5126	0	7085	28	72
	DW	0	0	0	353	0	0	20638	20991	2	98
	Total	15068	1396	13316	2838	1051	12887	20638	67194		
	O (%)	7	10	23	22	2	60	0		OA= 81%	
	PA(%)	93	90	77	78	98	40	100		K= 0.76	
OA: Overall Accuracy		B: Bog			S: Swamp			C: Commission			
K: Kappa Coefficient		F: Fen			Up: Upland			O: Omission			
PA: Producer Accuracy		M: Marsh			DW: Deep Water						
UA: User Accuracy		SW: Shallow Water			Ur: Urban						

Based on the results in all pilot sites, it was also concluded that treed swamps had similar spectral and backscattering behavior with the upland forest areas, as a result, there was much confusion between the Swamp and Upland classes. For instance, the PA for the Swamp class in the Gros Morne pilot site was low compared to the other classes (Figure 7.6 (d)), and according to the confusion matrix obtained for this pilot site, most of the swamps were mistakenly classified

as Upland. As another example, it can be seen from Figure 7.6 (c) and Table 7.3 that some of the upland forests were mistakenly classified as Swamp in the Deer Lake pilot site. The error of commission for the Swamp class was 42%, which was due to the misclassification of the Upland field data (654 pixels) as the Swamp class. In addition, since we defined the train and test data for the Upland class using the aerial imagery, it was possible that some miss-selection had occurred between these two classes in this step. Several studies, including Li et al. (2007), Henderson and Lewis (2008), and Hong et al. (2015), have reported that the L-band of SAR sensors can be useful in distinguishing swamps from upland forest and other wetland classes. The reason for this is that the penetration depth of the L-band is higher than C- and X-band, and thus, L-band signals can pass through the vegetation canopy and detect water beneath the dense vegetation and flooded trees characteristic of swamp wetlands.

Besides the high level of confusion between the Bog/Fen and Swamp/Upland classes, our analyses showed that the Marsh class was also often confused with the Shallow Water, Fen, and Bog classes in all study areas. As an example, according to Table 7.3, the error of commission for the Marsh class in the Deer Lake pilot site was considerably high (55%). In this study area, 1074 pixels of the Fen class were incorrectly identified as Marsh. The confusion between the Marsh and Shallow Water classes can be explained by the fact that, in all study areas, there are several emergent marsh areas that are spectrally similar to shallow water bodies containing lily pads. The confusion between peatlands (Bog and Fen classes) and Marsh class can be explained by the possible presence of water at bog and fen surfaces. Bogs can contain waterbodies, sometimes called bog pools, where water is present at the bog surface. These pools often contain emergent vegetation that

could cause both spectral and backscattering similar to marshes. Similarly, fens are often naturally associated with mineral ponds, lakes, and streams, which again, may contain emergent vegetation similar to marshes. In this way, confusion can arise, as wet and saturated emergent grasses in Bog, Fen, and Marsh will share similar spectral and backscattering values.

Moreover, the presence of water in wetlands is one of the main reasons of the difficulties in distinguishing wetland types. Water level in wetlands can change monthly and/or seasonally, sometimes rapidly resulting from snowmelt or precipitation, or gradually as a result of anthropogenic activities (Mitsch and Gosselink, 1993; Gallant, 2015). This fact shows that multi-temporal satellite data can be a considerable help in classifying wetlands (Li and Chen, 2005; Gosselin et al., 2014).

In addition to the spectral and backscattering similarity between wetland classes, which reduced the accuracy of the classifications, the PA and UA for each wetland class had a direct relationship with the amount of field data available for that class. Machine learning algorithms are sensitive to sample size, and thus decreasing the size of training samples generally results in a decrease in the accuracy of classification. This fact is more important for the RF algorithm, because it generates different trees, in which each tree needs an appropriate amount of training data to perform accurately (Figure 7.6). Since we had access to adequate amount of field data for the Bog class in all study areas except the Deer Lake pilot site, higher accuracies were also obtained for this class compared to the other wetland classes. However, since the amount of field data, and consequently train data, for the Swamp and Marsh classes were low in the Deer Lake pilot site, lower values for either PA or UA were obtained. As another example, we had access to insufficient

amount of field data for the Marsh class in the Gros Morne pilot site, which explained the lower accuracy for this class compared to the other wetland classes. In summary, it should be considered that most wetlands in the study areas were not accessible for field data collection. Additionally, even having GPS points, delineating a wetland boundary surrounding a sample point using high resolution imagery was challenging. This is because the boundaries of wetlands are often fuzzy as they gradually, rather than abruptly, transition to other wetland and non-wetland land cover classes (Gallant, 2015). In conclusion, it should be considered that having an insufficient amount of field data for some classes will result in lower accuracies for those particular classes, and consequently, reduce the reliability of the classified maps.

It is also worth noting that the RapidEye and RADARSAT 2 data were unavailable for the Deer Lake and Grand Falls-Windsor pilot sites, respectively, which limited the accuracy of the algorithm in the study areas. In Deer Lake, a pan-sharpened Landsat 8 image with a 15 m spatial resolution was used to segment the area instead of the RapidEye data with a 5 m spatial resolution. Thus, the produced objects were not as accurate and reliable as the obtained objects in the other pilot sites. Furthermore, the RADARSAT 2 data, which provide useful physical information to discriminate wetland classes, were not included in the classification of the Grand Falls-Windsor pilot site. This lack of data was also a limitation to achieving higher classification accuracy.

7.5. Conclusion

Wetland classification is a challenging issue in remote sensing because different wetland types are spectrally and texturally similar. However, this task can be effectively improved by the use of multi-source satellite data. In this research, we combined various types of remote sensing data to classify wetland areas into the five wetland classes of Bog, Fen, Marsh, Swamp, and Shallow Water, as well as four non-wetland classes of Deep Water, Upland, Urban, and Sand across five different study areas in NL. Different types of features, including topographic, spectral, SAR, and several pre-defined features in eCognition Developer™ 9, were evaluated to select those that were more useful for discriminating wetland classes. Then, the best features were inserted into a RF algorithm. According to the experts' knowledge and visual interpretation, the obtained maps were highly accordant with the actual objects. The overall classification accuracies obtained in all pilot sites were between 81% and 92%, proving the high performance of the methodology in classifying both wetland and non-wetland classes. In terms of class accuracies, the highest accuracies were generally obtained for the non-wetland classes. This was rooted in the fact that the non-wetland classes have distinguishable characteristics in terms of both spectral and backscattering information in remote sensing data. Among wetland classes, the highest confusion was between the Bog and Fen classes. Bogs and fens have many ecological similarities with each other and even with other wetlands, such as Marsh and Swamp, which cause many difficulties in differentiating these two classes. Moreover, the Swamp and Upland classes were mostly confused according to the calculated confusion matrices. This can be explained by the fact that most of the swamps in the study areas are treed swamps which have many similarities in the

backscattering and spectral information obtained by the SAR and optical data, respectively. In addition, several confusions were also observed between Marsh and the three classes of Shallow Water, Bog, and Fen. It should be noted that if there are little to no spectral and backscattering differences between some of the wetland types using satellite data, it is unlikely that any remote sensing algorithm could improve the accuracies for these classes. It was also found that the amount of field data has a significant effect on classification accuracy. For instance, since there were more field data for the Bog class compared to the other wetland classes, higher PA and UA were generally achieved for this class. In conclusion, our methodology proved to have a high potential for classifying wetland types in different study areas with various ecological characteristics. Therefore, based on accuracy levels, the proposed methodology will offers the potential to provide accurate results in different regions.

References

- Baatz, M., & Schäpe, A. (2000). Multiresolution segmentation: an optimization approach for high quality multi-scale image segmentation. *Angewandte Geographische Informationsverarbeitung XII*, 58, 12-23.
- Barbier, E. B., Acreman, M., & Knowler, D. (1997). Economic valuation of wetlands: a guide for policy makers and planners. *Gland: Ramsar Convention Bureau*.
- Breiman, L. (2001). Random forests. *Machine Learning*, 45(1), 5-32.
- Brisco, B., Kapfer, M., Hirose, T., Tedford, B., & Liu, J. (2011). Evaluation of C-band polarization diversity and polarimetry for wetland mapping. *Canadian Journal of Remote Sensing*, 37(1), 82-92.

- Cloude, S. R., & Pottier, E. (1997). An entropy based classification scheme for land applications of polarimetric SAR. *IEEE Transactions on Geoscience and Remote Sensing*, 35(1), 68-78.
- Dabboor, M., White, L., Brisco, B., & Charbonneau, F. (2015). Change detection with compact polarimetric SAR for monitoring wetlands. *Canadian Journal of Remote Sensing*, 41(5), 408-417.
- Definiens, A. G. (2009). Definiens eCognition developer 8 user guide. *Definiens AG, Munchen, Germany*.
- Duro, D. C., Franklin, S. E., & Dubé, M. G. (2012). A comparison of pixel-based and object-based image analysis with selected machine learning algorithms for the classification of agricultural landscapes using SPOT-5 HRG imagery. *Remote Sensing of Environment*, 118, 259-272.
- Ecological Stratification Working Group (Canada), Center for Land, Biological Resources Research (Canada), & Canada. State of the Environment Directorate. (1996). A national ecological framework for Canada. *Centre for Land and Biological Resources Research; Hull, Quebec: State of the Environment Directorate*.
- Freeman, A., & Durden, S. L. (1998). A three-component scattering model for polarimetric SAR data. *IEEE Transactions on Geoscience and Remote Sensing*, 36(3), 963-973.
- Gallant, A. L. (2015). The Challenges of Remote Monitoring of Wetlands. *Remote Sensing*, 7(8).
- Gosselin, G., Touzi, R., & Cavayas, F. (2014). Polarimetric Radarsat-2 wetland classification using the Touzi decomposition: case of the Lac Saint-Pierre Ramsar wetland. *Canadian Journal of Remote Sensing*, 39(6), 491-506.

- Grenier, M., Demers, A. M., Labrecque, S., Benoit, M., Fournier, R. A., & Drolet, B. (2007). An object-based method to map wetland using RADARSAT-1 and Landsat ETM images: test case on two sites in Quebec, Canada. *Canadian Journal of Remote Sensing*, 33(sup1), S28-S45.
- Henderson, F. M., & Lewis, A. J. (2008). Radar detection of wetland ecosystems: a review. *International Journal of Remote Sensing*, 29(20), 5809-5835.
- Hoag, R. S., & Price, J. S. (1995). A field-scale, natural gradient solute transport experiment in peat at a Newfoundland blanket bog. *Journal of Hydrology*, 172(1-4), 171-184.
- Hong, S. H., Kim, H. O., Wdowinski, S., & Feliciano, E. (2015). Evaluation of polarimetric SAR decomposition for classifying wetland vegetation types. *Remote Sensing*, 7(7), 8563-8585.
- Kumar, L., & Sinha, P. (2014). Mapping salt-marsh land-cover vegetation using high-spatial and hyperspectral satellite data to assist wetland inventory. *GIScience & Remote Sensing*, 51(5), 483-497.
- Lee, J. S., Grunes, M. R., & De Grandi, G. (1999). Polarimetric SAR speckle filtering and its implication for classification. *IEEE Transactions on Geoscience and remote sensing*, 37(5), 2363-2373.
- Li, J., & Chen, W. (2005). A rule-based method for mapping Canada's wetlands using optical, radar and DEM data. *International Journal of Remote Sensing*, 26(22), 5051-5069.
- Li, J., Chen, W., & Touzi, R. (2007). Optimum RADARSAT-1 configurations for wetlands discrimination: a case study of the Mer Bleue peat bog. *Canadian Journal of Remote Sensing*, 33(sup1), S46-S55.

- Mahoney, M. and Hanson A. (2006). Wetland Classification in a Sub-Urban Environment-Northeast Avalon Peninsula, Newfoundland. *Unpublished report. Canadian Wildlife Service, Sackville, New Brunswick.*
- Mahoney, M. L., Hanson, A. R., & Gilliland, S. (2007). An evaluation of a methodology for wetland classification and inventory for Labrador. *Canadian Wildlife Service.*
- Mitsch, W.J., and Gosselink, J.G. (1993). Wetlands (2nd edition). *Van Nostrand Reinhold, New-York. p. 600.*
- Mutanga, O., Adam, E., & Cho, M. A. (2012). High density biomass estimation for wetland vegetation using WorldView-2 imagery and random forest regression algorithm. *International Journal of Applied Earth Observation and Geoinformation*, 18, 399-406.
- Nyarko, B. K., Diekkrüger, B., Van De Giesen, N. C., & Vlek, P. L. (2015). Floodplain wetland mapping in the White Volta River Basin of Ghana. *GIScience & Remote Sensing*, 52(3), 374-395.
- Pal, M. (2005). Random forest classifier for remote sensing classification. *International Journal of Remote Sensing*, 26(1), 217-222.
- Powers, R. P., Hay, G. J., & Chen, G. (2012). How wetland type and area differ through scale: A GEOBIA case study in Alberta's Boreal Plains. *Remote Sensing of Environment*, 117, 135-145.
- Price, J. S. (1992). Blanket bog in Newfoundland. Part 2. Hydrological processes. *Journal of Hydrology*, 135(1-4), 103-119.
- RapidEye, A. G. (2011). Satellite imagery product specifications. *Satellite imagery product specifications: Version.*

- Reif, M., Frohn, R. C., Lane, C. R., & Autrey, B. (2009). Mapping isolated wetlands in a karst landscape: GIS and remote sensing methods. *GIScience & Remote Sensing*, 46(2), 187-211.
- Rundquist, D. C., Narumalani, S., & Narayanan, R. M. (2001). A review of wetlands remote sensing and defining new considerations. *Remote Sensing Reviews*, 20(3), 207-226.
- Salehi, B., Zhang, Y., & Zhong, M. (2013). A combined object-and pixel-based image analysis framework for urban land cover classification of VHR imagery. *Photogrammetric Engineering & Remote Sensing*, 79(11), 999-1014.
- Salehi, B., Zhang, Y., Zhong, M., & Dey, V. (2012). A review of the effectiveness of spatial information used in urban land cover classification of VHR imagery. *International Journal of Geoinformatics*, 8(2).
- Schmitt, A., & Brisco, B. (2013). Wetland monitoring using the curvelet-based change detection method on polarimetric SAR imagery. *Water*, 5(3), 1036-1051.
- Shiraishi, T., Motohka, T., Thapa, R. B., Watanabe, M., & Shimada, M. (2014). Comparative assessment of supervised classifiers for land use–land cover classification in a tropical region using time-series palsar mosaic data. *IEEE Journal of Selected Topics in Applied Earth Observations and Remote Sensing*, 7(4), 1186-1199.
- South, G. R. (1983). 10. Benthic marine algae. *Biogeography and Ecology of the Island of Newfoundland*, 48, 385.
- Tiner, R. W., Lang, M. W., & Klemas, V. V. (Eds.). (2015). Remote sensing of wetlands: applications and advances. *CRC Press*.
- Touzi, R., Deschamps, A., & Rother, G. (2007). Wetland characterization using polarimetric RADARSAT-2 capability. *Canadian Journal of Remote Sensing*, 33(sup1), S56-S67.

Wang, J., Shang, J., Brisco, B., & Brown, R. J. (1998). Evaluation of multitemporal ERS-1 and multispectral Landsat imagery for wetland detection in southern Ontario. *Canadian journal of remote sensing*, 24(1), 60-68.

Warner, B.G. and Rubec, C.D.A. eds. (1997). The Canadian wetland classification system. *Wetlands Research Branch, University of Waterloo*.

Whiteside, T. G., & Bartolo, R. E. (2015). Mapping Aquatic Vegetation in a Tropical Wetland Using High Spatial Resolution Multispectral Satellite Imagery. *Remote Sensing*, 7(9), 11664-11694.

CHAPTER 8. SUMMARY, CONCLUSION, AND RECOMMENDATIONS

8.1. Summary

Wetlands provide many ecological services to environment, and play an important role in providing water, food, and shelter to humans, animals and plants. Moreover, wetlands are important to be studied as they affect climate change, warming, global carbon and methane cycles. Thus, classifying and monitoring these valuable landscapes are of great importance for the countries. In this regard, satellites provide cost-effective, repetitive, and real-time data, which have been effectively applied to identify and distinguish different wetland species. Additionally, large coverage of the satellite imagery enables us to apply them to large scale applications and develop nation-wide wetland inventories. Different types of remote sensing data have so far been employed for wetland mapping, of which optical and Synthetic Aperture Radar (SAR) data are generally the most useful. Currently, object-based classification methods have been proved to provide higher accuracies compared to pixel-based methods by availability of medium and high spatial resolution imagery. Furthermore, there are currently several satellites that provide free data to users, causing satellites to be more useful for operational applications. Additionally, various classification algorithms have been developed to use satellite data for wetland classification.

In this research, multi-source optical and SAR data are applied to classify wetlands at five study areas in Newfoundland and Labrador (NL): Avalon, Deer Lake,

Grand Falls, Gros Morne, and Goose Bay. Several analyses are performed in this regard and several methods are proposed to accurately identify and differentiate five wetland classes: Bog, Fen, Marsh, Swamp, and Shallow Water. Initially, the object-based method is compared with the pixel-based method to show the high performance of the first approach for wetland studies in terms of both qualitative and quantitative accuracies. Moreover, different classification algorithms, including the Support Vector Machine (SVM), Maximum Likelihood (ML), Decision Tree (TD), K-Nearest Neighbor (KNN), and Random Forest (RF) are evaluated to select the most accurate method for further experiments and studies. The effects of tuning parameters, included in the non-parametric classifiers, on classification accuracy are also widely discussed. Moreover, the multi-temporal satellite images are briefly investigated to select the best time for wetland classification. Furthermore, an innovative Multiple Classifier System (MCS), fusing five classifiers, is proposed to improve the classification accuracy of complex land covers, such as wetlands, in terms of both overall and individual class accuracies using SAR data. Although limited numbers of classification algorithms and features are used in the proposed MCS, there is no limitation in terms of the number of input classifiers and features. Moreover, although the MCS is tested on the SAR data and using an object-based method, the proposed MCS is flexible to consider more remote sensing datasets and utilizes pixel-based methods. Finally, separability analyses are performed using field data and multi-source optical and SAR imagery to select the best remote sensing features for wetlands discrimination. To this end, two separability measures of T-statistics and U-statistics are utilized to obtain more reliable results.

8.2. Conclusion

The specific conclusions of this thesis are as follows:

- Although each of optical and SAR remote sensing data contains its own advantages and disadvantages for wetland classification, a combination of these two types of imagery causes the highest mapping accuracy.
- Object-based classification methods result in a higher classification accuracy and are superior to pixel-based methods when medium or high spatial resolution satellite imagery is available for wetland classification. Moreover, all wetland classes correspond well to real objects and are identified more accurately in terms of visual interpretation using object-based methods.
- Regarding object-based methods, segmenting a study area using SAR data produces noisy results due to speckle noise. Thus, it is better to use an optical satellite image for segmentation purposes. In this regard, as the image contains higher spatial resolution, more accurate objects are obtained by segmentation algorithms.
- RF provides the most accurate results compared to the most commonly used classification algorithms, such as DT, SVM, ML, and KNN.
- Using a single classifier for mapping dynamic wetland environments does not provide the highest classification accuracy, especially regarding the individual wetland classes. Thus, a promising approach is combining various classifiers as an MCS to use the advantages of each single classifier.
- The tuning parameters of non-parametric algorithms, especially those of RF and SVM, cause noticeable impacts on the classification accuracy. Therefore, the optimum values should be selected before classification.

Since there is no automatic technique to do this, the best values should be selected by trial and error. Moreover, since the optimum values depend on several factors, the most important of which is the number of samples, the optimum tuning values should be adjusted in each wetland study.

- The number of field samples, which are applied to train a classifier and test its accuracy, has direct effects on the final classification accuracy. As the amount of samples are high, the accuracy will most probably be higher and the results will be also more reliable.
- Comparing wetland and non-wetland classes, the second is identified more accurately using satellite data. The reason is that the spectral and backscattering responses of non-wetland classes are more distinguishable compared to wetland classes using remote sensing methods. However, there are significant confusions between different wetland classes. In this regard, the confusion between Bog and Fen is most serious. In addition, there are difficulties in discriminating Swamp/Upland, Marsh/Shallow Water, Marsh/Bog, and Marsh/Fen class pairs. The other reason for lower classification accuracies of wetlands compared to non-wetland classes is related to the number of field samples. Since the amount of samples for wetland classes are usually lower than those of non-wetland classes, wetlands are classified with lower accuracies.
- Comparing the optical images captured in June, August, and November, the ones acquired in August provide the highest classification accuracy. However, it should be noted that using a combination of multi-temporal satellite images is more promising than using a single-date image. This is

rooted in the fact that wetlands are highly changeable over time and using a single acquisition image cannot distinguish all wetland classes properly.

- Performing variance analyses on the field samples to remove poor and noisy features before classification is a critical step for image classification. This is more important in the case of complex landscapes, such as wetlands, where there is a high variance between the values of samples obtained for a particular class. Furthermore, both individual and class pair variance analyses of field samples are more important for the case of SAR data compared to optical data, because SAR features are generally noisier than most common satellite data.
- Because of high variance of field samples of wetland classes, the recommendation is to apply non-parametric separability measures, such as U-distance, for separability analyses.
- There are considerable overlaps between the spectral signatures of wetlands, especially vegetated wetlands (i.e. Bog, Fen, Marsh, and Swamp), demonstrating the difficulties in wetland discrimination using optical satellite data.
- Comparing optical spectral bands, the Near Infrared (NIR) and Red Edge (RE) are the most useful for differentiating wetland classes. The red band is also helpful for wetland studies, especially for separating the Bog class from other wetland types, because of its red appearance. The Short Wave Infrared (SWIR) and Thermal Infrared (TIR) bands are not as helpful as the above bands, and the blue band is not relatively useful.
- Considering the most useful spectral bands mentioned above, some optical satellites, such as RapidEye and Sentinel-2A, which contain both the NIR

and RE bands are more recommended for wetland mapping. In this regard, Sentinel-2A, which provides free data is superior, especially for operational wetland mapping and monitoring their changes over time. However, it is better to apply RapidEye imagery, which has a higher spatial resolution, for segmenting an imagery and, thus, it is proper for studies that apply an object-based method.

- Full polarimetric SAR (e.g. RADARSAT-2) data provide a higher wetland classification accuracy compared to dual polarimetric (e.g. Sentinel-1) data. One main reason for this is because various decomposition methods can be applied to full polarimetric data, and the corresponding features can be efficiently utilized for wetlands discrimination.
- Coherent decomposition methods, such as Krogager, are generally useful in identifying man-made structures and not useful for naturally distributed targets, such as those found in wetland environments.
- The H/A/Alpha and Freeman-Durden decompositions provide the highest separability, and the corresponding features are considerably useful in separating wetland species.
- Considering both optical and SAR features, the ratio features, extracted from the most useful optical and SAR features, provided the highest separability for wetland classes.
- In general, SAR features extracted from decomposing eigenvalues/eigenvectors of the coherency matrix demonstrate high potential for wetland classification.
- Comparing L-band, acquired by some satellites such as Advanced Land Observing Satellite (ALOS)-2, and C-band, acquired by some satellites such

as RADARSAT-2, L-band demonstrate a high performance in delineating wetland classes. This is particularly important when discriminating flooded wetlands (e.g., the Swamp class) from other wetland types.

- Comparing three mechanisms of single-bounce, double-bounce, and volume scattering, which are utilized in most decomposition methods (e.g., Freeman-Durden, Van Zyl, and Yamaguchi), volume scattering is the best. The double-bounce component is the second most useful, and is considerably helpful in identifying flooded wetlands. Single-bounce is not recommended for differentiating complex wetland classes, and can only provide good results for detecting open water regions.
- The achieved wetland classification accuracies in NL, obtained through this research, are comparatively higher than most Canadian provinces.

8.3. Recommendations

Based on the research conducted during this dissertation, the following suggestions are provided to address either the limitations of the proposed methods or developed new methods for improving the accuracy of wetland classification.

8.3.1. Separability analysis of wetlands using multi-temporal satellite data

In this study, multi-temporal Landsat-8 images are evaluated to select the month, in which wetlands are more separable (see Chapter 3). To this end, the classification accuracies obtained by the RF algorithm for three months of June, August, and November are compared. Moreover, the separability analyses of wetlands are performed and extensively discussed in Chapter 4 and Chapter 5 using both optical and SAR data. Because of the availability of satellite data, these analyses are performed during a specific month (Optical and SAR data were used

in June and August, respectively). However, since wetlands are highly dynamic environments (Tiner et al., 2015; Mahdavi et al., 2017), tools for mapping and monitoring wetlands should consider the high temporal variability within them. In fact, it is important to know how much wetland types are separable in different times. This can be efficiently performed by spectral and backscattering analyses of multi-temporal optical and SAR satellite data. This also helps to select the optimum date for purchasing satellite data for wetland studies.

8.3.2. Improving and validating the accuracy of the proposed MCS

A new MCS is proposed and discussed in Chapter 6. The system is applied to a limited number of SAR features to classify wetlands in a study area. Moreover, object-based image analysis is selected in this study, and the results of the proposed MCS are compared with five common individual classifiers. There are several methods to improve the accuracy of the proposed MCS: (1) use a combination of optical and SAR data; (2) include more features for the classification; and, (3) include more single classifiers in the MCS. Additionally, it is recommended that the proposed MCS be validated more through: (1) applying the system to more study areas with various ecological characteristics; (2) using the pixel-based method instead of an object-based approach; and, (3) using a limited amount of field samples to train and test the proposed MCS.

8.3.3. Improving the accuracy of the Bog/Fen discrimination

One of the differences between bog and fen in terms of ecological characteristics is the fact that bogs are usually isolated water bodies, while water flows through fens (Väliranta et al., 2017). Thus, there is a chance to discriminate these similar classes

using spatial analysis through object-based methods and assessing their connectivity to surrounding water bodies.

8.3.4. Wetland classification using EWCS

In Canada, there are two well-known wetland classification systems: Canadian Wetland Classification System (CWCS) and Enhanced Wetland Classification System (EWCS). Because wetlands are complex landscapes, each of the five main wetland classes, defined by the CWCS, contains various vegetation types, cover percentage, or forms. Therefore, the five main wetland classes are further divided into 19 subclasses through the EWCS (Figure 8.1, Smith et al., 2007). This is also illustrated in Chapter 5 (Figure 5.3), where the backscattering responses of field samples for a wetland class demonstrate a three-modal signature. Thus, it is recommended to apply EWCS for wetland classification and compare the results with those obtained from the CWCS.

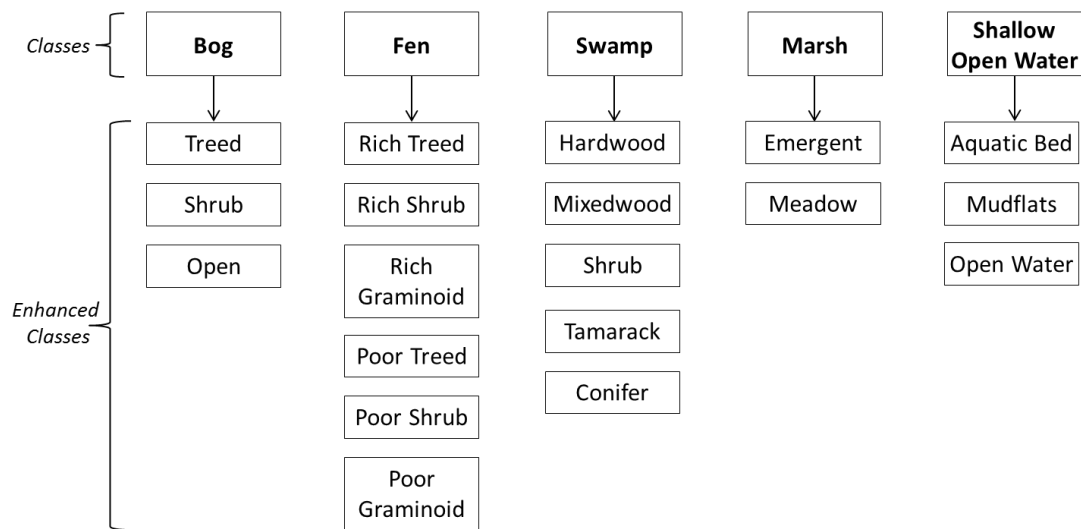


Figure 8.1. Wetland classification using the CWCS and EWCS (Smith et al., 2007).

8.3.5. Wetland classification using fuzzy methods

Wetlands do not occur in discrete units (Rocchini et al., 2013), and instead occur along a continuous gradient (Zoltai and Vitt, 1995). This means that there will inevitably be situations in nature where a wetland area cannot be all encompassing and perfectly classified without requiring a highly detailed and impractical classification system. An example of this confusion can be seen in the transitional areas that occur between a wetland and dry upland, or between one wetland type and another. At what point does wetland officially become upland? At what point does a wetland stop being one class and become another? Do these transitional areas meet the requirements of being assigned to a wetland class? Thus, it is a proper approach to apply a fuzzy method to assign a probability for each wetland class at each pixel/object.

8.3.6. Wetland classification using deep learning methods

Deep learning classification methods, such as the Convolutional Neural Network (CNN), have recently gained a significant attention in remote sensing image processing and classification. The methods have proved to provide a higher accuracy compared to conventional classifiers, including RF and SVM for various applications, including wetland classification (Kussul et al., 2017; Liu et al., 2017; Xu et al., 2018). However, the main disadvantages of deep learning methods are: 1) they need a large amount of samples to achieve a high accuracy; and, 2) it is significantly computationally expensive to train the corresponding algorithms (Liu

et al., 2018). Thus, there is need to a Graphics Processing Unit (GPU) rather than a Central Processing Unit (CPU) to process and classify the data. Currently, there are only a few studies worldwide that apply deep learning methods for wetland classification (e.g. Liu et al., 2018; Liu and Abd-Elrahman, 2018), and there is a desire to evaluate these methods and develop new deep learning approaches.

8.3.7. Improving wetland classification accuracy by incorporating DEM

Digital Elevation Model (DEM) along with the extracted features from it have demonstrated a high potential for wetland mapping (Brisco et al., 2011; Whiteside and Bartolo, 2015; Franklin and Ahmed, 2017). In this study, Canadian Digital Elevation Model (CDEM) is applied to classify wetlands in NL. Since the resolution of the products is low, they did not improve the accuracy considerably. However, it is a promising approach to include high resolution DEM in wetland classification and increase the accuracy. In this regard, Light Detection and Ranging (LiDAR) provides high resolution DEM or Digital Surface Model (DSM) and, thus, proved to be considerably helpful in wetland studies (Lang et al., 2012; Millard and Richardson, 2013; Franklin and Ahmed, 2017). However, it should be noted that LiDAR data are expensive and needs significant processing (Parsian and Amani, 2017).

8.3.8. Application of nanosatellites for wetland classification

Currently, there are many nanosatellites (CubeSats or SmallSats) in space. However, based on the author's literature review, there is no study which investigates their applications for wetland classification. These satellites provide high spatial resolution imagery and high temporal resolution data (e.g. daily data).

Therefore, they can be very helpful in classifying complex wetlands and monitor their changes over time. However, the data is relatively expensive and the number of spectral bands are mostly limited (e.g. RGB and NIR), which hinder their applications (Madry et al., 2018; Gao et al., 2018).

References

- Brisco, B., Kapfer, M., Hirose, T., Tedford, B., & Liu, J. (2011). Evaluation of C-band polarization diversity and polarimetry for wetland mapping. *Canadian Journal of Remote Sensing*, 37(1), 82-92.
- Franklin, S. E., & Ahmed, O. S. (2017). Object-based Wetland Characterization Using Radarsat-2 Quad-Polarimetric SAR Data, Landsat-8 OLI Imagery, and Airborne Lidar-Derived Geomorphometric Variables. *Photogrammetric Engineering & Remote Sensing*, 83(1), 27-36.
- Gao, S., Sweeting, M. N., Nakasuka, S., & Worden, S. P. (2018). Issue Small Satellites. *Proceedings of the IEEE*, 106(3), 339-342.
- Kussul, N., Lavreniuk, M., Skakun, S., & Shelestov, A. (2017). Deep learning classification of land cover and crop types using remote sensing data. *IEEE Geoscience and Remote Sensing Letters*, 14(5), 778-782.
- Lang, M., McDonough, O., McCarty, G., Oesterling, R., & Wilen, B. (2012). Enhanced detection of wetland-stream connectivity using LiDAR. *Wetlands*, 32(3), 461-473.
- Liu, P., Choo, K. K. R., Wang, L., & Huang, F. (2017). SVM or deep learning? A comparative study on remote sensing image classification. *Soft Computing*, 21(23), 7053-7065.

- Liu, T., & Abd-Elrahman, A. (2018). Deep convolutional neural network training enrichment using multi-view object-based analysis of Unmanned Aerial systems imagery for wetlands classification. *ISPRS Journal of Photogrammetry and Remote Sensing*, 139, 154-170.
- Liu, T., Abd-Elrahman, A., Jon, M., & Wilhelm, V. L. (2018). Comparing Fully Convolutional Networks, Random Forest, Support Vector Machine, and Patch-based Deep Convolutional Neural Networks for Object-based Wetland Mapping using Images from small Unmanned Aircraft System. *GIScience & Remote Sensing*, 55(2), 243-264.
- Madry, S., Martinez, P., & Laufer, R. (2018). Introduction to the World of Small Satellites. In *Innovative Design, Manufacturing and Testing of Small Satellites* (pp. 1-11). Springer, Cham.
- Mahdavi, S., Salehi, B., Granger, J., Amani, M., & Brisco, B. (2017). Remote sensing for wetland classification: a comprehensive review. *GIScience & Remote Sensing*, 1-36.
- Millard, K., & Richardson, M. (2013). Wetland mapping with LiDAR derivatives, SAR polarimetric decompositions, and LiDAR–SAR fusion using a random forest classifier. *Canadian Journal of Remote Sensing*, 39(4), 290-307.
- Parsian, S., & Amani, M. (2017). Building extraction from fused LiDAR and hyperspectral data using Random Forest Algorithm. *GEOMATICA*, 71(4), 185-193.
- Rocchini, D., Foody, G. M., Nagendra, H., Ricotta, C., Anand, M., He, K. S., ... & Feilhauer, H. (2013). Uncertainty in ecosystem mapping by remote sensing. *Computers & Geosciences*, 50, 128-135.

- Smith, K. B., Smith, C. E., Forest, S. F., & Richard, A. J. (2007). A field guide to the wetlands of the boreal plains ecozone of Canada. *Ducks Unlimited Canada, Western Boreal Office: Edmonton, Alberta.*
- Tiner, R. W., Lang, M. W., and Klemas, V. V. (Eds.). (2015). Remote Sensing of Wetlands: Applications and Advances. *CRC Press.*
- Väliranta, M., Salojärvi, N., Vuorsalo, A., Juutinen, S., Korhola, A., Luoto, M., & Whiteside, T. G., & Bartolo, R. E. (2015). Mapping Aquatic Vegetation in a Tropical Wetland Using High Spatial Resolution Multispectral Satellite Imagery. *Remote Sensing*, 7(9), 11664-11694.
- Xu, X., Li, W., Ran, Q., Du, Q., Gao, L., & Zhang, B. (2018). Multisource remote sensing data classification based on convolutional neural network. *IEEE Transactions on Geoscience and Remote Sensing*, 56(2), 937-949.
- Zoltai, S. C., & Vitt, D. H. (1995). Canadian wetlands: environmental gradients and classification. *Vegetatio*, 118(1-2), 131-137.

APPENDIX

In the following, the emails corresponding to the submitted papers are provided:

- Salehi, B., Mahdianpari, M., **Amani, M.**, Mohammadimanesh, F., Granger, J., Mahdavi, S., & Brisco, B. (2018). A collection of novel algorithms for wetland classification with SAR and optical data. "Minor revision", *InTech Open*.

Dear Ph.D. Salehi,

I am pleased to inform you that your chapter titled "A collection of novel algorithms for wetland classification with SAR and optical data," submitted to the book under the working title "Wetlands," has been reviewed. Based on the Editor's review, your chapter requires minor changes.

Below are some suggestions for you to incorporate in your full chapter manuscript:

"Dear Dr. Bahram Salehi,

Thank you for your revision manuscript to the Wetland Book. However, you should control some points carefully.

1. References [23], [29], [60], [67], [82] should be addressed in the full-text, while they are listing in the References List.

2. I strongly recommend that References should be in numerical order in the full-text ([43], [44], [47], [48], [49] [50], [52], [53], [54], [55], [56], [57], [58], [59], [62], [63], [65] [66]).

Please control carefully that references are in numerical order.

3. Table 2 caption. "wetlands [16,17]" should not be written in Bold.

4. Page 6. Please write in-situ in italic.

5. Table 3. I suggest that you write Table 3 caption under the table such as the other tables.

I hope you will implement the recommended changes successfully so your work can reach its maximum potential. Please submit the revised version of your chapter within the next 3 days.

If you have any questions or need any clarification regarding any of the Editor's suggestions, please let me know.

To sign in to your Author Panel please use the following link:

<https://mts.intechopen.com/booksprocess/action/chapter/161150>

Next Step:

Language Copyediting and Typeset Proof. Once your revision is uploaded, your paper will undergo specialized proofreading and editing to improve grammar, spelling, style, and accuracy at no additional charge, while our Technical Editors prepare your chapter for online publication.

Cordially,

Kristina Jurdana

Author Service Manager

IntechOpen

The Shard, 32 London Bridge Street, London SE1 9SG, United Kingdom

+44 20 8089 5700

www.intechopen.com

- **Amani, M.**, Salehi, B., Mahdavi, S., & Brisco, B. (2018). Separability analysis of wetland using multi-source SAR data. "Major revision", *ISPRS Journal of Photogrammetry and Remote Sensing*.

Ms. Ref. No.: PHOTO-D-18-00573

Title: Separability analysis of wetlands using multi-source SAR data

ISPRS Journal of Photogrammetry and Remote Sensing

Dear Mr. Meisam Amani,

Reviewers have now commented on your paper. I am pleased to say that it has been favourably received and publication with Major revision is recommended (see below and on <https://ees.elsevier.com/photo/>). If you are prepared to undertake the work required, I would be pleased to reconsider the revised paper for publication.

For your guidance, reviewers' comments are appended below.

To submit a revision, please go to <https://ees.elsevier.com/photo/> and login as an Author.

Your username is: meisam.amani69@gmail.com

If you need to retrieve password details, please go to:

http://ees.elsevier.com/photo/automail_query.asp

NOTE: Upon submitting your revised manuscript, please upload the source files for your article. For additional details regarding acceptable file formats, please refer to the Guide for Authors at: <http://www.elsevier.com/journals/isprs-journal-of-photogrammetry-and-remote-sensing/0924-2716/guide-for-authors>

When submitting your revised paper, we ask that you include the following items:

Response to Reviewers (mandatory)

This should be a separate file labeled "Response to Reviewers" that carefully addresses, point-by-point, the issues raised in the comments appended below. You should also include a suitable rebuttal to any specific request for change that you have not made.

Mention the page, paragraph, and line number of any revisions that are made.

Manuscript and Figure Source Files (mandatory)

We cannot accommodate PDF manuscript files for production purposes. We also ask that when submitting your revision you follow the journal formatting guidelines. Figures and

*tables may be embedded within the source file for the submission as long as they are of sufficient resolution for Production. For any figure that cannot be embedded within the source file (such as *.PSD Photoshop files), the original figure needs to be uploaded separately. Refer to the Guide for Authors for additional information.*

<http://www.elsevier.com/journals/isprs-journal-of-photogrammetry-and-remote-sensing/0924-2716/guide-for-authors>

Graphical Abstract (optional)

Graphical Abstracts should summarize the contents of the article in a concise, pictorial form designed to capture the attention of a wide readership online. Refer to the following website for more information: <http://www.elsevier.com/graphicalabstracts>

I would appreciate if you could submit your revised paper by Nov 6 2018 12:00:00:000AM.

On your Main Menu page is a folder entitled "Submissions Needing Revision". You will find your submission record there.

Given that the requested revisions are fairly major the new version is required within 4 weeks.

If you feel that you will be unable to submit your revision within the time allowed, please contact our editorial office to discuss an extension to your revision deadline.

Please proceed to the following link to update your personal classifications and keywords, if necessary:

<https://ees.elsevier.com/photo/l.asp?i=231285&l=NG8DLT1V>

Please note that this journal offers a new, free service called AudioSlides: brief, webcast-style presentations that are shown next to published articles on ScienceDirect (see also <http://www.elsevier.com/audioslides>). If your paper is accepted for publication, you will automatically receive an invitation to create an AudioSlides presentation.

ISPRS Journal of Photogrammetry and Remote Sensing features the Interactive Plot Viewer, see: <http://www.elsevier.com/interactiveplots>. Interactive Plots provide easy access to the data behind plots. To include one with your article, please prepare a .csv file with your plot data and test it online at <http://authortools.elsevier.com/interactiveplots/verification> before submission as supplementary material.

PLEASE NOTE: The journal would like to enrich online articles by visualising and providing geographical details described in ISPRS Journal of Photogrammetry and Remote Sensing articles. For this purpose, corresponding KML (GoogleMaps) files can be uploaded in our online submission system. Submitted KML files will be published with your online article on ScienceDirect. Elsevier will generate maps from the KML files and include them in the online article.

ISPRS Journal of Photogrammetry and Remote Sensing features the Interactive Map Viewer, <http://www.elsevier.com/googlemaps>. Interactive Maps visualize geospatial data provided by the author in a GoogleMap. To include one with your article, please submit a .kml or .kmz file and test it online at <http://elsevier-apps.sciiverse.com/GoogleMaps/verification> before uploading it with your submission. Include interactive data visualizations in your publication and let your readers interact and engage more closely with your research. Follow the instructions here: <https://www.elsevier.com/authors/author-services/data-visualization> to find out about available data visualization options and how to include them with your article.

Yours sincerely,

Derek Lichti

Editor-in-Chief

ISPRS Journal of Photogrammetry and Remote Sensing

- Mahdavi, S., Salehi, B., **Amani, M.**, Granger, J., Brisco, B., & Huang, W. (2018). A Dynamic Classification Scheme for Mapping Spectrally Similar Classes: Application to Wetland Classification. "Under review", *Remote Sensing of Environment*.

Dear Sahel,

Your submission entitled "A Novel Dynamic Classification Scheme for Mapping Spectrally Similar Classes: Application to Wetland Classification" as Research Paper has been received by Remote Sensing of Environment Journal Office.

You will be able to check on the progress of your paper by logging on to EES as an author.

The URL is <https://ees.elsevier.com/rse/>.

Your manuscript will be given a reference number once an Editor has been assigned.

Thank you for submitting your work to Remote Sensing of Environment.

Sincerely,

Betty Schiefelbein

Managing Editor

Remote Sensing of Environment

- Mahdavi, S., Salehi, B., **Amani, M.**, Brisco, B., & Huang, W. (2018). Change detection. "Under review", *IEEE Journal of Selected Topics in Applied Earth Observations and Remote Sensing*.

Dear Ms. Mahdavi:

The Editor of the IEEE Journal of Selected Topics in Applied Earth Observations and Remote Sensing acknowledges receipt of the following manuscript:

JSTARS-2018-00510

A Polarimetric Synthetic Aperture Radar Change Detection Index Based on Neighbourhood Information

It is understood that this manuscript is entirely original, has not been copyrighted, published, submitted, or accepted for publication elsewhere, and all necessary clearances and releases have been obtained. If the material in this paper has been published before in any form, it is imperative that you inform me immediately.

All JSTARS papers that are over 6 pages in the final published form will incur page charges of \$200.00 per page for pages 7 and beyond. Page charges are mandatory and non-negotiable. If you cannot pay these charges please shorten your paper accordingly.

Attention: Please do NOT attempt to resubmit any files or information in ScholarOne Manuscripts, as this will produce duplicate entries of the submission. If you find that you have made an error in the submission of your manuscript (i.e. uploaded the wrong file or selected the wrong issue designation) please contact me for assistance and further instructions.

You will be notified by e-mail when the review of this manuscript is completed. Please refer to the paper number in any communications regarding your manuscript. You may check the review status of your manuscript via the IEEE ScholarOne Manuscripts website. When the review of your manuscript has been completed, you will be notified of its disposition by e-mail and at that time reviewer comments will also be made available to you.

Sincerely,

Dr. Qian Du

Editor, IEEE Journal of Selected Topics in Applied Earth Observations and Remote Sensing

- Mahdavi, S., Maghsoudi, Y., & Amani, M. (2018). The effects of orbit type on Synthetic Aperture RADAR (SAR) backscatter. "Accepted", *Remote Sensing Letters*.

Dear Ms Mahdavi,

Thank you for making the further edits to your manuscript. It is a pleasure now to accept your research letter, TRES-LET-2018-0183.R3, entitled 'The effects of orbit type on Synthetic Aperture RADAR (SAR) backscatter', for publication in Remote Sensing Letters.

A copy of your manuscript files will be transferred electronically to the publishers, Taylor & Francis, in due course.

Once the paper has been transferred to the publishers, you will receive an email explaining how to follow its progress on their Central Article Tracking System (CATS). You will also receive a copy transfer agreement, information about obtaining reprints, and information about accessing and correcting the proofs.

If you do not receive an email about your proofs 2 weeks after you have received the initial CATS email, please contact the journal Administrator at craigcassells@hotmail.co.uk or submit an Article Status Form http://www.tandf.co.uk/journals/Article_status.asp directly to the publishers.

Thank you for your contribution to Remote Sensing Letters. We look forward to your continued contributions to the journal.

Yours sincerely,

Dr Craig Cassells

Administrator, Remote Sensing Letters

craigcassells@hotmail.co.uk

Ghahremanloo, M., **Amani, M.**, & Mobasheri, M. R. (2018). Soil moisture estimation at different depths using field soil temperature at various depths and remotely sensed surface temperature. "Under review", *International Journal of Remote Sensing*.

Dear Mr. Masoud Ghahremanloo

(cc'd to co-authors, if any)

Your manuscript entitled "Soil moisture estimation at different depths using field soil temperature at various depths and remotely sensed surface temperature" has been successfully submitted online and is presently being given full consideration for publication in International Journal of Remote Sensing.

Your manuscript ID is TRES-PAP-2018-1057.

Please mention the above manuscript ID in all future correspondence. If there are any changes in your contact details, please log in to the International Journal of Remote Sensing - ScholarOne Manuscripts site at <https://mc.manuscriptcentral.com/tres> and edit your user account information as appropriate.

You can also view the status of your manuscript at any time by checking the appropriate folder in your "Corresponding Author Centre" after logging in to <https://mc.manuscriptcentral.com/tres>.

The journal to which you are have submitted to is participating in the PEER project. This project, which is supported by the European Union EC eContentplus programme(http://ec.europa.eu/information_society/activities/econtentplus/index_en.htm), aims to monitor the effects of systematic self-archiving (author deposit in repositories) over time. If your submission is accepted, and you are based in the EU, you may be invited to deposit your accepted manuscript in a repository as part of this project. The project will develop models to illustrate how traditional publishing systems may coexist with self-

archiving For further information please visit the PEER project website at <http://www.peerproject.eu>.

Thank you for submitting your manuscript to the International Journal of Remote Sensing.

Yours sincerely

Mrs Catherine Murray

Administrator, International Journal of Remote Sensing

IIRS-Administrator@Dundee.ac.uk

- Mobasheri, M. R., Ranjbaran, M., **Amani, M.**, Mahdavi, S. & Zabihi, H. R. (2018). Determination of soil total nitrogen content in an agricultural area using spectrometry data. "Under review", *Journal of Applied Remote Sensing*.

Dear Mr. Amani,

I am pleased to acknowledge receipt of your manuscript entitled "Determination of soil total nitrogen content in an agricultural area using spectrometry data," which you have submitted to be considered for publication in the *Journal of Applied Remote Sensing (JARS)*.

The authors listed on this manuscript are:

Mohammad Reza Mobasheri

Maryam Ranjbaran

Meisam Amani

Sahel Mahdavi

Hamid Zabihi

All authors named on a manuscript are expected to have made a significant contribution to the writing, concept, design, execution, or interpretation of the work represented. If you

feel you are incorrectly included as an author on this manuscript, please respond immediately to this message indicating your concerns.

The manuscript control number for your paper is JARS 180713L. Please refer to this number in any correspondence.

You may check on the status of this manuscript at any time by selecting the "Check Manuscript Status" link after logging in at the following URL:

<https://jars.msubmit.net/cgi-bin/main.plex>

If you have any questions about your submission, please contact the editorial staff using the "Send Manuscript Correspondence" link, or send an e-mail to journals@spie.org.

Note to all authors: Please be sure to update your areas of expertise and contact information in your Journal of Applied Remote Sensing profile at <https://jars.msubmit.net/cgi-bin/main.plex>. If you are unsure of your login name or password, use the "Unknown/Forgotten Password" link. Once logged on, you can modify your account information via the "Modify Profile/Password" link at the bottom of your homepage.

Thank you for submitting your work to the Journal of Applied Remote Sensing.

Sincerely,

Dr. Ni-Bin Chang

Editor-in-Chief

Journal of Applied Remote Sensing

- *Mobasheri, M. R., Beikpour, M., **Amani, M.**, & Mahdavi, S. (2018). Soil moisture estimation using water absorption bands. "Under review", *Journal of Applied Remote Sensing*.*

Dear Dr. Mobasheri,

I am pleased to acknowledge receipt of your manuscript entitled "Soil moisture content estimation using water absorption bands," which you have submitted to be considered for publication in the Journal of Applied Remote Sensing (JARS).

The authors listed on this manuscript are:

MohammadReza Mobasheri

Mahin Beikpour

Meisam Amani

Sahel Mahdavi

All authors named on a manuscript are expected to have made a significant contribution to the writing, concept, design, execution, or interpretation of the work represented. If you feel you are incorrectly included as an author on this manuscript, please respond immediately to this message indicating your concerns.

The manuscript control number for your paper is JARS 180190. Please refer to this number in any correspondence.

You may check on the status of this manuscript at any time by selecting the "Check Manuscript Status" link after logging in at the following URL:

<https://jars.msubmit.net/cgi-bin/main.plex>

If you have any questions about your submission, please contact the editorial staff using the "Send Manuscript Correspondence" link, or send an e-mail to journals@spie.org.

Note to all authors: Please be sure to update your areas of expertise and contact information in your Journal of Applied Remote Sensing profile at <https://jars.msubmit.net/cgi-bin/main.plex>. If you are unsure of your login name or password, use the "Unknown/Forgotten Password" link. Once logged on, you can modify your account information via the "Modify Profile/Password" link at the bottom of your homepage.

Thank you for submitting your work to the Journal of Applied Remote Sensing.

Sincerely,

Dr. Ni-Bin Chang

Editor-in-Chief

Journal of Applied Remote Sensing